

Biomarkers Quantitative Imaging

Gastrointestinal (Rectal Cancer)

Sunday, Nov. 29 10:45AM - 12:15PM Location: E450A

GI BQ CT MR

AMA PRA Category 1 Credits ™: 1.50 ARRT Category A+ Credits: 1.50

Participants

Marc J. Gollub, MD, New York, NY (*Moderator*) Nothing to Disclose Kedar Jambhekar, MD, Little Rock, AR (*Moderator*) Nothing to Disclose

Sub-Events

SSA07-01 Correlations of Extramural Vascular Invasion on Preoperative MRI with Local Lymph Node Metastasis in Rectal Cancer

Sunday, Nov. 29 10:45AM - 10:55AM Location: E450A

Participants

Liheng Liu, MD, Beijing, China (*Presenter*) Nothing to Disclose Erhu Jin, Beijing, China (*Abstract Co-Author*) Nothing to Disclose Zhenghan Yang, MD, Beijing, China (*Abstract Co-Author*) Nothing to Disclose Zhenchang Wang, MD, PhD, Beijing, China (*Abstract Co-Author*) Nothing to Disclose

PURPOSE

To evaluate the possibility of predicting local lymph node metastasis by extramural vascular invasion (EMVI) on preoperative MRI in patients with rectal cancer.

METHOD AND MATERIALS

MR images and clinical pathologic data of 183 consecutive patients with rectal cancer (between Dec. 2011 and Dec. 2014) were reviewed. MRI-detected extramural vascular invasion (mr-EMVI), with clinical pathologic factors (including age, gender, T stage, differentiation, size and pathological EMVI), were analyzed by chi-square crosstabs test (or t test) and multivariate logistic regression to determine risk factors for lymph node metastasis.

RESULTS

A total of 183 rectal cancer patients who underwent radical surgery were included in our study. Of them, 78 (42.6%) patients had lymph node metastasis according to pathology at the time of surgery. Among those clinical pathologic factors, T stage (odds ratio, 1.848), pathological EMVI (odds ratio, 4.878) and MRI-detected EMVI (odds ratio, 3.884) were independent risk factors for LNM. The incidence of LNM in the patients with pathological EMVI and MRI-detected EMVI was 78.7% and 75.4% respectively. By using pathological EMVI as a gold standard, sensitivity, specificity and agreement rate of MRI-detected EMVI were 61.7%, 82.3% and 77.0%.

CONCLUSION

MRI-detected EMVI could be used as a predictor for lymph node metastasis in patients with rectal cancer.

CLINICAL RELEVANCE/APPLICATION

This paper has shown that the lymph node status at the time of surgery in rectal cancer is related to preoperative MRI-detected extramural vascular invasion. The results may be useful for patients' selection for preoperative neoadjuvant therapy.

SSA07-02 Reproducibility of Evaluation of Invasion Depth of Rectal Cancer into the Mesorectal Fat: Can We Reliably Discern T3ab from T3cd Tumours?

Sunday, Nov. 29 10:55AM - 11:05AM Location: E450A

Participants

Monique Maas, MD, Maastricht, Netherlands (*Presenter*) Nothing to Disclose Jasenko Krdzalic, MD, MSc, Maastricht, Netherlands (*Abstract Co-Author*) Nothing to Disclose Doenja M. Lambregts, MD, PhD, Maastricht, Netherlands (*Abstract Co-Author*) Nothing to Disclose Max Lahaye, MD, PhD, Maastricht, Netherlands (*Abstract Co-Author*) Nothing to Disclose Janna B. Houwers, MD, Maastricht, Netherlands (*Abstract Co-Author*) Nothing to Disclose Maria C. Ageitos Casais, MD, Santiago de Compostela, Spain (*Abstract Co-Author*) Nothing to Disclose Xubin Li, MD, PhD, Tianjin, China (*Abstract Co-Author*) Nothing to Disclose Rianne Beckers, Maastricht, Netherlands (*Abstract Co-Author*) Nothing to Disclose Miriam van Heeswijk, Maastricht, Netherlands (*Abstract Co-Author*) Nothing to Disclose Geerard L. Beets, MD, PhD, Maastricht, Netherlands (*Abstract Co-Author*) Nothing to Disclose Regina G. Beets-Tan, MD, PhD, Maastricht, Netherlands (*Abstract Co-Author*) Nothing to Disclose

PURPOSE

One of the important aspects of rectal cancer staging is the measurement of the invasion depth of a tumour into the mesorectal fat in millimetres. This determines whether there is a T3ab (<5mm) or T3cd (>5mm), which changes treatment for patients (CRT yes/no). Measurement of this factor is arbitrary. Aim was to evaluate reproducibility of the measurement of invasion depth into the mesorectal fat by different readers.

METHOD AND MATERIALS

Sixty-one patients with a pathologically proven T3 tumour were selected. Two readers with different experience in reading rectal

cancer MRI (2 years and 5 years) measured the maximal depth of invasion of tumour into mesorectal fat in the axial plane perpendicular to the tumour axis. Clock position of the measurement was registered. ICC and Bland-Altman plots were used for analyses.

RESULTS

Intraclass correlation coefficient was 0.61. The Bland-Altman plot showed a mean difference between measurements of 2.45 (SD 3.53) mm with limits of agreement of -4.45 to 9.39. Differences between measurements ranged from -9 to 15 mm. In 36% of patients the clock position of the measurements of both readers were was not in the same quadrant.

CONCLUSION

Reproducibility of measurement of invasion depth of tumour into the mesorectal fat is low, both with regard to the depth and to the location of the deepest invasion. Therefore, the distinction between T3ab and T3cd tumours is unreliable and should not be used for treatment decisions.

CLINICAL RELEVANCE/APPLICATION

The distinction between T3ab and T3cd tumours is deemed relevant to identify patients with a high risk tumor and administer neoadjuvant chemoradiation. Since measurement of invasion depth is only moderately reproducible, the use of this factor for risk and treatment stratification is questionable.

SSA07-03 Interobserver Variability in Interpretation of High Resolution MRI of Primary Rectal Cancer

Sunday, Nov. 29 11:05AM - 11:15AM Location: E450A

Participants

Ajaykumar C. Morani, MD, Houston, TX (*Presenter*) Nothing to Disclose Harmeet Kaur, MD, Houston, TX (*Abstract Co-Author*) Nothing to Disclose Raghunandan Vikram, MBBS, FRCR, Houston, TX (*Abstract Co-Author*) Nothing to Disclose Y. N. You, MD, Houston, TX (*Abstract Co-Author*) Nothing to Disclose Melissa W. Taggart, MD, Houston, TX (*Abstract Co-Author*) Nothing to Disclose George J. Chang, MD, Houston, TX (*Abstract Co-Author*) Nothing to Disclose Randy D. Ernst, MD, Houston, TX (*Abstract Co-Author*) Nothing to Disclose

PURPOSE

To assess interobserver variability in the interpretation of high resolution MRI scans for staging primary rectal cancer

METHOD AND MATERIALS

MRI of 22 randomly selected cases with known rectal cancer, were evaluated independently by 4 abdominal radiologists with approximately 2-4 years of experience in reading rectal MRI. Criteria evaluated included T stage and depth of tumor invasion separately assessed as measured in mm and < or > 5 mm, lymph node involvement and vascular invasion. The data was tabulated and interobserver agreement was calculated. For the small percentage of patients who went directly to surgery correlation with final pathology was performed.

RESULTS

There was wide range in interobserver agreement between 2 readers in different sets/combinations, ranging from 68-90% with overall complete agreement among all readers in only 68% of cases with respect to depth of tumor invasion which improved to 82%, if depth of tumor invasion was separated in <5 mm versus > 5 mm. 5 patients had undergone surgery immediately after MRI without preoperative chemoradiation. In these cases, individual reader accuracy for pT1/T2 versus T3 staging was 60-100% with overall mean accuracy of 80% among all readers. Agreement between 2 readers in different combinations, ranged from 68-81% with overall complete agreement among all readers in 54% of cases with respect to presence or absence of vascular invasion. Interobserver agreement was noted in 76-90% cases and complete agreement among all readers in 68% cases with respect to lymph node status.

CONCLUSION

High resolution MRI is now a widely accepted modality in the preoperative staging of primary rectal cancer. Inter-observer variability remains a significant limitation.

CLINICAL RELEVANCE/APPLICATION

High resolution MRI is now widely used for triaging patients directly to surgery or chemoradiation followed by surgery. However there is significant variation in the interpretation of key parameters. This should be recognized to avoid overtreatment or under-treatment of patients.

Honored Educators

Presenters or authors on this event have been recognized as RSNA Honored Educators for participating in multiple qualifying educational activities. Honored Educators are invested in furthering the profession of radiology by delivering high-quality educational content in their field of study. Learn how you can become an honored educator by visiting the website at: https://www.rsna.org/Honored-Educator-Award/

Raghunandan Vikram, MBBS, FRCR - 2012 Honored Educator

SSA07-04 Value of MRI in Prediction of Metachronous Distant Metastasis after Curative Surgery in Patients with Rectal Cancer versus Clinical and Pathologic Outcomes

Sunday, Nov. 29 11:15AM - 11:25AM Location: E450A

Caiyuan Zhang, MD, Shanghai, China (*Abstract Co-Author*) Nothing to Disclose Dengbin Wang, Shanghai, China (*Abstract Co-Author*) Nothing to Disclose

PURPOSE

To explore the risk factors for distant metastasis in patients with rectal cancer with MRI, clinical and pathologic outcomes.

METHOD AND MATERIALS

291 patients with surgico-pathologically confirmed rectal adenocarcinoma, who had undergone preoperative MRI before any treatment, were retrospectively collected. Preoperative MRI features (tumor location and size, MRI-TN stage, status of circumferential resection margin (CRM), lymphovascular invasion (LVI)), clinical characteristics (age, gender, preoperative CEA value), operation information (operation method, tumor location) and pathologic outcomes(pTN stage,status of pCRM, pLVI, nerve invasion(pNI), number of regional metastatic lymph nodes(pMLNNs), ratio of pMLN (pLNR),tumor grade) as well as immunohistochemical results were analyzed. Univariate and multivariate logistic regression models were performed to predict the risks of distant metastasis. The Kaplan-Meier method was used to analyze the disease-free survival (DFS) rate and 3-year overall survival (OS) rate.

RESULTS

Among 291 patients, 69 patients (23.7%) were confirmed to have distant metastasis. In univariate analysis, MRI-T stage (P=0.005), MRI-N stage (P<0.001), CEA value (P=0.007), pT stage (P<0.001), pN stage (P<0.001), pMLNNs (P<0.001), pLNR (P<0.001), tumor deposits (P=0.014), pLVI (P=0.005), pNI (P=0.003) correlated significantly with metachronous distant metastasis. In multivariate analysis, only preoperative CEA values (P=0.038, Exp(B)=2.102), pLNR(P<0.001, Exp(B)=23.780) and pT stage(P=0.005, Exp(B)=3.677) were independent risk factors for distant metastasis. The mean DFS period for both groups was significantly different (57.22±0.62 vs 18.88±1.98 months, P<0.001). The 3-year OS rate for patients with distant metastasis was 35.0% compared with 97.1% for those without distant metastasis (P<0.001).

CONCLUSION

Preoperative MRI provided limited value in prediction of metachronous distant metastasis in patients with rectal cancer as independent risk factor. Compared with MRI features, preoperative CEA values, pLNR and pT stage were independent risk factors. Patients with the risk factors should be closely followed up for monitoring the metachronous metastasis status in order to take measures for the hope of a good survival outcome.

CLINICAL RELEVANCE/APPLICATION

Compared with MRI features, CEA values, pLNR and pT stage were independent risk factors to predict metachronous distant metastasis in patients with rectal cancer.

SSA07-05 MRI Detected Tumor Response for Intermediate Stage Rectal Cancer(RC) Treated with Chemotherapy Predicts Disease Free Survival and Recurrence: A Collaborative Group Experience

Sunday, Nov. 29 11:25AM - 11:35AM Location: E450A

Participants

Uday B. Patel, MBBS, BSc, London, United Kingdom (Presenter) Nothing to Disclose Isidro Machado, Valencia, Spain (Abstract Co-Author) Nothing to Disclose Carlos Fernandez Martos, Valencia, Spain (*Abstract Co-Author*) Nothing to Disclose Rafael Estevan, Valencia, Spain (*Abstract Co-Author*) Nothing to Disclose Antonieta Salud, Lleida, Spain (Abstract Co-Author) Nothing to Disclose Maria Isabel Gil Garcia, Lleida, Spain (Abstract Co-Author) Nothing to Disclose Clara Montagut, Barcelona, Spain (Abstract Co-Author) Nothing to Disclose H Busto, Valencia, Spain (Abstract Co-Author) Nothing to Disclose Maria Rosa Safont, Sabadell, Spain (Abstract Co-Author) Nothing to Disclose Joan Maurel Santasusanaurel, Barcelona, Spain (Abstract Co-Author) Nothing to Disclose Juan R. Ayuso, MD, Barcelona, Spain (Abstract Co-Author) Nothing to Disclose J Aparicio, Madrid, Spain (Abstract Co-Author) Nothing to Disclose R Vera, Pamplona, Spain (Abstract Co-Author) Nothing to Disclose V Alonso, Zaragoza, Spain (Abstract Co-Author) Nothing to Disclose J Gallego, Elche, Spain (Abstract Co-Author) Nothing to Disclose M Martin, Barcelona, Spain (Abstract Co-Author) Nothing to Disclose C Pericay, Spain, Spain (Abstract Co-Author) Nothing to Disclose Eva Ballesteros JR, MD, Sabadell, Spain (Abstract Co-Author) Nothing to Disclose Jesus Santos Cores Santos Cores, Valencia, Spain (Abstract Co-Author) Nothing to Disclose Gina Brown, MD, MBBS, Sutton, United Kingdom (Abstract Co-Author) Nothing to Disclose

PURPOSE

'Intermediate risk' RC patients may benefit from neoadjuvant chemotherapy as staging MRI shows markers for distant disease but clear potential resection margins making local recurrence unlikely. This exhibit assesses MRI and pathological staging following neoadjuvant chemotherapy for intermediate risk RC in a prospectively enrolled multicenter phase II trial.

METHOD AND MATERIALS

The trial evaluated safety and efficacy of neoadjuvant Capecitabine, Oxliplatin and Bevacizumab(CAPOX-B). Forty-six patients were enrolled between 2009-11.Eligibility included baseline magnetic resonance(MR) showing a T3 tumour with mesorectal fascia (MRF) potentially clear.Baseline Nodal and Extra-mural venous invasion(EMVI) status was also recorded.Response was assessed by posttreatment MR and pathological T, N and EMVI status as well as Tumor regression grade(TRG).Additionally MR tumor length change,mrEMVI reversion and pathological T downstaging were recorded.Three-year disease free survival and recurrence were calculated using Kaplan-Meier.Cox proportional regression determined relationships between outcomes and all recorded imaging and pathology variables divided into good and poor responders.Three separate Cox-regression analyses were also performed for: baseline imaging, post-treatment imaging and pathology variables. Median follow-up was 36 months, fourteen patients experienced relapse. 3-year DFS was 69%. On Cox multivariate analysis including all factors mrEMVI(p=0.028) and T-downstaging(p=0.032) were independent prognostic factors for DFS. mrEMVI(p=0.040), T-downstaging(p=0.013) and ypN(p=0.041) were significant independent factors for recurrence.Significant univariate factors for DFS were: Baseline mrEMVI status(p=0.0001),mrEMVI reversion(p=0.003),post-treatment MR Tstaging(ymrT) (p=0.007),mrTRG(p=0.011),pathological nodal status(p=0.02) and Tdownstaging(p=0.0009).Significant univariate factors for recurrence were: mrEMVI(p=0.007),ymrT(p=0.008),mrTRG(p=0.019),Tdownstaging(p=<0.0001),ypN(p=0.002) and ypT(p=0.022).

CONCLUSION

Baseline MRI-EMVI is an independent prognostic factor for survival and recurrence in intermediate risk rectal cancer treated with neoadjuvant chemotherapy.

CLINICAL RELEVANCE/APPLICATION

Future randomised trials should evaluate primary chemotherapy verses standard treatment in patients with T3,MRF clear and mrEMVI positive disease. Moreover mrEMVI positive may be recommended as a stratification factor.

SSA07-06 Follow-up with MRI of Rectal Cancer Treated by TEM: Recurrence Detection and Inter-observer Reproducibility

Sunday, Nov. 29 11:35AM - 11:45AM Location: E450A

Participants

Monique Maas, MD, Maastricht, Netherlands (*Presenter*) Nothing to Disclose Britt Hupkens, Maastricht, Netherlands (*Abstract Co-Author*) Nothing to Disclose Milou Martens, Maastricht, Netherlands (*Abstract Co-Author*) Nothing to Disclose Jeroen Leijtens, Roermond, Netherlands (*Abstract Co-Author*) Nothing to Disclose Willem M. Deserno, MD,PhD, Almelo, Netherlands (*Abstract Co-Author*) Nothing to Disclose Camille van Berlo, Maastricht, Netherlands (*Abstract Co-Author*) Nothing to Disclose Geerard L. Beets, MD, PhD, Maastricht, Netherlands (*Abstract Co-Author*) Nothing to Disclose Regina G. Beets-Tan, MD, PhD, Maastricht, Netherlands (*Abstract Co-Author*) Nothing to Disclose

PURPOSE

Small rectal cancers can be treated with transanal endoscopic microsurgery(TEM). Postoperative changes make follow-up with MRI challenging. Aim was to evaluate post-TEM-MRI at different time points for recurrence detection and assess interobserver-reproducibility.

METHOD AND MATERIALS

38 patients underwent TEM (8 after CRT). 122 MRIs were performed with a mean of 3 MRIs per patient. Seven patients had a recurrence. MRI was performed every 3-4 months during follow-up and consisted of T2W-MRI±DWI. MRIs were evaluated by readers with different experience by confidence level (CL) scoring for recurrence, reproducibility was evaluated with weighted kappa statistics.

RESULTS

For all MRIs AUC for recurrence detection was 0.79and0.73 for T2W-MRI and 0.69and0.76 for DWI. During follow-up AUC increased from 0.55-0.57 at the first MRI to 0.67-0.73 at subsequent MRIs for T2W-MRI. Interobserver-reproducibility was increased during FU for T2W-MRI from kappa 0.09 to 0.77. For DWI reproducibility was fair-good (kappa 0.49-0.61) which increased slightly during FU. Reproducibility also increased during FU from kappa 0.36 to 0.84. At the first MRI after TEM higher CL scores were given at DWI than at T2W-MRI, this difference disappeared as of the second MRI during FU. Number of equivocal scores decreased during FU. Iso-intensity in bowel wall and/or mesorectal fat were predictive for recurrence.

CONCLUSION

The first post-TEM MRI is difficult to assess. After the first MRI accuracy for recurrence detection increases dramatically, due to comparison with earlier studies. There is a learning curve during FU per patient leading to more certainty in readers. Reproducibility is fair-moderate, but increases during FU. Iso-intensity in bowel wall and/or mesorectal fat were predictive for recurrence.

CLINICAL RELEVANCE/APPLICATION

After TEM follow-up is crucial to detect recurrences. MRI is a feasible and reliable modality to perform follow-up after TEM to both detect luminal and nodal recurrences.

SSA07-07 Imaging Genomics of Colorectal Cancer: Patterns of Metastatic Disease at Time of Presentation Based on Mutational Status

Sunday, Nov. 29 11:45AM - 11:55AM Location: E450A

Participants

Cinthia Cruz, MD, Boston, MA (Presenter) Nothing to Disclose

James H. Thrall, MD, Boston, MA (*Abstract Co-Author*) Board Member, Mobile Aspects, Inc; Board Member, WorldCare International Inc; Consultant, WorldCare International Inc; Shareholder, Antares Pharma, Inc; Shareholder, iBio, Inc; Shareholder, Peregrine Pharmaceuticals, Inc

Debra A. Gervais, MD, Chestnut Hill, MA (Abstract Co-Author) Nothing to Disclose

PURPOSE

To identify the most frequent genetic traits associated with metastatic colorectal tumors at time of presentation and whether there is a correlation between the genotypes and the metastatic disease patterns.

METHOD AND MATERIALS

Retrospective review of 713 subjects with cross-sectional imaging at time of diagnosis with no previous treatment. All tumor samples were tested for Single Nucleotide Polymorphisms (SNP). Mutations can be present individually or coexisting. Z tests were

used to assess differences.

RESULTS

Three-hundred-ninety-seven males and 316 females. Metastatic disease in 547/713 (76), 385/487(79) mutants (M) and 162/226(72) wild types (WT) (p=0.02). Incidence of metastatic disease per genotype as follows: NRAS 31/35(89%), KRAS 213/244 (87%), APC 47/55(85%), TP53 142/170(84%), PIK3C 59/81 (73%), BRAF 56/79(71%) and WT (72%)162/226. Metastasis to the liver, lymphnodes (LN), peritoneum and lung were observed with all genotypes. Liver:LN proportion of involvement was seen as follows: KRAS 62:28 (p<0.001), BRAF 55:62, NRAS 71:58, TP53 63:59, PIK3C 69:49, APC 64:47 and WT 51:49. Metastatic site involvement exclusive to certain genotypes was observed: duodenum/kidneys/uterus/cervix/vagina: KRAS+TP53, Brain:TP53, Appendix: KRAS, Retroperitoneum:PIK3C/WT and Bladder/Pancreas/Prostate/Mediastinum: WT. All genotypes except for BRAF demonstrated bone metastasis.

CONCLUSION

Our study suggests there is an association between mutational status and patterns of metastatic disease in Colorectal Cancer. Metastatic disease to the bladder, pancreas, prostate and mediastinum in CRC suggests wild type tumors. A lower involvement of LN suggests the presence of KRAS mutation.

CLINICAL RELEVANCE/APPLICATION

Genetic profiling should guide the search for specific metastatic patterns allowing special consideration for unusual sites of involvement of metastatic disease to suggest the presence of a specific mutation.

Honored Educators

Presenters or authors on this event have been recognized as RSNA Honored Educators for participating in multiple qualifying educational activities. Honored Educators are invested in furthering the profession of radiology by delivering high-quality educational content in their field of study. Learn how you can become an honored educator by visiting the website at: https://www.rsna.org/Honored-Educator-Award/

Debra A. Gervais, MD - 2012 Honored Educator

SSA07-08 The Application of 3.0T MR Intravoxel Incoherent Motion Imaging and Diffusion Weighed Imaging in Preoperative Diagnosis of Lymph Node Metastatic of Rectal Carcinoma

Sunday, Nov. 29 11:55AM - 12:05PM Location: E450A

Participants

Lin Qiu, Guangzhou, China (*Presenter*) Nothing to Disclose Xiang-Ran Cai, Guangzhou, China (*Abstract Co-Author*) Nothing to Disclose Sirun Liu, MSc, Guang-Zhou, China (*Abstract Co-Author*) Nothing to Disclose Meng Chen, Guangzhou, China (*Abstract Co-Author*) Nothing to Disclose You-Zhen Feng, Guangzhou, China (*Abstract Co-Author*) Nothing to Disclose Zhong-Ping Zhang, MMedSc, Guangzhou, China (*Abstract Co-Author*) Nothing to Disclose

PURPOSE

To evaluate the clinical value of Intravoxel Incoherent Motion imaging (IVIM) sequence in the diagnosis of lymph node metastatic of rectal carcinoma.

METHOD AND MATERIALS

87 lymph nodes from sixty-two rectal carcinoma patients with IVIM sequence

(b=0,25,50,75,100,150,200,400,600,800,1000,1200,1500 and 2000 s/mm2) at 3.0T MR scanner and pathology data were collected. The parameter of IVIM(standard ADC, D, D* and f values)and the DWI signal strength value with b=1000 s/mm2 (S1000)in non-metastatic lymph nodes and metastatic lymph nodes were measured and calculated. Pathology findings and MR sequence were compared. The difference of metastatic lymph nodes and non-metastatic lymph nodes were compared by paired-samples t test.

RESULTS

There were 25 metastatic lymph nodes was found in 62 patients. The standard-ADC= $(0.795 \pm 0.23) \times 10-3 \text{ s/mm2}, D= (0.649 \pm 0.11) \times 10-3 \text{ s/mm2}, D^* = (4.79\pm 2.38) \times 10-3 \text{ s/mm2}, f=(0.27\pm 0.09) \%$ and =348.25±26.74 in the metastatic lymph nodes ;the standard-ADC= $(0.995 \pm 0.34) \times 10-3 \text{ s/mm2}, D= (0.787 \pm 0.19) \times 10-3 \text{ s/mm2}, D^* = (4.86\pm 5.40) \times 10-3 \text{ s/mm2}, f=(0.33\pm 0.33) \%$ and S1000 =211.75±35.66 in non-metastatic lymph nodes. The difference of standard-ADC value(t=31.92,p<0.01), D(t=17.63,p=0.02) and S1000 (t=18.92,p<0.01) were statistically significant in the metastatic lymph nodes and non-metastatic lymph nodes;the standard-ADC value, D value and S1000 value of metastatic lymph nodes were higher than non-metastatic lymph nodes.

CONCLUSION

IVIM sequence can reveal standard ADC, D, D* , f and signal strength values ,they are helpful for diagnose metastatic lymph node.

CLINICAL RELEVANCE/APPLICATION

IVIM sequence is helpful for diagnose metastatic lymph node.

SSA07-09 CT Texture Analysis in Patients with Locally Advanced Rectal Cancer Treated with Neoadjuvant Chemoradiotherapy: A Potential Imaging Biomarker for Treatment Response and Prognosis

Sunday, Nov. 29 12:05PM - 12:15PM Location: E450A

Participants

Choong Guen Chee, MD, Seongnam, Korea, Republic Of (*Presenter*) Nothing to Disclose Young Hoon Kim, MD, PhD, Seongnam-Si, Korea, Republic Of (*Abstract Co-Author*) Nothing to Disclose Bohyoung Kim, PhD, Seongnam-Si, Korea, Republic Of (*Abstract Co-Author*) Nothing to Disclose Soyeon Ahn, Seongnam-Si, Korea, Republic Of (*Abstract Co-Author*) Nothing to Disclose Kyoung Ho Lee, MD, Seongnam-Si, Korea, Republic Of (*Abstract Co-Author*) Nothing to Disclose Yoon Jin Lee, MD, Seongnam-si, Korea, Republic Of (*Abstract Co-Author*) Nothing to Disclose Ji Hoon Park, MD, Seongnam-Si, Korea, Republic Of (*Abstract Co-Author*) Research Grant, Bracco Group

PURPOSE

To evaluate the association of texture of locally advanced rectal cancer in computed tomography (CT) with neoadjuvant concurrent chemoradiotherapy treatment (CRT) response and 3-year disease-free survival (DFS).

METHOD AND MATERIALS

Institutional review board approved this retrospective study and waived the requirement of informed patient consent. 95 consecutive patients who had neoadjuvant CRT followed by surgery for locally advanced rectal cancer have been included. Texture features were assessed with pretreatment CT scans by using independently developed software. Entropy, uniformity, kurtosis, skewness, and standard deviation were obtained from the largest axial image of the tumor (its boundary being manually drawn), without filtration and with Laplacian of Gaussian spatial filter of various filter values for fine (1.0), medium (1.5 and 2.0), and coarse (2.5) textures. Dworak pathologic grading was used for treatment response. Mean value of each texture parameter was compared between treatment responder (grade 3 and 4) and non-responder (grades 1 and 2) groups via independent t-test. Kaplan-Meier analysis was used to find the relationship between CT texture and 3-year DFS. Receiver operating characteristic curve was performed to determine the optimal threshold values. Using Cox proportional hazards model, independence of texture parameters from patient's stage and age was assessed.

RESULTS

Treatment responder group (n = 32) showed fine-texture features (lower entropy, higher uniformity, and lower standard deviation) with statistical significance in no filtration, and fine (1.0) and medium (1.5) filter values. Without filtration, Kaplan-Meier survival plots for entropy, uniformity, and standard deviation were significantly different (P = .03, P = .016, and P = .033) and fine-texture features (≤ 6.7 for entropy, > 0.0100 for uniformity, and ≤ 28.06 for standard deviation) were associated with higher 3-year DFS. Entropy, uniformity, and standard deviation were independent factors from the cancer stage and age in 3-year DFS (P = .033, P = .011, and P = .04).

CONCLUSION

Fine-texture features are associated with better neoadjuvant CRT response and higher 3-year DFS in patients with locally advanced rectal cancer.

CLINICAL RELEVANCE/APPLICATION

Our study implies the possibility of texture analysis as an imaging biomarker for the treatment response of neoadjuvant CRT and 3year DFS in locally advanced rectal cancer.

ISP: Gastrointestinal (HCC)

Sunday, Nov. 29 10:45AM - 12:15PM Location: E450B



AMA PRA Category 1 Credits ™: 1.50 ARRT Category A+ Credits: 1.50

Participants

Shahid M. Hussain, MD, PhD, Omaha, NE (*Moderator*) Nothing to Disclose Mustafa R. Bashir, MD, Cary, NC (*Moderator*) Research support, Siemens AG; Research support, Bayer AG; Research support,

Guerbet SA; Research support, General Electric Company; Consultant, Bristol-Myers Squibb Company

Sub-Events

SSA08-01 Gastrointestinal Keynote Speaker: Update on HCC Screening with Imaging

Sunday, Nov. 29 10:45AM - 10:55AM Location: E450B

Participants

Shahid M. Hussain, MD, PhD, Omaha, NE (Presenter) Nothing to Disclose

SSA08-02 Performances of Imaging for the Diagnosis of Small HCC Following the Recommendations of the European and American Association for the Study of the Liver

Sunday, Nov. 29 10:55AM - 11:05AM Location: E450B

Participants

Christophe Aube, MD, PhD, Angers, France (*Presenter*) Speaker, Bayer AG Support, General Electric Company Valerie Vilgrain, MD, Clichy, France (*Abstract Co-Author*) Nothing to Disclose Julie Lonjon, Montpellier, France (*Abstract Co-Author*) Nothing to Disclose Olivier Seror, Bondy, France (*Abstract Co-Author*) Consultant, Angiodynamics, Inc; Consultant, Olympus Corporation; Consultant, Bayer AG Ivan Bricault, PhD, Grenoble, France (*Abstract Co-Author*) Medical Advisory Board, IMACTIS Agnes Rode, MD, Lyon, France (*Abstract Co-Author*) Nothing to Disclose Christophe Cassinotto, MD, Pessac, France (*Abstract Co-Author*) Nothing to Disclose

Frederic Oberti, MD, PhD, Angers, France (*Abstract Co-Author*) Nothing to Disclose

PURPOSE

To evaluate, in a large population of patients with chronic liver disease, the performances of the different imaging techniques (contrast enhanced ultrasound (CEUS), CT scanner and MRI) alone and in combinations for the characterisation of hepatic nodules smaller than 3cm. This study was supported by a national institutional grant (PHRC 2008)

METHOD AND MATERIALS

From April 2010 to April 2013, 442 patients with a chronic liver disease have been prospectively included in 16 centres. They had 1 to 3 nodules 10 to 30 mm explored by CEUS, CT scanner and a MRI within a month. The examination was regarded as positive if the nodule displayed the typical landmark of HCC as defined by the European and American Association for the Study of the Liver (EASL and AASLD) recommendations. A composite gold standard was constructed with histology, imaging and follow up. We determined sensitivity and specificity for a given exam alone and for various combinations of exams as single tests. Results were given regarding the size of the nodules: 10-20mm and 20-30 mm.

RESULTS

382/442 patients with 551 nodules have been finally kept for the statistical analysis. They were 315 (82.46%) males; the mean age was 62.06 +/- 9.73 years. The causes of the chronic liver disease were mainly alcohol (58.12%), C virus (31.41%) and metabolic syndrome (19.11%). The mean size of the nodules was 18.15 +/- 5.74mm.For the 10 - 20mm nodules (n=347) sensibility for the diagnosis of HCC was 70.2% for MR, 67.6% for CT scanner and 39.9% for the CEUS; and the specificity was respectively 83.1%, 76.6% and 93.5%. For the 20 - 30mm nodules (n=204) sensibility for the diagnosis of HCC was 70.5% for MR, 67.5% for CT scanner and 52.4% for the CEUS; and the specificity was respectively 97.3%, 97.3% and 100%.For the 10 - 20mm nodules the sensibility and specificity were respectively 54.8% and 100% for the association of CT + MR; 27.7% and 100% for CT + CEUS; and 28.7% and 99.4% for MR and CEUS

CONCLUSION

This study validates the use of sequencial application of CT and MRI as recommended in the recent update of EASL and AASLD guidelines, in case of small HCC and in a large population. It shows the potential interest of CEUS for its high specificity. This study is part of the CHIC group.

CLINICAL RELEVANCE/APPLICATION

Recent updates of EASL and AASLD recommendations for the non invasive diagnosis of HCC are validated for the small HCC in a large population.

SSA08-03 Non-invasive Diagnostic Criteria of Hepatocellular Carcinoma: Comparison of Diagnostic Accuracy of Updated LI-RADS with Clinical Practice Guidelines of OPTN-UNOS, AASLD, NCCN, EASL-EORTC, and KLCSG-NCC

Sunday, Nov. 29 11:05AM - 11:15AM Location: E450B

Participants Burcu Akpinar, MD, Aurora, CO (*Presenter*) Nothing to Disclose Samuel Chang, MD, Aurora, CO (*Abstract Co-Author*) Nothing to Disclose Jeffrey Kaplan, MD, Aurora, CO (*Abstract Co-Author*) Nothing to Disclose

PURPOSE

To retrospectively compare the diagnostic accuracy of different noninvasive diagnostic criteria of hepatocellular carcinoma (HCC) by LI-RADS, OPTN-UNOS, AASLD, NCCN, EASL-EORTC, KLCSG-NCC

METHOD AND MATERIALS

We reviewed the medical records of 2,210 patients who had undergone biopsy, resection, or explantation of liver from January 2011 to November 2013 in our institution. Ninety three patients (M:F=69:24; mean age: 54.8, range 30-77) with chronic hepatitis B and/or cirrhosis for any etiology who had focal hepatic lesions \geq 5 mm reported on dynamic contrast enhanced CT or MR were included. The focal hepatic lesions treated prior to imaging were excluded. A total of 144 lesions were finally included in our study with 73 lesions \geq 2 cm, 55 lesions between 1-2 cm, and 16 lesions < 1 cm. The focal hepatic lesions were retrospectively evaluated on CT or MR by use of different noninvasive diagnostic criteria of HCC including LI-RADS (2014), OPTN-UNOS, AASLD, NCCN, EASL-EORTC, and KLCSG-NCC. Using the pathology reports as a gold standard, sensitivity, specificity, and accuracy of the diagnostic criteria were analyzed.

RESULTS

The sensitivity was highest and equal with AASLD, NCCN, EASL-EORTC and KLCSG-NCC criteria (84.4%), followed by LI-RADS (77.9%) and OPTN-UNOS criteria (75.3%). The specificity was highest with OPTN-UNOS criteria (92.5%), followed by LI-RADS (90.0%), AASLD, NCCN, EASL-EORTC and KLCSG-NCC (82.1%). The accuracies were 83.3%, equal for all noninvasive diagnostic criteria.

CONCLUSION

AASLD, NCCN, EASL-EORTC and KLCSG-NCC had the highest sensitivity whereas OPTN-UNOS had the highest specificity among all six guidelines. LI-RADS could not provide higher specificity than OPTN-UNOS criteria or high sensitivity than AASLD or EASL criteria.

CLINICAL RELEVANCE/APPLICATION

Though LI-RADS 2014 is widely used by radiologists, it provides lower specificity than OPTN-UNOS criteria as well as lower sensitivity than AASLD or EASL criteria for noninvasive diagnosis of HCC.

SSA08-04 Prognostic Stratification of Patients with Hepatocellular Carcinoma Undergoing Curative Resection: Comparison of Preoperative MRI Staging and Postoperative American Joint Committee on Cancer Staging Systems

Sunday, Nov. 29 11:15AM - 11:25AM Location: E450B

Participants

Chae Jung Park, MD, Seoul, Korea, Republic Of (*Presenter*) Nothing to Disclose Chansik An, MD, Seoul, Korea, Republic Of (*Abstract Co-Author*) Nothing to Disclose Yeun Yoon Kim, MD, Seoul, Korea, Republic Of (*Abstract Co-Author*) Nothing to Disclose Yong Eun Chung, MD, PhD, Seoul, Korea, Republic Of (*Abstract Co-Author*) Nothing to Disclose Jin-Young Choi, Seoul, Korea, Republic Of (*Abstract Co-Author*) Nothing to Disclose Myeong-Jin Kim, MD, PhD, Seoul, Korea, Republic Of (*Abstract Co-Author*) Nothing to Disclose

PURPOSE

To devise a preoperative staging system for hepatocellular carcinoma (HCC) undergoing resection using magnetic resonance imaging (MRI) findings, and to compare its prognostic ability with that of the American Joint Committee on Cancer (AJCC) staging.

METHOD AND MATERIALS

A total of 175 consecutive patients with HCC who underwent curative hepatic resection after preoperative MRI between January 2000 and December 2007 were analyzed. We devised an MRI staging system based on the number of nodules, a size criterion of 2 cm, gross vascular invasion, and two MRI features (rim enhancement and peritumoral parenchymal enhancement in the arterial phase) which were reported to be associated with worse prognosis after curative resection of HCC. In the devised MRI staging, instead of microvascular invasion which is used by the AJCC staging system, a size criterion of 2 cm was used to differentiate tumor stages 1 and 2. Each tumor stage was further divided into two substages; if both of the MRI features were absent, a patient was staged as T1a, 2a, or 3a, but staged as T1b, 2b, or 3b if any of these were present. Disease-free survival of both staging systems was analyzed using the Kaplan-Meier method with log-rank testing.

RESULTS

Both MRI and AJCC staging systems were excellent for predicting disease-free survival across different tumor stages 1, 2 and 3. Of 175 patients, 29 (16.6%), 6 (3.4%), 77 (44%), 51(29%), 6 (3.5%), and 6 (3.5%) were staged as T1a, T1b, T2a, T2b, T3a, and T3b by the preoperative MRI staging system, respectively. Disease-free survival was significantly different between T1 and T2a (median, 1925 days vs. 1668 days; P=0.048), between T2a and T2b (median, 1668 days vs. 799 days; P=0.0021), and between T2b and T3 (median survival, 799 days vs. 141 days; P=0.0015). However, no significant difference was found in disease-free survival between T1a and T1b, and between T3a and T3b.

CONCLUSION

Preoperative MRI staging system may be comparable to the postoperative AJCC staging system in predicting prognosis following

curative resection of HCC. Furthermore, tumor stage 2 of the MRI staging system may be further divided into T2a and T2b.

CLINICAL RELEVANCE/APPLICATION

These advantages (preoperative staging and further stratification of T2 into T2a/b) can make the devised MRI staging useful in deciding on treatment plans of patients with HCC.

SSA08-05 Utilising the Full Potential of MRI in the Diagnosis of HCC - Time for a Game Changer?

Sunday, Nov. 29 11:25AM - 11:35AM Location: E450B

Participants

Kelvin Cortis, MD, FRCR, Msida, Malta (*Presenter*) Nothing to Disclose Rosa Liotta, Palermo, Italy (*Abstract Co-Author*) Nothing to Disclose Roberto Miraglia, MD, Palermo, Italy (*Abstract Co-Author*) Nothing to Disclose Settimo Caruso, Palermo, Italy (*Abstract Co-Author*) Nothing to Disclose Fabio Tuzzolino, Palermo, Italy (*Abstract Co-Author*) Nothing to Disclose Angelo Luca, MD, Palermo, Italy (*Abstract Co-Author*) Nothing to Disclose

PURPOSE

The current cornerstone of HCC diagnosis is the wash-in/wash-out enhancement pattern. It is known that HCC might exhibit other MRI findings. Our aim was to retrospectively review the MRIs of histologically proven HCCs on liver explants, and to identify the best combination of sequences useful in HCC diagnosis.

METHOD AND MATERIALS

97 consecutive patients who underwent liver transplantation between 2004 and 2012 and Gd-BOPTA-MRI within 3 months of surgery were enrolled. A hepatobiliary histopathologist and two radiologists blinded to the radiological/histopathological findings performed a nodule by nodule analysis. The signal intensity of all nodules was assessed on the following axial sequences: T1 in/opposed phase, 3D fat suppressed (FS) T1 (pre-contrast, arterial, portal, equilibrium, and hepatobiliary phases), T2, T2 FS, and diffusion (B=800). Arterial enhancement was graded as none, mild, moderate, or intense. A multiple logistic regression analysis was performed following pathological/radiological correlation, and the Odds Ratio (OR) was calculated for every parameter analysed and adjusted for nodule size.

RESULTS

Imaging was performed 41.7±25.4 days pre-transplantation. 291 lesions were identified on histopathology, of which 193 were HCCs, 68 regenerative nodules, 8 low-grade dysplastic nodules (DN), 19 high-grade DNs, 2 cholangiocarcinomas, and 1 necrotic nodule. 48 HCCs (24.9%) were not detectable on imaging (24.9%), leaving a total of 145 HCCs (\leq 10 mm n=25;11-19 mm n=58; \geq 20 mm n=62).As expected, intense (OR 10.9, p<0.000) or moderate (OR 2.2, p=0.003) arterial enhancement and hypointensity on the portal venous (OR 14.3, p<0.000) or equilibrium (OR 15.9, p<0.000) phases were found to predict HCC.In addition, nodules showing hypointensity on the hepatobiliary phase and T2 hyperintensity were also highly likely to represent HCC. In the former, an OR of 10.2 was observed (p<0.000). The OR was 14.3 in non-FS T2 weighted sequences, and 10.2 in FS T2 weighted sequences (p<0.000).

CONCLUSION

In patients with a high risk of HCC, nodules lacking the typical hemodynamic findings are most likely HCC if they exhibit T2 hyperintensity and/or hypointensity on the hepatobiliary phase with an OR of 14.3 and 10.2, respectively (p<0.000).

CLINICAL RELEVANCE/APPLICATION

MRIs targeted at diagnosing HCC should include T2 weighted sequences with and without FS and Gd-BOPTA/Gd-EOB-enhanced hepatobiliary phases alongside standard sequences.

SSA08-06 A Tumor Suppression Factor HNF4a (Hepatocyte Nuclear Factor) Expression Correlates with Gadoxetic Acid Enhanced MRI Fndings in Hepatocellular Carcinoma

Sunday, Nov. 29 11:35AM - 11:45AM Location: E450B

Participants

Azusa Kitao, Kanazawa, Japan (*Presenter*) Nothing to Disclose Osamu Matsui, MD, Kanazawa, Japan (*Abstract Co-Author*) Research Consultant, Kowa Company, Ltd Research Consultant, Otsuka Holdings Co, Ltd Research Consultant, Eisai Co, Ltd Speakers Bureau, Bayer AG Speakers Bureau, Eisai Co, Ltd Norihide Yoneda, Kanazawa, Japan (*Abstract Co-Author*) Nothing to Disclose Kazuto Kozaka, MD, Kanazawa, Japan (*Abstract Co-Author*) Nothing to Disclose Satoshi Kobayashi, MD, Kanazawa, Japan (*Abstract Co-Author*) Nothing to Disclose Toshifumi Gabata, MD, Kanazawa, Japan (*Abstract Co-Author*) Nothing to Disclose Kotaro Yoshida, MD, Kanazawa, Japan (*Abstract Co-Author*) Nothing to Disclose Dai Inoue, Kanazawa, Japan (*Abstract Co-Author*) Nothing to Disclose Tetsuya Minami, MD, Kanazawa, Japan (*Abstract Co-Author*) Nothing to Disclose Wataru Koda, Kanazawa, Japan (*Abstract Co-Author*) Nothing to Disclose Junichiro Sanada, Kanazawa, Japan (*Abstract Co-Author*) Nothing to Disclose

PURPOSE

Hepatocyte nuclear factor (HNF) 4A is one of transcription factors with tumor suppression effect, and besides, regulates expression of many molecules including organic anion transporting polypeptide (OATP) 1B3 (uptake transporter of gadoxetic acid) in hepatocellular carcinoma (HCC) (Yamashita T, Hepatology 2014). The purpose of this study is to clarify the correlation between HNF4A expression, pathological findings and imaging findings on gadoxetic acid enhanced MRI.

METHOD AND MATERIALS

The subjects are 138 surgically resected HCCs. We semiquantitatively evaluated the immunohistochemical HNF4A and OATP1B3 expression of HCC into four grades: grade 0: no expression, grade 1: weak expression, grade 2: moderate expression and grade 3:

intensive expression. We compared HNF4A grade of HCCs with OATP1B3 grade, enhancement ratio on the hepatobiliary phase of gadoxetic acid enhanced MRI and histological tumor differentiation grade (well, moderately and poorly differentiated HCC).

RESULTS

HNF4A grade in HCC showed a significant positive correlation with OATP1B3 grade (P=0.003, r=0.46). There was also a significant positive correlation between HNF4A grade and enhancement ratio on the hepatobiliary phase of gadoxetic acid enhanced MRI (P<0.0001, r=0.49). Especially, intensive HNF4A expression was observed in atypical HCC showing high enhancement ratio and increased OATP1B3 expression. HNF4A grade was decreased according to the decline of differentiation grade of HCC (P=0.0007, r=0.29).

CONCLUSION

The expression of HNF4A in HCC correlated with both of OATP1B3 expression and enhancement ratio on the hepatobiliary phase of gadoxetic acid enhanced MRI. In addition, HNF4A expression was decreased during multistep hepatocarcinogenesis. Gadoxetic acid enhanced MRI is useful to evaluate the expression of HNF4A in HCC.

CLINICAL RELEVANCE/APPLICATION

Gadoxetic acid enhanced MRI has a potential to reflect the expression of many genes and molecules regulated by HNF4A as imaging biomarkers (radiogenomics), which will be important for future personalized medicine.

SSA08-07 Presence of Hypovascular and Hypointense Nodules on Preoperative Gadoxetic Acid-enhanced MR Imaging: An Important Risk Factor for Recurrence after Liver Resection for Hypervascular Hepatocellular Carcinoma

Sunday, Nov. 29 11:45AM - 11:55AM Location: E450B

Participants

Katsuhiro Sano, MD, PhD, Chuo, Japan (*Presenter*) Nothing to Disclose Tomoaki Ichikawa, MD, PhD, Yamanashi, Japan (*Abstract Co-Author*) Nothing to Disclose Tatsuya Shimizu, MD, Yamanashi, Japan (*Abstract Co-Author*) Nothing to Disclose Utaroh Motosugi, MD, Yamanashi, Japan (*Abstract Co-Author*) Nothing to Disclose Hiroyuki Morisaka, MD, Kofu, Japan (*Abstract Co-Author*) Nothing to Disclose Shintaro Ichikawa, MD, Chuo-Shi, Japan (*Abstract Co-Author*) Nothing to Disclose Hiroshi Onishi, MD, Yamanashi, Japan (*Abstract Co-Author*) Nothing to Disclose Masanori Matsuda, MD, Yamanashi, Japan (*Abstract Co-Author*) Nothing to Disclose Hideki Fujii, MD, Tamaho, Japan (*Abstract Co-Author*) Nothing to Disclose

PURPOSE

The hepatocyte phase (HP) of gadoxetic acid-enhanced magnetic resonance imaging (EOB-MRI) can reveal numerous hypovascular and hypointense nodules with malignant potential, which may progress to conventional hypervascular hepatocellular carcinoma (HCC). We retrospectively evaluated the prognostic factors for patients with hypervascular HCC after liver resection, including the presence of hypovascular hypointense nodules on HP of EOB-MRI (hypo-nodule).

METHOD AND MATERIALS

In total, 114 consecutive patients who had undergone surgical resection and were pathologically diagnosed with moderately differentiated HCC were included. For the analysis of risk factors for recurrence and a poor survival rate after liver resection, univariate and multivariate Cox regression analyses were performed for the following factors: age, tumor size, tumor number, vascular invasion, TNM stage, albumin level, prothrombin ratio, Child-Pugh class, alpha-fetoprotein level, protein induced by vitamin K absence/antagonist-II (PIVKA-II), liver cirrhosis, past history of HCC, and presence of hypo-nodules on HP of preoperative EOB-MRI. We compared the 5-year recurrence-free and overall survival rates between patients with and without hypo-nodules on HP of EOB-MRI.

RESULTS

Univariate and multivariate analyses revealed the presence of hypo-nodules as the only significant risk factor for recurrence after liver resection (risk ratio, 2.1 and 2.1; p-value, 0.014 and 0.020) and albumin level as the only significant risk factor for a poor survival rate (risk ratio, 10.3 and 6.1; p-value, <0.001 and 0.019). The 5-year recurrence-free rate was significantly lower for patients with hypo-nodules (13.1%) than for those without (48.8%; p = 0.008); similar results were observed for the 5-year survival rate (66.1% vs. 83.4%), although the difference was not significant (p = 0.222).

CONCLUSION

The presence of hypo-nodules on HP of preoperative EOB-MRI is an important risk factor for recurrence after liver resection for hypervascular HCC.

CLINICAL RELEVANCE/APPLICATION

The presence of hypovascular and hypointense nodules on hepatocyte phase of preoperative gadoxetic acid-enhanced MR imaging is an important risk factor for recurrence after liver resection for hypervascular hepatocellular carcinoma.

SSA08-08 Hepatocellular Carcinoma without Gadoxetic Acid Uptake on Preoperative MR Imaging: An Important Prognostic Risk Factor after Liver Resection

Sunday, Nov. 29 11:55AM - 12:05PM Location: E450B

Participants

Tatsuya Shimizu, MD, Yamanashi, Japan (*Presenter*) Nothing to Disclose Katsuhiro Sano, MD, PhD, Chuo, Japan (*Abstract Co-Author*) Nothing to Disclose Tomoaki Ichikawa, MD, PhD, Yamanashi, Japan (*Abstract Co-Author*) Nothing to Disclose Utaroh Motosugi, MD, Yamanashi, Japan (*Abstract Co-Author*) Nothing to Disclose Hiroyuki Morisaka, MD, Kofu, Japan (*Abstract Co-Author*) Nothing to Disclose Shintaro Ichikawa, MD, Chuo-Shi, Japan (*Abstract Co-Author*) Nothing to Disclose

```
Hiroshi Onishi, MD, Yamanashi, Japan (Abstract Co-Author) Nothing to Disclose
Masanori Matsuda, MD, Yamanashi, Japan (Abstract Co-Author) Nothing to Disclose
Hideki Fujii, MD, Tamaho, Japan (Abstract Co-Author) Nothing to Disclose
```

PURPOSE

Hepatocellular carcinomas (HCCs) commonly demonstrate hypointensity compared with the surrounding liver parenchyma on the hepatocyte phase (HP) of gadoxetic acid-enhanced MR imaging (EOB-MRI). However, some hypervascular HCCs with gadoxetic acid (EOB) uptake demonstrate iso- or hyperintensity on HP. Such lesions are known to be biologically less aggressive. A previous study showed a lower recurrence rate for hyperintense HCC than for hypointense HCC. In this study, we retrospectively evaluated the overall survival rate for patients with hyperintense and hypointense HCC on EOB-MRI.

METHOD AND MATERIALS

In total, 114 consecutive patients with moderately differentiated HCC that was surgically resected from January 2008 to December 2013 were included in this study. According to their signal intensity on HP of EOB-MRI, the 114 patients were classified as EOB uptake (+) HCC (n = 23) and EOB uptake (-) HCC (n = 91). Risk factors for recurrence and a poor survival rate after liver resection were analyzed by univariate and multivariate Cox regression analyses of the following factors: age, tumor size, tumor number, vascular invasion, TNM stage, albumin level, prothrombin ratio, Child-Pugh class, alpha-fetoprotein level, protein induced by vitamin K absence/antagonist-II (PIVKA-II), liver cirrhosis, past history of HCC, and EOB uptake on HP of preoperative EOB-MRI. Then, we calculated the overall survival and recurrence-free rates for both groups using Kaplan-Meier survival curves. The log-rank and Wilcoxon tests were used to analyze significant differences.

RESULTS

The absence of EOB uptake was found to be a significant risk factor for a poor survival rate after liver resection (risk ratio, 5.4; p < 0.05). The EOB uptake (+) group showed a higher overall survival rate compared with the EOB uptake (-) group (5-year survival rate, 100% and 73.3%; p < 0.05). However, the recurrence-free rate was not significantly different (p = 0.70).

CONCLUSION

The absence of EOB uptake was a significant risk factor for a poor survival rate after liver resection. The overall survival rate was higher for patients with EOB uptake than for those without.

CLINICAL RELEVANCE/APPLICATION

In patients with moderately-differentiated hepatocellular carcinoma, the absence of gadoxetic acid uptake is a significant risk factor for a poor survival rate after liver resection. The overall survival rate is higher for patients with gadoxetic acid uptake than for those without.

SSA08-09 Dual Energy Spectral CT Imaging for the Evaluation of Small Hepatocellular Carcinoma Microvascular Invasion

Sunday, Nov. 29 12:05PM - 12:15PM Location: E450B

Participants

Yang Chuangbo, MMed, Xianyang City, China (*Presenter*) Nothing to Disclose Chenglong Ren, Shanxi, China (*Abstract Co-Author*) Nothing to Disclose Xirong Zhang, Xianyang, China (*Abstract Co-Author*) Nothing to Disclose Haifeng Duan, Xianyang City, China (*Abstract Co-Author*) Nothing to Disclose Lei Yuxin, MMed, Xianyang City, China (*Abstract Co-Author*) Nothing to Disclose Ma Chunling, MMed, Xianyang City, China (*Abstract Co-Author*) Nothing to Disclose Taiping He, Xianyang, China (*Abstract Co-Author*) Nothing to Disclose Tian Xin, MMed, Xianyang City, China (*Abstract Co-Author*) Nothing to Disclose

PURPOSE

To evaluate small hepatocellular carcinoma microvascular invasion using dual energy spectral CT imaging.

METHOD AND MATERIALS

This study was approved by our ethics committee. We retrospectively analyzed the images of 50 patients with 56 small hepatocellular carcinoma who underwent preoperative contrast enhanced dual-phase spectral CT scans before surgical resection. Tumors were divided into two groups based on the pathological findings for analysis: with (n=37) and without (n=19) microvascular invasion. Iodine concentration (IC) for tumors was measured in arterial phase (AP) and venous phase (VP) on the iodine-based material decomposition images to calculate IC reduction rate (ICrr) between AP and VP. IC values were further normalized to that of aorta to obtain normalized IC (NIC). Tumor CT attenuation number was measured on the monochromatic image sets to generate spectral HU curve and to calculate a slope (k) for the curve: (CT(40keV)-CT(90keV))/50. Values of the 2 pathological groups were compared and ROC study was performed to assess the differential diagnosis performance.

RESULTS

The IC, NIC, ICrr and slope (k) values in AP for tumors with microvascular invasion(Fig 2A-2C) were significantly higher than those without microvascular invasion(Fig 1A-1C) (2.40 ± 0.80 mg/ml vs. 1.68 ± 0.47 mg/ml for IC; 0.22 ± 0.06 vs. 0.16 ± 0.05 for NIC; 0.27 ± 0.16 vs. 0.01 ± 0.25 for ICrr; and 3.28 ± 1.08 vs. 2.27 ± 0.63 for slope, all p<0.05)(Table 1). Using the normalized iodine concentration value of 0.18 in AP as a threshold, one could obtain an area-under-curve of 0.82 for ROC study with sensitivity of 82.4% and specificity of 70.0% for differentiating small hepatocellular carcinoma with and without microvascular invasion. These values were significantly higher than the sensitivity of 64.7% and specificity of 69.2% with conventional CT numbers at 70keV(Table 2).

CONCLUSION

Using quantitative parameters obtained in spectral CT in the arterial phase provides new method with high accuracy to evaluate small hepatocellular carcinoma microvascular invasion.

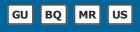
CLINICAL RELEVANCE/APPLICATION

Quantitative iodine concentration measurement in spectral CT may be used to provide a new method to evaluate small

hepatocellular carcinoma microvascular invasion.

Genitourinary (New Technologies for Imaging the Genitourinary Tract)

Sunday, Nov. 29 10:45AM - 12:15PM Location: E351



AMA PRA Category 1 Credits ™: 1.50 ARRT Category A+ Credits: 1.50

FDA Discussions may include off-label uses.

Participants

Julia R. Fielding, MD, Chapel Hill, NC (*Moderator*) Nothing to Disclose Erick M. Remer, MD, Cleveland, OH (*Moderator*) Nothing to Disclose

Sub-Events

SSA09-01 Simultaneous Conventional Dynamic MR Urography and High Temporal Resolution Perfusion MRI of Bladder Tumors Using a Novel Free-Breathing Golden-Angle Radial Compressed-Sensing Sequence

Sunday, Nov. 29 10:45AM - 10:55AM Location: E351

Participants

Nainesh Parikh, MD, New York, NY (*Presenter*) Nothing to Disclose Justin M. Ream, MD, Ann Arbor, MI (*Abstract Co-Author*) Nothing to Disclose Hoi Cheung Zhang, New York, NY (*Abstract Co-Author*) Nothing to Disclose Kai Tobias Block, PhD, New York, NY (*Abstract Co-Author*) Royalties, Siemens AG; Hersh Chandarana, MD, New York, NY (*Abstract Co-Author*) Equipment support, Siemens AG; Software support, Siemens AG; Consultant, Bayer, AG; Andrew B. Rosenkrantz, MD, New York, NY (*Abstract Co-Author*) Nothing to Disclose

PURPOSE

To investigate the feasibility of simultaneous conventional dynamic MR urography (MRU) and high temporal resolution perfusion MRI of bladder tumors using a novel free-breathing golden-angle radial acquisition scheme with compressed sensing reconstruction

METHOD AND MATERIALS

22 patients with bladder lesions underwent MRU using the GRASP (Golden-angle RAdial Sparse Parallel) technique. Following contrast injection, GRASP was performed of the abdomen and pelvis during free breathing (voxel size 1.4x1.4x3.0 mm, 1,000 radial spokes, acquisition time 3:44 min). Two dynamic data-sets were retrospectively reconstructed from this single acquisition by combining a distinct number of spokes into each dynamic frame: 110 spokes per frame to provide a resolution of approximately 30 seconds, serving as conventional MRU for clinical interpretation, and 8 spokes per frame to provide 2 second resolution images for quantitative perfusion. Using the 2 second resolution images, ROIs were placed within the bladder lesion and normal bladder wall for all patients, an arterial input function was generated from the femoral artery, and the GKM perfusion model was applied.

RESULTS

Follow-up cystoscopy and biopsy demonstrated 16 bladder tumors (13 stage \geq T2, 3 stage \leq T1) and 6 benign lesions. All lesions were well visualized using the conventional 25 second clinical dynamic images. Based on the 2 second resolution images, Ktrans was significantly higher in bladder tumors (0.38±0.24) than in either normal bladder wall (0.12±8, p<0.001) or in benign bladder lesions (0.15±0.04, p=0.033). The ratio between Ktrans of the lesion and of normal bladder wall in each patient was nearly double in tumors than in benign lesions (4.3±3.4 vs. 2.2±1.6), and Ktrans was nearly double in stage \geq T2 tumors than in stage \leq T1 tumors (0.44±0.24 vs. 0.24±0.24), although these did not approach significance (p=0.180-0.209), likely related to small sample size.

CONCLUSION

GRASP DCE-MRI provides simultaneous conventional dynamic MRU and high temporal resolution perfusion MRI of bladder tumors. Quantitative evaluation of bladder lesions based on the 2 second temporal resolution reconstructions showed associations with pathologic findings in our preliminary cohort.

CLINICAL RELEVANCE/APPLICATION

The novel GRASP sequence allows quantitative perfusion evaluation of bladder lesions within the context of a clinical MRU examination using a single contrast injection and without additional scan time.

SSA09-02 Magnetic Resonance Fingerprinting in Diagnosis of Prostate Cancer: Initial Experience

Sunday, Nov. 29 10:55AM - 11:05AM Location: E351

Participants

Shivani Pahwa, MD, Clevelnad, OH (*Presenter*) Nothing to Disclose Chaitra A. Badve, MD, MBBS, Cleveland, OH (*Abstract Co-Author*) Nothing to Disclose Yun Jiang, Cleveland, OH (*Abstract Co-Author*) Nothing to Disclose Alice Yu, BS, MS, Cleveland, OH (*Abstract Co-Author*) Nothing to Disclose Mark D. Schluchter, PhD, Cleveland, OH (*Abstract Co-Author*) Nothing to Disclose Mark A. Griswold, PhD, Cleveland, OH (*Abstract Co-Author*) Nothing to Disclose Electric Company Royalties, Bruker Corporation Contract, Siemens AG Lee E. Ponsky, MD, Cleveland, OH (*Abstract Co-Author*) Nothing to Disclose Vikas Gulani, MD, PhD, Ann Arbor, MI (*Abstract Co-Author*) Research support, Siemens AG

PURPOSE

 I o describe initial experience in detecting prostate cancer (PCa) using quantitative MRL parameters - 11 and 12 relaxation times derived from magnetic resonance fingerprinting (MRF-FISP), in combination with conventional ADC maps.

METHOD AND MATERIALS

63 patients with clinical suspicion of prostate cancer were imaged on 3T Siemens Skyra /Verio scanners. MRF has been shown to measure T1 and T2 relaxation times with high accuracy and precision2. In addition tothe standard multiparametric MRI exam, MRF-FISP was acquired (slice thickness: 6 mm, in-plane resolution:1×1 mm2,FOV:400 mm, TR:11-13 ms, flip angle:5-75 deg, duration:50s per slice).b-valuesfor DWI were0, 500, 1000 s/mm2.T1, T2 maps were generated from MRF-FISP dataand regions of interest (ROI)were drawn on T1, T2 and ADC maps in areas suspicious for cancer identified based on PIRADS score, and normal peripheral zone (NPZ). Matched pairs t-tests were used to compare T1, T2, ADC values in biopsy provenPCa and NPZ. Logistic regression model was applied to these parameters in differentiating PCa from NPZ. Receiver operating characteristic (ROC) analysis was performed for the parameters singly and in combination and area under the curve (AUC) was calculated

RESULTS

29 patients were diagnosed with cancer on transrectal biopsy. T1, T2, ADC values were significantly lower in cancer compared to NPZ (p<0.0001). Mean T1, T2, ADC for prostate cancer were 1413 ± 60 ms, 66 ± 3 ms, $745\pm54 \times 10-6$ mm2/s, respectively. For NPZ, these values were 2058 ± 77 ms, 165 ± 8 ms, $1736\pm37 \times 10-6$ mm2/s. The AUC for T1, T2, ADC values in separating PCa from NPZ was 0.978, 0.982, 0.801, respectively. The combination of T2 and ADC produced the most complete separation between cancer and normal tissues, resulting in AUC of 0.995.

CONCLUSION

MRF-FISP is a novel relaxometry sequence that allows quantitative examination of prostate in a clinical setting. The T1 and T2 relaxation times so obtained, in combination with ADC values show promising results in detecting prostate cancer.

CLINICAL RELEVANCE/APPLICATION

Quantitative MR parameters can help identify prostate cancer non-invasively. This could have broad applications in diagnosis, guiding biopsy, and following treatment

SSA09-03 Contrast-enhanced Ultrasound for Renal Mass Characterization: Comparison of Low MI Timeintensity Curves and Destruction Reperfusion Techniques

Sunday, Nov. 29 11:05AM - 11:15AM Location: E351

Participants

Wui K. Chong, MD, Chapel Hill, NC (*Presenter*) Nothing to Disclose
Emily Chang, MD, Chapel Hill, NC (*Abstract Co-Author*) Nothing to Disclose
Sandeep Kasoji, Chapel Hill, NC (*Abstract Co-Author*) Nothing to Disclose
Paul Dayton, PhD, Chapel Hill, NC (*Abstract Co-Author*) Co-founder, SonoVol LLC; Board Member, SonoVol LLC
Ersan Altun, MD, Istanbul, Turkey (*Abstract Co-Author*) Nothing to Disclose
Julia R. Fielding, MD, Chapel Hill, NC (*Abstract Co-Author*) Nothing to Disclose
Kevin O. Herman, MD, Raleigh, NC (*Abstract Co-Author*) Nothing to Disclose
W K. Rathmell, Chapel Hill, NC (*Abstract Co-Author*) Research support, GlaxoSmithKline plc
Lee Mullin, PhD, Chapel Hill, NC (*Abstract Co-Author*) Nothing to Disclose

PURPOSE

To evaluate contrast enhanced US (CEUS) for renal mass characterization in chronic renal insufficiency (CRI), comparing nondestructive (low MI) and destruction-reperfusion techniques.

METHOD AND MATERIALS

Prospective study comparing 48 subjects: 24 with normal function and renal masses scheduled for excision; 24 with CRI and indeterminate renal lesions on non-contrast US/CT.CEUS was performed on an Acuson Sequoia with CPS software. Perflutren (Definity) 1.3ml was administered IV. Lesions were imaged at a low MI of 0.2. A 3 minute videoclip was recorded. Time Intensity curves (TICs) of the lesion and adjacent parenchyma were generated. After 30 minutes, a 2nd dose of Definity was given and a Destruction Reperfusion (DR) sequence performed on the same lesion. DR was performed under an IND exemption from the FDA. Bubble destruction was performed at an MI of 0.9. Reperfusion images were obtained using Motion Stabilized Persistence software (Siemens). A color-coded parametric map quantifying arrival time was generated in which Green=faster arrival, Red=slower, Black=no contrast. (Arrow=Bosniak IV mass).Reference standard was pathology, contrast CT/MR or absence of change on follow up imaging for benign lesions. Two blinded readers reviewed the low MI images and classified the lesions using Bosniak criteria.

RESULTS

Lesion size ranged from 1.7-7.6cm (mean 3.5cm). Histopathology of resected masses showed no cavitation or cellular injury from high MI of DR. DR arrival times correlated with low MI TIC parameters. Sensitivity for distinguishing Bosniak I/II/IIF from III and higher was: Reader 1-96%, Reader 2-100%. Specificity was 78% and 63%. Specificity is lower because CEUS detects smaller amounts of contrast than CT/MR, leading to 'overstaging' with standard Bosniak. Reduced time to peak and arrival time (p<0.05) was seen in the parenchyma of CRI subjects compared to parenchyma of those with normal renal function.

CONCLUSION

CEUS can characterize renal lesions, but Bosniak criteria must be modified because US is more sensitive to slight enhancement. DR does not cause tissue injury, correlates with low MI findings, and takes less time. The parenchyma in CRI showed reduced/ delayed contrast uptake, suggesting CEUS may also be useful for renal functional imaging.

CLINICAL RELEVANCE/APPLICATION

CEUS can evaluate indeterminate renal lesions and renal function in CRI, a population where CT and MR contrast are contraindicated.

SSA09-04 ARFI Evaluation of Small (<4 cm) Renal Masses. A Preliminary Study

Participants Costanza Bruno, Verona, Italy (*Abstract Co-Author*) Nothing to Disclose Alessandra Bucci, MD, Verona, Italy (*Presenter*) Nothing to Disclose Matteo Brunelli, PhD, Verona, Italy (*Abstract Co-Author*) Nothing to Disclose Salvatore Minniti, MD, Verona, Italy (*Abstract Co-Author*) Nothing to Disclose Chiara Dalla Serra, Verona, Italy (*Abstract Co-Author*) Nothing to Disclose Roberto Pozzi Mucelli, Verona, Italy (*Abstract Co-Author*) Nothing to Disclose

PURPOSE

To evaluate if ARFI can be a reliable technique in distinguish ccRCCS from other solid and fluid-containing small renal masses.

METHOD AND MATERIALS

31 small (<4 cm) renal masses (27 were solid - 17/27 ccRCCs, 3/27 papillary RCCs, 2/27 chromophobe RCCs, 4 oncocytomas and 1 angiomyolipoma - and 4 were cysts) were prospectively evaluated using US and ARFI. Each lesion was assigned an ARFI value obtained from the average of 12 measurements. All the solid masses underwent resection; all the cystic lesions were Bosniak 2, so were evaluated with follow up. The difference existing between the two groups was evaluated by means of Student's t test. A cut off value was determined to distinguish between ccRCCs and other lesions and sensibility, specificity, PPV, NPV and accuracy were determined.

RESULTS

ccRCCs are characterized by an higher ARFI value and - when compared with all the other lesions - the difference existing between the two groups was statistically significant (p<0.001). Considering a cut off value of 1.95 m/sec sensibility, specificity, PPV, NPV and accuracy were respectively 94.1%, 78.6%, 84.2%, 91.7% and 87.1%.

CONCLUSION

ccRCC is characterized by an higher ARFI value which can be used to distinguish it from other solid and fluid containing masses.

CLINICAL RELEVANCE/APPLICATION

ARFI can be an useful tool in the evaluation of small renal masses, helping distinguish cc RCCs from other lesions.

SSA09-05 Fusion Imaging of (Contrast-enhanced) Ultrasound with CT or MRI for Kidney Lesions

Sunday, Nov. 29 11:25AM - 11:35AM Location: E351

Participants

Thomas Auer, Innsbruck, Austria (*Abstract Co-Author*) Nothing to Disclose Tobias De Zordo, MD, Innsbruck, Austria (*Presenter*) Nothing to Disclose Daniel Junker, Innsbruck, Austria (*Abstract Co-Author*) Nothing to Disclose Isabel M. Heidegger, Innsbruck, Austria (*Abstract Co-Author*) Nothing to Disclose Werner R. Jaschke, MD, PhD, Innsbruck, Austria (*Abstract Co-Author*) Nothing to Disclose Friedrich H. Aigner, MD, Innsbruck, Austria (*Abstract Co-Author*) Nothing to Disclose

PURPOSE

The aim of the study was to evaluate the feasibility of fusion imaging (FI) of (contrast-enhanced) ultrasound (CEUS) with CT/MRI in localization of sonographically challenging kidney lesions and usefulness for assessment of indeterminate kidney lesions

METHOD AND MATERIALS

From March 2013 to January 2014, 30 consecutive patients were included in this retrospective studyAll patients presented with previously in CT/MRI detected indeterminate kidney lesions that were either not detectable or hard to distinguish in conventional gray-scale ultrasoundIn these patients additional FI was performed by fusion of ultrasound with CT/MRI datasets. In 26 (86.7%) of these patients FI and CEUS was simultaneously conducted

RESULTS

FI could be performed in all of the 30 patientsFI-indication: In 18 of 30 patients (60%) FI was performed because a lesion of interest could not clearly be allocated due to multiple and directly adjacent similar lesions within one kidney. In 12 of 30 patients (40%) the kidney lesions were solitary or at least isolated but could not be detected with gray-scale US alone.CEUS-indication: Insufficient CT protocol (without NECT) and a not-water-isodens lesion (>20 HU) in 8 (30.8%) patients borderline CE in CT (10HU-20HU) in 11 (42.3%) patients non-conclusive CT/MRI studies in 5 (19.2%) patients CEUS for follow-up in 2 (7.7%) patients.Combined FI-CEUS: FI-CEUS could clearly differentiate between a surgical and non-surgical finding in 24 (80%) of 30 patients In 2 (6.7%) of 30 patients with conducted FI-CEUS lesions remained indeterminateFinal dignosis: Histology revealed a surgical lesion in 6 (20%) patients, while in 18 (60%) patients a non-surgical lesion such as BII/BIIF cysts, abscess formations, cicatricial tissue and a pseudotumor could be found. FI-CEUS didn't determine a final diagnosis in 2 patients (6.7%) In one elderly patient (3.3%) FI was conducted without CEUS because only size control of was demanded In 3 (10%) patients kidney lesions were not confidently detected with FI due to general US limitations

CONCLUSION

Our data suggest that FI of the kidney is a feasible examination regarding the localization and further assessment of indeterminate kidney lesions.

CLINICAL RELEVANCE/APPLICATION

The combination of FI with a synchronous CEUS examination can clarify indeterminate renal CT or MRI findings, reduce radiation exposure and is cost effective.

SSA09-06 Optimal Energy for Kidney Parenchymal Visualization in Monoenergetic Images Generated from Dual Energy CT

Participants

Jason DiPoce, MD, Jerusalem, Israel (Presenter) Nothing to Disclose

Zimam Romman, Haifa, Israel (Abstract Co-Author) Employee, Koninklijke Philips NV

Jacob Sosna, MD, Jerusalem, Israel (Abstract Co-Author) Consultant, ActiViews Ltd Research Grant, Koninklijke Philips NV

PURPOSE

To evaluate image quality of kidney parenchyma in a spectrum of CT monoenergy levels and to select the optimal Monoenergy levels for visualization.

METHOD AND MATERIALS

IRB approval was obtained. 30-corticomedullary phase, IV contrast-enhanced CT abdomen scans (18 males, 12 females, mean age of 50 years) were evaluated. In each scan, kidney parenchyma (60 regions) was assessed. The scans were obtained from a 64-slice spectral detector CT prototype (Philips Healthcare, Cleveland, OH, USA) at 120 kVp with an average of 150 mAs. For each scan, simultaneous conventional polyenergetic and monoenergetic image datasets at 50, 60, 70, 100, and 140 keV were reconstructed. Two experienced radiologists analyzed subjectively in consensus visualization of the kidney parenchyma and selected the optimal visualization dataset based on the conspicuity of the cortex and medulla and compared to the conventional images. Objective kidney signal-to-noise ratio (SNR) in the optimal monoenergy images was measured and compared to data from the conventional CT images.

RESULTS

Optimal image quality for kidney visualization was subjectively selected with 60 - 70 keV monoenergy images and was judged to be better than the conventional dataset. The kidney SNR values in optimal monoenergy were highly significantly different (p<0.01) from conventional CT images. Average SNR was 10.9 and 16.3 in the conventional and optimal monoenergy respectively.

CONCLUSION

Optimal visualization of the kidney parenchyma on dual energy CT images is achieved with monoenergy image reconstruction at 60 - 70 keV based on both subjective and objective assessments and seems to improve image quality compared to conventional images.

CLINICAL RELEVANCE/APPLICATION

Optimal image quality in monoenergy images may be supplemental to conventional polyenergetic images and potentially increase the diagnostic yield.

Honored Educators

Presenters or authors on this event have been recognized as RSNA Honored Educators for participating in multiple qualifying educational activities. Honored Educators are invested in furthering the profession of radiology by delivering high-quality educational content in their field of study. Learn how you can become an honored educator by visiting the website at: https://www.rsna.org/Honored-Educator-Award/

Jason DiPoce, MD - 2013 Honored Educator Jacob Sosna, MD - 2012 Honored Educator

SSA09-07 The Use of New Tissue Strain Analytics Measurement in Testicular Lesions

Sunday, Nov. 29 11:45AM - 11:55AM Location: E351

Participants

Dirk-Andre Clevert, MD, Munich, Germany (*Presenter*) Speaker, Siemens AG; Speaker, Koninklijke Philips NV; Speaker, Bracco Group; Matthias Trottmann, Munich, Germany (*Abstract Co-Author*) Nothing to Disclose Julian Marcon, Munich, Germany (*Abstract Co-Author*) Nothing to Disclose Melvin D'Anastasi, MD, New York, NY (*Abstract Co-Author*) Nothing to Disclose Alexander Karl, Munich, Germany (*Abstract Co-Author*) Nothing to Disclose Maximilian F. Reiser, MD, Munich, Germany (*Abstract Co-Author*) Nothing to Disclose

PURPOSE

Virtual touch tissue imaging quantification (VTIQ) is a newly developed technique for the sonographic quantification of tissue elasticity. It has been used in the assessment of breast lesions. The purpose of this study was to determine the diagnostic performance of VTIQ in unclear testicular lesions.

METHOD AND MATERIALS

Twenty patients with known testicular pathology underwent conventional B-mode sonography with additional VTIQ of the testicular lesions using a Siemens Acuson S2000[™] and S3000[™] (Siemens Medical Solutions, Mountain View, CA, USA) system. Tissue mechanical properties were interpreted and compared in the VTIQ examination. The pathologic diagnosis was established after surgery or in the follow up examination in highly suspicious of benign lesions.

RESULTS

Over 36 months, 22 focal testicular lesions (median lesion size, 18 mm; range, 4-36 mm in 20 patients (median age, 43 years; range, 22-81 years) were examined. Lesions were hyperechoic (n = 1), hypoechoic (n = 14), isoechoic (n = 1), mixed echogenicity (n = 3) or anechoic (n = 3). Histological examination showed one benign lesion (6.25 %) with a mean size of 7 mm and 15 malignant lesions (93.75 %) with a mean size of 20 mm. The value of the shear wave velocity in normal testis tissue showed a mean shear wave velocity of 1.17 m/s. No value of the shear wave velocity could the measured in cystic lesions. The rest of the benign lesions showed a mean shear wave velocity of 1.94 m/s and for seminoma it showed a mean shear wave velocity of 2.42 m/s.

CONCLUSION

VTIQ is a reliable new method for measuring qualitative and quantitative stiffness of testis lesions and tissue. The qualitative shear-

wave elastography features were highly reproducible and showed good diagnostic performance in unclear testicular lesions. The VTIQ technique is a useful in assessing small testicular nodules and pseudo lesions.

CLINICAL RELEVANCE/APPLICATION

VTIQ is a reliable user independent new method for measuring qualitative and quantitative stiffness of different testis lesions and tissue. The VTIQ technique allows to distinguished different testis lesions and pseudo lesions.

SSA09-08 One-stop-shot MRI for Infertility Evaluation: Comparison with US and CT-HSG

Sunday, Nov. 29 11:55AM - 12:05PM Location: E351

Participants

Javier Vallejos, MD, MBA, Vicente Lopez, Argentina (*Abstract Co-Author*) Nothing to Disclose Jimena B. Carpio, MD, Buenos Aires, Argentina (*Presenter*) Nothing to Disclose Ezequiel Salas, MD, Buenos Aires, Argentina (*Abstract Co-Author*) Nothing to Disclose Carlos Capunay, MD, Buenos Aires, Argentina (*Abstract Co-Author*) Nothing to Disclose Mariano Baronio, Buenos Aires, Argentina (*Abstract Co-Author*) Nothing to Disclose Patricia M. Carrascosa, MD, Buenos Aires, Argentina (*Abstract Co-Author*) Nothing to Disclose Lorena I. Sarati, Vicente Lopez, Argentina (*Abstract Co-Author*) Nothing to Disclose

PURPOSE

Demonstrate the utility of MRI-HSG in the diagnosis of infertility, can through this method show uterine, tubal, ovarian and pelvic causes.

METHOD AND MATERIALS

14 patients between 31 and 41 year-old diagnosed with infertility were studied. We performed a transvaginal ultrasound, virtual CT-HSG and MRI- HSG at the same day. MRI protocol include high-resolution T2 sequences, fat-suppressed T1, diffusion weighted imaging and contrast dynamic sequence (3D time-resolved imaging of contrast kinetics [TRICKS]). A contrast dilution of saline, iodine and gadolinium was instilled. Antral follicle counts, endometrial cavity findings, uterine wall pathology, tubal patency, and pelvic cavity findings were assessed with modalities.

RESULTS

In all cases it was observed more ovarian follicles on MRI-HSG than in US. In 65% of patients, Fallopian tubes were visualized completely with MRI-HSG, whereas in the remaining 35% only look at its distal portion. In all cases was demonstrated tubal patency with free peritoneal spillage. In 45% of patients, MRI-HSG showed endoluminal lesions, likes polyps and miomas, that were corroborated with CT-HSG. In 14% of patients, MRI-HSG detected endometrial implants in pelvic cavity that could not be corroborated by the other methods.

CONCLUSION

MRI-HSG allows a comprehensive evaluation for infertility diagnosis, with visualization and quantification of antral follicles, endometrial cavity, uterine wall and fallopian tubes as well as pelvic cavity findings such as endometrial implants.

CLINICAL RELEVANCE/APPLICATION

MRI techniques could be combined with HSG procedure in order to enables a one-step-shot imaging for evaluation of female infertility with the advantages of causing less pain and avoidance of exposure to ionizing radiation.

4D Ultrasound Cistoscopy with Fly through in the Evaluation of Urinary Bladder Tumors Preliminary Experience

Sunday, Nov. 29 12:05PM - 12:15PM Location: E351

Participants

Vito Cantisani, MD, Roma, Italy (*Abstract Co-Author*) Speaker, Toshiba Corporation; Speaker, Bracco Group; Speaker, Samsung Electronics Co, Ltd;

Nicola Di Leo, MD, Rome, Italy (*Abstract Co-Author*) Nothing to Disclose Valerio Forte, MD, Rome, Italy (*Presenter*) Nothing to Disclose Flavio Malpassini, Rome, Italy (*Abstract Co-Author*) Nothing to Disclose Mauro Ciccariello, Rome, Italy (*Abstract Co-Author*) Nothing to Disclose Francesco Flammia, Rome, Italy (*Abstract Co-Author*) Nothing to Disclose Francesco M. Drudi, MD, Rome, Italy (*Abstract Co-Author*) Nothing to Disclose Carlo Catalano, MD, Rome, Italy (*Abstract Co-Author*) Nothing to Disclose Federica Flammia, Roma, Italy (*Abstract Co-Author*) Nothing to Disclose Giuseppe Schillizzi, Roma, Italy (*Abstract Co-Author*) Nothing to Disclose Ferdinando D'Ambrosio, Rome, Italy (*Abstract Co-Author*) Nothing to Disclose

PURPOSE

To assess the feasibility and diagnostic efficacy 4D Ultrasound cystoscopy with Fly through as compared with trasditional cystoscopy in evaluating Urinary Bladder tumors.

METHOD AND MATERIALS

30 consecutive patients with previous detected urinary bladder lesions at cystoscopy were prospectively evaluated with 2D baseline US, and 4D Ultrasound with fly through (US virtual navigation system) by an expert radiologist blinded to cystoscopy results. The two imaging modalities were compared with cystoscopy and surgical results (N=8 patients) in order to assess the sensitivity and specificity in tumor detection and characterization. The diagnostic performance of 2D features and 4D ultrasound were estimated and compared using ROC curve analysis.

RESULTS

24/33 and 31/33 urinary bladder lesions were detected by 2 D US and 4 D Ultrasound respectively. The latter was also able to

identify two additional lesions not previously detected at traditional cystoscopy. The US features of the lesions were consistent with the one provided at cystoscopy with not significant differences in term of characterization.Conclusion: Our preliminary results shows that 4 D ultrasound cystoscopy with fly through is more accurate than baseline 2D ultrasound to detect and characterize urinary bladder lesions with results comparable with traditional cystoscopy.

CONCLUSION

Our preliminary results shows that 4 D ultrasound cystoscopy with fly through is more accurate than baseline 2D ultrasound to detect and characterize urinary bladder lesions with results comparable with traditional cystoscopy.

CLINICAL RELEVANCE/APPLICATION

New ultrasound software such as 4 D ultrasound cystoscopy with fly through may help us to follow-up patients treated conservatively for urinary bladder lesions.

Physics (Image Processing/Analysis I)

Sunday, Nov. 29 10:45AM - 12:15PM Location: S405AB



AMA PRA Category 1 Credits ™: 1.50 ARRT Category A+ Credit: 1.00

FDA Discussions may include off-label uses.

Participants

Kenneth R. Hoffmann, PhD, Buffalo, NY (*Moderator*) Vice President, Imagination Software Corporation; Stockholder, Imagination Software Corporation; Officer, Imagination Software Corporation; Rebet M. Nichikawa, PhD, Pitteburgh, PA (*Moderator*) Pavaltics, Hologic, Inc.

Robert M. Nishikawa, PhD, Pittsburgh, PA (Moderator) Royalties, Hologic, Inc;

Sub-Events

SSA21-01 Mapping the Brain by a New Multiparametric Quantitative MRI Method

Sunday, Nov. 29 10:45AM - 10:55AM Location: S405AB

Participants

Giuseppe Palma, PhD, Naples, Italy (*Presenter*) Nothing to Disclose Enrico Tedeschi, MD, Napoli, Italy (*Abstract Co-Author*) Nothing to Disclose Pasquale Borrelli, Naples, Italy (*Abstract Co-Author*) Nothing to Disclose Sirio Cocozza, MD, Napoli, Italy (*Abstract Co-Author*) Nothing to Disclose Carmela Russo, Naples, Italy (*Abstract Co-Author*) Nothing to Disclose Antonietta Canna, Naples, Italy (*Abstract Co-Author*) Nothing to Disclose Marco Comerci, Naples, Italy (*Abstract Co-Author*) Nothing to Disclose Bruno Alfano, PhD, Napoli, Italy (*Abstract Co-Author*) Nothing to Disclose Marcello Mancini, MD, Naples, Italy (*Abstract Co-Author*) Nothing to Disclose

Background

Multi-parametric quantitative MRI (qMRI) has long been an active field of research, with several approaches aiming to estimate a subset of R1, R2, R2*, proton density (PD) and magnetic susceptibility (QSM) maps of the tissues. We used a set of Steady-State sequences, acquired with variable flip angles (FAs) and different phase coherence, to derive, in a fully analytical way, quantitative volumetric R1, R2, R2*, PD and QSM maps.

Evaluation

Two dual-echo fully flow-compensated (FC) FLASH and one phase-cycled balanced Steady-State Free-Precession (bSSFP) sequences were acquired at different FAs with very low sensitivity to blood or Cerebrospinal Fluid (CSF) flow. The full brain of each volunteer was scanned in a total acquisition time of 14 minutes with a voxel size of 0.6 mm3. The datasets were processed to remove banding artifacts and used to invert voxelwise the relaxometry equations in the FOV.

Discussion

Unlike most existing approaches, the maps obtained by our method entirely rely on widely available 3D sequences, thus overcoming usual 2D resolution constraints, and are not affected by intra-voxel biases arising from imperfect 2D radio frequency-pulse profiles, which in turn cause different isochromat evolutions in response to different effective FAs. Moreover, unlike other 3D schemes based on unbalanced SSFP, our method does not suffer from high sensitivity to flow of relatively long T2 fluids (as CSF), thus being apt to image other body districts. Also, several issues of the DESPO methods are solved. In particular, the B1± inhomogeneity dependence can be either removed by providing a measured B1 field map, if an ad hoc protocol is available on the scanner, or largely compensated for by the proposed information theory approach. Furthermore, a judicious use of the Bloch equations for the acquired MR signals proved useful to skip the acquisition of the high-FA bSSFPs required by DESPOT2, thus limiting the acquisition time and avoiding at once SAR issues and CSF pulsation artifacts.

Conclusion

Our method allows for the quantitation of 5 independent parameters and gets rid of the sensitivity to B0 inhomogeneity by means of a fully analytical solution, thus also speeding up the computation step.

SSA21-02 Hybrid Exact Maximum Likelihood Estimation (HE-ML) Algorithm for Accurate qMRI Over the Full T2 Biological Spectrum with Only Two Echoes

Sunday, Nov. 29 10:55AM - 11:05AM Location: S405AB

Participants

Hernan Jara, PhD, Belmont, MA (*Presenter*) Patent holder, qMRI algorithms Research Grant, General Electric Company Royalties, World Scientific Publishing Co

Stephan W. Anderson, MD, Boston, MA (Abstract Co-Author) Nothing to Disclose

Osamu Sakai, MD, PhD, Boston, MA (Abstract Co-Author) Speaker, Bracco Group; Speaker, Eisai Co, Ltd; Consultant, Guerbet SA

Background

To develop a T2 qMRI mapping algorithm for the DE-TSE pulse sequence that is accurate over the full T2 biological range. To create a T2 mapping program that combines the exact dual echo T2 formula and the methods of maximum likelihood (ML) estimation for estimating long T2 values. The dual echo turbo spin echo (DE-TSE) pulse sequence is consistently being adopted for routine clinical use and for research protocols: it is fast, efficient, highly resilient to susceptibility artifacts, and diffusion insensitive. It also has qMRI applications for mapping T2 and the proton density (PD). The main limitation in terms of qMRI is that only two echoes are

available for T2 mapping, thus limiting the accuracy range of T2 estimation. The purpose of this work was to develop a T2 qMRI mapping algorithm for the DE-TSE pulse sequence that is accurate over the full T2 biological range, from soft tissues to pure cerebrospinal fluid (CSF). Specifically, to create a T2 mapping program that combines the exact dual echo T2 formula as well as the methods of maximum likelihood (ML) estimation for estimating long T2 values. ML estimators are optimal in the sense that the variance of the estimates reaches asymptotically the greatest lower bound of the variance.

Evaluation

HE-MLE algorithm was programed in Mathcad using the formulation of Bonny el al. (MRM 1996; 36(2):287-293.) and used to process the images of a phantom and the head images of a volunteer. The T2 values were compared to those obtained with a single slice multi spin echo (mSE) sequence. The phantom T2 obtained with both techniques are graphed in Fig. 1a: linear correlation analysis reveals strong linear relationship (R2=0.9988) with a slope of 0.975.

Discussion

DE-TSE is available from all major MRI manufacturers and efficiently produces excellent PD- and T2-weighted images with high anatomic coverage in less than four minutes.

Conclusion

The developed hybrid exact maximum likelihood T2 qMRI algorithm produces accurate measurements over the full T2 biological spectrum and could extend the usefulness of the DE-TSE pulse sequence in clinical and research applications.

Honored Educators

Presenters or authors on this event have been recognized as RSNA Honored Educators for participating in multiple qualifying educational activities. Honored Educators are invested in furthering the profession of radiology by delivering high-quality educational content in their field of study. Learn how you can become an honored educator by visiting the website at: https://www.rsna.org/Honored-Educator-Award/

Hernan Jara, PhD - 2014 Honored Educator Osamu Sakai, MD, PhD - 2013 Honored Educator Osamu Sakai, MD, PhD - 2014 Honored Educator Osamu Sakai, MD, PhD - 2015 Honored Educator

SSA21-03 Prognostic Value of Quantitative MRI Biomarkers for Treatment Response Assessment of Multiple Myeloma

Sunday, Nov. 29 11:05AM - 11:15AM Location: S405AB

Participants

Chuan Zhou, PhD, Ann Arbor, MI (*Presenter*) Nothing to Disclose Qian Dong, MD, Ann Arbor, MI (*Abstract Co-Author*) Nothing to Disclose Heang-Ping Chan, PhD, Ann Arbor, MI (*Abstract Co-Author*) Institutional research collaboration, General Electric Company Daniel R. Couriel, Ann Arbor, MI (*Abstract Co-Author*) Nothing to Disclose Attaphol Pawarode, Ann Arbor, MI (*Abstract Co-Author*) Nothing to Disclose Jun Wei, PhD, Ann Arbor, MI (*Abstract Co-Author*) Nothing to Disclose Lubomir M. Hadjiiski, PhD, Ann Arbor, MI (*Abstract Co-Author*) Nothing to Disclose

PURPOSE

We are investigating a radiomics approach to treatment response assessment of multiple myeloma (MM) using MRI. This study assessed the value of our developed MRI biomarkers as prognostic factors in patients with MM after autologous bone marrow transplant (BMT).

METHOD AND MATERIALS

With IRB approval, 63 pairs of spine MRI scans performed pre- and post-BMT (3-6 months) and clinical tests ($< \pm 7$ days of post-MRI) were collected retrospectively from 63 MM patients. A 3D dynamic intensity entropy transformation (DIET) method was developed to transform MR T1-weighted signal voxel by voxel to a quantitative entropy enhancement value (qEEV), from which two MR image biomarkers, the mean difference in qEEV between the pre- and post-BMT MR scans over the vertebras (m-qEEV) and the percentage of vertebras with an increased qEEV in the post-BMT scan (p-qEEV), were derived for each patient to estimate progression-free survival. The values of age, gender, and the clinical test outcomes including M-protein in serum and urine, ratio of free light chain (FLC), % plasma cell (PC), beta-2-microglobulin and immunoglobulin levels were also assessed. Univariate analysis was performed with the Kaplan-Meier method and log-rank test, and multivariate analysis was performed with the Cox proportional hazards regress model, with respect to the time to progression (TTP) censored at 3 years.

RESULTS

The univariate analysis showed that the patients with optimal cutoff points of m-qEEV < -0.1 and p-qEEV < 10% determined by the maximally selected rank statistics had significantly shorter TTP (P = 0.047 and P < 0.001, respectively). The age (<60), gender and all individual clinical tests in their normal ranges did not significantly predict longer TTP, except normal FLC (P = 0.040) and PC (P = 0.022). The multivariate analysis showed that the best predictive factor for TTP was p-qEEV (P < 0.018; hazard ratio (HR) 31.2). Other factors such as m-qEEV (P = 0.276; HR=5.6), FLC(P = 0.510; HR = 1.4) and PC (P < 0.217; HR = 1.2) did not provide significant predictive value for TTP.

CONCLUSION

The study demonstrated the feasibility of using the quantitative MRI biomarker (p-qEEV) as prognostic predictor for patients with MM after BMT.

CLINICAL RELEVANCE/APPLICATION

MR-based radiomic biomarker with prognostic significance may improve the accuracy for staging and assessing treatment response for MM, allowing clinicians to optimize therapy for individual patients.

SSA21-04 Validation of a Quantitative Masking Index for Digital Mammography

Sunday, Nov. 29 11:15AM - 11:25AM Location: S405AB

Participants

James G. Mainprize, PhD, Toronto, ON (*Presenter*) Institutional research agreement, General Electric Company Olivier Alonzo-Proulx, Toronto, ON (*Abstract Co-Author*) Institutional research agreement, General Electric Company Martin J. Yaffe, PhD, Toronto, ON (*Abstract Co-Author*) Research collaboration, General Electric Company Founder, Matakina International Ltd Shareholder, Matakina International Ltd Co-founder, Mammographic Physics Inc

PURPOSE

Mammography has reduced sensitivity for detecting cancer in dense breasts, for which superposition of shadows of normal structures can "mask" the presence of cancer either by a loss of contrast or by the distracting complexity of the surrounding parenchymal structures. We have developed a quantitative measure of masking by evaluating the signal-to-noise ratio (SNR) of a localized model observer.

METHOD AND MATERIALS

On a grid of sub-regions (ROIs), the parenchymal texture was quantified by extracting the inverse power-law exponent, β , from the noise power spectrum (NPS). The localized detection task SNR, d_L, for a simulated 5 mm diameter lesion was estimated using a non-prewhitening observer and measurements of the system MTF, and NPS from each ROI. The resulting map of d_L is analyzed to extract the masking potential of each mammogram. The d_L maps were validated with a 4 alternative forced choice (4AFC) of a simulated lesion (diameter 5 mm) inserted into ROIs randomly selected from a single mammogram, across 7 β categories (0.5 intervals from 1.5-5.0). A second reader study compared a radiologist's perception and accuracy to the d_L maps generated for a set of 78 screening cases.

RESULTS

The 4AFC study was performed on 20 mammograms and over 5000 ROIs. Preliminary results on one reader showed that mean d_L was highly correlated with inverse threshold lesion thickness (r=0.897, p<1e-10). In the second study, a radiologist estimated the probability of malignancy, BIRADS density and assessed the difficulty level of each case. Initial results showed a 36% difference (p<1e-6) in mean d_L between non-dense and dense mammograms and a 28% difference (p<1e-3) in mean d_L between "easy" and "hard" images.

CONCLUSION

A quantitative measure of masking by background parenchyma has been developed. Strong correlation is seen with both breast density and texture. Two preliminary reader studies confirm that local task SNR tracks with reader performance, in both simulated conditions and clinical evaluations of mammograms.

CLINICAL RELEVANCE/APPLICATION

A measure of masking by mammographic density can have a number of applications, e.g., to conform to recent changes to BIRADS density assessment, to categorize mammograms that require more careful assessment, or as a selection tool to identify those women who should be invited to be screened with alternative technologies.

SSA21-05 Virtual Monochromatic CT Numbers from a Dual-Energy MDCT Acquisition: Comparison between Single-Source Projection-Based and Dual-Source Image-Based Platforms in a Phantom Environment

Sunday, Nov. 29 11:25AM - 11:35AM Location: S405AB

Participants

Achille Mileto, MD, Durham, NC (*Presenter*) Nothing to Disclose Andrew R. Barina, MD, Durham, NC (*Abstract Co-Author*) Nothing to Disclose Daniele Marin, MD, Cary, NC (*Abstract Co-Author*) Nothing to Disclose Sandra Stinnett, MS, MPH, Durham, NC (*Abstract Co-Author*) Nothing to Disclose Kingshuk Choudhury, PhD, Durham, NC (*Abstract Co-Author*) Nothing to Disclose Rendon C. Nelson, MD, Durham, NC (*Abstract Co-Author*) Consultant, General Electric Company Consultant, Nemoto Kyorindo Co, Ltd Consultant, VoxelMetrix, LLC Research support, Bracco Group Research support, Becton, Dickinson and Company Speakers Bureau, Siemens AG Royalties, Wolters Kluwer nv

PURPOSE

To investigate in a phantom experiment whether there is any variability in virtual monochromatic CT numbers from a dual energy MDCT acquisition, across single- and dual-source hardware implementations.

METHOD AND MATERIALS

A polyethylene terephthalate torso phantom, filled with water, was employed to simulate the human abdominal environment. This contained a cylindrical polypropylene bottle, filled with 12 mg/mL of iopamidol 300, with serially suspended polyethylene terephthalate spheres (15 and 18 mm) filled with two iodine-to saline iodine dilutions (0.8 mgI/mL and 1.2 mgI/mL). Dual energy (80/140 kVp) and single energy (100 and 120 kVp) scans were performed using single-source (HD750 GSI, GE Healthcare) and dual-source (SOMATOM Definition Flash, Siemens Healthcare) MDCT systems. Virtual monochromatic images were reconstructed at energy levels ranging from 40 to 140 keV (at 10 keV increments), in either the projection- or the image-space domains.

RESULTS

There were significant differences between the single-source projection-based platform and the dual-source image-based platform in the measured attenuation values of the simulated lesions tested (P < 0.001, for all comparisons). The magnitude of these differences was greatest at lower monochromatic energy levels and at lower iodine concentrations. The dual energy hardware platform, the virtual monochromatic energy level, and the lesion iodine concentration had a highly statistically significant effect on the difference in the measured attenuation values between the two platforms, indicating that the platforms respond differently to changes in these variables (P < 0.001, for all comparisons).

CONCLUSION

A significant variability in CT numbers exists between single-source projection-based and dual-source image-based virtual monochromatic datasets, as a function of the selected energy level and the lesion iodine content.

CLINICAL RELEVANCE/APPLICATION

The variability in monochromatic CT numbers between the two clinically available dual energy platforms may impact clinical decisions that depend on subtle differences in measured attenuation values. For example, when minimally-vascularized abdominal neoplasms are repeatedly imaged with different dual energy platforms, differences in measured attenuation values between the imaging studies due to variability between scanners might be erroneously attributed to changes in tumor vascularity.

SSA21-06 Accuracy Enhancement with Deep Convolutional Neural Networks for Classifying Regional Texture Patterns of Diffuse Lung Disease in HRCT

Sunday, Nov. 29 11:35AM - 11:45AM Location: S405AB

Participants

Guk-Bae Kim, Seoul, Korea, Republic Of (*Abstract Co-Author*) Nothing to Disclose Yeha Lee, Seoul, Korea, Republic Of (*Abstract Co-Author*) CEO, VUNO Korea Inc Hyun-Jun Kim, Seoul, Korea, Republic Of (*Abstract Co-Author*) Founder, VUNO Korea Inc Kyu-Hwan Jung, Seoul, Korea, Republic Of (*Abstract Co-Author*) Employee, VUNO Korea Inc Namkug Kim, PhD, Seoul, Korea, Republic Of (*Presenter*) Stockholder, Coreline Soft, Inc Joon Beom Seo, MD, PhD, Seoul, Korea, Republic Of (*Abstract Co-Author*) Nothing to Disclose June-Goo Lee, PhD, Seoul, Korea, Republic Of (*Abstract Co-Author*) Nothing to Disclose

PURPOSE

To introduce deep learning-based feature extraction method which adaptively learns the most significant features for the given task using deep structure to classify six kinds of regional patterns in diffuse lung disease.

METHOD AND MATERIALS

HRCT images were selected from images of 106 patients having diffuse lung disease from a Siemens CT scanner (Sensation 16, Siemens, Forchheim, Germany) and 212 patients from a GE CT scanner (Lightspeed 16, GE, Milwaukee, WI, USA). Two experienced radiologists marked sets of 600 rectangular regions of interest (ROIs) with 20×20 pixels on HRCT images obtained from GE and Siemens scanners, respectively. These were consisted of a hundred of ROIs for each of six local patterns including normal, consolidation, emphysema, ground-glass opacity, honeycombing, and reticular opacity (Fig. 1(a)). Performance of convolution neural network (CNN) classifier having a deep architecture (Fig. 1(b)) was compared with that of support vector machine (SVM) having a shallow architecture. In the SVM classifier, 22 features including histogram, gradient, run-length, gray level co-occurrence matrix, low-attenuation area cluster, and top-hat transform were extracted. In the CNN classifier, a hundred features in the last layer (FC #1), however, were extracted automatically with deep learning classifier manner. All experiments were performed based on forward feature selection and five fold cross-validation with 20 repetitions.

RESULTS

The accuracies of the SVM classifier were achieved 92.34 ± 2.26 % at 600 ROI images acquired in a single scanner (GE) and 91.18 ± 1.91 % at 1200 ROI images of the integrated data set (GE and Siemens). The accuracies of the CNN classifier showed a higher performance of 93.72 ± 1.95 % and 94.47 ± 1.19 % in a single and the integrated HRCT, respectively (Fig. 1(c)).

CONCLUSION

The SVM accuracy in the integrated data showed not inferior to that in a single vender data, due to the effect of different scanners. In the CNN classifier, however, the CNN performance in the integrated data might be better, due to more robustness to image noise and higher performance in larger data set. In addition, the CNN shows higher performance than the SVM in both of data types.

CLINICAL RELEVANCE/APPLICATION

Deep learning based automated quantification system of regional disease patterns at HRCT of interstitial lung diseases can be more useful in the diagnosis, severity assessment, and monitoring of treatment effects.

SSA21-07 Predicting Radiologists' Diagnostic Performances Using Quantitative Image Features: Preliminary Analysis

Sunday, Nov. 29 11:45AM - 11:55AM Location: S405AB

Participants

Juhun Lee, PhD, Pittsburgh, PA (*Abstract Co-Author*) Nothing to Disclose Robert M. Nishikawa, PhD, Pittsburgh, PA (*Presenter*) Royalties, Hologic, Inc; Ingrid Reiser, PhD, Chicago, IL (*Abstract Co-Author*) Nothing to Disclose John M. Boone, PhD, Sacramento, CA (*Abstract Co-Author*) Research Grant, Siemens AG Research Grant, Hologic, Inc Consultant, Varian Medical Systems, Inc

PURPOSE

The endpoint for assessing image quality should be related to radiologists' diagnostic performances, instead of imaging statistics, such as contrast to noise ratio. The purpose of this preliminary study is to evaluate breast computed tomography (CT) image quality using quantitative image features that are correlated with radiologists' diagnostic performances.

METHOD AND MATERIALS

A total of 102 pathology proven breast lesions in 92 dedicated breast CT images were used. An iterative image reconstruction (IIR) algorithm was used to obtain CT images with different image qualities (28 different qualities). Through image feature analysis from breast lesions (developing classifiers on image features from the lesion), two reconstruction options (i.e., 2 out of 28 different qualities) and one clinical reconstruction with area under the ROC curve (AUC) values of 0.67, 0.75, and 0.86 were selected for a reader study. A subset of breast lesions (N = 50, half malignant) were selected for the reader study. One experienced MQSA

radiologist read 150 cases (50 lesions x 3 image qualities) and reported each lesion's probability of malignancy following BI-RADS. The radiologist's performance was evaluated by measuring the AUC. Under leave-one-out-cross-validation, a logistic regression classifier was trained and tested over the image features (via a feature selection technique) and the probability of malignancy from the radiologist. The classifier's AUC was measured and compared with that of the radiologist.

RESULTS

The radiologist's AUCs for each quality were 0.74, 0.79, and 0.81. The trained classifier achieved averaged AUCs of 0.72, 0.76, and 0.77. The linear correlation coefficients between the classifier's probability and the radiologist's probability on the test set were 0.51, 0.6, and 0.54 (all p-values < 0.001).

CONCLUSION

The classifier was able to learn the radiologist's estimation of lesion malignancy. More readers are required to generalize our results.

CLINICAL RELEVANCE/APPLICATION

Quantitative image features were used to correlate radiologists' diagnostic performances. These features may be useful for optimizing reconstruction algorithms and evaluating dose reduction techniques.

SSA21-08 Multivariate Modeling for Prediction of Cervical Cancer Treatment Outcomes

Sunday, Nov. 29 11:55AM - 12:05PM Location: S405AB

Participants

Baderaldeen A. Altazi, MS, Tampa, FL (*Presenter*) Nothing to Disclose Daniel Fernandez, MD, PhD, Tampa, FL (*Abstract Co-Author*) Nothing to Disclose Geoffery Zhang, PhD, Tampa, FL (*Abstract Co-Author*) Nothing to Disclose Eduardo G. Moros, PhD, MS, Tampa, FL (*Abstract Co-Author*) Nothing to Disclose

Background

Several studies reported univariate correlation analysis of radiomics as predictive factors for treatment clinical outcomes. This study investigated building a multivariate linear regression model that combines several predictive metrics in correlation with treatment outcomes.

Evaluation

Our dataset consisted of the pretreatment PET/CT scans from a cohort of 74 patients diagnosed with cervical cancer, FIGO stage IB-IVA, age range 31-76 years, treated with external beam radiation therapy to a dose range between 45-50.4 Gy (median dose: 45 Gy), concurrent cisplatin chemotherapy and MRI-based Brachytherapy to a dose of 20-30 Gy (median total dose: 28 Gy). Pearson's correlation (PC) and Area under (AUC) the receiver operator curve (ROC) were used to assess the correlation with treatment outcomes. Radiomics features were extracted; Co-occurrence (COM), Gray Level Size Zone (GLSM) and Run Length (RLM) and Intensity Based (IBM) Matrices algorithms. Afterwards, they were selected using sequential backward selection to predict for distant metastases (DM), Locoregional recurrence (LRR) and last follow-up status (LFS).

Discussion

The models consisted of linear combination of 2 to 3 radiomics features for each outcome. LRR model consisted of (Intensity contrast and Low Gray-Level Run Emphasis). LFS model consisted of (Different Entropy, Intensity contrast and Low-Intensity small-area emphasis). DM models consisted of (size zone variability and small-area emphasis) and (surface/Area and Volume). Models showed PC scores range (0.3-0.5) and AUC range (0.75-0.9) with 95% CI (0.6-1.0). All models scored low Variance Inflation Factor (VIF < 5) based on multicolinearity diagnostics test. All tests were statistically significant (p<0.05).

Conclusion

Multivariate linear regression models of radiomics features improved prediction power of treatment outcomes in comparison to univariate analysis. Morever, all models passed multicolinearity diagnostics test. LRR model scored highest improved predictive power followed by LFU then DM models respectively. This approach may contribute to incorporate PET radiomics in patient's response analysis in clinic.

SSA21-09 Increasing the Interscan Reproducibility of Coronary Calcium Scoring by Partial Volume Correction in Low-Dose non-ECG Synchronized CT: Phantom Study

Sunday, Nov. 29 12:05PM - 12:15PM Location: S405AB

Participants

Jurica Sprem, MSc, Urecht, Netherlands (*Presenter*) Nothing to Disclose Bob De Vos, MSc, Utrecht, Netherlands (*Abstract Co-Author*) Nothing to Disclose Rozemarijn Vliegenthart, MD, PhD, Groningen, Netherlands (*Abstract Co-Author*) Nothing to Disclose Max A. Viergever, Utrecht, Netherlands (*Abstract Co-Author*) Research Grant, Pie Medical Imaging BV; Pim A. De Jong, MD, PhD, Utrecht, Netherlands (*Abstract Co-Author*) Nothing to Disclose Ivana Isgum, PhD, Utrecht, Netherlands (*Abstract Co-Author*) Research Grant, Pie Medical Imaging BV; Research Grant, 3mensio Medical Imaging BV;

PURPOSE

Coronary calcium (CAC) scores obtained in low-dose chest CT without ECG-synchronization, as acquired in lung cancer screenings, are strong and independent predictors of cardiovascular events (CVE). However, due to acquisition, interscan CAC score reproducibility is moderate. This may result in incorrect CVE risk prediction. To increase the interscan reproducibility of CAC scores, we have developed a method to quantify CAC using partial volume correction (PVC).

METHOD AND MATERIALS

Three phantoms were scanned (Philips Brilliance 64, 120 kVp, 20 mAs, 3.0 mm slice thickness, 3.0 mm increment), each containing 3 inserts differing in size (9.1, 24.6 and 62.8 mm³) and calcium density (0.197, 0.401 and 0.796 mg/mm³). Total CAC volume per scan

was 96.5 mm³. Each phantom was scanned 3 times with slight rotation and translation between acquisitions, and in 3 different scenarios: 1 stationary and 2 moving with speed of 10 mm/s and 30 mm/s without ECG-synchronization, resulting in total of 27 scans. CAC was scored by clinically used thresholding at 130 HU. Thereafter, PVC employing Expectation-maximization algorithm for learning a multi-dimensional Gaussian mixture was used to determine partial content of calcium in the voxels of each identified calcification and its vicinity. The total CAC volumes per scan were computed by thresholding and using the proposed PVC method.

RESULTS

For the stationary phantom with low, medium and high density inserts, thresholding resulted in CAC volumes of 60.9, 142.9 and 213.2 mm³, while PVC determined 70.4, 88.9 and 92.9 mm³, respectively. For the phantom moving at 10 mm/s, thresholding resulted in CAC volumes of 50.3, 149.8 and 224.6 mm³, while PVC gave 58.2, 91.2 and 96.7 mm³, respectively. For the phantom moving at 30 mm/s, thresholding resulted in CAC volumes of 15.1, 147.2, and 306.3 mm³ and PVC determined 51.8, 78.8 and 106.5 mm³, respectively.

CONCLUSION

Thresholding underestimates volume of low density and overestimates volume of high density calcifications. The effect is emphasized with increasing motion artefacts. PVC provides better estimates of true calcium volume and it is less affected by motion.

CLINICAL RELEVANCE/APPLICATION

CAC quantification using PVC may increase interscan reproducibility of the CAC volume score.

Quantitative Imaging Mini-Course: Promise and Challenges

Sunday, Nov. 29 2:00PM - 3:30PM Location: S502AB

BQ

AMA PRA Category 1 Credits ™: 1.50 ARRT Category A+ Credits: 1.50

Participants

Michael F. McNitt-Gray, PhD, Los Angeles, CA (*Director*) Institutional research agreement, Siemens AG; Research support, Siemens AG; ; ; ; ;

Sub-Events

RC125A The Perspective of the RSNA Quantitative Imaging Biomarker Alliance (QIBA)

Participants

Edward F. Jackson, PhD, Madison, WI, (efjackson@wisc.edu) (Presenter) Nothing to Disclose

LEARNING OBJECTIVES

1) Describe the need for and benefits of implementing quantitative image analyses in clinical trials and clinical radiology practice. 2) Understand the activities that RSNA supports to help move the profession of radiology from a primarily qualitative interpretation paradigm to a more quantitative-based interpretation model. 3) Describe the challenges of extracting uniform, standardized quantitative measures from clinical imaging scans. 4) Provide examples of approaches to resolving some of these challenges.

ABSTRACT

The RSNA Strategic Plan strives to advance the radiological sciences and foster the development of new technologies in part by promoting the quantification of imaging results. The added value of quantification in both research and clinical environments is likely to increase as health care initiatives place increased pressure on radiologists to provide decision support for evidence-based care. There remain substantial barriers to the widespread use of quantitative measures in clinical radiology, including an inherently large number of variables that impede validation of specific metrics, diversity of proprietary industry platforms, and lack of acceptance by radiologists. A critical barrier to the implementation of quantitative imaging in radiology is the lack of standardization among vendor platforms. Collaboration in the pre-competitive space is challenging yet crucial to address standardization, and integrating quantitative measurement into workflow will be necessary for wide adoption. The Quantitative Imaging Biomarkers Alliance (QIBA) was officially launched in 2007 as a means to unite researchers, healthcare professionals, and industry stakeholders in the advancement of quantitative imaging. QIBA's mission is to improve the value and practicality of quantitative biomarkers by reducing variability across devices, patients, and time. The four QIBA modality-driven Coordinating Committees (CT, MR, Nuclear Medicine, US) currently oversee nine Biomarker Committees, and associated task forces, that develop QIBA Profiles (i.e., documents) of standardized technical performance specifications for image acquisition, data processing and analysis, and compliance.

RC125B NCI's Quantitative Imaging Network (QIN) Perspective

Participants

Robert J. Nordstrom, PhD, Rockville, MD (Presenter) Nothing to Disclose

LEARNING OBJECTIVES

1) Gain an overview of the NCI Quantitative Imaging Network (QIN). 2) Identify conditions for application submission and review. 3) Identify the needs and benefits for implementing quantitative imaging principles aimed at measurement or prediction of response to therapy in clinical trials. 4) Understand the need for network involvement in these activities.

ABSTRACT

The NCI Quantitative Imaging Network (QIN) is an international association of research teams with the mission to improve the role of quantitative imaging for clinical decision making in oncology by the development and validation of data acquisition, analysis methods, and tools to tailor treatment to individual patients and to predict or monitor the response to drug or radiation therapy. To that end, the teams are moving from the activities of developing and optimizing decision support tools to validating them in clinical environments. This lecture will chart the history of the QIN, show examples of the research results from several teams, and review results of the recent annual meeting.

RC125C Clinical Trial Perspective

Participants

Lawrence H. Schwartz, MD, New York, NY (*Presenter*) Committee member, Celgene Corporation; Committee member, Novartis AG; Committee member, ICON plc; Committee member, BioClinica, Inc

LEARNING OBJECTIVES

1) Gain an overview of the NCI's National Clinical Trials Network (NCTN). 2) Identify the need for Quantitative Imaging within the trial network and in specific trials. 3) Review examples of trial design incorporating Quantitative Imaging. 4) Review recent initiatives in Precision Medicine and the potential role for Quantitative Imaging.

ABSTRACT

Advances in the understanding of the cancer genome has supported the development of targeted therapeutics such as imatinib, erlotinib, crizotinib, and vemurafenib that have changed the approach to cancer treatment, allowing for individualized therapy. In order to study these targeted therapies in an individual manner, cancer clinical trials will need to screen large numbers of patients

in order to identify the subset with the molecular targets that are appropriate to study. In addition, improved efficiencies have been implemented to streamline important central functions related to tissue banks, regulatory approvals and imaging transfer and archiving. The role of imaging both within the NCTN and in precision medicine is undergoing change as well. This will be explored and discussed to understand how we can optimize the role of Quantitative Imaging.

Precision Medicine through Image Phenotyping

Sunday, Nov. 29 2:00PM - 3:30PM Location: S403A

CA CH VA BQ IN

AMA PRA Category 1 Credits ™: 1.50 ARRT Category A+ Credits: 1.50

Participants

Ella A. Kazerooni, MD, Ann Arbor, MI (Moderator) Nothing to Disclose

LEARNING OBJECTIVES

1) To learn what the term precision medicine means. 2) To understand how informatics intersects with clinical radiology to enable precision medicine in practice. 3) To learn through concrete examples how informatics based radiology precision medicine impacts health

ABSTRACT

Biomarkers have been emrabced by both the scientific and regulatory communities as surrogates end points for clinical trials, paving the way for their widespread use in medicine. The field of imaging biomarkers has exploded, and the their integration into clinical practice relies heaving on and intersects with the field of bioinformatics.. Once specific biomakers are show to have value, easily integrating them into the digital environment of the radiologist and communcating them to the health care providers and or directly to patients effeiciently and seamlessly is important for their value and impact on health to be realized. Culturally, it is taking radiologists from the era of description and largely qualitative reporting, into a quantitative future state, and leveraging informatics to extract information from imaging alone ot together with data available in the electronic medical record is essential for future sucess in this new world. To get there, understanding the impact of this approach as a value of our services, and standardization of imaging technques along the lines of what the RSNA QIBA initiative is designing, are essential, so that imaging biomarkers are robust, accurate and reprodicbile. Embraching this approach enables and facilitates new appracohes, relationships of imaging and IT researchers, vendors and consumers, to fully realize the possibilities. This course will discuss and describe the overall constructs, and use tangible exams of using this in practice today and for the future.

Sub-Events

RC154A Lung Nodules: Combining Population and Patient Specific Data to Inform Personalized Decision Making

Participants

Eliot L. Siegel, MD, Severna Park, MD (*Presenter*) Research Grant, General Electric Company; Speakers Bureau, Siemens AG; Board of Directors, Carestream Health, Inc; Research Grant, XYBIX Systems, Inc; Research Grant, Steelcase, Inc; Research Grant, Anthro Corp; Research Grant, RedRick Technologies Inc; Research Grant, Evolved Technologies Corporation; Research Grant, Barco nv; Research Grant, Intel Corporation; Research Grant, Dell Inc; Research Grant, Herman Miller, Inc; Research Grant, Virtual Radiology; Research Grant, Anatomical Travelogue, Inc; Medical Advisory Board, Fovia, Inc; Medical Advisory Board, Toshiba Corporation; Medical Advisory Board, McKesson Corporation; Medical Advisory Board, Carestream Health, Inc; Medical Advisory Board, Bayer AG; Research, TeraRecon, Inc; Medical Advisory Board, Bracco Group; Researcher, Bracco Group; Medical Advisory Board, Merge Healthcare Incorporated; Medical Advisory Board, Microsoft Corporation; Researcher, Microsoft Corporation

LEARNING OBJECTIVES

1) Describe how data from a clinical trial can be repurposed as a decision support tool. 2) List some of the potential techniques that can be utilized to predict likelihood of a malignant nodule from the NLST database. 3) Explain how the Fleischner Guidelines can be personalized utilizing data from NLST and PLCO. 4) Detail the implications for lung screening trials of having access to NLST and PLCO data. 5) Demonstrate how a healthcare enterprise can create their own local reference database using information from their own patient population.

ABSTRACT

The era of personalized/precision medicine offers the potential to utilize patient and lesion specific data to personalize screening and diagnostic work-up, diagnosis, and treatment selection to a particular patient to optimize effectiveness. Although recently, the emphasis has been on utilization of genomic data in personalized medicine, there is a 'gold mine' of useful data in previously conducted clinical trials as well as patient medical electronic records that has, until now, gone largely untapped. The purpose of this presentation is to describe how the screening, diagnosis, and treatment of lung nodules can be personalized utilizing data from the NLST and PLCO clinical trials and how the Fleischner Guidelines and screening criteria for lung cancer can be modified according to the characteristics of an individual patient and individual nodule. The presentation will also include ways in which a facility can collect local data on their own patients to supplement these reference databases with experience from their own patient population.

RC154B Managing Cardiovascular Care through Image Phenotyping Combined with Patient Level Data

Participants John J. Carr, MD, MS, Nashville, TN (*Presenter*) Nothing to Disclose

LEARNING OBJECTIVES

View learning objectives under main course title.

ABSTRACT

Cardiovascular diseases(CVD) develop over an individual's lifetime. CVD is the number one cause of death and morbidity worldwide. Integrated application of genomics, quantitative imaging and "big data" has the potential to positively transform cardiovascular

prevention and care and reduce the health and economic consequence of CVD. In this talk we will review how easily obtainable imaging biomarkers, already available, can power this change. Measures of cardiac and vascular structure and function as well as body composition provide great insight into and individual's risk of CVD, level of physical activity, diet, vascular health and general well-being.

Molecular Imaging Symposium: Basics of Molecular Imaging

Monday, Nov. 30 8:30AM - 10:00AM Location: S405AB



AMA PRA Category 1 Credits ™: 1.50 ARRT Category A+ Credits: 1.50

FDA Discussions may include off-label uses.

Participants

Jan Grimm, MD, PhD, New York, NY (*Moderator*) Nothing to Disclose Zaver M. Bhujwalla, PhD, Baltimore, MD (*Moderator*) Nothing to Disclose

Sub-Events

MSMI21A MI Using Radioactive Tracers

Participants

Jan Grimm, MD, PhD, New York, NY (Presenter) Nothing to Disclose

LEARNING OBJECTIVES

1) In this course, we will discuss the various radio tracers and their applications in Molecular Imaging studies. Participants will understand in which situations to use which radio tracers, what to consider when developing the imaging construct and what controls to obtain for nuclear imaging studies. Examples will contain imaging with small molecules, with antibodies and nanoparticles as well as with cells in order to provide the participants with examples how o correctly perform their imaging studies. Most of the examples will be from the oncology field but their underlying principles are universally applicable to other areas as well.

ABSTRACT

Nuclear Imaging is currently the only true "molecular" imaging method utilized in clinic. It offers quantitative imaging of biological processes in vivo. Therefore, it is not surprising that it is also highly frequented in preclinical imaging applications since it is currently the only true quantitative imaging method. Multiple agents have been developed, predominantly for PET imaging but also for SPECT imaging. In this talk, we will discuss the application of radio tracers to molecular imaging and what to consider. Common pitfalls and mistakes as well as required measures to avoid these will be discussed. We will discuss various examples of imaging constructs, ranging from small molecules to antibodies, nanoparticles and even cells. In addition, the imaging modalities will also briefly discussed, including PET, SPECT and Cherenkov imaging.

MSMI21B Molecular MRI and MRS

Participants

Zaver M. Bhujwalla, PhD, Baltimore, MD, (zbhujwa1@jhmi.edu) (Presenter) Nothing to Disclose

LEARNING OBJECTIVES

To define the role of MRI and MRS in molecular and functional imaging and cover specific applications in disease processes. The primary focus will be advances in novel theranostic approaches for precision medicine.

ABSTRACT

With an array of functional imaging capabilities, magnetic resonance imaging (MRI) and spectroscopy (MRS) techniques are valuable in obtaining functional information, but the sensitivity of detection is limited to the 0.1-1 mM range for contrast agents and metabolites, respectively. Nevertheless, MRI and MRS are finding important applications in providing wide-ranging capabilities to tackle key questions in cancer and other diseases with a 'molecular-functional' approach. An overview of these capabilities and examples of MR molecular and functional imaging applications will be presented with a focus on theranostic imaging for precision medicine.

MSMI21C Nanoparticles

Participants Heike E. Daldrup-Link, MD, Palo Alto, CA (*Presenter*) Nothing to Disclose

LEARNING OBJECTIVES

1) To understand important safety aspects of USPIO. 2) To recognize the value of immediately clinically applicable iron oxide nanoparticles for tumor MR imaging applications. 3) To learn about clinically relevant new developments of theranostic USPIO.

ABSTRACT

Nanoparticles Nanoscale materials can be employed to develop novel platforms for understanding, diagnosing, and treating diseases. Integrating nanomedicine with novel multi-modality imaging technologies spurs the development of new personalized diagnostic tests and theranostic (combined diagnostic and therapeutic) procedures. This presentation will provide an overview over the safety, diagnostic applications and theranostic developments of clinically applicable ultrasmall superparamagnetic iron oxide nanoparticles (USPIO). USPIO which are currently used for clinical applications include ferumoxytol (Feraheme), an FDA-approved iron supplement, and ferumoxtran-10 (Combidex/Sinerem), which is currently undergoing renewed clinical trials in Europe. Safety considerations for these agents will be discussed. Both compounds provide long lasting blood pool enhancement, which can be used for MR angiographies and tissue perfusion studies. Subsequently, USPIO are slowly phagocytosed by macrophages in the reticuloendothelial system (RES), which can be used to improve MRI detection of tumors in liver, spleen, lymph nodes and bone marrow. A slow phagocytosis by macrophages in inflammations and high grade tumors can be used to grade the severity of the disease process and monitor new immune-modulating therapies. Novel developments include synthesis of multi-functional nanoparticles, which can be detected with two or more imaging modalities, as well as clinically applicable approaches for in vivo tracking of stem cell therapies. Since USPIO are not associated with any risk of nephrogenic sclerosis, they can be used as alternative contrast agents to gadolinium chelates in patients with renal insufficiency or in patients in whom creatinine lab values are not available. Ongoing pre-clinical developments include the development of improved, targeted and activatable nanoparticle formulations, which can further improve sensitivity, specificity and theranostic imaging capabilities.

MSMI21D Contrast Ultrasound

Participants

Steven B. Feinstein, MD, Chicago, IL (*Presenter*) Research support, General Electric Company; Consultant, General Electric Company; Investor, SonoGene LLC;

LEARNING OBJECTIVES

1) Inform: Clinical utility and safety of contrast enhanced ultrasound (CEUS) imaging. 2) Educate: Current diagnostic and therapeutic approaches. 3) Introduce: Newer concepts for combined diagnostic and therapeutic applications.

MSMI21E Quantitative Imaging Biomarkers

Participants

Richard L. Wahl, MD, Saint Louis, MO (Presenter) Research Consultant, Nihon Medi-Physics Co, Ltd;

LEARNING OBJECTIVES

1) Identify at least one method of assessing anatomic tumor response quantitatively. 2) Identify at least one method of assessing metabolic tumor response using FDG PET quantitative. 3) Identify an MRI quantitative metric which is associated with cellularity of biological processes.

ABSTRACT

Radiology initially developed as an analog imaging method in which non quantitative data were interpreted in a 'qualitative and subjective' manner. This approach has worked well, but modern imaging also is digital, quantitative and has the opportunity for more quantitative and objective interpretations. This lecture will focus on a few areas in which quantitative imaging is augmenting qualitative image assessments to lead to more precise interpretation of images. Examples of such an approach can include measuremental of tumor 'metabolic' activity using formalisms such as PERCIST 1.0; methods of assessment of tumor size and volumes using the RECIST 1.1 and emerging formalisms and metrics of tumor heterogeneity, density, receptor density, diffusion, vascular permeability and elasticity using techniques incuding PET/SPECT, MRI, CT and ultrasound. With quantitative imaging, the opportunity to move from qualitative methods to precise in vivo quantitative pheontyping is a real one, with a quantitative 'phenome' complementing other 'omics' such as genomics. However, the quality of quantitation may vary and close attention to technical methodologies and process are required to have reliable and accurate quantitation. The RSNA QIBA effort will be briefly reviewed as one approach to achieve precise quantitative phenotyping. Examples of the use of quantitative phenotyping to inform patient management will be discussed.

Honored Educators

Presenters or authors on this event have been recognized as RSNA Honored Educators for participating in multiple qualifying educational activities. Honored Educators are invested in furthering the profession of radiology by delivering high-quality educational content in their field of study. Learn how you can become an honored educator by visiting the website at: https://www.rsna.org/Honored-Educator-Award/

Richard L. Wahl, MD - 2013 Honored Educator

BOOST: Gynecology-Oncology Anatomy - Radiologic Evaluation of Pelvic Malignancies in the Era of Imaging Biomarkers (An Interactive Session)

Monday, Nov. 30 8:30AM - 10:00AM Location: S103AB



AMA PRA Category 1 Credits ™: 1.50 ARRT Category A+ Credits: 1.50

FDA Discussions may include off-label uses.

Participants

Saurabh Gupta, MD, Milwaukee, WI (*Presenter*) Nothing to Disclose Robert S. Hellman, MD, Milwaukee, WI (*Presenter*) Nothing to Disclose Paul M. Knechtges, MD, Milwaukee, WI (*Presenter*) Nothing to Disclose Mark D. Hohenwalter, MD, Milwaukee, WI (*Presenter*) Nothing to Disclose Beth A. Erickson, MD, Milwaukee, WI (*Presenter*) Nothing to Disclose

LEARNING OBJECTIVES

1) Review uterine/cervical anatomy and current anatomic imaging methods for the evaluation of pelvic malignancy. 2) Review the current role of PET in the imaging of pelvic malignancy. 3) Discuss the growing role of imaging biomarkers (e.g. diffusion weighted imaging and perfusion imaging) in determining prognosis and treatment response for pelvic malignancies.

Nuclear Medicine Series: Assessment of Cancer Treatment Response: Updates

Monday, Nov. 30 8:30AM - 12:00PM Location: S505AB

BQ NM OI

AMA PRA Category 1 Credits ™: 3.25 ARRT Category A+ Credits: 3.75

Participants

Terence Z. Wong, MD, PhD, Chapel Hill, NC (*Moderator*) Nothing to Disclose Haesun Choi, MD, Houston, TX (*Moderator*) Nothing to Disclose

Sub-Events

RC211-01 Imaging Response - Earning Biomarker Status

Monday, Nov. 30 8:30AM - 9:15AM Location: S505AB

Participants

Terence Z. Wong, MD, PhD, Chapel Hill, NC (Presenter) Nothing to Disclose

LEARNING OBJECTIVES

1) Compare and contrast prognostic, predictive, and pharmacodynamic biomarkers. 2) Understand the difference between integrated and integral biomarkers in clinical trials. 3) Discuss advantages and limitations of imaging biomarkers.

ABSTRACT

Serum, pathological, and imaging biomarkers are becoming increasingly important to define potential biological targets, select which patients may benefit from a particular targeted agent, and to follow patients during and following therapy. Traditionally, imaging has not been formally recognized as a biomarker, and standardization of quantitative imaging techniques remains a major challenge. However, functional and quantitative imaging techniques are now being used routinely to evaluate early response to therapy. Unlike conventional cytotoxic chemotherapy, targeted therapy can be cytostatic and selects only susceptible populations of cells. Imaging response criteria is therefore often different from standard anatomic (RECIST, WHO) criteria, and the response may be heterogeneous. In the future, both serum and imaging biomarkers will have an increasingly important role in managing patients undergoing conventional and targeted therapy.

RC211-02 Can Interim [18F]-FDG-PET or Diffusion-weighted MRI Predict End-of-Treatment Outcome in MALT Lymphoma after Immunotherapy? A Prospective Study in 15 Patients

Monday, Nov. 30 9:15AM - 9:25AM Location: S505AB

Participants

Marius E. Mayerhoefer, MD, PhD, Vienna, Austria (*Presenter*) Nothing to Disclose Georgios Karanikas, MD, Vienna, Austria (*Abstract Co-Author*) Nothing to Disclose Kurt Kletter, MD, Vienna, Austria (*Abstract Co-Author*) Nothing to Disclose Matthias Pones, MD, Vienna, Austria (*Abstract Co-Author*) Nothing to Disclose Michael Weber, Vienna, Austria (*Abstract Co-Author*) Nothing to Disclose Markus Raderer, MD, Vienna, Austria (*Abstract Co-Author*) Nothing to Disclose

PURPOSE

To determine whether, in in patients with MALT lymphoma, quantitative changes of glycolytic activity on interim [18F]-FDG-PET, or quantitative changes of cell density on interim diffusion-weighted MRI (DWI), relative to pre-therapeutic scans, can predict the end-of-treatment (EOT) outcome after immunotherapy.

METHOD AND MATERIALS

Our prospective IRB-approved study included patients with untreated, histologically proven, FDG-avid MALT lymphoma that underwent whole-body [18F]-FDG-PET/CT and DWI at three time-points: before treatment (baseline); after three cycles (interim); and after six cycles of rituximab-based immunotherapy (EOT). The up to three largest nodal or extranodal lymphoma lesions that were visible on both [18F]-FDG-PET and DWI were defined as target lesions at baseline. Maximum and mean SUVs (SUVmax, SUVmean), and minimum and mean apparent diffusion coefficients (ADCmin, ADCmean) were measured, and their rates of change between baseline and interim examinations (Δ SUVmax, Δ SUVmean, Δ ADCmin, and Δ ADCmean) were compared, using ANOVAs, between the four EOT outcomes: complete remission (CR), partial remission (PR), stable disease (SD), or progressive disease (PD). The relationship between Δ SUVs and Δ ADCs was also assessed by Pearson correlation coefficients (r).

RESULTS

Fifteen patients with 25 lesions were included. Lesion-based post-hoc tests showed significant differences between CR and PR for Δ SUVmax (P<0.001), Δ SUVmean (P<0.001), and Δ ADCmin (P=0.044); and between CR and SD for Δ SUVmax (P<0.001), Δ SUVmean (P<0.001), Δ ADCmin (P=0.021), and Δ ADCmean (P=0.022); but not between CR and PR for Δ ADCmean (P=0.012); and also not between PR and SD for Δ SUVmax (P=0.98), Δ SUVmean (P=0.96), Δ ADCmin (P=0.85), or Δ ADCmean (P=0.99). No lesion showed PD at EOT. A substantial and significant, negative correlation between Δ SUVmax and Δ ADCmin (r=-0.71, P<0.001), and Δ SUVmean and Δ ADCmean (r=-0.70, P<0.001), was observed.

CONCLUSION

Both quantitative interim [18F]-FDG-PET measures and interim DWI measures may be able to predict lesion-based complete response to immunotherapy at end-of-treatment in MALT lymphoma.

CLINICAL RELEVANCE/APPLICATION

[18F]-FDG-PET and DWI may be useful for early treatment outcome prediction in patients with MALT lymphoma undergoing rituximab-based immunotherapy.

RC211-03 Whole-Body FDG-PET/MRI vs. Whole-Body MRI with DWI vs. Integrated FDG-PET/CT with Brain CE-MRI: Capability for Recurrence Assessment in Patients with Postoperative Non-Small Cell Lung Cancer

Monday, Nov. 30 9:25AM - 9:35AM Location: S505AB

Participants

Yoshiharu Ohno, MD, PhD, Kobe, Japan (*Presenter*) Research Grant, Toshiba Corporation; Research Grant, Koninklijke Philips NV; Research Grant, Bayer AG; Research Grant, DAIICHI SANKYO Group; Research Grant, Eisai Co, Ltd; Research Grant, Terumo Corporation; Research Grant, Fuji Yakuhin Co, Ltd; Research Grant, FUJIFILM Holdings Corporation; Research Grant, Guerbet SA; Shinichiro Seki, Kobe, Japan (*Abstract Co-Author*) Nothing to Disclose Hisanobu Koyama, MD, PhD, Kobe, Japan (*Abstract Co-Author*) Nothing to Disclose Kota Aoyagi, Otawara, Japan (*Abstract Co-Author*) Employee, Toshiba Corporation Hitoshi Yamagata, PhD, Otawara, Japan (*Abstract Co-Author*) Employee, Toshiba Corporation Takeshi Yoshikawa, MD, Kobe, Japan (*Abstract Co-Author*) Research Grant, Toshiba Corporation Sumiaki Matsumoto, MD, PhD, Kobe, Japan (*Abstract Co-Author*) Research Grant, Toshiba Corporation Sumiaki Matsumoto, MD, PhD, Kobe, Japan (*Abstract Co-Author*) Research Grant, Toshiba Corporation Sumiaki Matsumoto, MD, PhD, Kobe, Japan (*Abstract Co-Author*) Research Grant, Toshiba Corporation Sumiaki Matsumoto, MD, PhD, Kobe, Japan (*Abstract Co-Author*) Research Grant, Toshiba Corporation Sumiaki Matsumoto, MD, PhD, Kobe, Japan (*Abstract Co-Author*) Employee, Toshiba Corporation Yoshimori Kassai, MS, Otawara, Japan (*Abstract Co-Author*) Employee, Toshiba Corporation Katsusuke Kyotani, RT, Kobe, Japan (*Abstract Co-Author*) Nothing to Disclose Kazuro Sugimura, MD, PhD, Kobe, Japan (*Abstract Co-Author*) Nothing to Disclose Kazuro Sugimura, MD, PhD, Kobe, Japan (*Abstract Co-Author*) Research Grant, Toshiba Corporation Research Grant, Koninklijke Philips NV Research Grant, Bayer AG Research Grant, Eisai Co, Ltd Research Grant, DAIICHI SANKYO Group

PURPOSE

To compare the diagnostic performance for postoperative lung cancer recurrence assessment among whole-body FDG-PET/MRI, MRI with diffusion weighted imaging (DWI) and integrated FDG-PET/CT with brain contrast-enhanced (CE-) MRI in non-small lung cancer (NSCLC) patients.

METHOD AND MATERIALS

96 consecutive postoperative NSCLC patients (52 men, 44 women; mean age 72 years) prospectively underwent whole-body MRI with and without DWI at 3T MRI system, integrated PET/CTs and conventional radiological examinations as well as follow-up examinations. When recurrence was suspected in each NSCLC patients, pathological examination was performed. Then, all patients were divided into recurrence (n=17) and non-recurrence (n=79) groups based on pathological and follow-up examinations. All corregistered PET/MRIs were generated by means of our proprietary software. Then, probability postoperative recurrence in each patient was visually assessed on all methods by means of 5-point visual scoring system. To compare diagnostic performance among all methods, receiver operating characteristic analyses were performed. Finally, diagnostic accuracy of each factor and clinical stage was statistically compared each other by using McNemar's test.

RESULTS

Area under the curves (Azs) of whole-body PET/MRI (Az=0.99) and MRI with DWI (Az=0.99) were significantly larger than that of PET/CT (Az=0.92, p<0.05) and conventional examination (Az=0.91, p<0.05). When applied feasible threshold values, specificities (SPs) and accuracies (ACs) of PET/MRI (SP: 96.2 [76/79] %, and AC: 96.8 [93/96] %) and MRI with DWI (SP: 100 [79/79] %, and AC: 96.8 [93/96] %) were significantly higher than those of PET/CT with CE-brain MRI (SP: 81.0 [64/79] %, p<0.05; AC: 84.4 [81/96] %, p<0.05) and conventional radiological examination (SP: 79.7 [63/79] %, p<0.05; AC: 83.3 [80/96] %), p<0.05).

CONCLUSION

Whole-body PET/MRI and MRI with DWI have better potential for recurrence evaluation than PET/CT with CE-brain MRI and conventional radiological examination in postoperative NSCLC patients.

CLINICAL RELEVANCE/APPLICATION

Whole-body PET/MRI and MRI with DWI have better potential for recurrence evaluation than PET/CT with CE-brain MRI and conventional radiological examination in postoperative NSCLC patients.

RC211-04 Lung Cancer: PET/CT Interpretation (Hopkins Criteria) for Therapy Assessment and Survival Outcome Prediction

Monday, Nov. 30 9:35AM - 9:45AM Location: S505AB

Participants

Rick Wray, MD, Baltimore, MD (*Presenter*) Nothing to Disclose Charles Marcus, MD, Baltimore, MD (*Abstract Co-Author*) Nothing to Disclose Sara Sheikhbahaei, MD, MPH, Baltimore, MD (*Abstract Co-Author*) Nothing to Disclose Rathan M. Subramaniam, MD, PhD, Baltimore, MD (*Abstract Co-Author*) Travel support, Koninklijke Philips NV

PURPOSE

The aim of the study was to test a simple, reproducible, qualitative, therapy response interpretation method (Hopkins Criteria) that can be implemented on the post treatment 18F-FDG PET/CT study and to evaluate its impact on prognosis in patients with lung cancer.

METHOD AND MATERIALS

This was a retrospective study of 204 biopsy-proven lung cancer patients, who underwent a post treatment PET/CT study after completion of primary treatment from 2003 to 2012. The median follow-up was 12.1 months. The PET/CT studies were interpreted using a qualitative 5-point scoring system - Hopkins Criteria. The primary outcome was overall survival (OS), which was analyzed by Kaplan-Meier plots with a Mantel-Cox long-rank test.

Of the 204 patients, 88 were women and 116 were men. A total of 140 (68.6%) patients died during the follow-up period. There were 123 (61.3%) with a positive Hopkins Criteria score for residual disease and 81 (39.7%) patients with a negative score. The median survival time for patients with a positive score was 29.6 months in comparison to 51.2 months in those with a negative score (p<0.001). There was a significant difference in the OS between patients with a positive score versus those with a negative score (HR 2.01; 95%CI: 1.42-2.84; Logrank P<0.001). The Kaplan-Meier analysis also showed a significant difference in OS between patients with a positive and negative score who were treated with surgery (HR 4.72; 95%CI: 1.84-12.08; Logrank P<0.001) and those treated with chemoradiation alone (HR 1.62; 95%CI: 1.11-2.37; Logrank P=0.012). There was also a significant difference in the OS between 3 versus score 4 and 5 (Logrank P<0.001).

CONCLUSION

The 5-point qualitative therapy response Hopkins Criteria provides valuable prognostic information in patients with lung carcinoma.

CLINICAL RELEVANCE/APPLICATION

The 5-point qualitative therapy response Hopkins Criteria can predict survival outcome in post therapy patients with lung carcinoma and is recommended for surveillance in this population.

RC211-05 Response Assessment Recommendations in Solid Tumors: RECIST vs PERCIST

Monday, Nov. 30 9:45AM - 10:30AM Location: S505AB

Participants

Heather Jacene, MD, Boston, MA (Presenter) Nothing to Disclose

LEARNING OBJECTIVES

1) To compare anatomic and metabolic imaging for response assessment. 2) To discuss limitations of current widely used criteria for assessing response. 3) To discuss the benefits and limitations of metabolic imaging for response assessment.

ABSTRACT

RC211-06 Challenges of Solid Tumor Measurements and Techniques to Address This

Monday, Nov. 30 10:45AM - 11:30AM Location: S505AB

Participants

Haesun Choi, MD, Houston, TX (Presenter) Nothing to Disclose

LEARNING OBJECTIVES

1) The currently available response evaluation criteria of solid tumors and its limitations. 2) New concept of response evaluation of solid tumors. 3) Future of response evaluation of solid tumors.

ABSTRACT

RC211-07 Is There an Influence of the PERCIST Analysis Approach Used with FDG PET/CT for Evaluation of Tumor Response on Outcome Prediction in Stage IV Breast Cancer Patients?

Monday, Nov. 30 11:30AM - 11:40AM Location: S505AB

Participants

Katja Pinker, MD, New York, NY (*Presenter*) Nothing to Disclose
Christopher C. Riedl, MD, New York, NY (*Abstract Co-Author*) Nothing to Disclose
Leonard Ong, MD, New York, NY (*Abstract Co-Author*) Nothing to Disclose
Maxine S. Jochelson, MD, New York, NY (*Abstract Co-Author*) Nothing to Disclose
Gary A. Ulaner, MD, PhD, New York, NY (*Abstract Co-Author*) Research support, General Electric Company; Research support, F.
Hoffmann-La Roche Ltd
Maura Dickler, New York, NY (*Abstract Co-Author*) Nothing to Disclose
Wolfgang A. Weber, MD, New York, NY (*Abstract Co-Author*) Consultant, Endocyte, Inc

PURPOSE

PET Response Criteria in Solid Tumors (PERCIST) 1.0, is a framework for the evaluation of tumor response to therapy by FDG PET/CT. PERCIST recommends measuring changes in tumor FDG uptake of 1-5 lesions as measured by SUVpeak normalized for body weight. The purpose of this study was to compare analysis of 1 lesion (PERCIST_1) to analysis of up to 5 lesions (PERCIST_5) and to changes of tumor/liver ratio (TLR) of one lesion for prediction of progression-free (PFS) and disease-specific survival (DSS) in stage IV breast cancer patients under systemic therapy.

METHOD AND MATERIALS

This HPAA compliant IRB approved retrospective study included 65 patients with stage IV breast cancer who received 1st or 2nd line systemic therapy in clinical trials and had a FDG PET/CT at baseline and within 3 months after therapy initiation. Treatment response according to PERCIST_1, PERCIST_5 and TLR was correlated with PFS and DSS using Kaplan-Meier analysis/log-rank tests.

RESULTS

Response classifications using PERCIST_1, PERCIST_5 and tumor/liver ratio analysis are summarized in Table 1. All three approaches resulted in highly significant (p<0.01) differences between responders (CR+PR) and nonresponders (SD+PD) for both PFS and DSS (Figure 1). When comparing the PFS and DSS of responders there were no significant differences for PERCIST_1 vs PERCIST_5 (p=0.74), PERCIST_1 vs TLR (p=0.88) and PERCIST_5 vs TLR (p=0.64). There were also no significant differences of PFS in the group of nonresponders: (PERCIST_1 vs PERCIST_5, p=0.3; PERCIST_1 vs TLR, p=0.54; and PERCIST_5 vs TLR, p=0.62).

CONCLUSION

In metastatic breast cancer a metabolic response according to PERCIST 1 5 and TLR is bighly significantly correlated with PES and

cust current a metabolic response according to r Erecor I, J and TEXIS Inginy Significancy Lonciacea mich i i o ana DSS. The exact definition of a metabolic response does not have a major impact on the prognostic value of response assessment.

CLINICAL RELEVANCE/APPLICATION

Response assessment by FDG PET/CT appears to be a robust approach for monitoring tumor response to therapy in patients with metastatic breast cancer.

RC211-08 Assessment of Early Response to Treatment Using FDG PET/CT in Patients with Advanced Melanoma **Receiving Immune Checkpoint Inhibitors**

Monday, Nov. 30 11:40AM - 11:50AM Location: S505AB

Participants

Steve Cho, MD, Madison, WI (Abstract Co-Author) Nothing to Disclose Evan J. Lipson, MD, Baltimore, MD (Abstract Co-Author) Nothing to Disclose Hyung-Jun Im, MD, PhD, Madison, WI (Presenter) Nothing to Disclose Esther Mena, MD, Bethesda, MD (Abstract Co-Author) Nothing to Disclose Steven P. Rowe, MD, PhD , Parkville, MD (Abstract Co-Author) Nothing to Disclose Drew M. Pardoll, MD, PhD, Baltimore, MD (Abstract Co-Author) Nothing to Disclose Suzanne Topalian, MD, Baltimore, MD (Abstract Co-Author) Consultant, Bristol-Myers Squibb Company Research Grant, Bristol-Myers Squibb Company

Richard L. Wahl, MD, Saint Louis, MO (Abstract Co-Author) Research Consultant, Nihon Medi-Physics Co, Ltd;

PURPOSE

Immune checkpoint inhibitors (ICI) have demonstrated antitumor activity and prolonged survival in patients with advanced melanoma. Evaluation of response to early treatment response with these agents using standard CT imaging can be challenging. A recent report of FDG-PET/CT after two cycles of ICI has been reported to be highly predictive of the final outcome. We evaluated the use of FDG-PET/CT scans as early predictors of response to therapy in patients with melanoma receiving ICI.

METHOD AND MATERIALS

Twenty patients with advanced melanoma treated with ICI therapy underwent FDG PET/CT prior to initiation of therapy (day -28 to 0; SCAN1), at day 23-28 (SCAN2) and at 16 weeks (SCAN3). FDG-PET scans were evaluated for changes in maximum standardized uptake value (SUVmax), peak SUV (SUVpeak), metabolic tumor volume (MTV), and total lesion glycolysis (TLG). CT images were used to evaluate response according to RECIST 1.1 and immune-related response criteria (irRC). Receiver-operating characteristic (ROC) analysis for prediction of tumor response used area under curve (AUC) to compare baseline SCAN1 and the percent change in PET and CT parameters between SCAN1 and SCAN2. These values were also compared to the standard RECIST 1.1 response at SCAN3.

RESULTS

Twenty evaluable patients who had completed SCAN1 and SCAN2 and had a documented radiologic and/or clinical outcome were evaluated. By RECIST 1.1 criteria 2 had partial responses (PR) and 2 complete responses (CR) at 16 weeks. One patient had stable disease >6 months and 15 had progressive disease (PD). SUVmax and SUVpeak at SCAN1 and SUVmax and SUVpeak percent change from SCAN1 to SCAN2 were not strongly predictive of tumor response, with AUC of 0.480, 0.547, 0.680, and 0.680, respectively. CT-based irRC and RECIST 1.1 were also not strongly predictive of tumor response with AUC of 0.760 and 0.787, respectively. Analyses of PET based MTV and TLG parameters are in progress.

CONCLUSION

Standard parameters of PET and CT response at baseline and early in the course of ICI therapy were not strongly predictive for response to ICI treatment in patients with advanced melanoma. These findings require further validation in a larger cohort of patients.

CLINICAL RELEVANCE/APPLICATION

Standard PET and CT parameters of early tumor response to ICI therapy are not sufficient for predicting response to therapy, and therefore development of improved imaging metrics and methods are needed.

Honored Educators

Presenters or authors on this event have been recognized as RSNA Honored Educators for participating in multiple qualifying educational activities. Honored Educators are invested in furthering the profession of radiology by delivering high-quality educational content in their field of study. Learn how you can become an honored educator by visiting the website at: https://www.rsna.org/Honored-Educator-Award/

Richard L. Wahl, MD - 2013 Honored Educator

RC211-09 Analysis of PET/CT Patterns of Response to Ipilimumab in Patients with Metastatic Melanoma

Monday, Nov. 30 11:50AM - 12:00PM Location: S505AB

Participants

Brandon A. Howard, MD, Durham, NC (*Presenter*) Nothing to Disclose

Bhavana Singh, Durham, NC (Abstract Co-Author) Nothing to Disclose

April Salama, Durham, NC (Abstract Co-Author) Consultant, Bristol-Myers Squibb Company; Advisory Board Member, Bristol-Myers Squibb Company; Institutional Research Grant, Bristol-Myers Squibb Company; Institutional Research Grant, Merck & Co, Inc Brent Hanks, MD, PhD, Durham, NC (Abstract Co-Author) Nothing to Disclose

Mustafa R. Bashir, MD, Cary, NC (Abstract Co-Author) Research support, Siemens AG; Research support, Bayer AG; Research support, Guerbet SA; Research support, General Electric Company; Consultant, Bristol-Myers Squibb Company

Tracy A. Jaffe, MD, Durham, NC (Abstract Co-Author) Nothing to Disclose

Andrew R. Barina, MD, Durham, NC (Abstract Co-Author) Nothing to Disclose

Melanoma is a serious public health problem with rising incidence worldwide. Although surgery is efficacious for early stage disease, prognosis is poor for metastatic melanoma, with median survival of less than 1 year. Previous therapies, such as interleukin-2 and chemoradiation, have had minimal impact on survival. Ipilimumab (Ipi; Bristol- Meyers Squibb, Princeton, NJ), a human monoclonal antibody against the cytotoxic T-lymphocyte associated antigen 4 (CTLA-4), was recently introduced and demonstrates improved survival in metastatic melanoma. CTLA-4 is a negative regulator of T cell activation and is exploited by melanoma cells to evade T cell immune- mediated destruction. CTLA-4 blockade by Ipi enhances host anti-tumor response. F-18 fluorodeoxyglucose PET-CT is routinely used in melanoma, however is subject to false positives when inflammatory or immune mediated processes are involved. It has recently been reported that in the setting of Ipi therapy, certain findings such as colitis, lymphadenopathy, inflammatory fat stranding may portend a favorable prognosis. We aim to further characterize the spectrum of PET/CT findings relevant to response to ipilimumab in our population.

METHOD AND MATERIALS

Patients who underwent FDG PET-CT from 2005 through Sept. 2014, and received at least one cycle of Ipi were retrospectively reviewed. PET/CT results, including unusual findings (i.e. those neither clearly malignant or benign on imaging) were recorded and correlated with clinicopathologic records and subsequent imaging.

RESULTS

103 patients met criteria for the study. Indeterminate findings on PET-CT included FDG-avid lymphadenopathy, diffuse thyroid uptake, subcutaneous nodularity, gallbladder uptake, and intracardiac uptake. A mixed pattern of response was often reported.

CONCLUSION

The most common PET/CT findings in metastatic melanoma patients on ipilimumab were FDG- avid lymphadenopathy, thyroid uptake, and subcutaneous nodularity, which did not correlate with an adverse outcome. A mixed response was often noted. Further analysis of clinical outcome data and clinical benefit analysis will be performed, including Kaplan-Meier analysis, to determine whether these correlated with improved outcomes.

CLINICAL RELEVANCE/APPLICATION

Characteristic patterns on PET/CT may imply a favorable outcome to treatment with ipilimumab in melanoma. Care must be taken not to interpret FDG uptake in lymph nodes, thyroid, and subcutaneous fat as progression.

Quantitative CT and MR Perfusion Imaging

Monday, Nov. 30 8:30AM - 10:00AM Location: S504CD

CT GI MR OI BQ

AMA PRA Category 1 Credits ™: 1.50 ARRT Category A+ Credits: 1.50

Participants

Max Wintermark, MD, Lausanne, Switzerland, (max.wintermark@gmail.com) (Moderator) Advisory Board, General Electric Company;

LEARNING OBJECTIVES

1) To understand the principles of CT perfusion analysis for tumor assessment. 2) To understand the pathophysiological basis of CT perfusion parameters for tumors. 3) To understand unique CT perfusion analysis of the liver due to its characteristic dual blood supply. 4) To describe the potential clinical applications, with a focus on hepatic and extrahepatic applications and clinical trials. 5) To discuss several recent challenging issues regarding CT perfusion. 6) To discuss areas for further development including assessment of tumor heterogeneity.

ABSTRACT

With the emergence of novel targeted therapies for cancer, imaging techniques that assess tumor vascular support have gained credence for response assessment alongside standard response criteria. CT perfusion techniques that quantify regional tumour blood flow, blood volume, flow-extraction product, and permeability-surface area product through standard kinetic models, are attractive in this scenario by providing evidence of a vascular response or non-response. Additionally, these techniques may provide prognostic and predictive information to the clinician. Their increasing acceptance in oncological practice in recent years has been related to the combination of clinical need and technological improvements in CT, including faster tube rotation speeds, higher temporal sampling rates, the development of dynamic 3D acquisitions and development of commercial software programmes embedded within the clinical workflow. Recently published consensus guidelines provide a way forward to perfoming studies in a more standardized manner. To date single centre studies have provided evidence of clinical utility. Future studies that include good quality prospective validation correlating perfusion CT to outcome endpoints in the trial setting are now needed to take CT perfusion forward as a biomarker in oncology.These presentations will cover the principles of CT perfusion analysis for tumor assessment and its pathophysiological basis. Clinical applications will be discussed focusing on hepatic and extrahepatic applications and clinical trials. Areas for further development including assessment of tumor heterogeneity will also be discussed.

Sub-Events

RC217A CT Perfusion in Oncology: Hepatic Imaging

Participants

Se Hyung Kim, Seoul, Korea, Republic Of (Presenter) Research Grant, Mallinckrodt plc; Research Grant, Samsung Electronics Co Ltd

LEARNING OBJECTIVES

1) To understand basic principles, acquisition protocol, and pharmacokinetic models of CT perfusion. 2) To learn unique CT perfusion analysis of the liver due to its characteristic dual blood supply. 3) To describe the potential clinical applications, with a focus on hepatic applications. 4) To discuss several recent challenging issues regarding CT perfusion.

ABSTRACT

RC217B CT Perfusion in Oncology: Extrahepatic Imaging

Participants

Vicky J. Goh, MBBCh, London, United Kingdom (Presenter) Research Grant, Siemens AG; Speaker, Siemens AG

LEARNING OBJECTIVES

1) To understand the principles of CT perfusion analysis for tumor assessment. 2) To understand the pathophysiological basis of CT perfusion parameters for tumors. 3) To describe the potential clinical applications, with a focus on extrahepatic applications and clinical trials. 4) To discuss areas for further development including assessment of tumor heterogeneity.

ABSTRACT

With the emergence of novel targeted therapies for cancer, imaging techniques that assess tumor vascular support have gained credence for response assessment alongside standard response criteria. CT perfusion techniques that quantify regional tumour blood flow, blood volume, flow-extraction product, and permeability-surface area product through standard kinetic models, are attractive in this scenario by providing evidence of a vascular response or non-response. Additionally, these techniques may provide prognostic and predictive information to the clinician. Their increasing acceptance in oncological practice in recent years has been related to the combination of clinical need and technological improvements in CT, including faster tube rotation speeds, higher temporal sampling rates, the development of dynamic 3D acquisitions and development of commercial software programmes embedded within the clinical workflow. Recently published consensus guidelines provide a way forward to perfoming studies in a more standardized manner. To date single centre studies have provided evidence of clinical utility. Future studies that include good quality prospective validation correlating perfusion CT to outcome endpoints in the trial setting are now needed to take CT perfusion forward as a biomarker in oncology. This presentation will cover the principles of CT perfusion analysis for tumor assessment and its pathophysiological basis. Clinical applications will be discussed focusing on extrahepatic applications and clinical trials. Areas for further development including assessment of tumor heterogeneity will also be discussed.

RC217C Quantitative MR Perfusion Imaging of the Brain

Participants Max Wintermark, MD, Lausanne, Switzerland, (max.wintermark@gmail.com) (*Presenter*) Advisory Board, General Electric Company;

LEARNING OBJECTIVES

1) Understand the difference between quantitative and qualitative perfusion measurements. 2) Distinguish several approaches for obtaining quantitative perfusion maps in the brain. 3) Appreciate the strengths and weaknesses between the two major techniques, arterial spin labeling and bolus contrast dynamic susceptibility imaging.

Physics Series: Quantitative Imaging Mini-Course: Image Modality Specific Issues

Monday, Nov. 30 8:30AM - 12:00PM Location: S403B

BQ CT MR NM PH

AMA PRA Category 1 Credits ™: 3.25 ARRT Category A+ Credits: 3.75

FDA Discussions may include off-label uses.

Participants

Michael F. McNitt-Gray, PhD, Los Angeles, CA (*Director*) Institutional research agreement, Siemens AG; Research support, Siemens AG; ; ; ; ;

Edward F. Jackson, PhD, Madison, WI, (efjackson@wisc.edu) (Moderator) Nothing to Disclose

Paul L. Carson, PhD, Ann Arbor, MI (*Moderator*) Research collaboration, General Electric Company; Research collaboration, Light Age, Inc

Sub-Events

RC225-01 Quantitative Imaging for Computed Tomography: Applications and Future Directions

Monday, Nov. 30 8:30AM - 9:00AM Location: S403B

Participants Samuel G. Armato III, PhD, Chicago, IL, (s-armato@uchicago.edu) (*Presenter*) Nothing to Disclose

LEARNING OBJECTIVES

1) Describe the role of computed-tomography-based quantitative imaging in the clinical and research settings.

ABSTRACT

RC225-02 Quantification of Vascular Response in Rodent Brown Adipose Tissue Using Spectral CT

Monday, Nov. 30 9:00AM - 9:10AM Location: S403B

Participants

Xin-Gui Peng, MD,PhD, Nanjing, China (*Presenter*) Nothing to Disclose Zhen Zhao, Nanjing, China (*Abstract Co-Author*) Nothing to Disclose Di Chang, Nanjing, China (*Abstract Co-Author*) Nothing to Disclose Shenghong Ju, MD, PhD, Nanjing, China (*Abstract Co-Author*) Nothing to Disclose

PURPOSE

Brown adipose tissure (BAT) has abundant mitochondrion, uncoupling protein 1 and vascularizaiton to provide sufficient energy compared to white adipose tissure (WAT). Our study is to assess the changes of iodine/water base material concentration in BAT after injecting norepinephrine (NE).

METHOD AND MATERIALS

The animal study was approved by the institutional Committee on Animal Research. Spetral CT scan (GE, Discovery CT750) was performed to measure the iodine/water concentration based on base material mapping in the BAT (interscapular) and WAT (visceral) of Wistar rat (n=6, 14 weeks, $304g\pm12g$) at baseline condition. To induce the blood flow increase, animals were given NE (1µg/kg/min, 10min, totle 1ml) or saline (1ml) from caudal vein. The enhanced CT imaging (6ml/kg, iopromide 300) was performed after the injection of the drug. The iodine/water concentraction of BAT and WAT, the BAT/Arota and WAT/Arota ratio were calculated. Statistical analysis was performed with independent sample t test and paired sample t test .

RESULTS

There was no difference in mean base iodine (water) material concentration of BAT and WAT at the baseline condition between the NE and saline groups (P>0.05). After injecting NE, the base iodine material concentration of BAT increased significantly compared to controls (NE: -5.41±1.20mg/cm3 and 23.57±8.71mg/cm3; saline: -7.66±2.01mg/cm3 and 8.71±3.68mg/cm3, respectively; P<0.001) (Fig.A). However, there were no statistically significant changes observed in iodine and water material concentration of WAT between both groups. The BAT/Arota ratio, WAT/Arota ratio of iodine concentration and BAT/Arota ratio of water concentration after injection NE increased significantly (iodine: BAT/Arota ratio, 0.26±0.96 and 0.10±0.04, WAT/Arota ratio, -0.12±0.04 and -0.16±0.03; water: BAT/Arota ratio:1.06±0.02 and 0.93±0.04, respectively; P<0.001) (Fig.B). There was no difference of WAT/Arota ratio in water concentration imaging between both groups (P>0.05) (Fig.C).

CONCLUSION

The iodine/water base material concentration detected the pharmacologic activation of BAT. Energy spectrum CT has protential to evaluate the change of BAT and WAT after treatment.

CLINICAL RELEVANCE/APPLICATION

Spectral CT provided a new noninvasive method to be translated to a clinical setting for evaluation the difference of adipose tissue and monitoring the responses to specific therapeutic strategies.

RC225-03 Determinants of the Accuracy of the Quantification of Glandularity and Iodine Uptake in Contrast-Enhanced Digital Mammography

Participants Kristen C. Lau, MS, Philadelphia, PA (*Presenter*) Nothing to Disclose Moez K. Aziz, Philadelphia, PA (*Abstract Co-Author*) Nothing to Disclose Young Joon Kwon, Philadelphia, PA (*Abstract Co-Author*) Nothing to Disclose Andrew D. Maidment, PhD, Philadelphia, PA (*Abstract Co-Author*) Research support, Hologic, Inc; Research support, Barco nv; Spouse, Employee, Real-Time Radiography, Inc; Spouse, Stockholder, Real-Time Radiography, Inc

PURPOSE

To develop a method for determining breast tissue composition in dual-energy (DE) contrast-enhanced digital mammography (CE-DM). The motivation for this arises from our difficulty to resolve contrast uptake at the boundaries of the breast in DE subtraction.

METHOD AND MATERIALS

Phantoms were constructed using 1 cm thick uniform blocks of 100% glandular-equivalent and 100% adipose-equivalent materials (CIRS, Norfolk, VA). The thickness of the phantoms ranged from 3 to 8 cm, in 1 cm increments. For a given thickness, the glandular/adipose composition of the phantom was varied using different combinations of blocks. The phantoms were imaged using a prototype DE Hologic Selenia Dimensions DBT system. A 0.3 mm copper filter is used for the high-energy (HE) x-rays (49 kVp) and a 0.7 mm aluminum filter is used for the low-energy (LE) x-rays (32 kVp). X-ray energies were chosen so the k-edge of the contrast agent was in the range spanned by the LE and HE x-ray spectra. DE images were obtained by a weighted logarithmic subtraction of the HE and LE image pairs. The images were smoothed using a 2D convolution with a 4x4 matrix prior to quantitative analysis. LE and HE signal intensities were normalized by the mAs, and mean and standard deviation values were calculated for the normalized log HE and log LE images.

RESULTS

The mean LE and HE values varied with phantom thickness and glandularity. The log LE and log HE signals decrease linearly with increasing glandularity for a given thickness. The signals decrease with increasing phantom thickness; for a given glandularity, the x-ray signal decreases linearly with thickness. As the thickness increases, the attenuation difference per additional glandular block decreases, indicating beam hardening. Using these data, we have created a mapping between signal intensity and breast thickness. These data facilitate the subtraction of tissue in the periphery of the breast, and aid in discriminating between contrast agent uptake in glandular tissue and subtraction artifacts.

CONCLUSION

We have shown that breast thickness and composition can be predicted based on signal intensities in DE CE-DM. This has implications for the weighting factor used in DE subtraction.

CLINICAL RELEVANCE/APPLICATION

DE CE-DM can be improved by taking into account breast thickness and composition. Combining these techniques into a single procedure is a powerful tool for the detection and diagnosis of breast cancer.

RC225-04 Mapping of Medullar Adiposity of the Lumbar Spine in MRI

Monday, Nov. 30 9:20AM - 9:30AM Location: S403B

Participants

Nicolas Demany, Brest, France (*Abstract Co-Author*) Nothing to Disclose Julien Ognard, MD, MSc, Brest, France (*Presenter*) Nothing to Disclose Jawad Mesrar, MD, Brest, France (*Abstract Co-Author*) Nothing to Disclose Serge Ludwig Aho-Glele, Dijon, France (*Abstract Co-Author*) Nothing to Disclose Alain Saraux, Brest, France (*Abstract Co-Author*) Nothing to Disclose Douraied Ben Salem, MD, PhD, Brest, France (*Abstract Co-Author*) Nothing to Disclose

PURPOSE

The bone medullar adiposity is a marker of bone quality to the point that it should be better to know the factors which influence or not the density and distribution of this fat in the spine, especially at the lumbar level.

METHOD AND MATERIALS

A sagittal sequence IDEAL IQ (MRI GE 1.5T) was performed on the lumbar spine of 46 subjects without bone disease (21 women and 25 men, aged 18 to 77 years old). Medulla adiposity was determined directly from the measurement of the fat fraction of each vertebral body (T12 to S1) obtained on the fat cartography automatically generated by the IDEAL sequence.

RESULTS

Average vertebral fat fraction was 36.48% (DS 12.82 ; 14.69% - 72.8%], increasing with age, and it is higher among men. We observed a craniocaudal gradient of the fat fraction (B = 1,37 ; p < 0,001 ; DS 0,06) increasing with age in the lumbar spine from T12 to L5. Through a multivariate analysis, this gradient was independent of sex, weight and height of subjects.

CONCLUSION

This study shows the existence of a physiological craniocaudal gradient of vertebral medullar adiposity from T12 to L5. This gradient increases with age but it is independent of sex or BMI. The IDEAL sequence allows quick and reproducible measurement of the spine vertebral medullar adiposity.

CLINICAL RELEVANCE/APPLICATION

IDEAL IQ is a Rapid sequence, Allowing easy and reproducible measurements with ROIs. The need is to recruit a wider population to establish standards fat percentage by age strata and compare them with bone mineral density obtained by densitometry. For example, in an attempt to establish thresholds for a subject to beconsidered as osteopenic or osteoporotic. The IDEAL IQ sequence allows a fast and reproductible measure of the bone marrow fat of the spine, that could easily completing a lumbar MRI assessment

RC225-05 Automatic Quantification of Iodine and Calcium using Monoenergetic Virtual Images Generated by

Spectral Detector Dual-Layer CT: A Phantom Study

Monday, Nov. 30 9:30AM - 9:40AM Location: S403B

Participants

Isaac Leichter, PhD, Jerusalem, Israel (*Presenter*) Nothing to Disclose Tzvi Lipschuetz, Jerusalem, Israel (*Abstract Co-Author*) Nothing to Disclose Tzvi Vichter, Jerusalem, Israel (*Abstract Co-Author*) Nothing to Disclose Zimam Romman, Haifa, Israel (*Abstract Co-Author*) Employee, Koninklijke Philips NV Jacob Sosna, MD, Jerusalem, Israel (*Abstract Co-Author*) Consultant, ActiViews Ltd Research Grant, Koninklijke Philips NV

PURPOSE

To use Monoenergetic Virtual images generated by Spectral Detector Dual-Layer CT (SDCT) for automatic reliable identification and concentration calculation of calcium and iodine solutions.

METHOD AND MATERIALS

Tubes of 11.1 mm diameter filled with iodine and calcium solutions at concentrations of 10 to 60 mg/ml and 100 to 1000 mg/ml, respectively, were inserted in a water-equivalent anthropomorphic CT phantom (QRM, Moehrendorf, Germany). The phantom, of two sizes (25×35 cm and 30×40 cm), was scanned with a SDCT (Philips Healthcare, Cleveland, OH, USA) at 120kVp and 200 mAs. Software was developed to calculate the relationship between gray-level values of pixels containing iodine and calcium solutions in the monoenergetic virtual images generated by SDCT. The relationship obtained for the image of the small phantom was used to create spectral maps that uniquely characterize the material in the pixel, independently of its concentration. For any given image, the software searched and identified pixels which fitted into the spectral map equations of calcium and iodine and displayed them in different colors. In order to evaluate the effect of beam hardening, iodine and calcium was searched in images of both phantom sizes. The concentration of each solution identified by the software was evaluated.

RESULTS

In the small phantom (98.9 \pm 1.6)% of the pixels containing iodine or calcium were correctly identified and displayed in different colors. In the large phantom the identification accuracy was (92.7 \pm 10.4)%. The calculated solution concentrations in the small phantom were higher by (4.6 \pm 2.6)% from the actual concentrations, and lower by (5.7 \pm 4.6)% in the large phantom.

CONCLUSION

SDCT can differentiate between calcium and iodine solutions in a phantom model and calculate their concentrations with good accuracy on a pixel by pixel analysis. Beam hardening effects had only a small impact on the results which depended very slightly on the phantom size or the solution location within the phantom.

CLINICAL RELEVANCE/APPLICATION

By the use of Spectral Detector CT, contrast agents in blood and tumors may be reliably differentiated from adjacent skeletal components, and their concentration can be accurately assessed.

Honored Educators

Presenters or authors on this event have been recognized as RSNA Honored Educators for participating in multiple qualifying educational activities. Honored Educators are invested in furthering the profession of radiology by delivering high-quality educational content in their field of study. Learn how you can become an honored educator by visiting the website at: https://www.rsna.org/Honored-Educator-Award/

Jacob Sosna, MD - 2012 Honored Educator

RC225-06 Quantitative Imaging for PET-CT: Applications and Future Directions

Monday, Nov. 30 9:40AM - 10:10AM Location: S403B

Participants

Robert Jeraj, Madison, WI (*Abstract Co-Author*) Founder, AIQ Services Tyler Bradshaw, Madison, WI (*Presenter*) Nothing to Disclose

LEARNING OBJECTIVES

1) Describe the role of PET/CT-based quantitative imaging in the clinical and research settings.

RC225-07 Quantitative Imaging for DCE-MRI: Applications and Future Directions

Monday, Nov. 30 10:25AM - 10:55AM Location: S403B

Participants

Yue Cao, PhD, Ann Arbor, MI (Presenter) Research Grant, Siemens AG; Speaker, Siemens AG

LEARNING OBJECTIVES

1) Describe the role of quantitative DCE MR imaging in the clinical and research settings.

RC225-08 Measuring Blood Velocity with Doppler-CT (part 1): Theoretical Aspects and Simulations

Monday, Nov. 30 10:55AM - 11:05AM Location: S403B

Participants

Johannes G. Korporaal, PhD, Forchheim, Germany (*Abstract Co-Author*) Employee, Siemens AG Rainer Raupach, PhD, Forchheim, Germany (*Abstract Co-Author*) Employee, Siemens AG Thomas G. Flohr, PhD, Forchheim, Germany (*Abstract Co-Author*) Employee, Siemens AG Bernhard Schmidt, PhD, Forchheim, Germany (*Presenter*) Employee, Siemens AG

PURPOSE

Measuring blood velocity with computed tomography (CT) has been subject of numerous studies, most of which used the time-offlight technique. With that method, data acquisition should be performed with a stationary table (sequence mode) and the clinical applicability and measurement accuracy are limited by the detector size. The purpose of this study is to introduce Doppler-CT as a new method of measuring blood velocity by describing the theory, simulating its expected behavior and deriving clinical acquisition strategies.

METHOD AND MATERIALS

In general, the speed v [m/s] of a wave with wavelength λ [m] and frequency f [1/s] is given by v = f* λ . When considering a straight vessel segment and assuming a linear increase in contrast enhancement after injecting an iodinated contrast agent, the blood velocity can be analogously calculated from the spatial [m/HU] and temporal [HU/s] contrast gradients within the vessel. In case the observer O (the scan plane of the CT scanner) and the source S (the human heart) are moving with respect to each other, i.e. during a spiral acquisition, the well-known Doppler-equations can be applied, e.g. fO = fS(1±v/c) [eq.1], with fO being the measured temporal gradient [HU/s] of the spiral scan, fS the temporal gradient [HU/s] produced by the heart, ±v the table speed and c the blood velocity. For table velocities of ±70cm/s and blood velocities of ±100cm/s, fO was simulated as fraction of fS, since the relative change in fO is independent of fS.

RESULTS

With a known direction of table movement, the direction of the blood flow can be qualitatively determined, since the relative gradient of fO is centrally symmetric. With increasing table speed and decreasing blood speed, the deviation of fO from fS increases, indicating better quantitative measurement accuracy. For equal image noise, low tube voltages and high iodine delivery rates will further improve the measurement sensitivity.

CONCLUSION

High table speed and low blood velocity are favorable for quantifying blood velocity with Doppler-CT. Implementation in clinical routine can be simple, e.g. with two (or more) sweeps of a dynamic scan mode with alternating scan direction (part 2) or with a bolus tracking scan followed by a CT angiography (part 3).

CLINICAL RELEVANCE/APPLICATION

Measuring blood velocity is no longer reserved for wide-detector CT-systems in sequence mode, but can also be performed with CT-systems with smaller detectors in spiral scan mode.

RC225-09 Quantification of Hepatic Tumor Viability in Multi-phase MDCT Images

Monday, Nov. 30 11:05AM - 11:15AM Location: S403B

Participants

Wenli Cai, PhD, Boston, MA (*Presenter*) Nothing to Disclose Anand K. Singh, MD, Boston, MA (*Abstract Co-Author*) Nothing to Disclose Yin Wu, Boston, MA (*Abstract Co-Author*) Nothing to Disclose Gordon J. Harris, PhD, Boston, MA (*Abstract Co-Author*) Medical Advisory Board, Fovia, Inc

PURPOSE

The purpose of this study was to develop a quantitative imaging biomarker, denoted as hepatic tumor viability (HTV), for quantification of viable and necrotic tumor volumes in addition to the size of liver and tumors in the assessment of tumor progression and treatment responses for patients with hepatocellular carcinoma (HCC) and metastasis.

METHOD AND MATERIALS

Based on the pattern analysis of time-intensity curve (TIC) in multi-phase MDCT images, we developed the automated HTV scheme for segmentation of liver and liver tumors, and classification of viable and necrotic tumor regions. To depict a TIC pattern, a group of TIC features was extracted including the peak CT value, the time to peak (TTP), the area under the curve (AUC), the AUC of wash-in/out, the max/average wash-in/out derivative, and a group of spatiotemporal textures: skewness, kurtosis, energy, and entropy. A K-mean cluster was applied to classify each voxels into four different types of materials: vessel, normal liver tissue, tumor tissue, and necrotic tissue. Liver, liver tumor and viable regions were segmented using the likelihood to each material. Forty (40) IV-contrast enhanced hepatic multi-phase MDCT cases with biopsy-confirmed HCC or metastases were used for evaluation of the proposed HTV biomarker. The MDCT imaging parameters settings were: 2.5-5 mm collimation, 1.25-2.5 mm reconstruction interval, 175 mA tube current, and 120 kVp tube voltage.

RESULTS

In reference to the liver and tumor segmentation by manual-contouring of two radiologists, the volumetric size of these 40 HCC or metastasis livers ranged from 1079.2 CC to 4652.3 CC, in which the tumor volume percentages ranged from 1.77% to 53.54%. The proposed HTV scheme achieved a liver volumetric difference of $3.27\pm2.58\%$ and tumor percentage difference of $1.33\pm1.44\%$. Viable tumor volume showed significant better performance than RECIST and total tumor volume in prediction of treatment response in the case of overall and progression-free survival.

CONCLUSION

Our HTV biomarker can achieve accurate and reliable quantification results in segmentation of liver and liver tumors, classification of viable and necrotic tumor regions, and thus provides a better prediction of treatment response.

CLINICAL RELEVANCE/APPLICATION

Our HTV biomarker can provide an accurate and reliable tumor quantification for assessment of tumor progression and treatment response for HCC and liver metastasis.

RC225-10 Fully Automated Quantitative Analysis of Myocardial Perfusion in First-pass MR Images

Monday, Nov. 30 11:15AM - 11:25AM Location: S403B

Participants

Luan Jiang, PhD, Shanghai, China (*Presenter*) Nothing to Disclose

Shan Ling, Shanghai, China (Abstract Co-Author) Nothing to Disclose

Jichao Yan, Shanghai, China (Abstract Co-Author) Nothing to Disclose

Qiang Li, PhD, Shanghai, China (*Abstract Co-Author*) Patent agreement, General Electric Company Patent agreement, Hologic, Inc Patent agreement, Riverain Technologies, LLC Patent agreement, MEDIAN Technologies Patent agreement, Mitsubishi Corporation

PURPOSE

We are developing a fully automated scheme for quantitative analysis of myocardial perfusion in short-axis first-pass MR images.

METHOD AND MATERIALS

We obtained 8 short-axis myocardial perfusion MR scans from xxx Hospital in xxx with an xxx 1.5-T MR scanner. Each MR scan has 40 time frames with slice thickness 8 mm and in-plane resolution 1.37 mm × 1.37 mm. Our automated method consists of three steps, i.e., cardiac registration, myocardium segmentation, and empirical indexes quantification. Based on the region of interest (ROI) automatically identified from the image at the reference time phase with better contrast of left ventricle and myocardium, a multiscale affine transformation using Sobel gradient information and a non-rigid Demons registration using pseudo ground truth images were sequentially applied to correct the deformations caused by respiratory and cardiac motion. We then further used fuzzy c-means clustering method in the reference image and dynamic programming method in the maximum intensity projection image of all time phases to delineate, respectively, the endo- and epicardial boundaries of the myocardium. Finally, several empirical perfusion indexes (peak signal intensity, time to peak, and maximum upslope) were quantified from the time-intensity curves of segments of myocardium.

RESULTS

Dice index based on apical, midventricular, and basal slices was improved from $78.4\% \pm 12.5\%$ to $85.9\% \pm 5.3\%$ using cardiac registration, and Dice index of $82.2\% \pm 5.9\%$ was achieved for myocardium segmentation. Subjective judgment showed that the empirical indexes were able to identify the ischemia in myocardium.

CONCLUSION

Our fully automated scheme for quantitative analysis of myocardial perfusion MR images would be useful for myocardium perfusion assessment and early diagnosis of myocardium with ischemia.

CLINICAL RELEVANCE/APPLICATION

Our CAD scheme could help the radiologists to quantitatively analyze myocardium perfusion and to improve the accuracy and efficiency for diagnosis of myocardium with ischemia.

Active Handout:Luan Jiang

http://abstract.rsna.org/uploads/2015/15016295/RC225-10.pdf

RC225-11 Laws Textures: A Potential MRI Surrogate Marker of Hepatic Fibrosis in a Murine Model

Monday, Nov. 30 11:25AM - 11:35AM Location: S403B

Participants

Baojun Li, PhD, Boston, MA (*Presenter*) Nothing to Disclose Hei Shun Yu, MD, Boston, MA (*Abstract Co-Author*) Nothing to Disclose Hernan Jara, PhD, Belmont, MA (*Abstract Co-Author*) Patent holder, qMRI algorithms Research Grant, General Electric Company Royalties, World Scientific Publishing Co Jorge A. Soto, MD, Boston, MA (*Abstract Co-Author*) Nothing to Disclose Stephan W. Anderson, MD, Boston, MA (*Abstract Co-Author*) Nothing to Disclose

PURPOSE

To study the effect of disease progression on liver parenchymal Laws textures of ex vivo murine liver specimens imaged using 11.7 Tesla MRI. To compare Laws textures to other imaging-based surrogate markers (T2, PD, ADC, and degrees of inflammation).

METHOD AND MATERIALS

This animal study was IACUC approved. Seventeen male, C57BL/6 mice were divided into control (n=2) and experimental groups (n=15). The latter were fed a 3,5-dicarbethoxy-1, 4-dihydrocollidine (DDC) supplemented diet to induce hepatic fibrosis. Ex vivo liver specimens were imaged using an 11.7T MRI scanner, from which the parametric proton density (PD), T2, and ADC maps were generated from spin-echo pulsed field gradient and multi-echo spin-echo acquisitions. The PD maps were first preprocessed to eliminate the low-intensity histogram bias arisen from partial volume effect. The PD maps were further corrected by mean and standard deviation in order to minimize discrimination by overall graylevel variation, which is unrelated to liver parenchymal texture. Laws textures were extracted from the PD maps. Degrees of fibrosis and inflammation were assessed by an experienced pathologist (subjective scores) and digital image analysis (DIA, %Area Fibrosis). Scatterplot graphs comparing Laws texture, T2, PD, ADC, inflammation score to degrees of fibrosis were generated and correlation coefficients were calculated.

RESULTS

Hepatic fibrosis and Laws textures were strongly correlated with higher %Area Fibrosis associated with higher Laws textures (r=0.89, p<0.001). Strong correlation also existed between T2 and Laws textures (r=0.85, p<0.01). Moderate correlations were seen between %Area Fibrosis and PD (r=0.65), ADC (r=0.67), and Subjective Fibrosis Score (r=0.51). The Subjective Inflammation Score was poorly correlated with hepatic fibrosis (r=0.20). Without proposed corrections, there was only a moderate correlation between %Area Fibrosis and Laws textures (r=0.70).

CONCLUSION

Higher degree of hepatic fibrosis is associated with increased liver parenchymal Laws textures. Laws textures may be more accurate than PD, ADC, and subjective fibrosis and inflammation scores in assessing degrees of fibrosis. The proposed corrections are critical.

CLINICAL RELEVANCE/APPLICATION

Laws textures are potentially accurate surrogate marker for diagnosing and staging hepatic fibrosis.

Honored Educators

Presenters or authors on this event have been recognized as RSNA Honored Educators for participating in multiple qualifying educational activities. Honored Educators are invested in furthering the profession of radiology by delivering high-quality educational content in their field of study. Learn how you can become an honored educator by visiting the website at: https://www.rsna.org/Honored-Educator-Award/

Hernan Jara, PhD - 2014 Honored Educator Jorge A. Soto, MD - 2013 Honored Educator Jorge A. Soto, MD - 2014 Honored Educator Jorge A. Soto, MD - 2015 Honored Educator

RC225-12 Grading of Diffuse Liver Diseases Using Phase-Contrast-Imaging

Monday, Nov. 30 11:35AM - 11:45AM Location: S403B

Participants

Marco Armbruster, Munich, Germany (*Presenter*) Co-Founder of medical software company. Blaz Zupanc, MA, Munich, Germany (*Abstract Co-Author*) Nothing to Disclose Emmanuel Brun, Grenoble, France (*Abstract Co-Author*) Nothing to Disclose Alberto Mittone, Munich, Germany (*Abstract Co-Author*) Nothing to Disclose Wieland H. Sommer, MD, Munich, Germany (*Abstract Co-Author*) Founder, QMedify GmbH Wolfgang Thasler, MD, Munich, Germany (*Abstract Co-Author*) Nothing to Disclose Maximilian F. Reiser, MD, Munich, Germany (*Abstract Co-Author*) Nothing to Disclose Paola Coan, Grenoble, France (*Abstract Co-Author*) Nothing to Disclose

CONCLUSION

X-ray PCI allows grading of diffuse liver diseases, is correlated to histopathology and might be a valuable technique for non-invasive diagnosis and grading of liver fibrosis and steatosis.

Background

Diffuse liver pathologies like steatosis, fibrosis or cirrhosis are an increasing cause of morbidity and mortality worldwide. Liver biopsy is currently the gold standard for the diagnosis and monitoring of disease progression and is essential both for treatment decisions and the prognosis of patients. However, liver biopsy has non-negligible risks, is prone to sampling erros and cannot be used as a screening method. Therefore, the purpose of this study was a proof-of-concept that high resolution X-ray phase contrast imaging (PCI) in computer tomography mode is able to directly visualize pathological changes of the microstructure and that grading of diffuse liver diseases is feasible using PCI-CT.

Evaluation

Synchrotron-based PCI-CT volumetric imaging was performed for human, ex-vivo liver samples from 20 patients (male: 12, female: 8, age: 62+12 yrs). Histopathological workup included hematoxylin-and-eosin-, elastica-van-Gieson-, and iron-straining. For PCI-CT, propagation based imaging technique was used with X-ray of 30 keV and a sample-to-detector distance of 11m. Images were acquired at a spatial resolution of 8 microns.All dataset were graded for the presence of fibrotic changes and the amount of fatty vacuoles. PCI-CT- and histopathological grading of fibrosis and steatosis was correlated using pearson's correlation-coefficient. Both fatty vacuoles, portal, and septal fibrougenous deposites were identifiable in PCI-CT. Visual grading of fibrosis and steatosis correlated moderatly but significantly to the histopathological assessment (r=0.682; p<0.05 for fibrosis; r=0.764; p<0.05 for steatosis).

Discussion

In this study we used X-ray PCI for a direct visualization of microstructural changes within the liver tissue of patients suffering from diffuse liver diseases. Detailed grading of fibrosis and steatosis was feasible. Due to the three-dimensionality of PCI datasets this technique has the potential to decrease interobserver variability and sampling errors in the grading of diffuse liver diseases.

RC225-13 Question and Answer

Monday, Nov. 30 11:45AM - 12:00PM Location: S403B

Participants

ISP: Musculoskeletal (Cartilage: Mechanics, Quantitative MRI and Repair)

Monday, Nov. 30 10:30AM - 12:00PM Location: E450B

MK BQ MR

AMA PRA Category 1 Credits ™: 1.50 ARRT Category A+ Credits: 1.50

Participants

Daniel B. Nissman, MD, MPH, Raleigh, NC (*Moderator*) Royalties, John Wiley & Sons, Inc Michael P. Recht, MD, New York, NY (*Moderator*) Nothing to Disclose

Sub-Events

SSC07-01 Musculoskeletal Keynote Speaker: Cartilage: Understanding Quantitative Evaluation through Structure and Biomechanics

Monday, Nov. 30 10:30AM - 10:50AM Location: E450B

Participants

Michael P. Recht, MD, New York, NY (Presenter) Nothing to Disclose

SSC07-03 Weight Loss Is Associated with Slower Cartilage Degeneration Over 48 Months in Obese and Overweight Subjects: Data from the Osteoarthritis Initiative

Monday, Nov. 30 10:50AM - 11:00AM Location: E450B

Participants

Alexandra S. Gersing, MD, San Francisco, CA (*Presenter*) Nothing to Disclose Martin Solka, San Francisco, CA (*Abstract Co-Author*) Nothing to Disclose Gabby B. Joseph, San Francisco, CA (*Abstract Co-Author*) Nothing to Disclose Benedikt J. Schwaiger, MD, San Francisco, CA (*Abstract Co-Author*) Nothing to Disclose Ursula R. Heilmeier, MD, Munich, Germany (*Abstract Co-Author*) Nothing to Disclose Georg Feuerriegel, San Francisco, CA (*Abstract Co-Author*) Nothing to Disclose John Mbapte Wamba, MD, San Francisco, CA (*Abstract Co-Author*) Nothing to Disclose Charles E. McCulloch, San Francisco, CA (*Abstract Co-Author*) Nothing to Disclose Charles E. McCulloch, San Francisco, CA (*Abstract Co-Author*) Instructor, F. Hoffmann-La Roche Ltd Expert Witness, Mallinckrodt plc Consultant, Mallinckrodt plc Michael C. Nevitt, PhD, San Francisco, CA (*Abstract Co-Author*) Nothing to Disclose Thomas M. Link, MD, PhD, San Francisco, CA (*Abstract Co-Author*) Research funded, General Electric Company; Research funded, InSightec Ltd; Royalties, Springer Science+Business Media Deutschland GmbH; Research Consultant, Pfizer Inc;

PURPOSE

To investigate the association of different degrees of weight loss with progression of knee cartilage degeneration in overweight and obese subjects.

METHOD AND MATERIALS

In this study, 290 subjects (age 61.7 \pm 9.1y; 171 females) with a BMI>25kg/m2 from the Osteoarthritis Initiative (OAI) with risk factors for OA or radiographically mild to moderate OA were included. Subjects with weight loss were categorized into groups with a large (\geq 10%, n=36) or moderate amount of weight loss (5-10%, n=109) over 48 months, and were frequency matched to a group with stable weight (BMI change <3%, n=145). Changes of focal cartilage defects assessed with 3T MRI cartilage WORMS (Whole-Organ Magnetic Resonance Imaging Score) and T2 maps of the right knee for five cartilage compartments (patella, medial and lateral femur, medial and lateral tibia) including laminar and texture analysis, were analyzed using multivariate regression models adjusting for age, sex, baseline BMI and KL.

RESULTS

Overall cartilage WORMS showed significantly less progression in both weight loss groups compared to the stable weight group (5-10% weight loss, P=0.035; >10% weight loss, P<0.0001) over 48 months and changes were associated with changes of BMI (r=0.31, P=0.02). Subjects with >10% weight loss showed significantly less T2 value increase in the bone layer averaged over all compartments compared with stable weight subjects (mean diff. 1.0msec [95%CI 1.3, 0.6] P=0.01), suggesting slower cartilage deterioration, yet no significant change in T2 was found between 5-10% weight loss and stable weight group. In the medial compartment of the >10% weight loss group, overall T2 and cartilage WORMS changes were significantly less (P<0.0001, for each) and homogeneity was increased (P=0.004), compared to the group with stable weight.

CONCLUSION

While changes in cartilage defects were significantly associated with the amount of weight loss in all subjects, only subjects with >10% weight loss showed significantly reduced cartilage deterioration measured with T2. Our data show evidence that weight loss has a protective effect against cartilage degeneration and that a larger amount of weight loss is more beneficial.

CLINICAL RELEVANCE/APPLICATION

MR-based knee cartilage T2 measurements and semiquantitative grading allow monitoring of the protective effect of weight loss on joint health and are useful to determine which amount of weight loss is most beneficial in overweight and obese patients.

SSC07-04 The TEFR Field Study: Results of Continuous Biochemical and Morphological Cartilage Analysis of Hindfoot, Ankle, and Knee Joints in Course of a 4,500 km Ultramarathon Race throughout Whole Europe Using T2*-mapping on a Mobile MRI Truck Trailer

Awards RSNA Country Presents Travel Award

Participants Uwe H. Schuetz, MD, Ulm, Germany (*Presenter*) Nothing to Disclose Christian Billich, Ulm, Germany (*Abstract Co-Author*) Nothing to Disclose Jutta Ellermann, MD, PhD, Minneapolis, MN (*Abstract Co-Author*) Nothing to Disclose Martin Ehrhardt, MD, Ulm, Germany (*Abstract Co-Author*) Nothing to Disclose Daniel Schoss, MD, Ulm, Germany (*Abstract Co-Author*) Nothing to Disclose Martin Brix, Vienna, Austria (*Abstract Co-Author*) Nothing to Disclose Siegfried Trattnig, MD, Vienna, Austria (*Abstract Co-Author*) Nothing to Disclose Sabine Goed, Vienna, Austria (*Abstract Co-Author*) Nothing to Disclose Antje Reiner, MD, Ulm, Germany (*Abstract Co-Author*) Nothing to Disclose Meinrad J. Beer, MD, Wuerzburg, Germany (*Abstract Co-Author*) Research Consultant, Shire plc

PURPOSE

We took advantage of the possibility for a continuous, mobile MR surveillance of cartilage integrity during a transcontinental ultramarathon over 4,486 km. Biochemical changes, thickness and focal lesions of the cartilage of knee, ankle, and hindfoot joints as well as muscle mass and respective relationships were presented.

METHOD AND MATERIALS

MRI data were acquired with a mobile 1.5T scanner travelling with 44 participants of the TransEurope FootRace (TEFR) for 64 days. Repeated follow-up scans were obtained using a T2* GRE-, a TIRM-, and a fat-saturated PD-sequence. T2* values were obtained from inline reconstructed T2* maps by using a pixelwise, monoexponential nonnegative least squares fit analysis. Statistical analyses regarding cartilage T2* and thickness changes and influencing factors were done on the finishers of the race.

RESULTS

With exception of the patellar joint, nearly all cartilage segments showed a significant initial mean T2* signal increase within the first 1500km run: ankle 25.6%, subtalar joint 20.9%, midtarsal joint 26.3%, femorotibial Joint (FTJ) 25.1 to 44.0%. Interestingly, an unexpected secondary T2* decrease was observed in ankle (-30.6%) and hindfoot joints (-28.5% and -16.0%), but not in the FTJ. A significant loss of cartilage thickness was detected in the FTJ, but not in the other joints. A side dependent, positive relationship between muscle volumes of the thigh and cartilage T2* at baseline could be found in the FTJ. Osteochondral lesions were detected, however all were already present at baseline and showed no changes throughout TEFR. Reasons for stopping the race were not associated with joint problems.

CONCLUSION

After initial significant intrachondral matrix changes, a subsequent T2* value recovery indicates the ability of the cartilage matrix to regenerate under ongoing running burden in ankle and hindfoot joints. In contrast, for the FTJ no T2* signal recovery could be observed accompanied by loss of cartilage thickness. No new lesions were observed during TEFR. Asymmetry of cartilage T2* behavior is in line with the hypothesis of the "breaking" limb and demonstrates leg-preference even in well-trained ultra-runners.

CLINICAL RELEVANCE/APPLICATION

The capability of most parts of human cartilage to recover in the presence of extreme physical stress has not been shown previously indicating a high regenerative potential of human joint cartilage.

SSC07-05 The Evaluation of Clinical Reliability and Speed of a Triple-echo Steady-state T2 Mapping for in Vivo Evaluation of Articular Cartilage in Comparison to Multi-echo Spin-echo Sequence

Monday, Nov. 30 11:10AM - 11:20AM Location: E450B

Participants

Vladimir Juras, BMedSc, PhD, Vienna, Austria (*Presenter*) Nothing to Disclose Klaus Bohndorf, MD, Augsburg, Germany (*Abstract Co-Author*) Nothing to Disclose Claudia Kronnerwetter, Vienna, Austria (*Abstract Co-Author*) Nothing to Disclose Pavol Szomolanyi, PhD, Vienna, Austria (*Abstract Co-Author*) Nothing to Disclose Stefan Zbyn, Vienna, Austria (*Abstract Co-Author*) Nothing to Disclose Siegfried Trattnig, MD, Vienna, Austria (*Abstract Co-Author*) Nothing to Disclose

PURPOSE

To assess the clinical relevance of T2 relaxation times, measured by 3D triple-echo steady-state (3D-TESS), in knee articular cartilage compared to conventional multi-echo spin-echo T2-mapping.

METHOD AND MATERIALS

Thirteen volunteers and ten patients with focal cartilage lesions were included in the study. All subjects underwent 3-Tesla MRI consisting of a multi-echo multi-slice spin echo sequence (CPMG) as a reference method for T2 mapping, and 3D TESS with the exact same geometry settings, but variable acquisition times: standard (TESSs 4:35 min) and quick (TESSq 2:05 min). T2 values were compared in six different regions in the femoral and tibial cartilage using a paired t-test and the Pearson correlation coefficient (r).

RESULTS

The mean quantitative T2 values measured by CPMG (mean: 46±9ms) in volunteers were significantly higher compared to those measured with TESS (mean: 31±5ms) in all regions. Both methods performed similarly in patients, but CPMG provided a slightly higher difference between lesions and native cartilage (CPMG: 90ms?61ms [31%],p=0.0125; TESS 32ms?24ms [24%],p=0.0839).

CONCLUSION

This work compared a newly developed 3D-TESS sequence with a CPMG method to evaluate T2-mapping of human articular

cartilage. 3D-TESS provided results comparable to CMPG with a substantially shorter acquisition time. This novel sequence may replace the conventional approach with CMPG

CLINICAL RELEVANCE/APPLICATION

3D-TESS T2 mapping provides clinically comparable results to CPMG in shorter scan-time Cartilage loading studies might benefit from high temporal resolution of 3D-TESS. 3D-TESS T2 values are able to differentiate between healthy and damaged cartilage

SSC07-06 A Comprehensive 7 Tesla Hip Cartilage Protocol Including Morphological and Quantitative MRI Techniques and Its Application in Patients after Acetabular Autologous Chondrocyte Transplantation

Monday, Nov. 30 11:20AM - 11:30AM Location: E450B

Participants

Andrea Lazik, MD, Essen, Germany (*Presenter*) Nothing to Disclose Oliver Kraff, MSc, Essen, Germany (*Abstract Co-Author*) Nothing to Disclose Konrad Koersmeier, Essen, Germany (*Abstract Co-Author*) Nothing to Disclose Soren Johst, Essen, Germany (*Abstract Co-Author*) Nothing to Disclose Christina Geis, Essen, Germany (*Abstract Co-Author*) Nothing to Disclose Harald H. Quick, PhD, Essen, Germany (*Abstract Co-Author*) Nothing to Disclose Jens M. Theysohn, MD, Essen, Germany (*Abstract Co-Author*) Nothing to Disclose

PURPOSE

To evaluate morphological and quantitative 7 Tesla MRI techniques for hip cartilage imaging in patients with acetabular cartilage lesions, treated by autologous chondrocyte transplantation (ACT).

METHOD AND MATERIALS

Hips of 11 healthy volunteers were examined to establish a 7T hip cartilage protocol including high-resolution DESS (0.7mm3 isotropic), T1 VIBE (0.4x0.4x0.8mm3) and PDw sequences (sagittal and coronal) for morphological imaging, multi-contrast sequences (5 echoes) for T2- and T2*-mapping and a dual flip angle technique for T1-mapping prior to and after contrast agent administration following a dGEMRIC-protocol. Accurate and reproducible scan-rescan conditions were monitored with a fast B1-mapping technique (DREAM). After reviewing image quality by means of acetabular and femoral cartilage delineation (4-point scale, 4 being best) and comparing relaxation times in correlating regions (Pearson's correlation) this protocol was applied in 9 patients treated by ACT. Here, over-all image quality, delineation of the cartilage transplants and their relaxation times were compared to 3T MRI.

RESULTS

Volunteer study: The delineation of acetabular and femoral cartilage was excellent in T2- (3.2 ± 0.9) and T2*-maps (3.2 ± 0.4) . Gadolinium improved cartilage delineation in T1-maps $(2.9\pm0.8 \text{ vs. } 1.7\pm0.6)$ as well as in T1 VIBE $(3.3\pm0.6 \text{ vs. } 2.2\pm0.9)$. T1-, T2and T2*-relaxation times showed a high correlation in unenhanced and contrast-enhanced sequences (all p<0.001) in volunteers with mean values of 931ms (T1 enhanced), 43ms (T2) and 15ms (T2*).Patient study: Compared to 3T, image quality at 7T was clearly superior in sagittal PDw, T1 VIBE, DESS and T1-mapping with enhanced delineation of the transplants. Mean relaxation times of the cartilage transplants were reduced at 7T comparted to 3T for T1 (537 vs. 757ms), T2 (42 vs. 45ms) and T2* (11 vs. 14ms).

CONCLUSION

A comprehensive hip cartilage protocol after contrast agent administration was established at 7T MRI, including morphological sequences as well as T1-mapping for dGEMRIC, T2- and T2*-mapping. The application of this protocol in patients after ACT showed predominantly superior image quality with better evaluation of the cartilage transplants compared to 3T.

CLINICAL RELEVANCE/APPLICATION

7 Tesla can help to noninvasively follow up patients after acetabular cartilage transplantation, as imaging of the thin and spherical shaped hip cartilage remains challenging at lower field strengths.

SSC07-07 Quantitative T2* Analysis of Articular Cartilage of the Tibiotalar Joint in Professional Soccer Players and Healthy Individuals at 3T MRI

```
Monday, Nov. 30 11:30AM - 11:40AM Location: E450B
```

Participants

Marc Regier, Hamburg, Germany (*Presenter*) Nothing to Disclose Cyrus Behzadi, Hamburg, Germany (*Abstract Co-Author*) Nothing to Disclose Azien Laqmani, Hamburg, Germany (*Abstract Co-Author*) Nothing to Disclose Chressen C. Remus, MD, Hamburg, Germany (*Abstract Co-Author*) Nothing to Disclose Michael G. Kaul, Hamburg, Germany (*Abstract Co-Author*) Nothing to Disclose Gerhard B. Adam, MD, Hamburg, Germany (*Abstract Co-Author*) Nothing to Disclose

PURPOSE

To quantitatively evaluate the tibiotalar cartilage of professional soccer players by T2* relaxation measurements in comparison to age-matched healthy volunteers.

METHOD AND MATERIALS

Using a 3T MRI system both ankles of 20 elite professional soccer players from the highest european level and 20 age-matched healthy individuals were investigated. After resting in supine position for 30 minutes, all individuals were examined appliying multiplanar T1w and Pdw sequences. For quantitative measurements a 3D T2* (24 echoes ranging from 4.6-52.9ms; image resolution 0.5x2x2mm) sequence was performed in sagittal orientation. Using a dedicated software tool (ImageJ) data were postprocessed and quantitative maps were generated. The articular cartilage was subdivided into 6 areas and regions-of-interest (ROI) were manually placed in all zones of the tibial and talar cartilage. For statistical workup Pearson product-moment correlation coefficients and confidence intervals were calculated.

RESULTS

In professional soccer players the T2* values were significantly higher in all tibial and talar compartments than those in healthy participants (mean, 21.36ms vs. 16.44ms; p<0.001). This difference was most evident in the posterior zones of the tibiotalar cartilage. In the athletes, there was a trend towards higher T2* values at the anterior medial compartments of the articular cartilage, however, compared to the healthy control group this was not statistically significant (p,0.08).

CONCLUSION

Based on these initial results, T2* values of the tibiotalar joint seem to be elevated in professional soccer players compared to an age-matched control group indicating cartilage degeneration. T2* measurements might potentially serve as a quantitative noninvasive tool for the detection of articular cartilage lesions at early stage.

CLINICAL RELEVANCE/APPLICATION

Quantitative MR imaging of tibiotalar articular cartilage using T2* measurements could serve as a complementary tool for early detection of subtle cartilage defects and further investigation should be encouraged.

SSC07-08 MRI-T2 Mapping Assessment after Treatment of Knee Osteoarthritis with Mesenchymal Stem Cells at One Year Follow-up

Monday, Nov. 30 11:40AM - 11:50AM Location: E450B

Participants

Joan C. Vilanova, MD, PhD, Girona, Spain (*Presenter*) Nothing to Disclose Marina Huguet, MD, Barcelona, Spain (*Abstract Co-Author*) Nothing to Disclose Lluis Orozco, Barcelona, Spain (*Abstract Co-Author*) Nothing to Disclose Robert Soler, Barcelona, Spain (*Abstract Co-Author*) Nothing to Disclose Anna Munar, Barcelona, Spain (*Abstract Co-Author*) Nothing to Disclose

PURPOSE

To confirm the feasibility of osteoarthritis treatment with mesenchymal stem cells (MSCs) in humans, and to demonstrate its efficacy on MRI and clinical outcome on a larger population with osteoarthritis of the knee

METHOD AND MATERIALS

Fifty patients with clinical and radiologic diagnosis of osteoarthritis of the knee (graded according to the ICRS (International Cartilage Repair Society) were treated with autologous MSCs by intrarticular injection. Clinical outcomes were followed for 1 year (including pain, disability, and quality of life). Cartilage assessment was performed using MRI T2-mapping at 88 pre-determined anatomical regions previous to treatment at 12 months after treatment; by determining the T2 relaxation values (RV) in each region of the knee. Inter, intraobserver and equipment errors were calculated for reproducibility, and for the statistical analysis to determine significant differences on T2 RV's before and after treatment. Statistical analysis was performed by Students t-test or by one-way analysis of variance (ANOVA) and the corresponding non-parametric tests

RESULTS

The mean T2 RV's (ms) previous to treatment (mean±SD) (60.3 ± 6.1) was significantly higher than at 12 months (53.1 ± 6.2) (p<0.04). A positive correlation was identified between the baseline mean average T2 RV's and the mean final average (ms) improvement T2 RV's score (r=0.38; p<0.05). T2 RV's decreased in 37 of 50 patients, 10 remained the same and 3 worsened between 7 and 10%. The median pain reduction was 60% for daily activities and 63% for sport activities. A good positive correlation was observed between the amount of clinical improvement and the initial score (r=0.49), (P<0.001)

CONCLUSION

Non-invasive technique MRI T2-mapping is a valuable tool to assess the follow up of cartilage after MSC therapy for knee osteoarthritis

CLINICAL RELEVANCE/APPLICATION

Stem cell therapy could be an effective, feasible and safe treatment for knee osteoarthritis; and MRI T2-mapping can be a useful imaging biomarker tool to correlate and assess the clinical outcome

SSC07-09 Prevalent Partial and Full-thickness Focal Cartilage Defects Predict Cartilage Damage Progression in the Same Subregion and Development of Incident Cartilage Damage in the Same Tibiofemoral Compartment: The MOST Study

Monday, Nov. 30 11:50AM - 12:00PM Location: E450B

Participants

Ali Guermazi, MD, PhD, Boston, MA (*Presenter*) President, Boston Imaging Core Lab, LLC; Research Consultant, Merck KgaA; Research Consultant, Sanofi-Aventis Group; Research Consultant, TissueGene, Inc; Research Consultant, OrthoTrophic; Research Consultant, AstraZeneca PLC Daichi Hayashi, MBBS, PhD, Bridgeport, CT (*Abstract Co-Author*) Nothing to Disclose Frank W. Roemer, MD, Boston, MA (*Abstract Co-Author*) Chief Medical Officer, Boston Imaging Core Lab LLC Research Director, Boston Imaging Core Lab LLC Shareholder, Boston Imaging Core Lab LLC

Emily K. Quinn, Boston, MA (*Abstract Co-Author*) Nothing to Disclose Michel D. Crema, MD, Boston, MA (*Abstract Co-Author*) Shareholder, Boston Imaging Core Lab, LLC

David T. Felson, MD, MPH, Boston, MA (*Abstract Co-Author*) Consultant, Zimmer Holdings, Inc

PURPOSE

To assess if depth of focal cartilage damage affects the risk of incidence and progression of cartilage loss in the tibiofemoral joint (TFJ).

Persons with or at high risk of knee OA with MRI readings at baseline and 30-month were included. Semiquantitative MRI analysis was done using the Whole Organ MRI Score (WORMS) for cartilage damage, meniscal damage and extrusion, bone marrow lesions (BMLs), effusion and synovitis. Baseline focal cartilage damage was defined as grade 2 (partial-thickness) or grade 2.5 (full-thickness). In a subregion-based analysis, we assessed the risk of cartilage loss over 30 months comparing subregions of TFJ with baseline cartilage grade 2.5 vs grade 2. In the compartment-based analysis, we included only knees with a solitary grade 2 or 2.5 lesion at baseline and all other subregions in the same compartment having no cartilage damage. We estimated the risk of incident cartilage loss (grade \geq 2) in any non-damaged subregions for compartments with baseline full-thickness and partial thickness defects. In addition knees or compartments with grade 2 and 2.5 cartilage damage at baseline were compared to those without. Logistic regression was used to account for correlations among multiple subregions/compartments within a knee.

RESULTS

927 subregions (683 knees) were included in the subregion-based analysis. Risk of cartilage damage progression for grade 2.5 lesions compared to grade 2 lesions were comparable. However, compared to subregions with no cartilage damage, subregions with grade 2 or 2.5 cartilage defects had higher risk for cartilage loss (aOR 8.2, 95%CI 6.7-10.0). 374 compartments were included in the compartment-based analysis. There was no significant difference in regard to risk of incident damage between compartments that had grade 2 and grade 2.5 cartilage defects at baseline. However, compared to compartments with no baseline cartilage damage, those with grade 2 or 2.5 cartilage defects in a subregion had higher risk for incident cartilage damage in other subregions at follow-up (aOR 1.7, 95%CI 1.2-2.5).

CONCLUSION

Prevalent focal cartilage defects are a risk factor for local cartilage damage progression in the same subregion and increase risk for development of incident cartilage damage in the same TFJ compartment regardless of defect depth.

CLINICAL RELEVANCE/APPLICATION

Even small superficial cartilage lesions are relevant for cartilage damage progression.

Honored Educators

Presenters or authors on this event have been recognized as RSNA Honored Educators for participating in multiple qualifying educational activities. Honored Educators are invested in furthering the profession of radiology by delivering high-quality educational content in their field of study. Learn how you can become an honored educator by visiting the website at: https://www.rsna.org/Honored-Educator-Award/

Ali Guermazi, MD, PhD - 2012 Honored Educator

Neuroradiology (Parkinson Disease)

Monday, Nov. 30 3:00PM - 4:00PM Location: N228

NR BQ

AMA PRA Category 1 Credit [™]: 1.00 ARRT Category A+ Credit: 1.00

Participants

Christopher P. Hess, MD, PhD, Mill Valley, CA (*Moderator*) Research Grant, General Electric Company; Research Grant, Quest Diagnostics Incorporated; Research Grant, Cerebrotech Medical Systems, Inc; Jay J. Pillai, MD, Baltimore, MD (*Moderator*) Medical Advisory Board, Prism Clinical Imaging, Inc; Author with royalties, Springer Science+Business Media Deutschland GmbH; Author with royalties, Reed Elsevier

Sub-Events

SSE17-01 A Voxel-based Evaluation of Parkinson's Disease Using Quantitative Susceptibility Mapping and Neuromelanin Imaging

Monday, Nov. 30 3:00PM - 3:10PM Location: N228

Participants

Hiroto Takahashi, MD, Suita, Japan (*Presenter*) Nothing to Disclose Yoshiyuki Watanabe, MD, PhD, Suita, Japan (*Abstract Co-Author*) Nothing to Disclose Hisashi Tanaka, MD, Suita, Japan (*Abstract Co-Author*) Nothing to Disclose Masashi Mihara, Suita, Japan (*Abstract Co-Author*) Nothing to Disclose Yi Wang, PhD, New York, NY (*Abstract Co-Author*) Nothing to Disclose Noriyuki Tomiyama, MD, PhD, Suita, Japan (*Abstract Co-Author*) Nothing to Disclose Hiroki Kato, Suita, Japan (*Abstract Co-Author*) Nothing to Disclose Atsuko Arisawa, MD, Suita, Japan (*Abstract Co-Author*) Nothing to Disclose Chisato Matsuo, MD, Suita, Japan (*Abstract Co-Author*) Nothing to Disclose Tian Liu, PhD, New York, NY (*Abstract Co-Author*) Nothing to Disclose Hideki Mochizuki, Suita, Japan (*Abstract Co-Author*) Nothing to Disclose

PURPOSE

To assess dopaminergic neurodegeneration with iron deposition of the substantia nigra pars compacta (SNpc) in patients with Parkinson's disease (PD) in a quantitative and reproducible fashion.

METHOD AND MATERIALS

This study included 14 patients with PD (Group A) and 14 normal controls (Group B) who underwent quantitative susceptibility mapping (QSM), neuromelanin (NM) imaging and three-dimensional (3D) T1W imaging on a 3T magnetic resonance imager. Both QSM and NM values of the SNpc were calculated using a region of interest (ROI) based automated segmentation system with the voxel-based morphometric technique. Images were preprocessed as follows (Figure): All QSM and NM images were coregistered with 3D T1-weighted structural images and were spatially normalized using Statistical Parametric Mapping, thus allowing voxel-based measurement with automatic setting of the ROI encompassing the SNpc. The spatially normalized images of all subjects were smoothed. Finally, the SNpc ROI was set on the QSM-NM fused image. Signal to noise ratio (SNR) of the SNpc in the NM images was calculated on the basis of mean value of the automatically segmented background region (tegmentum in the midbrain). The significance of intergroup differences in each QSM value and NM area of higher SNR than that of the background region was tested using Mann-Whitney's U test.

RESULTS

For mean QSM value of the SNpc, no significant difference was shown between both groups [Group A/B: mean value (ppb) = 75.72/64.62, SD = 21.24/27.75]. But when comparing the highest 5% of QSM values in each group, the mean in Group A was significantly larger than that in Group B [Group A/B: mean value (ppb) = 175.21/133.33, SD = 45.44/41.75] (P < 0.05). The NM area of higher SNR in Group A was significantly less than that in Group B [Group A/B: mean value (pixel) = 85.79/104.07, SD = 13.66/13.56] (P < 0.05).

CONCLUSION

An automatic measurement system for structural and functional changes in the SNpc with voxel-based analysis can provide clinically useful information in the diagnosis of PD.

CLINICAL RELEVANCE/APPLICATION

SNpc is a small region, but can be assessed quantitatively and reproducibly with voxel-based analysis in the diagnosis of Parkinson's disease.

SSE17-02 Drug-induced Parkinsonism versus Idiopathic Parkinson's Disease: Diagnostic Utility of Nigrosome 1 MRI at 3T

Monday, Nov. 30 3:10PM - 3:20PM Location: N228

Participants

Min Ju Jung, Incheon, Korea, Republic Of (*Presenter*) Nothing to Disclose Eung Yeop Kim, MD, Incheon, Korea, Republic Of (*Abstract Co-Author*) Nothing to Disclose Byong Ho Goh, Incheon, Korea, Republic Of (*Abstract Co-Author*) Nothing to Disclose Young Hee Seong, MD, Incheon, Japan (*Abstract Co-Author*) Nothing to Disclose Young Noh, Incheon, Korea, Republic Of (*Abstract Co-Author*) Nothing to Disclose

PURPOSE

Discrimination between drug-induced parkinsonism (DIP) and idiopathic Parkinson's disease (IPD) is challenging because they may be clinically indistinguishable. Dopamine transporter imaging can help differentiate them, but it is expensive and imposes radiation on patients. We hypothesized that the nigrosome 1 is not affected in patients with DIP unlike in those with PD. The aim of this study was to investigate whether nigrosome 1 imaging at 3T can help differentiate PD from DIP.

METHOD AND MATERIALS

We enrolled 20 patients with DIP (16 female; mean age, 74) who showed normal activity on 18F-FP-CIT PET (CIT PET), 29 patients with IPD (10 female; mean age, 71; HandY stage \leq 2) who showed abnormality on CIT PET, and 18 healthy subjects (10 female; mean age, 66). All participants underwent 3D multi-echo gradient-recalled echo imaging (number of echoes, 6) covering the midbrain parallel to the plane from the posterior commissure and top of the pons (spatial resolution, $0.5 \times 0.5 \times 1$ mm). Two independent reviewers assessed nigrosome 1 on three slices: an upper slice at the lower tip of red nucleus, and two successive lower slices by comparing the signal intensity of the central portion of the nigrosome 1 with that of the white matter lateral to decussation of the superior cerebellar peduncles. Relative hypointensity in either side of nigrosome 1 was considered abnormal. Interobserver observer agreement, diagnostic sensitivity, specificity, and accuracy were analyzed.

RESULTS

Inter-rater agreement was excellent ($\kappa = 0.821$). All 29 patients with IPD and three of 18 healthy subjects were rated as abnormal on nigrosome 1 MRI (sensitivity, 100%; specificity, 83.3%; accuracy, 93.6%; positive predictive value [PPV], 90.6%; negative predictive value [NPV], 100% between the patients with IPD and healthy subjects). Three of 20 patients with DIP were considered abnormal on nigrosome 1 MRI (sensitivity, 100%; specificity, 85%; accuracy, 93.9%; PPV, 90.6%; NPV, 100% between the patients with IPD and DIP). Abnormality on MRI was significantly more frequent in patients with IPD (P < 0.0001).

CONCLUSION

Nigrosome 1 imaging at 3T can differentiate IPD from DIP with accuracy of 93.9%.

CLINICAL RELEVANCE/APPLICATION

High diagnostic accuracy and perfect NPV of nigrosome imaging at 3T between patients with IPD and DIP can help manage them properly and may reduce dependence on dopamine transporter imaging.

SSE17-03 The Pattern of Iron Deposition in the Progression of Parkinson's Disease by Quantitative Susceptibility Mapping

Monday, Nov. 30 3:20PM - 3:30PM Location: N228

Participants

Xiaojun Guan, Hangzhou, China (*Presenter*) Nothing to Disclose Min Xuan, HangZhou, China (*Abstract Co-Author*) Nothing to Disclose Quanquan Gu, MD, PhD, Hangzhou, China (*Abstract Co-Author*) Nothing to Disclose Chunlei Liu, PhD, Durham, NC (*Abstract Co-Author*) Nothing to Disclose Peiyu Huang, Hangzhou, China (*Abstract Co-Author*) Nothing to Disclose Xu Xiaojun, Hangzhou, China (*Abstract Co-Author*) Nothing to Disclose Wei Luo, Hangzhou, China (*Abstract Co-Author*) Nothing to Disclose Minming Zhang, MD, PhD, Hangzhou, China (*Abstract Co-Author*) Nothing to Disclose

PURPOSE

The influence of iron on the pathophysiological progression of Parkinson's disease (PD) and the pattern of iron accumulation in the subregions of substantia nigra (SN) were unclear. In the present cross-section study, we aimed to clarify the potential pattern of iron deposition in the subcortical nuclei, especially in the SN, among the controls and PD subgroups, thus the possible underlying iron-related pathogenesis of PD.

METHOD AND MATERIALS

Forty-eight PD patients (H-Y stage <= 2.5, n=16, belonged to mild subgroup; H-Y stage >= 3, n=32, belonged to severe subgroup), and 47 gender-, age-, duration- matched healthy controls were included in our study. All subjects participated in the 3D-enhanced T2 star weighted angiography (ESWAN) scanning. The phase images of ESWAN data were processed to generate quantitative susceptibility mapping (QSM). Then, we measured the iron content within the ROIs and the relevant clinical assessments of these patients.

RESULTS

After controlling for age as a covariant (Bonfferoni corrected), QSM values within the medSNc and latSNc increased significantly in both PD subgroups compared with controls respectively (both p<0.01), while QSM values within medSNr (p<0.01) and latSNr (p<0.05) only increased in the severe subgroup of PD. More interestingly, medSNc had higher iron content in the severe group of PD than the mild one (p<0.05), while that could not observe in the latSNc. Further, in the severe subgroup iron content within medSNr (p<0.01) and latSNr (p<0.01) and latSNr (p<0.05) elevated greatly compared with the mild subgroup.

CONCLUSION

Due to the limitation of present study, which recruited symptomatic patients, we didn't observe the presymptomatic or early changes in the latSNc between 2 PD subgroups. After all, we had investigated the dynamic pattern of iron deposition in the SN during the progression of PD, which was perfectly consistent with the work of Fearnley JM (Brain 1991). As the disease proceeding, the iron deposition accumulated first in the latSNc (Martin W.R. et al., 2008), and then involved the medSNc, finally reached the medSNr and latSNr.

CLINICAL RELEVANCE/APPLICATION

Firstly, present work would help understand the possible pathogenesis of PD indirectly; secondly, the pattern of iron deposition would indicate the imaging biomarker of early diagnosis of PD.

Resting State Functional Connectivity in Parkinson's Patients with Implanted Deep Brain Stimulation Electrodes

Monday, Nov. 30 3:30PM - 3:40PM Location: N228

Subhendra N. Sarkar, PhD, RT, Boston, MA (*Presenter*) Nothing to Disclose Neda I. Sedora-Roman, MD, Boston, MA (*Abstract Co-Author*) Nothing to Disclose Michael D. Fox, Boston, MA (*Abstract Co-Author*) Nothing to Disclose Ron L. Alterman, MD, Boston, MA (*Abstract Co-Author*) Nothing to Disclose Fernando A. Barrios, PhD, Juriquilla, Mexico (*Abstract Co-Author*) Nothing to Disclose David B. Hackney, MD, Boston, MA (*Abstract Co-Author*) Nothing to Disclose Rafeeque A. Bhadelia, MD, Chestnut Hill, MA (*Abstract Co-Author*) Nothing to Disclose Rafael Rojas, MD, Chestnut Hill, MA (*Abstract Co-Author*) Nothing to Disclose

PURPOSE

rs-fcMRI, if performed within MR safety limits, could help evaluate electrode placement and the effects of DBS on brain connectivity for Parkinson's patients. However, fMRI traditionally requires high speed and high field MRI violating RF and gradient safety for DBS (1).

METHOD AND MATERIALS

10 PD patients with DBS electrodes were imaged within MR safety limits (SAR <0.1 W/kg, dB/dT <20 mT/S, B0=1.5T) by single-shot EPI (TR/TE/Voxel/# brain volumes = 3-4s/50ms /4x4x5mm3 /interleaved/100-120 volumes/ scan time 6 min). 5 PD patients prior to DBS implantation were imaged at high SAR (>0.8 W/kg, 3T) by a single-shot EPI (TR/TE/Voxel/whole brain volumes = 2s/30ms /3.4x3.4x3.4xm3 /interleaved/100-140 volumes/ scan time 3-4 min/2-3 runs).Motion corrected, normalized images were corregistered with 3D MPRAGE using SPM. Several resting state networks were computed (default mode/DMN, executive control/ECN and sensory motor/SMN) using common seed regions and CONN rs-fMRI processing algorithm(2). The networks for low and high SAR groups were averaged and objectively compared by two independent readers.

RESULTS

The group average network images at low SAR were similar to those imaged pre-DBS at high SAR. The spatial correlation coefficients between the high and low SAR for each network were: DMN 0.70, ECN 0.64 and SMN 0.64, supporting the maps similarities.Zhang et al (3) have shown that PD patients with Tremor show increased centrality in rs networks in frontal, parietal and occipital lobes that are supported by our results although low SAR maps were weaker perhaps due to the susceptibility from electrodes. Anticorrelations among networks were also preserved at low SAR even after using global regressors that are quite acceptable (4).

CONCLUSION

High quality rs fc-MRI images can be safely obtained at 1.5T at about10% of routine SAR at high fields. Abnormal brain connectivity may be used to modulate DBS settings.Resting state fc-MRI is promising toward understanding and manipulating the stimulation effects on brain cognition and motor control in refractory PD.Reference(1) Kahan et al Brain Feb 2014; (2) Whitfield-Gabrieli et al Neuroimage 2011; (3) Zhang et al Front. Aging Neurosc 2015; (4) Chai et al Neuroimage 2012

CLINICAL RELEVANCE/APPLICATION

High quality resting state fc images can be obtained for DBS patients within MR safety margin, with device programming and understanding stimulation effects on brain connectivity in refractory PD.

SSE17-05 Chemical Exchange Saturation Transfer Signal of the Substantia Nigra as Imaging Biomarker for Assessing Progression of Parkinson's Disease

Monday, Nov. 30 3:40PM - 3:50PM Location: N228

Participants

Chunnei Li, MD, Beijing, China (*Presenter*) Nothing to Disclose Na X. Zhao, PhD, Beijing, China (*Abstract Co-Author*) Nothing to Disclose Jinyuan Zhou, PhD, Baltimore, MD (*Abstract Co-Author*) Nothing to Disclose Min Chen, MD, PhD, Beijing, China (*Abstract Co-Author*) Nothing to Disclose

PURPOSE

To evaluate chemical-exchange-saturation-transfer (CEST) signal of the substantia nigra (SN) in Parkinson's disease (PD) patients, as well as their relationship to clinical progression.

METHOD AND MATERIALS

CEST MR imaging of 26 normal controls and 61 PD patients [18 early stage (disease duration \leq 1 year), 19 mid stage (disease duration 2~5 years) and 24 late stage (disease duration \geq 6 years)] were acquired on a Philips 3 Tesla MRI system. Magnetization transfer spectra with 31 different frequency offsets (-6 to 6 ppm) were acquired at the slice of the SN. The FLAIR image was used as the anatomical reference to draw regions of interest. MTRasym(3.5ppm) and MTRtotal (the integral of the MTRasym spectrum in the range of 0 to 4 ppm) of the total SN were measured. Clinical measures were obtained for PD patients, such as the Hoehn and Yahr (HandY) scale and the unified Parkinson's disease rating scale (UPDRS), etc. One-way ANOVA was used to compare the CEST signal differences between normal controls and PD patients of all stages. Correlation analysis was made for the CEST signal of SN and clinical progression.

RESULTS

Compared to normal controls, the MTRasym(3.5ppm) and MTRtotal values of the SN were significantly lower in PD patients of all stages. Both the MTRasym(3.5ppm) and MTRtotal values of the SN strongly associated with HandY scale, UPDRS, UPDRS-3 and disease duration.

CONCLUSION

CECT signal of the CN has the extential to some as imaging hismarker for accessing progression of DD

CEST SIGNAL OF THE SIN HAS THE POTENTIAL TO SERVE AS IMAGING DIOMATKET FOR ASSESSING PROGRESSION OF PD.

CLINICAL RELEVANCE/APPLICATION

CEST signal could provide information additional to conventional MR imaging and potentially serve as imaging biomarker in the progression assessment of PD.

SSE17-06 Multivariate Pattern Analysis of Paroxysmal Kinesigenic Dyskinesia Using Diffusion Tensor Imaging

Monday, Nov. 30 3:50PM - 4:00PM Location: N228

Participants

Lei Li, Chengdu, China (*Presenter*) Nothing to Disclose Xinyu Hu, Chengdu, China (*Abstract Co-Author*) Nothing to Disclose Du Lei, Chengdu, China (*Abstract Co-Author*) Nothing to Disclose Xueling Suo, Chengdu, China (*Abstract Co-Author*) Nothing to Disclose Xiaoqi Huang, MD, Chengdu, China (*Abstract Co-Author*) Nothing to Disclose Dong Zhou, ChenDu, China (*Abstract Co-Author*) Nothing to Disclose Qiyong Gong, Chengdu, China (*Abstract Co-Author*) Nothing to Disclose

PURPOSE

Paroxysmal kinesigenic dyskinesia (PKD) is a rare movement disorder. Available researches using diffusion tensor imaging (DTI) have shown that PKD is accompanied by abnormalities in white matter (WM). However, results of those publications were based on average differences between groups, which permitted little use in clinical practice. Multivariate pattern analysis (MVPA) approach is a promising analytical technique which allows the classification of individual observations into distinct classes. Thus, in current study, we aimed to (i) apply MVPA approach known as Support Vector Machine (SVM) for investigating whether fractional anisotropy (FA) of WM can be used to discriminate between patients with PKD and healthy control subjects (HCS) at the level of the individual; (ii) explore which WM regions contributed to such discrimination.

METHOD AND MATERIALS

DTI data were acquired from 48 PKD patients and 48 demographically matched HCS using a 3T MRI system. Differences in FA values of WM were used to discriminate between PKD patients and HCS using leave-one-out cross-validation with SVM based on Probid software (http://www.brainmap.co.uk/probid.htm), and to find a spatially distributed pattern of regions with maximal classification weights. We also drew a receiver operating characteristic (ROC) curve to help evaluate the performance of the classifier.

RESULTS

SVM applied to FA images correctly identified PKD patients with a sensitivity of 91.67% and a specificity of 87.50% resulting in a statistically significant accuracy of 89.58% (P <0.001). This discrimination was based on a distributed network including anterior thalamic radiation temporoparietal junction, inferior fronto-occipital fasciculus, inferior longitudinal fasciculus, corpus callosum, and cingulum.

CONCLUSION

The present study demonstrates subtle and spatially distributed WM abnormalities in individuals with PKD, indicating neuroanatomical basis for the involvement of the basal ganglia-thalamocortical pathway in PKD, and provides preliminary support for the suggestion that SVM approach could be used to aid the identification of individuals with PKD in clinical practice.

CLINICAL RELEVANCE/APPLICATION

The current study illustrated that the application of SVM to FA images could allow accurate discrimination between PKD patients and HCS, which indicated its potential diagnostic value in helping detecting this disease.

Special Interest Session: Radiology and Pathology Diagnostics: Examples in Practice

Monday, Nov. 30 4:30PM - 6:00PM Location: E352

BQ

AMA PRA Category 1 Credits ™: 1.50 ARRT Category A+ Credits: 1.50

Participants

Mitchell D. Schnall, MD, PhD, Philadelphia, PA (Moderator) Nothing to Disclose

LEARNING OBJECTIVES

1) Explain the concepts of integrated radiology and pathology reports. 2) Outline how computers can extract information from pathology and radiology images to improve cancer diagnosis. 3) Develop integrated diagnostic pathways.

Sub-Events

SPSI22A Integrated Diagnostic Pathways

Participants

Mitchell D. Schnall, MD, PhD, Philadelphia, PA (Presenter) Nothing to Disclose

LEARNING OBJECTIVES

View learning objectives under main course title.

Honored Educators

Presenters or authors on this event have been recognized as RSNA Honored Educators for participating in multiple qualifying educational activities. Honored Educators are invested in furthering the profession of radiology by delivering high-quality educational content in their field of study. Learn how you can become an honored educator by visiting the website at: https://www.rsna.org/Honored-Educator-Award/

Mitchell D. Schnall, MD, PhD - 2013 Honored Educator

SPSI22B Combined Radiology/Pathology Phenotype Biomarkers

Participants

Anant Madabhushi, MS, Piscataway, NJ (*Presenter*) Research partner, Siemens AG Research partner, General Electric Company Research partner, F. Hoffmann-La Roche Ltd Founder and President, IbRiS, Inc

LEARNING OBJECTIVES

View learning objectives under main course title.

SPSI22C Integrated Pathology and Radiology Reporting Tool

Participants Patricia Goede, PhD, Salt Lake City, UT, (pgoede@xifin.com) (*Presenter*) Employee, XIFIN, Inc

LEARNING OBJECTIVES

View learning objectives under main course title.

ABSTRACT

Clinical collaboration across multidisciplinary teams from radiology, pathology and oncology has a significant role in the diagnostic and treatment planning process. Specialists and sub-specialists rely on the ability to view imaging and findings together for diagnosis, clinical correlation and treatment planning. The following paper proposes a patient centric model and tools for image management, collaboration and a use case for integrated continuity of care (CCD) reporting.

SPSI22D Integrated Radiology and Pathology Reporting

Participants Dieter R. Enzmann, MD, Los Angeles, CA (*Presenter*) Nothing to Disclose

LEARNING OBJECTIVES

View learning objectives under main course title.

Hot Topic Session: Quantitative MR Biomarkers in the MSK System

Tuesday, Dec. 1 7:15AM - 8:15AM Location: E350



FDA Discussions may include off-label uses.

Participants

Martin Torriani, MD, Boston, MA (Moderator) Nothing to Disclose

LEARNING OBJECTIVES

1) To discuss how MRI-based cartilage mapping techniques yield biomarkers of cartilage integrity, and discuss the technical requirements and current indications for clinical use of these methods. 2) To describe the emerging capabilities of high-resolution MR imaging to examine bone microarchitecture and its potential in providing biomarkers of bone strength. 3) To discuss potential applications of MR spectroscopy in musculoskeletal neoplasms and fat quantification of musculoskeletal tissues such as marrow and muscle.

ABSTRACT

There is strong incentive to increase the role of quantitative techniques in clinical musculoskeletal imaging, especially applications related to cartilage health, bone structure, tumor and metabolic imaging. This Hot Topic session will discuss clinical applications of biomarkers of cartilage integrity (T1rho, T2, T2* and dGEMRIC), bone structure by high-resolution MRI, and tissue metabolism (MR spectroscopy for tumor imaging, muscle and marrow fat content).

Sub-Events

SPSH30A T2, T2*, T1rho and dGEMRIC as Biomarkers of Cartilage Integrity

Participants

Thomas M. Link, MD, PhD, San Francisco, CA, (thomas.link@ucsf.edu) (*Presenter*) Research funded, General Electric Company; Research funded, InSightec Ltd; Royalties, Springer Science+Business Media Deutschland GmbH; Research Consultant, Pfizer Inc;

LEARNING OBJECTIVES

1) To define how T2, T2*, T1rho and dGEMRIC quantitatively assess cartilage matrix composition. 2) To describe the requirements for applying these quantitative measurements to clinical imaging. 3) To critically assess previous clinical studies and list indications for using quantitative cartilage imaging biomarkers.

SPSH30B Bone Microarchitecture by MRI

Participants

Gregory Chang, MD, New York, NY (Presenter) Speaker, Siemens AG

LEARNING OBJECTIVES

1) To define bone microarchitecture and its contribution to bone strength and fracture risk. 2) To describe the technical requirements for MRI of bone microarchitecture, including hardware, pulse sequences, and image post-processing. 3) To provide an overview of clinical studies of MRI of bone microarchitecture.

SPSH30C MR Spectroscopy of the Musculoskeletal System

Participants Martin Torriani, MD, Boston, MA (*Presenter*) Nothing to Disclose

LEARNING OBJECTIVES

1) To define how MR spectroscopy quantitatively measures tissue biochemistry. 2) To describe general guidelines for usage of MR spectroscopy in musculoskeletal clinical imaging, including technical factors, quantification/analysis and interpretation. 3) To assess the state-of-the-science in regards to the use of MR spectroscopy for musculoskeletal tissues.

PET-MR/Hyperpolarized MR

Tuesday, Dec. 1 8:30AM - 10:00AM Location: S504CD

MR NM BQ

AMA PRA Category 1 Credits ™: 1.50 ARRT Category A+ Credits: 1.50

FDA Discussions may include off-label uses.

Participants

Heike E. Daldrup-Link, MD, Palo Alto, CA (Moderator) Nothing to Disclose

Sub-Events

RC317A Hyperpolarized 13C MR-A Complementary Method to PET for Imaging in Vivo Metabolism

Participants

Daniel M. Spielman, PhD, Stanford, CA (Presenter) Nothing to Disclose

LEARNING OBJECTIVES

1) Assess the basic principles of hyperpolarized 13C MRS, including sample preparation, image acquisition, and data analysis. 2) Differentiate metabolic parameters measurable by hyperpolarized 13C MRS from though obtained with PET. 3) Compare PET versus hyperpolarized 13C MRS sensitivities, spatial resolution, and temporal resolution.

RC317B PET/MR: Applications in Clinical Imaging

Participants

Karin A. Herrmann, MD, PhD, Cleveland, OH (Presenter) Nothing to Disclose

LEARNING OBJECTIVES

1) To understand technical limitations, workflow and current challenges of PET/MR compared to PET/CT. 2) To learn about most successful applications of PET/MR in clinical practice. 3) To be informed about the incremental value of PET/MR over current imaging strategies in selected clinical scenarios. 4) Identify appropriate clinical indications for PET/MR in current clinical practice. 5) Understand and manage procedural and logistic challenges of PET/MR.

RC317C The Emerging Clinical Role of Hyperpolarized ¹³C MR in Prostate Cancer Imaging

Participants

John Kurhanewicz, PhD, San Francisco, CA (Presenter) Nothing to Disclose

LEARNING OBJECTIVES

1) Understand the clinical need and biochemical rationale for the use of hyperpolarized [1-13C] pyruvate for prostate cancer imaging. 2) Demonstrate a multi-hyperpolarized probe approach for simultaneously measuring prostate cancer metabolism and tumor micro-environment. 3) Demonstrate the utility of hyperpolarized 13C MR for measuring prostate cancer aggressiveness and response to therapy. 4) Demonstrate the safety, clinical feasibility, sensitivity and resolution, and future availability of clinical hyperpolarized 13C MR.

Quantitative Imaging Mini-course: Modality Independent Issues

Tuesday, Dec. 1 8:30AM - 10:00AM Location: S502AB

BQ CT PH

AMA PRA Category 1 Credits ™: 1.50 ARRT Category A+ Credits: 1.50

Participants

Michael F. McNitt-Gray, PhD, Los Angeles, CA (*Director*) Institutional research agreement, Siemens AG; Research support, Siemens AG; ; ; ; ;

Sub-Events

RC325A The Role of Physical Phantoms in Quantitative Imaging

Participants

Paul E. Kinahan, PhD, Seattle, WA (Presenter) Research Grant, General Electric Company; Co-founder, PET/X LLC

LEARNING OBJECTIVES

1) To understand the definitions and requirements of quantitative medical imaging. 2) To learn the role of phantoms and tradeoffs in comparison with simulations and patient studies. 3) To review the classes of phantoms available: Commercial, experimental, and virtual (digital reference objects).

ABSTRACT

RC325B Digital Reference Objects

Participants Daniel P. Barboriak, MD, Durham, NC (*Presenter*) Advisory Board, General Electric Company

LEARNING OBJECTIVES

1) Explain why digital reference objects are useful for evaluation of software packages used to derive quantitative imaging biomarkers. 2) State the difference between bias and precision, and describe how aggregate and disaggregate measures of software performance differ.

ABSTRACT

This lecture will familiarize the audience with digital reference objects (DROs) and their place in the development of quantitative imaging biomarkers (QIBs). To determine whether a quantitative imaging study is measuring a pathological or physiological process in an unbiased way, the quantitative imaging result would need to be compared to an independently ascertained unbiased measurement in the imaged subject or animal. Unfortunately, obtaining a precise and unbiased measurement (also known as ground truth) is generally impractical or impossible. Frequently there are several software packages that can be used to create maps reflecting the spatial distribution of the QIB. Because different software packages often give different quantitative results, the choice of software contributes to the variability of the result. Without ground truth data, it can be difficult to determine which softwares calculate the underlying biomarker with sufficient precision and lack of bias to be applicable for a particular use case.DROs are synthetic images whose pixel values are partially or completely determined by mathematical equations. Although these images may be designed to mimic real imaging data, their content is ultimately determined by mathematical models. Even though DROs do not perfectly simulate real data, they are useful because they are created assuming particular underlying parameter values, which can be regarded as ground truth for these objects. DROs can be particularly valuable for evaluation of software packages. Because they are created using known ground truth, they can be used to determine whether a particular image analysis strategy introduces biases when used to extract a QIB. (This is not possible with real data if the ground truth is not known). Assuming that realistic image noise and/or artifact can be included in the DRO, they can also be used to estimate how precisely a software package is deriving quantitative metrics in real images. This lecture will describe how DROs are used in the RSNA Quantitative Imaging Biomarker Alliance (QIBA) process. Topics that will be discussed include: 1) the variety of metrics that can be used to evaluate software performance with DROs; 2) the differences between aggregated and disaggregated measures of performance, and the relevance of this for determining whether software complies with a standard; and 3) best practices for creation of DROs.

Honored Educators

Presenters or authors on this event have been recognized as RSNA Honored Educators for participating in multiple qualifying educational activities. Honored Educators are invested in furthering the profession of radiology by delivering high-quality educational content in their field of study. Learn how you can become an honored educator by visiting the website at: https://www.rsna.org/Honored-Educator-Award/

Daniel P. Barboriak, MD - 2013 Honored Educator

RC325C CT Image Analysis and Sources of Variation

Participants

Binsheng Zhao, DSc, New York, NY (*Presenter*) License agreement, Varian Medical Systems, Inc; License agreement, Keosys SAS; License agreement, Hinacom Software and Technology, Ltd; License agreement, ImBio, LLC; License agreement, AG Mednet, Inc

LEARNING OBJECTIVES

1) To familiarize the audience with the basic image analysis methods such as segmentation and feature extraction, using tumor

quantification in oncology as an example. 2) To discuss sources of variation in image analysis, using both phantom and in-vivo tumors as examples. 3) To raise awareness of the need for harmonization of imaging and quantification techniques in quantitative radiology.

ISP: Genitourinary (Imaging Gynecological Malignancy)

Tuesday, Dec. 1 10:30AM - 12:00PM Location: N229

GU MR OI BQ

AMA PRA Category 1 Credits ™: 1.50 ARRT Category A+ Credits: 1.50

Participants

Susanna I. Lee, MD, PhD, Boston, MA (*Moderator*) Nothing to Disclose Andrea G. Rockall, MRCP, FRCR, London, United Kingdom (*Moderator*) Nothing to Disclose

Sub-Events

SSG06-01 Genitourinary Keynote Speaker: Gynecologic Cancer Imaging-Present and Future

Tuesday, Dec. 1 10:30AM - 10:40AM Location: N229

Participants

Susanna I. Lee, MD, PhD, Boston, MA (Presenter) Nothing to Disclose

ABSTRACT

The past decade has seen the development of MRI and FDG PET-CT, both of which now play central and complementary roles in treatment planning and followup of women with uterine, ovarian and vulvar cancer. Ongoing investigations of novel techniques such as diffusion and perfusion imaging, and of PET tracers capable of targeting hypoxia and hormone receptors, will push cancer radiology firmly into the realm of the molecular, quantitative and predictive in the coming decade. PET-MRI, capable of concurrent multi-modality functional imaging, will likely prove to be a mainstay in personalized gynecologic cancer care.

Honored Educators

Presenters or authors on this event have been recognized as RSNA Honored Educators for participating in multiple qualifying educational activities. Honored Educators are invested in furthering the profession of radiology by delivering high-quality educational content in their field of study. Learn how you can become an honored educator by visiting the website at: https://www.rsna.org/Honored-Educator-Award/

Susanna I. Lee, MD, PhD - 2013 Honored Educator

SSG06-02 High Grade Serous Ovarian Cancer: BRCA Mutation Status and CT Imaging Phenotypes

Tuesday, Dec. 1 10:40AM - 10:50AM Location: N229

Participants

Stephanie Nougaret, MD, New York, NY (*Presenter*) Nothing to Disclose Yuliya Lakhman, MD, New York, NY (*Abstract Co-Author*) Nothing to Disclose Hebert Alberto Vargas, MD, New York, NY (*Abstract Co-Author*) Nothing to Disclose Maura Micco, MD, Rome, Italy (*Abstract Co-Author*) Nothing to Disclose Melvin D'Anastasi, MD, New York, NY (*Abstract Co-Author*) Nothing to Disclose Sarah A. Johnson, MD, Toronto, ON (*Abstract Co-Author*) Nothing to Disclose Ramon E. Sosa, BA, New York, NY (*Abstract Co-Author*) Nothing to Disclose Krishna Juluru, MD, New York, NY (*Abstract Co-Author*) Nothing to Disclose Noah Kauff, New York, NY (*Abstract Co-Author*) Nothing to Disclose Hedvig Hricak, MD, PhD, New York, NY (*Abstract Co-Author*) Nothing to Disclose Evis Sala, MD, PhD, New York, NY (*Abstract Co-Author*) Nothing to Disclose

PURPOSE

To investigate the associations between BRCA mutation status and preoperative CT imaging phenotypes in women with high-grade serous ovarian cancer (HGSOC).

METHOD AND MATERIALS

115 patients with HGSOC (76 BRCA mutation-positive and 39 BRCA mutation-negative) and CT scans prior to the primary cytoreductive surgery were included in this retrospective HIPAA-compliant study. Two radiologists (R1 and R2) independently reviewed all CT scans and R1 determined total measurable peritoneal tumor volume (TPTV) for each patient. Associations between BRCA mutation status, CT imaging features, and TPTV were analyzed using Fisher exact test and Mann Whitney test. Inter-reader agreement was assessed with the Cohen's kappa. Kaplan-Meier and Cox proportional hazards regression survival analyses were performed.

RESULTS

BRCA mutation-positive HGSOC had less frequent peritoneal disease, mesenteric infiltration, and lymphadenopathy at CT (p = 0.0002, < 0.0001-0.03, 0.03 for both readers, respectively). Furthermore, the pattern of peritoneal implants was correlated with the BRCA mutation status: nodular pattern was more common in BRCA-associated tumors whereas infiltrative pattern was more frequent in sporadic tumors (p = 0.0009 and p = 0.0005 for R1 and R2, respectively). BRCA mutation-positive HGSOC had higher mean TPTV (125 cm3 ± 171) than sporadic tumors (56 cm3 ± 95) (p<0.001). Irrespective of BRCA mutation status, mesenteric involvement by tumor was associated with shorter progression-free survival (p <0.0001 for both readers) and overall survival (p<0.0002 and p<0.0001 for R1 and R2, respectively).

CONCLUSION

BRCA mutation status in HGSOC was linked to the distinct CT imaging phenotypes. Mesenteric disease at CT was an independent

predictor of reduced survival in both BRCA mutation-positive and sporadic tumors.

CLINICAL RELEVANCE/APPLICATION

BRCA-associated HGSOC have characteristic prognostically significant morphology on CT.

Honored Educators

Presenters or authors on this event have been recognized as RSNA Honored Educators for participating in multiple qualifying educational activities. Honored Educators are invested in furthering the profession of radiology by delivering high-quality educational content in their field of study. Learn how you can become an honored educator by visiting the website at: https://www.rsna.org/Honored-Educator-Award/

Stephanie Nougaret, MD - 2013 Honored Educator Evis Sala, MD, PhD - 2013 Honored Educator

SSG06-03 Advanced Cervical Cancer: Quantitative Assessment of Early Response to Neoadjuvant Chemotherapy with Intravoxel Incoherent Motion Diffusion-weighted Magnetic Resonance Imaging

Tuesday, Dec. 1 10:50AM - 11:00AM Location: N229

Participants

Yanchun Wang, Wuhan, China (*Presenter*) Nothing to Disclose Dao Y. Hu, MD, PhD, Wuhan, China (*Abstract Co-Author*) Nothing to Disclose

PURPOSE

To investigate the utility of intravoxel incoherent motion (IVIM) diffusion-weighted magnetic resonance imaging (MRI) for predicting and monitoring the response of cervical cancer to neoadjuvant chemotherapy (NACT).

METHOD AND MATERIALS

This prospective study was approved by an institutional review board, and informed consent was obtained from all patients. A total of 42 patients with primary cervical cancer were recruited into this study. IVIM diffusion-weighted MRI was performed on all patients at three time points (prior to NACT, 3 weeks after the first NACT, and 3 weeks after the second NACT). The response to treatment was determined according to the Responded Evaluation Criteria in Solid Tumors (RECIST) three weeks after the second NACT treatment, and the subjects were categorized into responders and non-responders. The standard ADC, true diffusion coefficient (D), perfusion-related pseudo-diffusion coefficient (D*), and perfusion fraction (f) values were determined.

RESULTS

Patients were divided into responders (n=24) and non-responders (n=18) according to the RECIST guidelines. Before treatment, the D and standard ADC values were significantly higher in responders than in non-responders (both p<0.01). No significant differences were observed in D* and f. Analysis of the receiver operating characteristic (ROC) curves indicated that the threshold of $D<0.93\times10-3mm2/s$ and the standard ADC<1.11×10-3mm2/s could be used to differentiate responders from non-responders, yielding area under curve (AUC) values of 0.804 and 0.768, respectively. Three weeks after both the first and second NACT treatments, the D and standard ADC values in the responders were still significantly higher than those in the non-responders.D* and f values still showed no significant differences.The ROC curve analysis indicated that the AUC values for D and standard ADC were 0.823 and 0.763 for the second time point and 0.787 and 0.794 for the last time point.

CONCLUSION

IVIM may be useful for predicting and monitoring the efficacy of NACT in cervical cancer. D and standard ADC values could represent reliable early predictors of the NACT response prior to treatment. Furthermore, these parameters can be used to monitor NACT responses during and after therapy.

CLINICAL RELEVANCE/APPLICATION

These results should be useful for both patients and clinical doctors. Patients who are unsuitable for NACT could be given radiation or surgical treatment in a more timely manner.

SSG06-04 Prognostic Value of Diffusion-weighted MRI and PET/CT During Concurrent Chemoradiotherapy in Uterine Cervical Cancer

Tuesday, Dec. 1 11:00AM - 11:10AM Location: N229

Participants

Jung Jae Park, MD, Seoul, Korea, Republic Of (*Presenter*) Nothing to Disclose Chan Kyo Kim, MD, PhD, Seoul, Korea, Republic Of (*Abstract Co-Author*) Nothing to Disclose Byung Kwan Park, MD, Seoul, Korea, Republic Of (*Abstract Co-Author*) Nothing to Disclose

PURPOSE

To evaluate the prognostic value of diffusion-weighted MRI (DWI) and PET/CT during concurrent chemoradiotherapy (CCRT) of cervical cancer for predicting disease progression.

METHOD AND MATERIALS

This retrospective study included 67 consecutive patients (median age, 55 years; range, 28-78 years) who received CCRT for locally advanced cervical cancer. All patients underwent both 3T-DWI and PET/CT before and during (at 4 weeks) treatment. The mean apparent diffusion coefficient (ADC) and maximum standardized uptake value (SUVmax) were measured on the tumors and the percentage changes of each parameter between the two time points (Δ ADC and Δ SUVmax) were calculated. In the prediction of disease progression, the diagnostic performance of tumor Δ ADC and Δ SUVmax was evaluated using the time-dependent receiver operating characteristics (ROC) curve analysis. The relationship between disease progression and clinical and imaging parameters was investigated using univariate and multivariate Cox regression analyses.

During a mean follow-up of 2.7 years, disease progression was identified in 16 patients (23.9%): local recurrence (n= 7), distant metastasis (n= 8) and both local recurrence and distance metastasis (n= 1). During treatment, the mean ADC and SUVmax significantly increased and decreased, respectively (both P < 0.001). The mean Δ ADC and Δ SUVmax were 42.6 ± 17% and 67.6 ± 16.5%, respectively. In the prediction of disease progression, the integrated area under the curve of Δ ADC (0.791) and Δ SUVmax (0.781) were not significantly different (P = 0.88) and the optimal cut-offs of Δ ADC and Δ SUVmax were 35.1% and 60.7%, respectively. On multivariate Cox regression analysis, the Δ ADC (< 35.1%) and Δ SUVmax (< 60.7%) were the only independent predictors of disease progression after treatment (hazard ratio, 4.1 and 4.5; P , 0.04 and 0.03, respectively).

CONCLUSION

The percentage changes of DWI and PET/CT parameters during CCRT offer similar prognostic value for the prediction of posttreatment disease progression in patients with cervical cancer.

CLINICAL RELEVANCE/APPLICATION

DWI, as a noninvasive tool, can be used in the prediction of therapeutic outcomes following concurrent chemoradiotherapy in patients with cervical cancer, instead of PET/CT with the risk of ionizing radiation exposure.

SSG06-05 Application of Non-Gaussian Water Diffusional Kurtosis Imaging in the Assessment of Uterine Tumors: A Preliminary Study

Tuesday, Dec. 1 11:10AM - 11:20AM Location: N229

Participants

Aliou A. Dia, MD, Suita, Japan (*Presenter*) Nothing to Disclose Masatoshi Hori, MD, Suita, Japan (*Abstract Co-Author*) Nothing to Disclose Hiromitsu Onishi, MD, Suita, Japan (*Abstract Co-Author*) Nothing to Disclose Makoto Sakane, MD, Suita, Japan (*Abstract Co-Author*) Nothing to Disclose Takahiro Tsuboyama, MD, Suita, Japan (*Abstract Co-Author*) Nothing to Disclose Noriyuki Tomiyama, MD, PhD, Suita, Japan (*Abstract Co-Author*) Nothing to Disclose Mitsuaki Tatsumi, MD, PhD, Suita, Japan (*Abstract Co-Author*) Nothing to Disclose Tomoyuki Okuaki, RT, Chuo-Ku, Japan (*Abstract Co-Author*) Employee, Koninklijke Philips NV

PURPOSE

To retrospectively evaluate the feasibility and the value of diffusional kurtosis imaging (DKI) in the assessment of uterine tumors compared with that of conventional diffusion weighted imaging (DWI) and with pathological findings as gold-standard.

METHOD AND MATERIALS

Sixty-one women (mean age: 54.85 years \pm 14.09, range 26-89 years) with histopathologically proven uterine cancers (51 cervical cancers and 10 corpus cancers) underwent 3-T MR imaging using DKI with high b values (b=700, 1000, 1700 and 2500 s/mm2) and DWI (b=0 s/mm2, b=700 s/mm2). Thirteen of the 61 patients (21.3 %) had coexisting leiomyomas.ROI-based measurements of diffusivity (D), kurtosis (K) and ADC of the uterine cancers, leiomyomas, healthy myometrium and endometrium were performed.The areas under the ROC curve (AUC) in differentiating malignant from benign lesions were also compared.

RESULTS

Mean D of uterine cancers (0.879 mm/s2 \pm 0.30) was significantly lower than that of the leiomyomas (1.174 mm/s2 \pm 0.43) (P=0.006), the healthy myometrium (1.178 mm/s2 \pm 0.27) (P=0.000) and the healthy endometrium (1.308 mm/s2 \pm 0.5) (P=0.013). Mean K of uterine cancers (0.754 mm/s2 \pm 0.22) was moderately higher than that of leiomyomas (0.686 mm/s2 \pm 0.24), the healthy myometrium (0.708 mm/s2 \pm 0.19) and the healthy endometrium (0.568mm/s2 \pm 0.25).No significant difference was found between the mean K of the uterine cancers, the leiomyomas, the healthy myometrium and endometrium (P=0.33, 0.27 and 0.23).There was no significant difference in AUC between D and ADC.

CONCLUSION

D is not superior or inferior to the conventional ADC in the differentiation between benign and malignant uterine lesions. The K that is related to the microstructural complexity was higher in uterine cancers than that of leiomyomas but without any significant difference, opposite to K values in white matter tissue of the brain, in breast or prostate cancers where the mean K of malignant lesions was significantly higher than of the benign lesions.

CLINICAL RELEVANCE/APPLICATION

The D, in non-Gaussian DKI, is equal to the conventional ADC in differentiating benign from malignant uterine lesions. The K of uterine malignant tumors was not significantly higher than that of the benign lesions, unlike in breast or prostate cancers.

SSG06-06 Clinical Value of Proton (1H-) Magnetic Resonance Spectroscopy (MRS) Using Body-phased Array Coil at 3.0 T in Pretreatment Assessment for Cervical Cancer Patients

···---

.

Tuesday, Dec. 1 11:20AM - 11:30AM Location: N229

Participants

Gigin Lin, MD, Guishan, Taiwan (*Presenter*) Nothing to Disclose Yu-Ting Huang, Guishan, Taiwan (*Abstract Co-Author*) Nothing to Disclose Koon-Kwan Ng, Guishan, Taiwan (*Abstract Co-Author*) Nothing to Disclose Yu-Chun Lin, MSC, Taoyuan, Taiwan (*Abstract Co-Author*) Nothing to Disclose Tzu-Chen Yen, MD, PHD, Taoyuan, Taiwan (*Abstract Co-Author*) Nothing to Disclose Hung-Hsueh Chou, MD, Taoyuan, Taiwan (*Abstract Co-Author*) Nothing to Disclose Angel Chao, MD, Taoyuan, Taiwan (*Abstract Co-Author*) Nothing to Disclose Chiun-Chieh Wang, Guishan, Taiwan (*Abstract Co-Author*) Nothing to Disclose Chyong-Huey Lai, Guishan, Taiwan (*Abstract Co-Author*) Nothing to Disclose Pen-An Liao, MD, Taipei City, Taiwan (*Abstract Co-Author*) Nothing to Disclose

PURPOSE

To determine the clinical value of proton (1H-) magnetic resonance spectroscopy (MRS) using body-phased array coil at 3.0 T, in pretreatment assessment for cervical cancer patients.

METHOD AND MATERIALS

We prospectively enrolled 52 histology proven cervical cancer patients (age 27-80 years) and 30 age-matched surgical candidates for benign uterine myoma without evidence of cervical cancer. Pretreatment MR study plus MRS and diffusion weighted imaging (DWI) sequences were carried out at a 3.0 T system using body-phased array coil for the pelvis. PRESS localized 1H-MRS was applied to cervical tumor or normal tissue, with resonances analyzed by using the LC-Model algorithm. Cramer-Rao lower bound (CRLB) threshold of 20% was used as quality control. We compared resonances based on: (1) tumor vs normal cervical tissue, (2) histopathology type (squamous vs adenocarcinoma) (3) T stage = IIb (4) nodal metastasis (5) distant metastasis using Mann-Whitney test.

RESULTS

Cervical tumor showed a lower 1.3-ppm lipid level (0.30 vs 1.01 μ M, P < .05), as compared with normal cervical tissue. Squamous cell carcinoma demonstrated lower levels in 1.3-ppm lipid (0.17 μ M vs 0.59 μ M, P < .05) and 0.9-ppm lipid (0.04 μ M vs 0.16 μ M, P < .05), as compared with adenocarcinoma. Tumor with T stage >= IIb had lower levels in 1.3-ppm lipid (0.15 μ M vs 0.53 μ M, P < .05), 0.9-ppm lipid (0.04 μ M vs 0.15 μ M, P < .05) and total choline (0.04 μ M vs 0.16 μ M, P < .05). Tumors with nodal metastasis contained lower levels of 1.3-ppm lipid (0.16 μ M vs 0.44 μ M, P < .05) and glutamine (0.01 μ M vs 0.02 μ M, P < .05), whereas tumors with distant metastasis contained a lower level of 1.3-ppm lipid (0.12 μ M vs 0.50 μ M, P < .05). However, resonances from cervical tumor were independent to maximal tumor size or ADC value on MRI.

CONCLUSION

1H-MRS using body-phased array coil at 3.0 T in cervical cancer patients is useful in differentiating tumor, histopathology type, T stage >= IIb, nodal or distant metastasis, and is independent to maximal tumor size or ADC value on MRI.

CLINICAL RELEVANCE/APPLICATION

1H-MRS using body-phased array coil at 3.0 T added additional dimensions for pretreatment assessment in cervical cancer patients.

SSG06-07 Impact of Multiparametric MRI (mMRI) on the Therapeutic Management of Suspicious Adnexal Masses Detected by Transvaginal Ultrasound (TVUS)

Tuesday, Dec. 1 11:30AM - 11:40AM Location: N229

Participants

Simone Schrading, MD, Aachen, Germany (*Presenter*) Nothing to Disclose Sabine M. Detering, Aachen, Germany (*Abstract Co-Author*) Nothing to Disclose Dirk Bauerschlag, Aachen, Germany (*Abstract Co-Author*) Nothing to Disclose Christiane K. Kuhl, MD, Bonn, Germany (*Abstract Co-Author*) Nothing to Disclose

PURPOSE

Incidental adnexal masses at TVUS are common and diagnostically challenging. The primary goal of imaging is accurate tissue characterization to guide further management, i.e. the choice between plain follow-up vs laparoscopic surgery vs. open surgery. Aim of this study was to evaluate the diagnostic utility of mMRI for further management stratification in patients with such adnexal masses

METHOD AND MATERIALS

Prospective IRB-approved trial on 126 women (mean age 54.6 years) with inconclusive adnexal masses at TVUS. All women underwent conventional work up, including pelvic examination, TVUS, and CA-125 levels. In addition, all women underwent mMRI at 3T with high resolution T2-TSE in three planes, DWI (max. b-800) and DCE. Likelihood of malignancy and appropriate management (i.e. follow-up vs. laparoscopic vs. open surgery) was first determined based on results of conventional methods, and then, independently, based on mMRI. Then, all methods were reviewed in synopsis. Final surgical pathology served as standard-of-reference or clinical and imaging follow-up of at least 24 months

RESULTS

In 65% (82/126) of patients the adnexal mass finally classified as benign, in 29% (36/126) as malignant and in 6% (8/126) as borderline. The diagnostic indices for TVUS+CA-125 alone vs. MRI alone vs. all methods combined were as follows: Sensitivity: 86% (31/36) vs. 97% (35/36) vs. 100% (36/36); Specificity: 32% (29/90) vs. 83% (75/90) vs. 80% (68/90); PPV: 34% (31/91) vs. 70% (35/50) vs. 74% (40/54), NPV: 65% (29/44) vs. 98% (75/76) vs. 100% (72/72). After mMRI, the therapeutic management was changed in 41/126 (34%) of patients. In 30 patients in whom surgery had been recommended based on conventional assessment, mMRI correctly diagnosed typical benign findings; these patients underwent follow-up instead of surgery. None of these women developed malignancy during follow-up. In another 11 patients, mMRI results correctly suggested malignancy such that open surgery was performed instead of laparoscopic surgery

CONCLUSION

Compared with conventional assessment (pelvic exam, TVUS, CA-125), mMRI correctly changed the management in one-third of women with incidental adnexal masses. It helps avoid unnecessary surgery, or unnecessary surgical steps (conversion from laparoscopic to open surgery)

CLINICAL RELEVANCE/APPLICATION

Pelvic mMRI helps to significantly improve clinical management of asymptomatic women with incidental adnexal masses identified on TVUS

SSG06-08 Preoperative Tumor Texture Analysis from MRI Predicts Deep Myometrial Invasion and High Risk Histology in Endometrial Carcinomas

Tuesday, Dec. 1 11:40AM - 11:50AM Location: N229

Sigmund Ytre-Hauge, MD, Bergen, Norway (*Presenter*) Nothing to Disclose Erik Hanson, PhD, Bergen, Norway (*Abstract Co-Author*) Nothing to Disclose Arvid Lundervold, MD, PhD, Bergen, Norway (*Abstract Co-Author*) Nothing to Disclose Jone Trovik, MD, Bergen, Norway (*Abstract Co-Author*) Nothing to Disclose Helga Salvesen, MD, PhD, Bergen, Norway (*Abstract Co-Author*) Nothing to Disclose Ingfrid S. Haldorsen, MD, PhD, Bergen, Norway (*Abstract Co-Author*) Nothing to Disclose

PURPOSE

Tumor heterogeneity is a key feature of malignant disease. Heterogeneity in MR images can be quantified by texture analysis. We aimed to explore whether high risk histological features are reflected in texture parameters derived from preoperative MRI in endometrial carcinomas.

METHOD AND MATERIALS

Preoperative pelvic contrast-enhanced MRI (1.5T) including diffusion-weighted imaging (DWI) was prospectively performed in 99 patients with histologically confirmed endometrial carcinomas. Tumor region of interest (ROI) was manually drawn encircling the uterine tumor on axial T1-weighted contrast-enhanced (CE) series on the slice displaying the largest cross-section tumor area. Histogram based texture features (standard deviation, skewness and kurtosis) were calculated from these tumor ROIs. Texture parameters were analyzed in relation to established histological subtype and grade, surgicopathological staging parameters (deep myometrial and cervical stroma invasion and lymph node metastases) and MRI based tumor volume and tumor apparent diffusion coefficient (ADC) value using Mann-Whitney U test, Jonckheere-Terpsta trend test and Pearson's bivariate correlation test.

RESULTS

Large standard deviation (SD) in the tumor ROIs was significantly associated with presence of deep myometrial invasion (p=0.009). Lower values for skewness were observed in the tumor ROIs from endometrioid high grade tumors (p=0.012) and from nonendometrioid tumors (by definition always high grade lesions, p=0.020). Kurtosis was positively correlated to tumor volume (r=0.27; p=0.006) and negatively correlated to tumor ADC value (r=-0.28; p=0.006).

CONCLUSION

MRI derived tumor texture features reflecting tumor heterogeneity are significantly related to high risk histology and predict deep myometrial invasion in endometrial carcinomas. Thus, tumor texture features based on MRI represent promising biomarkers to aid preoperative tumor characterization for risk stratified surgical treatment.

CLINICAL RELEVANCE/APPLICATION

Tumor texture features derived from MRI reflect high risk endometrial carcinoma and may aid preoperative risk classification for stratified surgery.

SSG06-09 Endometrial Cancer MR Staging Accuracy in a Large Multi-site UK Cancer Network Over Three Years: Can the Reported Single Centre Staging Accuracies be Met in Clinical Practice?

Tuesday, Dec. 1 11:50AM - 12:00PM Location: N229

Participants

Neil Soneji, BSC, MBBS, London, United Kingdom (*Abstract Co-Author*) Nothing to Disclose Annarita Ferri, MD, Chieti, Italy (*Presenter*) Nothing to Disclose Victoria Stewart, London, United Kingdom (*Abstract Co-Author*) Nothing to Disclose Roberto Dina, MD, London, United Kingdom (*Abstract Co-Author*) Nothing to Disclose Nishat Bharwani, MBBS, FRCR, London, United Kingdom (*Abstract Co-Author*) Nothing to Disclose Andrea G. Rockall, MRCP, FRCR, London, United Kingdom (*Abstract Co-Author*) Nothing to Disclose

PURPOSE

To determine the radiological staging accuracy of endometrial cancer (EC) from images acquired from multiple MR scanners across a 10 centre UK cancer network over three years.

METHOD AND MATERIALS

Retrospective study of 382 consecutive patients with EC imaged in 9 external hospitals and 3 internal hospital sites discussed at our tertiary gyne-oncology centre between October 2011-October 2014. All patients with tertiary centre reports for both final histology and MRI were included (n=270). The radiological stage provided at MDT discussion was compared to the 'gold standard' histological report. Parameters assessed included depth of myometrial invasion, cervical and nodal stage. The use of DWI or DCE and the site for incorrect staging were recorded. MedCalc statistical software version 15.2.2 was used.

RESULTS

242 of 270 MRI reports (90%) included a final FIGO stage; of these 147 scans were performed internally and 95 at an external hospital. Accuracy of the reported depth of invasion was 72.7% for all cases (72.8% for internal and 72.6% for external scans). Sensitivity, specificity, positive and negative predictive values & accuracy with DWI (n=204) were 67%, 77%, 64%, 79%, 73% and without DWI (n=38) were 75%, 69%, 53%, 86%, 71% (p>.05). Accuracy with DCE (n=109) was 72% and without (n=130) was 73%. For cervical stromal invasion, sensitivity, specificity, PPV, NPV and accuracy for all scans were 59%, 94%, 64%, 93% and 89%. As a percentage of all causes of staging error, depth of invasion accounted for 41-52%, cervix stromal invasion 20-32% and nodal stage 8-16% depending on whether the patient was scanned internally or externally, or whether DWI or DCE were included (p>.05).

CONCLUSION

Staging accuracy in a large multi-site cancer network over three years does not meet the reported staging accuracies in metaanalyses of smaller single centre published research (pooled sensitivity/specificity of 86-90%). DWI and DCE did not affect staging accuracy, although only a small number of cases did not have these. The underlying causes for the reduction in sensitivity and specificity need to be evaluated in order to translate the highest achievable MR staging accuracy to long term routine practice.

CLINICAL RELEVANCE/APPLICATION

Accuracy of MR staging of endometrial cancer in a multi-site cancer network over three years does not reach single centre study results. The causes for staging inaccuracies need to be understood.

Breast Imaging (Quantitative)

Tuesday, Dec. 1 3:00PM - 4:00PM Location: Arie Crown Theater

BR BQ MR

AMA PRA Category 1 Credit [™]: 1.00 ARRT Category A+ Credit: 1.00

Participants

Fiona J. Gilbert, MD, Cambridge, United Kingdom (*Moderator*) Medical Advisory Board, General Electric Company; Research Grant, GlaxoSmithKline plc; Research Grant, General Electric Company Despina Kontos, PhD, Philadelphia, PA (*Moderator*) Nothing to Disclose

Sub-Events

SSJ01-01 Relationship between Computer-extracted MRI-based Phenotypes and the Risk of Breast Cancer Recurrence as Predicted by PAM50 Gene Expression Array

Tuesday, Dec. 1 3:00PM - 3:10PM Location: Arie Crown Theater

Participants

Elizabeth S. Burnside, MD, MPH, Madison, WI (Presenter) Stockholder, NeuWave Medical Inc Hui Li, MD, PhD, Chicago, IL (Abstract Co-Author) Nothing to Disclose Charles Perou, PhD, Chapel Hill, NC (Abstract Co-Author) Nothing to Disclose Karen Drukker, PhD, Chicago, IL (Abstract Co-Author) Nothing to Disclose Elizabeth A. Morris, MD, New York, NY (Abstract Co-Author) Nothing to Disclose Maryellen L. Giger, PhD, Chicago, IL (Abstract Co-Author) Stockholder, Hologic, Inc; Shareholder, Quantitative Insights, Inc; Royalties, Hologic, Inc; Royalties, General Electric Company; Royalties, MEDIAN Technologies; Royalties, Riverain Technologies, LLC; Royalties, Mitsubishi Corporation; Royalties, Toshiba Corporation; Researcher, Koninklijke Philips NV; Researcher, U-Systems, Inc Ermelinda Bonaccio, MD, Amherst, NY (Abstract Co-Author) Nothing to Disclose Margarita L. Zuley, MD, Pittsburgh, PA (Abstract Co-Author) Research Grant, Hologic, Inc; Marie A. Ganott, MD, Pittsburgh, PA (Abstract Co-Author) Nothing to Disclose Jose M. Net, MD, Miami, FL (Abstract Co-Author) Nothing to Disclose Elizabeth J. Sutton, MD, New York, NY (Abstract Co-Author) Nothing to Disclose Kathleen R. Brandt, MD, Rochester, MN (Abstract Co-Author) Nothing to Disclose Gary J. Whitman, MD, Houston, TX (Abstract Co-Author) Book contract, Cambridge University Press Suzanne Conzen, MD, Chicago, IL (Abstract Co-Author) Nothing to Disclose Li Lan, Chicago, IL (Abstract Co-Author) Nothing to Disclose Yitan Zhu, PhD, Evanston, IL (Abstract Co-Author) Nothing to Disclose Yuan Ji, Chicago, IL (Abstract Co-Author) Nothing to Disclose Erich Huang, PhD, Bethesda, MD (Abstract Co-Author) Nothing to Disclose John B. Freymann, BS, Rockville, MD (Abstract Co-Author) Nothing to Disclose Justin Kirby, Bethesda, MD (Abstract Co-Author) Stockholder, Myriad Genetics, Inc C. Carl Jaffe, MD, Boston, MA (Abstract Co-Author) Nothing to Disclose

PURPOSE

Clinical teams are increasingly relying on genetic profiles for breast cancer subtyping, prognostication, and treatment decisions. We investigate the relationship between computer-extracted breast MRI phenotypes with the PAM50 gene array (which includes two methods: PAM50 Risk of Relapse Subtype [ROR-S] and PAM50 Risk of Relapse Subtype + Proliferation [ROR-P]) in order to understand MRI's potential role in assessing risk of breast cancer recurrence.

METHOD AND MATERIALS

We analyzed a retrospective dataset of 84 de-identified, breast MRIs contributed by 5 institutions to the NCI's "The Cancer Imaging Archive" (TCIA), along with clinical, histopathological, and genomic data from "The Cancer Genome Atlas" (TCGA). Each MRI examination imaged a biopsy proven invasive breast cancer comprised of 74 (88%) ductal; 8 (10%) lobular, and 2 (2%) mixed. Of these cancers, 73 (87%) were ER +, 67 (80%) were PR +, and 19 (23%) were HER-2 +. We performed computerized analysis on each cancer yielding computer-extracted image-based tumor phenotypes (CEIPs), quantifying size, shape, morphology, enhancement texture, kinetic curve assessment, and enhancement variance kinetics. Regression and ROC analysis were conducted to assess the predictive ability of CEIPs relative to the multi-gene assays' continuous outputs.

RESULTS

Multiple linear regression analyses demonstrated statistically significant Pearson correlations (0.5-0.55) between CEIP signatures and the PAM50 recurrence scores. The most important CEIPs included tumor size and enhancement texture patterns characterizing tumor heterogeneity. Use of CEIP in the tasks of distinguishing between good and poor prognosis in terms of levels of recurrence yielded area under the ROC curve values (standard error) of 0.88 (0.05), 0.73 (0.06), 0.72 (0.08), and 0.61 (0.09) for MammaPrint, Oncotype DX, PAM50 Risk of Relapse Subtype (ROR-S), and PAM50 ROR-P (subtype+proliferation), respectively, with all but the latter showing statistical difference from chance.

CONCLUSION

Quantitative breast MRI radiomics shows promise as a method for image-based phenotyping to assess risk of breast cancer recurrence. This work helps us begin to understand which MRI features may be most powerfully correlated with genetic recurrence risk.

CLINICAL RELEVANCE/APPLICATION

Computerized MRI tumor phenotyping yield quantitative predictive features that have the potential to advance precision medicine and affect patient treatment strategy.

SSJ01-02 Dynamic Contrast Enhanced (DCE) Breast MR Features Associated with Prognostic Factors in Triple Negative Breast Cancers (TNBC)

Tuesday, Dec. 1 3:10PM - 3:20PM Location: Arie Crown Theater

Participants

Bo La Yun, MD, Seongnam, Korea, Republic Of (*Presenter*) Nothing to Disclose Sun Mi Kim, MD, PhD, Seongnam-Si, Korea, Republic Of (*Abstract Co-Author*) Nothing to Disclose Mijung Jang, Seongnam, Korea, Republic Of (*Abstract Co-Author*) Nothing to Disclose Jong Yoon Lee, MD, Seongnam-Si, Korea, Republic Of (*Abstract Co-Author*) Nothing to Disclose Ja Yoon Jang, MD, Seongnam-Si, Korea, Republic Of (*Abstract Co-Author*) Nothing to Disclose

PURPOSE

To assess the association of DCE MR features including texture and histogram analysis with pathologic prognostic factors in TNBC.

METHOD AND MATERIALS

From June 2012 to February 2015, 92 TNBC patients (mean age 53 ±13 years) based on immunohistochemical staining (IHC) enrolled our study. We excluded patient underwent primary systemic therapy. For texture (13 grey level co-occurrence matrix features) and histogram analysis using in-house program, the ROIs were drawn along the margin of the cancer in the largest diameter image at 1.5 minute after contrast injection. For dynamic enhancement pattern analysis, MR CAD system (CADstream) was used. The percentage of fast or medium initial enhancement and persistent, plateau and washout delayed enhancement were analyzed. The pathologic results of specimens were categorized according to histologic grade and axillary nodal status, and IHC result (Ki-67, cytokeratin 5/6, EGFR, p53). The correlation of texture features and enhancement patterns with each pathological prognostic factor were assessed. Interobserver agreement was also investigated.

RESULTS

High histologic grade was associated with low angular second moment (ASM, p=0.025). Axillary nodal metastasis was associated with high maximum MR diameter (p=0.013), high entropy (p=0.024), and low ASM (p=0.026), low information measure of correlation (IMC1, p=0.046). High Ki-67 index (\geq 14%) tumors showed high percentage of fast initial enhancement (p=0.015), high percentage of plateau or washout delayed enhancement (p<0.001, p=0.001) on dynamic enhancement pattern, high entropy (p<0.001), low ASM (p=0.004) and low IMC1 (p=0.004) on texture analysis. The positivity of cytokeratin 5/6 or EGFR associated with high entropy (p=0.004), high inverse difference moment (IDM, p=0.029), low sum average (p=0.038), low IMC1 (p=0.005) and low IMC2 (p=0.038) on texture analysis, and low mean (p=0.042) and low median (p=0.037) on histogram analysis. Positivity of p53 was not associated with DCE MR features. The agreement of texture and histogram features was good (ICCs>0.9).

CONCLUSION

Dynamic enhancement pattern, texture and histogram features in DCE MR were associated with pathologic prognosis factors in TNBC. These image features would predict aggressiveness of TNBC on preoperative MR.

CLINICAL RELEVANCE/APPLICATION

DCE MR features would predict TNBC aggressiveness. It could be used for non-invasive evaluation of TNBC before chemotherapy or surgery.

SSJ01-03 Automatic and Accurate Breast Cancer Volumetric Segmentation on MRI with Varying Degrees of Background Parenchymal Enhancement

Tuesday, Dec. 1 3:20PM - 3:30PM Location: Arie Crown Theater

Participants

Harini Veeraraghavan, New York, NY (*Presenter*) Nothing to Disclose Brittany Dashevsky, MD, DPhil, New York, NY (*Abstract Co-Author*) Nothing to Disclose Girard Gibbons, BA, New York, NY (*Abstract Co-Author*) Nothing to Disclose Elizabeth A. Morris, MD, New York, NY (*Abstract Co-Author*) Nothing to Disclose Joseph O. Deasy, PhD, New York, NY (*Abstract Co-Author*) Nothing to Disclose Elizabeth J. Sutton, MD, New York, NY (*Abstract Co-Author*) Nothing to Disclose

PURPOSE

Breast MRI background parenchymal enhancement (BPE) varies between women and can limit the radiologists ability to accurately define breast cancer extent of disease. Here we sought to develop a computer model that could automatically generate volumetric segmentations of breast cancers on MRI with varying degrees of BPE.

METHOD AND MATERIALS

46 patients with HER2+ invasive breast cancers were included with either mild (n=23) or marked (n=23) BPE. We developed inhouse software that combines dynamic contrast enhanced (DCE) MR images acquired at multiple time points (1 pre and 3 post contrast) to generate volumetric tumor segmentation. The DCE-MR images are combined through spectral embedding from which scalar images are computed. The algorithm is initialized with a manually delineated contour of the tumor on a single slice. A model of the tumor is automatically learned using a Gaussian mixtures model (GMM) using the individual time series and the computed scalar images. The GMM classifications are used to refine a joint segmentation generated from the individual sequences using an automatically seeded grow cut method.

RESULTS

The computer-generated volumetric segmentations were compared with a radiologist-delineated segmentation by computing DICE overlap scores (1.0 -best, 0 -worst). For tumors with mild BPE, the maximum DICE score was 0.92, the lowest was 0.28 and the median was 0.79. For tumors with marked BPE, the maximum DICE score was 0.90, the lowest was 0.04 and the median was 0.71. Two sampled t-test between the scores computed for the mild and marked BPE tumors failed to reject the null hypothesis indicating that there was no difference in the segmentation performance regardless of the extent of BPE.

CONCLUSION

Our method achieves reasonably accurate volumetric tumor regardless of the extent of BPE.

CLINICAL RELEVANCE/APPLICATION

Automatic and accurate segmentation of breast cancers with marked BPE can aid the radiologist in accurately defining the extent of disease and minimizing inter-observer variability.

SSJ01-04 Association between Quantitative Measures of Breast Parenchymal Complexity and False-Positive Recall from Digital Mammography: Results from a Large Prospective Screening Cohort

Tuesday, Dec. 1 3:30PM - 3:40PM Location: Arie Crown Theater

Participants

Shonket Ray, PhD, Philadelphia, PA (*Abstract Co-Author*) Nothing to Disclose Brad M. Keller, PhD, Philadelphia, PA (*Presenter*) Nothing to Disclose Jinbo Chen, PhD, Philadelphia, PA (*Abstract Co-Author*) Nothing to Disclose Emily F. Conant, MD, Philadelphia, PA (*Abstract Co-Author*) Speaker, Hologic, Inc; Scientific Advisory Board, Hologic, Inc; Consultant, Siemens AG Despina Kontos, PhD, Philadelphia, PA (*Abstract Co-Author*) Nothing to Disclose

PURPOSE

To investigate associations between quantitative features of breast parenchymal complexity and false-positive (FP) recall from breast cancer screening with digital mammography.

METHOD AND MATERIALS

Digital mammography (DM) images from an entire one-year cohort of women screened for breast cancer at our institution (Sept. 2010 - Aug. 2011) were retrospectively analyzed. A total of 10,571 screening mammography exams were acquired using either a GE Essential or Hologic Selenia full-field digital mammography (FFDM) unit. All images sets consisted of bilateral cranio-caudal (CC) and medio-lateral oblique (MLO) views and were vendor post-processed (i.e., "For Presentation" images). To characterize breast tissue complexity, thirteen texture features were extracted using a locally adaptive computerized parenchymal texture analysis algorithm. As a comparative established risk factor for FP recall, breast percent density (PD) was estimated on a per-woman basis using previously validated automated software. Logistic regression was performed to evaluate associations between FP recall and the extracted complexity features, using a case-control design where FP-recalls (N=1064) were randomly age-matched to negative screening controls (N=3192) at a 1:3 ratio. Odds ratios (OR) and area under the curve (AUC) of the receiver operating characteristic (ROC) were used to assess strength of associations.

RESULTS

Combining PD and texture features yielded an AUC=0.62 (95%CI: 0.60-0.64), with PD (OR=1.01; 95%CI: 1.00-1.01), texture energy (OR=1.43; 95%CI: 1.27-1.61) and sum variance (OR=1.23; 95%CI: 1.07-1.52) associated to higher risk of FP recall (p<0.05), while texture difference variance (OR=0.67; 95%CI: 0.58-0.78) and information correlation (OR=0.77; 95%CI: 0.69-0.85) were inversely associated to FP recall (p<0.05). A baseline model of PD alone yielded had AUC=0.52 (95%CI: 0.50-0.54, PD OR=1.00; 95%CI: 1.00-1.01).

CONCLUSION

Quantitative features of mammographic parenchymal texture complexity may be indicative of the risk for false-positive recall from screening with digital mammography.

CLINICAL RELEVANCE/APPLICATION

Incorporating quantitative features of breast parenchymal texture may augment breast density as a parenchymal complexity descriptor to help guide personalized breast cancer screening recommendations.

SSJ01-05 Prediction of False-Negative Breast Cancer Screens with Digital Mammography: Preliminary evaluation of a Quantitative Breast Complexity Index

Tuesday, Dec. 1 3:40PM - 3:50PM Location: Arie Crown Theater

Participants

Andrew Oustimov, Philadelphia, PA (*Presenter*) Nothing to Disclose Emily F. Conant, MD, Philadelphia, PA (*Abstract Co-Author*) Speaker, Hologic, Inc; Scientific Advisory Board, Hologic, Inc; Consultant, Siemens AG Lauren Pantalone, BS, Philadelphia, PA (*Abstract Co-Author*) Nothing to Disclose Brad M. Keller, PhD, Philadelphia, PA (*Abstract Co-Author*) Nothing to Disclose Meng-Kang Hsieh, Philadelphia, PA (*Abstract Co-Author*) Nothing to Disclose

Despina Kontos, PhD, Philadelphia, PA (Abstract Co-Author) Nothing to Disclose

PURPOSE

Breast density is a known confounder of mammographic sensitivity, and increasingly reported for guiding supplemental screening recommendations. We assess the predictive value of a refined quantitative index of dense tissue complexity in identifying women at high-risk of false-negative screens.

METHOD AND MATERIALS

We retrospectively analyzed data from an entire one-year (09/01/10 to 08/30/11) screening cohort at our institution (N = 10,728). Among women with negative screening, false negatives (FNs) were defined as cancer detected in a follow up period of 12 and up to 24 months prior to the next routine screening exam (N=11). Controls were identified as women confirmed negative also at subsequent screening, and were randomly selected and matched to FNs based on age and race, at a 1:3 ratio (N=33). To specifically determine the added value of our breast complexity index (BCI), controls were also matched to FNs based on BIRADS density, and on the interpreting radiologist. The BCI was derived from a range of computer-extracted parenchymal texture descriptors, including Grey-level Histogram, Haralick, and Edge-enhancement features (N=29), summarized via principal component analysis (PCA). Associations between the BCI-PCA components and the odds of FN screening were determined via univariate logistic regression and discriminatory capacity was assessed via receiver operating characteristic (ROC) curve analysis.

RESULTS

The BCI was significantly associated with the odds of FN screening (OR: 0.67, 95% CI: 0.45 - 1.00, p = 0.05), while exhibiting potential to discriminate between false negative screeners and controls confirmed as negative at subsequent screening (AUC = 0.69, 95% CI: 0.48 to 0.88). The first 3 principle components accounted for 88% of the total variance in the features.

CONCLUSION

The significant association between BCI and the odds of FN screen, in a case-control sample with identical BIRADS density distributions, suggests that refined quantitative measures of breast complexity may be more sensitive than qualitative BIRADS density in identifying women at high-risk for a false-negative screening exam.

CLINICAL RELEVANCE/APPLICATION

Quantitative measures of breast complexity may result in more sensitive markers for guiding supplemental screening recommendations, than the reporting of conventional BIRADS breast density.

SSJ01-06 Dedicated Computer Aided Detection for Automated 3D Breast Ultrasound Detects Invasive Ductal Cancers Independent of Hormonal Receptor Status

Tuesday, Dec. 1 3:50PM - 4:00PM Location: Arie Crown Theater

Participants

Jan Van Zelst, Nijmegen, Netherlands (*Presenter*) Nothing to Disclose Tao Tan, Nijmegen, Netherlands (*Abstract Co-Author*) Research Grant, QView Medical, Inc Nico Karssemeijer, PhD, Nijmegen, Netherlands (*Abstract Co-Author*) Shareholder, Matakina Technology Limited; Consultant, QView Medical, Inc; Shareholder, QView Medical, Inc; Director, ScreenPoint Medical BV; Shareholder, ScreenPoint Medical BV; Ritse M. Mann, MD, PhD, Nijmegen, Netherlands (*Abstract Co-Author*) Speakers Bureau, Bayer AG

PURPOSE

Prognostic factors such as hormonal receptor (HR) status (estrogen and progestron) in invasive ductal cancers (IDC) are associated with ultrasonographic imaging phenotypes that may limit differentiating aggressive IDC from benign masses. Therefore, in this study we compared the relative sensitivity of a commercially developed computer aided detection (CADe) program in the detection of HR+ and HR- IDCs and biopsied benign breast lesions.

METHOD AND MATERIALS

The local IRB waived the need for informed consent for this study. ABUS exams of 101 women with 66 IDCs and 35 biopsied benign lesions were randomly selected from a large image archive. All IDCs were examined by a pathologist on the surgical specimen and benign lesions were examined on a histological core needle biopsy specimen. For all IDCs we extracted HR status from the pathology reports. All lesions were annotated by outlining the contour of the lesion based on radiology and pathology reports. After reading the cases, the CADe program (Qview Medical Inc., Los Altos, ca., USA) generated a series of suspicious region candidates that were marked in the ABUS scans. The location of these candidates were objectively compared to the location of the annotations. Thereafter, the relative sensitivity of the CADe program was computed for the HR+ IDCs, HR- IDCs and the benign lesions. Chi-square tests were used to analyze the differences between the sensitivities of these three groups. Statistical differences are considered significant when p < 0.05.

RESULTS

CADe marked 71.2% of the IDC's as suspicious versus 45.7% of the benign lesions (p=0.012). Of the HR+ IDCs, 69.2% were marked by CADe. This is significantly higher than the marked proportion of benign lesions (p=0.028). Also the detection of HR- IDC's (78.6%) was better than that of the benign lesions (p=0.037). The detection of HR+ IDC's did not statistically differ from the HR-IDC's that were marked by CADe (p=0.48).

CONCLUSION

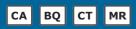
Computer Aided Detection software can detect and mark IDCs independent from the hormonal status. Furthermore, CADe differentiates between suspicious benign breast lesions and HR negative IDC's that are known for their benign-like ultrasonographic appearance.

CLINICAL RELEVANCE/APPLICATION

Computer Aided Detection software has the potential to aid radiologists in detecting even the more aggressive breast cancers and may aid in differentiating between aggressive subtypes of cancer and suspicious benign lesions.

Cardiac (Quantitative Imaging)

Tuesday, Dec. 1 3:00PM - 4:00PM Location: S504AB



AMA PRA Category 1 Credit [™]: 1.00 ARRT Category A+ Credit: 1.00

FDA Discussions may include off-label uses.

Participants

Lisa Diethelm, MD, New Orleans, LA (*Moderator*) Nothing to Disclose Frank J. Rybicki III, MD, PhD, Ottawa, ON (*Moderator*) Research Grant, Toshiba Corporation; Dianna M. Bardo, MD, Seattle, WA (*Moderator*) Speaker, Koninklijke Philips NV; Consultant, Koninklijke Philips NV; Author, Thieme Medical Publishers, Inc

Sub-Events

ssj04-01 Diagnostic Value of Quantitative Edema Detection Using T2-mapping in Acute Myocarditis

Tuesday, Dec. 1 3:00PM - 3:10PM Location: S504AB

Awards

Trainee Research Prize - Resident

Participants

Bettina Baessler, MD, Cologne, Germany (*Presenter*) Nothing to Disclose Frank Schaarschmidt, Hannover, Germany (*Abstract Co-Author*) Nothing to Disclose Anastasia Dick, Cologne, Germany (*Abstract Co-Author*) Nothing to Disclose Christian Stehning, Hamburg, Germany (*Abstract Co-Author*) Employee, Koninklijke Philips NV Bernhard Schnackenburg, PhD, Hamburg, Germany (*Abstract Co-Author*) Employee, Koninklijke Philips NV Guido Michels, Cologne, Germany (*Abstract Co-Author*) Nothing to Disclose David C. Maintz, MD, Koln, Germany (*Abstract Co-Author*) Nothing to Disclose Alexander C. Bunck, Koln, Germany (*Abstract Co-Author*) Nothing to Disclose

PURPOSE

To investigate the diagnostic value of T2-mapping in patients with acute myocarditis (ACM) and to define an appropriate cut-off value for edema detection.

METHOD AND MATERIALS

CMR data of 35 patients with clinically suspected ACM and confirmation of diagnosis by CMR according to the Lake Louise criteria were retrospectively analyzed. 30 healthy volunteers (HV) served as a control. All patients and HV were examined on a clinical 1.5T scanner, where - in addition to the routine CMR protocol - a breathhold Gradient Spin Echo (GraSE) T2-mapping sequence had been acquired at a basal, midventricular and apical slice in short axis view. T2-maps were segmented according to the 16-segments AHA-model and segmental T2 values as well as the segmental pixel-SD were analyzed. Statistical analysis was conducted using independent t-test, multiple logistic regression analyses, random forests, and decision trees.

RESULTS

Means of global myocardial T2 or pixel-SD showed only small differences between HV and ACM patients (T2: 58.7 \pm 0.3 ms vs. 63.1 \pm 0.4, p < .001; pixel-SD: 7.7 \pm 0.1 vs. 8.6 \pm 0.2, p < .001), lying in the observed normal range of HV. In contrast, variation of T2 values as well as of pixel-SD was much larger in ACM patients compared to HV. In random forests and multiple logistic regression analyses, the combination of the highest segmental T2 value within each patient (maxT2) and the mean absolute deviation (MAD) of log-transformed pixel-SD (madSD) over all 16 segments within each patient proved to be the best discriminators between HV and ACM patients with an AUC of 0.85 in ROC-analysis. In decision trees, a cut-off of 0.22 for madSD and of 67.7 ms for maxT2 resulted in 83% specificity and 97% sensitivity for classification between HV and ACM, even when not taking into account Lake Louise criteria.

CONCLUSION

The proposed cut-off values for maxT2 and madSD in the setting of ACM allow edema detection with high sensitivity and specificity and in a quantitative manner. The two parameters have the potential to overcome the hurdles of T2-mapping for its integration into clinical routine and should be validated in a greater patient cohort.

CLINICAL RELEVANCE/APPLICATION

Myocardial edema is an important factor not only in ACM. T2-mapping promises to be a quantitative approach in edema imaging, overcoming some limitations of qualitative edema assessment.

SSJ04-02 Myocardial T1 Mapping in Asymptomatic Subjects: Variations According to Left Ventricular Segments and Correlation with Cardiovascular Risk Factors

Tuesday, Dec. 1 3:10PM - 3:20PM Location: S504AB

Participants

Moon Young Kim, MD, Seoul, Korea, Republic Of (*Presenter*) Nothing to Disclose Soo Jin Cho, Seoul, Moldova, Republic Of (*Abstract Co-Author*) Nothing to Disclose Hae Jin Kim, Seoul, Korea, Republic Of (*Abstract Co-Author*) Nothing to Disclose Sung Mok Kim, MD, Seoul, Korea, Republic Of (*Abstract Co-Author*) Nothing to Disclose Sang-Chol Lee, Seoul, Korea, Republic Of (*Abstract Co-Author*) Nothing to Disclose Yeon Hyeon Choe, MD, PhD, Seoul, Korea, Republic Of (Abstract Co-Author) Nothing to Disclose

PURPOSE

To evaluate whether there is variation in precontrast and postcontrast myocardial T1 time (prT1 and poT1, respectively) and extracelluar volume fraction (ECVF) according to left ventricular (LV) segments and to search for any correlation between them and known cardiovascular risk factors.

METHOD AND MATERIALS

This study included 198 asymptomatic subjects (180 men and 18 women, age 54.4 \pm 6.12 years) who underwent cardiac MR imaging. Precontrast T1 mapping and postcontrast T1 mapping 15 minutes after 0.2 mmol gadobutrol injection were performed using shortened modified look-locker inversion recovery [ShMOLLI] sequence at 1.5T (Magnetom Avanto, Siemens). Short-axial cine MR imaging was performed with SSFP technique. T1 values and ECVFs were calculated in 16 AHA myocardial segments. Those values were compared among LV segments and correlated with presence of hypertension (n = 52), diabetes mellitus (DM, n = 15), or both (n = 17). ECVF was also correlated with LV mass.

RESULTS

The overall prT1 and poT1 values and ECVF were 1006 \pm 291.5 ms, 454.2 \pm 38.5 ms, and 0.24 \pm 0.04, respectively. There was significant difference between apical segments and mid-basal segments in poT1 value and ECVF (p<0.03) and between mid-septal segments and mid-lateral segments in T1 values and ECVF (p<0.04). ECVF showed reverse correlation with LV mass (p=0.002). There was significantly lower poT1 value (449 \pm 35.6 ms) and higher ECVF (0.24 \pm 0.04) in subjects with hypertension compared with those (459 \pm 43.3 ms and 0.23 \pm 0.02) of subjects without hypertension (p<0.05). Subjects with DM showed no difference in all T1 values from subjects with both risk factors showed no difference in all T1 values from subjects with both risk factors showed no difference in all T1 values from subjects with both risk factors showed no difference in all T1 values from subjects without DM or hypertension, except poT1 values from subjects without DM or hypertension, except poT1 values from subjects without DM or hypertension, except poT1 values from subjects without DM or hypertension, except poT1 values from subjects without DM or hypertension, except poT1 values from subjects without DM or hypertension, except prT1 values from subjects without DM or hypertension, except prT1 values from subjects without DM or hypertension, except prT1 values from subjects without DM or hypertension, except prT1 values from subjects without DM or hypertension, except prT1 values from subjects without DM or hypertension, except prT1 values from subjects without DM or hypertension, except prT1 values from subjects without DM or hypertension, except prT1 values from subjects without DM or hypertension, except prT1 value between apical septal and lateral segments (1007 \pm 126 ms vs 999 \pm 156 ms, p=0.03).

CONCLUSION

The septal wall showed higher prT1 value and ECVF but lower poT1 value than the lateral wall of mid- and basal levels. PoT1 value and ECVF are significantly affected by hypertension and LV mass.

CLINICAL RELEVANCE/APPLICATION

Normal range of T1 values and ECVF and their segmental variation should be differentiated from myocardial pathologic conditions. Moreover the cardiovascular risk factors may affect T1 values, ECVF, and LV function in asymptomatic subjects before cardiovascular symptoms develop.

SSJ04-03 3D-Dixon MRI Based Volumetry of Peri- and Epicardial Fat

Tuesday, Dec. 1 3:20PM - 3:30PM Location: S504AB

Participants

Rami Homsi, Bonn, Germany (*Presenter*) Nothing to Disclose Michael Meier-Schroers, Bonn, Germany (*Abstract Co-Author*) Nothing to Disclose Juergen Gieseke, DSc, Bonn, Germany (*Abstract Co-Author*) Employee, Koninklijke Philips NV Julian A. Luetkens, Bonn, Germany (*Abstract Co-Author*) Nothing to Disclose Darius Dabir, Bonn, Germany (*Abstract Co-Author*) Nothing to Disclose Claas P. Naehle, MD, Bonn, Germany (*Abstract Co-Author*) Consultant, Medtronic, Inc Daniel Kuetting, MD, Bonn, Germany (*Abstract Co-Author*) Nothing to Disclose Hans H. Schild, MD, Bonn, Germany (*Abstract Co-Author*) Nothing to Disclose Daniel K. Thomas, MD, PhD, Bonn, Germany (*Abstract Co-Author*) Nothing to Disclose Alois Martin Sprinkart, MSc, Bonn, Germany (*Abstract Co-Author*) Nothing to Disclose

PURPOSE

There is growing evidence that pericardial and epicardial fat volume (PFV, EFV) are associated with cardiovascular risk. The aim of this study was to develop a novel approach to accurately measure PFV and EFV using a 3D-Dixon based MRI approach.

METHOD AND MATERIALS

A cardiac triggered and respiratory navigator gated 3D-gradient echo pulse sequence (TR=5.4ms, TE1/TE2 = 1.8/4.0ms, a=20°, voxel size 1.5x1.5x3.0mm3) was developed for cardiac Dixon imaging. Based on this sequence fat fraction maps were computed. After correction for relaxation effects and setting of an appropriate noise threshold, voxels with more than 50% signal from fat were added for volumetry. Validation of the measurement accuracy was performed in a phantom consisting of muscle tissue and five different known volumes of fat (50-200ml). The proposed sequence was acquired in 34 healthy volunteers (22 male, BMI range 14-42 kg/m2, age range 21-79y) at 1.5T (Ingenia, Philips). Analysis was performed independently by two readers by drawing two 3D-region of interests, one for EFV and one for PFV. Additionally, EFV and PFV were compared between overweighted and non-overweighted subjects.

RESULTS

The phantom study showed an excellent agreement of measured and true fat volumes (maximum difference = 5 ml, linear correlation R>0.99). PFV over all volunteers was 158.0 \pm 126.4ml and EFV was 77.0 \pm 55.3ml. PFV and EFV were highly correlated (R=0.96). Inter-reader agreement was good with a mean difference of 0.2 \pm 5.6ml and 4.5 \pm 4.2ml for PFV/EFV, (R>0.99, each). EFV and PFV differed significantly between overweighted and non-overweighted subjects (BMI >25kg/m2 and BMI <25kg/m2, n=17 each) with PFV 219.0 \pm 151.8ml vs. 96.9 \pm 44.7ml and EFV 102.3 \pm 66.3ml vs. 51.7 \pm 23.6ml (p<0.001, each). There was no significant difference in age between the two groups (41.4 \pm 14.3y vs. 42.9 \pm 16.0y, p= 0.76).

CONCLUSION

The implemented Dixon method allows accurate measurement of PFV and EFV with all benefits of a 3D-approach similar to CT.

CLINICAL RELEVANCE/APPLICATION

The proposed 3D-Dixon based method allows accurate measurement of cardiac fat volumes, free of ionizing radiation and provides a

valuable tool for cardiovascular risk stratification.

ssj04-04 Reproducibility of Cine Displacement Encoding with Stimulated Echoes (DENSE) in Human Subjects

Tuesday, Dec. 1 3:30PM - 3:40PM Location: S504AB

Participants Kai Lin, MD, MSc, Chicago, IL (*Presenter*) Nothing to Disclose Michael Markl, PhD, Chicago, IL (*Abstract Co-Author*) Nothing to Disclose Jeremy D. Collins, MD, Chicago, IL (*Abstract Co-Author*) Nothing to Disclose Varun Chowdhary, MD, BS, Chicago, IL (*Abstract Co-Author*) Nothing to Disclose Julie A. Blaisdell, Chicago, IL (*Abstract Co-Author*) Nothing to Disclose Gong Feng, MD,PhD, Chicago, IL (*Abstract Co-Author*) Nothing to Disclose Bruce Spottiswoode, Chicago, IL (*Abstract Co-Author*) Nothing to Disclose Bruce Spottiswoode, Chicago, IL (*Abstract Co-Author*) Nothing to Disclose Bruce Spottiswoode, Chicago, IL (*Abstract Co-Author*) Research Grant, Astellas Group Research support, Siemens AG Speaker, Siemens AG Advisory Board, Guerbet SA

PURPOSE

To test the hypothesis that two-dimensional (2D) displacement encoding via stimulated echoes (DENSE) is a reproducible technique for the depiction of segmental myocardial motion in human subjects.

METHOD AND MATERIALS

Following the approval of the institutional review board (IRB), 10 healthy volunteers without documented history of cardiovascular disease were recruited. For each participant, 2D DENSE were performed twice (at different days) and the data were obtained at basal, midventricular and apical levels of the LV with a short-axis view. The first and second principal strains (E1 and E2), radial thickening strain (Err), circumferential rotating strain (Ecc), twist and torsion were calculated. The intra-, inter-observer and inter-study variances were evaluated using coefficient of variation (CoV) and intra-class correlation coefficient (ICC).

RESULTS

In total, there are 160 pairs of myocardial segments (from 2 scans on 10 subjects) for quantitative analysis and comparison. Figure 1 shows an example set of DENSE images demonstrating myocardial displacement maps from a single subject for scan #1 and #2. The images demonstrated similar image quality and systolic displacement patterns for both acquisitions. These observations were confirmed by segment-by-segment comparisons which showed no significant differences in peak Ecc, E1, E2, twist and torsion between two sequential scans. A difference in radial strain was noted, Err ($0.43 \pm 0.22 \text{ vs}.0.38 \pm 0.19$, p = 0.008). There was good scan-rescan reproducibility of peak Ecc (CoV = 20.59%, ICC = 0.815, p < 0.001), E2 (CoV = 14.85%, ICC = 0.757, p < 0.001), twist (CoV = 34.12%, ICC = 0.911, p < 0.001) and torsion (CoV = 11.07%, ICC = 0.818, p < 0.001). There was moderate scan-rescan reproducibility of Err (CoV = 36.36%, ICC = 0.664, p < 0.001) and E1 (CoV = 32.74%, ICC = 0.646, p < 0.001). The figure shows similar segmental patterns for all indices, significant differences only for 2 apical segments between two scans.

CONCLUSION

DENSE is a reproducible MRI technique for characterizing regional myocardial motion on a per-segment basis in human subjects.

CLINICAL RELEVANCE/APPLICATION

In the present study, we demonstrated the overall reproducibility of DENSE for the description of LV motion on a per-segment basis for human subjects.

SSJ04-05 The Relationship between the Transluminal Attenuation Gradient (TAG) Measured from Coronary CT Angiography (CTA) and Coronary Blood Flow: Validation in Left- versus Right-Dominant Circulation

Tuesday, Dec. 1 3:40PM - 3:50PM Location: S504AB

Participants

Dimitris Mitsouras, PhD, Boston, MA (*Presenter*) Research Grant, Toshiba Corporation; Speakers Bureau, Toshiba Corporation Rani S. Sewatkar, MBBS, Edison, NJ (*Abstract Co-Author*) Nothing to Disclose Mukta Agarwal, MD, Boston, MA (*Abstract Co-Author*) Nothing to Disclose Andreas Giannopoulos, MD, Boston, MA (*Abstract Co-Author*) Nothing to Disclose Marcus Y. Chen, MD, Bethesda, MD (*Abstract Co-Author*) Institutional research agreement, Toshiba Corporation Frank J. Rybicki III, MD, PhD, Ottawa, ON (*Abstract Co-Author*) Research Grant, Toshiba Corporation; Elizabeth George, MD, Boston, MA (*Abstract Co-Author*) Nothing to Disclose Michael Cheezum, MD, Boston, MA (*Abstract Co-Author*) Nothing to Disclose

PURPOSE

TAG characterizes the dropoff in contrast enhancement across a coronary artery in a CT angiogram. We sought to validate a theoretical relationship to coronary flow using the known relationships of physiologic flow amongst the three main coronary arteries.

METHOD AND MATERIALS

We hypothesized that during changing inflow contrast concentration (eg, during bolus up-/down-slope), TAG relates to volumetric flow as Q~Lumen Area [mm^2]×Inflowing Contrast Enhancement Change [HU/sec]/TAG [HU/mm]. TAG and relative flow metrics using this equation were calculated in 25 patients with <25% diameter stenoses imaged with 320-row CTA (AquilionOne, Toshiba), and compared between those with right- (RD) vs left-/co-dominant (LD) circulation. Lumen area was determined for the arterial length used for TAG measurement. For 22 patients with bolus tracking images additionally available, inflow contrast enhancement change during the CTA was estimated in the ascending aorta. TAG-derived flow was averaged for each major coronary artery of LD and RD patients separately, and compared to invasively-measured flows reported in the PREDICTION trial (n=496 patients; Sakamoto et al, Am J Cardiol 2013;111:1420-).

RESULTS

20 patients were RD and 5 LD. In those with bolus tracking images, TAG-derived flow in the LAD and LCX was within 4-16% of physiologic values; RCA flow was over/underestimated by 21-40%. In terms of physiologic LD/RD ratios, TAG-derived flow in the

LAD for LD vs RD patients was 1.09 (104 vs 92.5 ml/min), which compares well to the known physiologic ratio of 1.07 (2% difference). Similarly, the ratio for the LCX was 1.47 (113 vs 76 ml/min) compared to the physiologic ratio of 1.57 (6% difference), and in the RCA it was 0.37 (56 vs 158 ml/min) compared to 0.50 (26% difference).

CONCLUSION

The TAG in coronary arteries appears inversely proportional to resting coronary flow. Knowledge of the temporal change of inflow contrast concentration further enables derivation of coronary flow from TAG.

CLINICAL RELEVANCE/APPLICATION

Knowledge of the relationship of TAG to coronary flow can enhance detection of functionally significant CAD. We have used this relationship to increase TAG accuracy for predicting a significant invasive fractional flow reserve (FFR<0.8), and to obtain more accurate hyperemic blood flow boundary conditions for FFR-CT estimation via computational fluid dynamics.

SSJ04-06 Feasibility of the Combined CT Assessment of Coronary CT Angiography and Quantitative Myocardial CT Perfusion Imaging for the Detection of Obstructive Coronary Artery Disease Assessed by Invasive Coronary Angiography and Cardiac Magnetic Resonance

Tuesday, Dec. 1 3:50PM - 4:00PM Location: S504AB

Participants

Yuki Tanabe, Toon, Japan (*Presenter*) Nothing to Disclose Teruhito Kido, MD, PhD, Toon, Japan (*Abstract Co-Author*) Nothing to Disclose Takahiro Yokoi, Toon, Japan (*Abstract Co-Author*) Nothing to Disclose Naoki Fukuyama, Toon, Japan (*Abstract Co-Author*) Nothing to Disclose Ryo Ogawa, MD, Toon, Japan (*Abstract Co-Author*) Nothing to Disclose Rami Yokoyama, Toon, Japan (*Abstract Co-Author*) Nothing to Disclose Yoshiko Nishiyama, MD, Toon, Japan (*Abstract Co-Author*) Nothing to Disclose Tomoyuki Kido, Toon, Japan (*Abstract Co-Author*) Nothing to Disclose Akira Kurata, PhD, Toon, Japan (*Abstract Co-Author*) Nothing to Disclose Masao Miyagawa, MD, PhD, Toon, Japan (*Abstract Co-Author*) Nothing to Disclose Teruhito Mochizuki, MD, Toon, Japan (*Abstract Co-Author*) Nothing to Disclose

PURPOSE

The aim of this study was to evaluate the diagnostic performance of the combined assessment of coronary computed tomography angiography (CTA) and quantitative myocardial CT perfusion (CTP) to identify obstructive coronary artery disease (CAD).

METHOD AND MATERIALS

The study group comprised consecutive 34 patients (mean age 68.7 years) who underwent combined CT protocol and cardiac magnetic resonance (CMR) prior to invasive coronary angiography (ICA). CT scan protocol consisted of pharmacological stress dynamic myocardial CTP and coronary CTA using 256-slice CT. Obstructive CAD was defined as stenosis>=50% on ICA with a corresponding myocardial ischemia on CMR. Quantitative CTP assessment was performed with myocardial blood flow (MBF), which was calculated by model-based deconvolution method using semi-automated prototype software (FUJIFILM RI Pharma Co., Ltd., Tokyo, Japan) built on MATLAB (The MathWorks Inc, Natick, MA). A cut-off value of CT-MBF was determined for detecting myocardial ischemia assessed by CMR using receiver operating characteristic (ROC) analysis at a vessel level. The presence of coronary stenosis was assessed with lesions defined as follows: 0-no luminal stenosis; 1-minimal (<25% stenosis); 2-mild (25-49% stenosis); 3-moderate (50-69% stenosis); 4-severe (70-99% stenosis); and 5-occlusion. Coronary stenosis >= 50% or unavailable vessels were defined as significant, and CT-MBF was referred consequently. A vascular territory with a significant stenosis on CTA along with CT-MBF less than the cut-off value was considered to be positive. Diagnostic performance (sensitivity, specificity, positive and negative predictive value [PPV and NPV]) of CTA, CTP and combined assessment (CTA+CTP) for detecting obstructive CAD.

RESULTS

A cut-off value of CT-MBF was 1.28 ml/g/min. In comparison with ICA and CMR, sensitivity, specificity, PPV and NPV were 97%, 47%, 52% and 97% for CTA, 84%, 76%, 67% and 89% for CTP and 84%, 89%, 82% and 90% for combined assessment. Area under the ROC curve of CTA, CTP and combined assessment were 0.79, 0.83 and 0.88.

CONCLUSION

Combined CT assessment of CTA and quantitative CTP imaging allows for evaluating obstructive CAD with high diagnostic accuracy using single modality.

CLINICAL RELEVANCE/APPLICATION

Combined CT protocol of CTA and CTP allows for anatomical and physiological assessment of coronary artery disease with high diagnostic accuracy by using a single modality.

Molecular Imaging (Prostate/Neuroendocrine Tumors)

Tuesday, Dec. 1 3:00PM - 4:00PM Location: S504CD

GU BQ MI MR

AMA PRA Category 1 Credit ™: 1.00 ARRT Category A+ Credit: 1.00

FDA Discussions may include off-label uses.

Participants

Peter L. Choyke, MD, Rockville, MD (*Moderator*) Researcher, Koninklijke Philips NV Researcher, General Electric Company Researcher, Siemens AG Researcher, iCAD, Inc Researcher, Aspyrian Therapeutics, Inc Researcher, ImaginAb, Inc Researcher, Aura Biosciences, Inc

Vikas Kundra, MD, PhD, Houston, TX (Moderator) License agreement, Introgen Therapeutics, Inc

Sub-Events

SSJ14-01 Promising Role of Ga-68 PSMA PET/CT over Conventional Imaging in Staging and Restaging of Carcinoma Prostate

Tuesday, Dec. 1 3:00PM - 3:10PM Location: S504CD

Participants

Venkatesh Rangarajan, MBBS, Mumbai, India (*Presenter*) Nothing to Disclose Archi Agrawal, MBBS, Mumbai, India (*Abstract Co-Author*) Nothing to Disclose Rasika Kabnurkar, MBBS, Mumbai, India (*Abstract Co-Author*) Nothing to Disclose Nilendu C. Purandare, DMRD, Mumbai, India (*Abstract Co-Author*) Nothing to Disclose Sneha A. Shah, Mumbai, India (*Abstract Co-Author*) Nothing to Disclose

PURPOSE

1) To study the utility of Ga-68 Prostate Specific Membrane Antigen (PSMA) Positron Emission Tomography/Computed Tomography (PET/CT) for staging and restaging of Carcinoma Prostate (CaP).2) To compare the efficacy of Ga-68 PSMA PET/CT with Contrast Enhanced Computed Tomography (CECT) and F18 Sodium Fluoride (NaF) PET/CT for lesion detection

METHOD AND MATERIALS

Retrospective audit of prospectively maintained data of 25 patients of CaP (3 for staging and 22 with biochemical failure for restaging) who underwent Ga-68 PSMA PET/CT, CECT and F18 NaF PET/CT scan. The imaging findings were analyzed on lesion-lesion and patient-patient basis for concordance and discordance.

RESULTS

All the 3 cases imaged for staging evaluation demonstrated Ga-68 PSMA uptake at the site of primary while CECT demonstrated lesion in only 1 patient. In cases with suspected biochemical failure, local recurrence was detected in 59% (13/22) patients on Ga-68 PSMA PET/CT as against 9 % (2/22) detected on CECT. In 25 patients studied, Ga-68 PSMA PET/CT detected 43 metastatic nodes compared to 29 detected on CECT. Ga-68 PSMA detected additional metastases in sub cm sized nodes in 24% (6/25) patients. Ga-68 PSMA had incremental value in detecting occult extranodal metastases involving urinary bladder, pararectal nodule and peritoneal deposit in 8% (2/25) patients .In 25 patients, 109 skeletal lesions were detected on Ga-68 PSMA while F18 NaF PET/CT demonstrated147 lesions. Concordance in imaging findings of Ga-68 PSMA PET/CT and F 18 Fluoride PET/CT was noted in 68% (17/25) patients. Ga-68 PSMA PET/CT had an incremental value in staging of 1 patient where it detected lytic and marrow metastases. In restaging group, 7 patients showed additional lesions on F18 NaF PET/CT.

CONCLUSION

Ga-68 PSMA PET/CT is superior in detection of primary, nodal and soft tissue metastases as compared to conventional imaging techniques. However, F18 NaF PET/CT appears to detect more skeletal lesions in patients with biochemical failure in our study and further prospective trials are warranted to confirm these findings.

CLINICAL RELEVANCE/APPLICATION

Ga-68 PSMA PET/CT has an incremental value as a one stop shop in staging and restaging of carcinoma prostate

SSJ14-02 18F-fluoro-4-thia-palmitate (18F-FTP) PET Imaging for Evaluation of Exogenous Fatty Acid Metabolism in Prostate Cancer: Implications for Treatment Optimization

Tuesday, Dec. 1 3:10PM - 3:20PM Location: S504CD

Participants

Pedram Heidari, MD, Boston, MA (*Presenter*) Nothing to Disclose Shadi A. Esfahani, MD, MPH, Boston, MA (*Abstract Co-Author*) Nothing to Disclose Giorgia Zadra, PhD, Boston, MA (*Abstract Co-Author*) Nothing to Disclose Michael S. Placzek, PhD, Charlestown, MA (*Abstract Co-Author*) Nothing to Disclose Benjamin Larimer, PhD, Charlestown, MA (*Abstract Co-Author*) Nothing to Disclose Jacob M. Hooker, PhD, Charlestown, MA (*Abstract Co-Author*) Nothing to Disclose Massimo Loda, MD, Boston, MA (*Abstract Co-Author*) Nothing to Disclose Umar Mahmood, MD, PhD, Charlestown, MA (*Abstract Co-Author*) Research Grant, Sabik Medical Inc; Advisory Board, Blue Earth Diagnostics Limited;

PURPOSE

Upregulation of de novo lipogenesis is a major metabolic change in PCa development, and correlates with tumor progression and poor prognosis. Differentiation of diet-derived versus de novo fatty acid (FA) utilization in PCa is essential in designing anti-lipogenic therapeutics. We aim to evaluate the use of 18F-fluoro-4-thia-palmitate (18F-FTP) PET for assessment of exogenous FA utilization by PCa.

METHOD AND MATERIALS

14C incorporation into lipids of LNCaP cells by a glucose donor (marker of de novo lipogenesis) was measured by a beta-counter after treatment with vehicle, IPI-9119, or C75. Growth inhibition rescue of LNCaP cells was performed using Cell Titer Glo assay after incubation with IPI-9119 alone or in the presence of BSA or of BSA-conjugated palmitate. For in-vitro 18F-FTP uptake study LNCaP cells were incubated with IPI-9119, C75, Etomoxir, SSO, DMSO, and combination of IPI-9119 with Etomoxir or C75 for 24 hours. The cells were then incubated with 18F-FTP and harvested to measure retained activity corrected for cell count. IACUC approval was obtained. Mice with subcutaneous LNCaP xenografts were fasted. PET data was acquired in list mode after injection of 18F-FTP. The SUVmean and tracer influx constant were measured.

RESULTS

14C incorporation in lipids decreased to approximately 25% of control using both IPI-9119 and C75 indicating FASN inhibition. LNCaP growth inhibition was aborted by BSA-conjugated palmitate. 18F-FTP uptake significantly increased with IPI-9119 treatment, while C75, etomoxir, SSO treatment reduced 18F-FTP uptake. 18F-FTP PET demonstrated significantly decreased uptake in LNCaP tumors following treatment with C75 and etomoxir compared to control (SUVmean=0.20±0.01, 0.25±0.2, and 0.40±0.02, respectively).

CONCLUSION

We demonstrated that metabolic imaging using 18F-FTP can be used to assess the exogenous FA utilization by PCa. As expected, IPI-9119 (selective FASN inhibitor) increased the exogenous FA (18F-FTP) uptake while C75, which induces a host of metabolic modulations other than FASN inhibition paradoxically reduces 18F-FTP uptake. Etomoxir (FAO inhibitor) and SSO (FA transporter inhibitor) reduce 18F-FTP uptake as expected.

CLINICAL RELEVANCE/APPLICATION

Understanding the effect of exogenous lipid availability on therapeutic potential of targeting de novo lipogenesis is critical in prostate cancer treatment. This could lead to treatment strategies that result in maximal efficacy.

SSJ14-03 Feasibility of Hyperpolarized 13C-Pyruvate Magnetic Resonance Spectroscopy for Pancreatic Cancer Diagnostic Imaging

Tuesday, Dec. 1 3:20PM - 3:30PM Location: S504CD

Participants

Stephanie K. Carlson, MD, Rochester, MN (*Presenter*) Royalties, Medspira, LLC Alan Penheiter, PhD, Rochester, MN (*Abstract Co-Author*) Nothing to Disclose Prasanna K. Mishra, PhD, Rochester, MN (*Abstract Co-Author*) Nothing to Disclose Fergus J. Couch, PhD, Rochester, MN (*Abstract Co-Author*) Nothing to Disclose Slobodan I. Macura, PhD, Rochester, MN (*Abstract Co-Author*) Nothing to Disclose John D. Port, MD, PhD, Rochester, MN (*Abstract Co-Author*) Nothing to Disclose Malgorzata Marjanska, PhD, Minneapolis, MN (*Abstract Co-Author*) Nothing to Disclose Claire E. Bender, MD, Rochester, MN (*Abstract Co-Author*) Nothing to Disclose

PURPOSE

Hyperpolarized (HP) 13C magnetic resonance spectroscopic imaging (MRSI) is a recently developed technique that allows the detection of injected 13C-labeled agents and their metabolites in real-time. The purpose of this study was to identify and explore potential metabolic pathways in pancreatic ductal adenocarcinoma (PDAC) that could be targeted with HP-13C MRSI to increase the diagnostic accuracy of pancreatic cancer imaging.

METHOD AND MATERIALS

We performed gene expression profiling using laser capture microdissection and RNAseq on histologically-confirmed primary PDAC tumors and normal pancreas tissue from 21 patients. A promising, highly upregulated and imageable metabolic pathway (the conversion of pyruvate to lactate) was identified. To further explore this pathway in vivo, mice bearing genetically-engineered PDAC tumors were injected with 200 microliters of 80 mM [1-13C]-pyruvate. Tumors were quench-frozen and excised 30 s post-injection. Spectroscopic data on tumor lysates was obtained using 1H and 13C nuclear magnetic resonance. Studies were approved by our IRB and IACUC.

RESULTS

Gene expression studies showed that transcripts encoding transporters and enzymes responsible for cellular import of pyruvate, export of lactate, and conversion of pyruvate to lactate are almost universally upregulated in PDAC compared to normal pancreas, while competing pathways of mitochondrial pyruvate metabolism and cytoplasmic pyruvate to alanine conversion are consistently low. NMR analysis of PDAC tumors showed a tumor metabolic signature consistent with a very high lactate concentration and high lactate-to-alanine ratio. Quantitative analysis after injection of [1-13C]-pyruvate showed a 4.8-fold enrichment of intratumoral [1-13C]-lactate over natural abundance, indicating that ~5% of the total lactate in the tumor at 30 s post-injection was derived from the injected [1-13C]-pyruvate.

CONCLUSION

PDAC tumors have a pyruvate-lactate metabolic signature that can be quantitated with 13C-pyruvate NMR. Further exploration of HP-13C-pyruvate MRSI for PDAC is warranted.

CLINICAL RELEVANCE/APPLICATION

A new molecular imaging strategy for PDAC used in conjunction with existing morphological imaging could transform patient management in clinically-challenging scenarios.

System for Patients with Neuroendocrine Tumours: Direct Comparison to Multiphase Contrastenhanced PET/CT

Tuesday, Dec. 1 3:30PM - 3:40PM Location: S504CD

Participants

Ferdinand F. Seith, BSC, Tuebingen, Germany (*Presenter*) Nothing to Disclose Christian la Fougere, Munich, Germany (*Abstract Co-Author*) Nothing to Disclose Christina Pfannenberg, MD, Tuebingen, Germany (*Abstract Co-Author*) Nothing to Disclose Konstantin Nikolaou, MD, Tuebingen, Germany (*Abstract Co-Author*) Speakers Bureau, Siemens AG Speakers Bureau, Bracco Group Speakers Bureau, Bayer AG Nina Schwenzer, MD, Tuebingen, Germany (*Abstract Co-Author*) Nothing to Disclose Cornelia Brendle, MD, Tubingen, Germany (*Abstract Co-Author*) Nothing to Disclose Christina Schraml, MD, Tuebingen, Germany (*Abstract Co-Author*) Nothing to Disclose

PURPOSE

In patients with neuroendocrine tumours (NET), kidney failure is a common complication of radionuclide therapy. It is known that multiphase contrast-enhanced PET/CT is superior to non-enhanced PET/CT in diagnosing metastases with low or no tracer uptake as well as small lesions especially in the liver. However, due to the superior soft tissue contrast of MRI it is possible that non-enhanced PET/CT. The aim of the study was therefore to evaluate a fast protocol in PET/MR without contrast agent in direct comparison to multiphase contrast-enhanced PET/CT as gold standard.

METHOD AND MATERIALS

39 Patients (22 female, 58±13 years) were examined in multiphase contrast-enhanced 68Ga-DOMITATE-PET/CT in a clinical setup and in PET/MR subsequently. 2 blinded readers investigated PET/MR examinations of the abdomen with 3 different setups: T2HASTE+PET (30min), T2HASTE+TSET2+PET (35min) and T2HASTE+TSET2+DWI+PET (35min). The T2HASTE was acquired under free breathing with continuous table move. DWI was acquired with two b-values (0, 800 s/mm2). Metastatic lesions were defined as functional and/or morphological suspicious lesions or lymph nodes. The results were compared with the contrast-enhanced PET/CT, follow-up examinations and histopathology, if available.

RESULTS

T2HASTE sequences were of diagnostic quality in all patients. DWI suffered from artefacts especially in the upper regions of the liver. Compared with contrast-enhanced PET/CT high agreement was found with T2HASTE+TSET2+DWI+PET.

CONCLUSION

A protocol for PET/MR including T2HASTE, TSET2, DWI and PET seems to provide comparable results compared with multiphase contrast-enhanced PET/CT. With an estimated time of 35 min for a whole body examination, this might serve as a legitimate alternative to contrast-enhanced PET/CT for patients with kidney failure in the future.

CLINICAL RELEVANCE/APPLICATION

In patients with neuroendocrine tumours (NET) and kidney failure, fast non-enhanced PET/MR protocols can serve as a legitimate alternative to multiphase contrast-enhanced PET/CT examinations.

SSJ14-05 Qualitative and Quantitative Comparison of 68Ga-DOTATATE PET/CT and PET/ MRI in Neuroendocrine Tumours

Tuesday, Dec. 1 3:40PM - 3:50PM Location: S504CD

Participants

Francesco Fraioli, MD, London, United Kingdom (*Presenter*) Nothing to Disclose Alshaima Alshammari, London, United Kingdom (*Abstract Co-Author*) Nothing to Disclose Evangelia Skoura, Athens, Greece (*Abstract Co-Author*) Nothing to Disclose Rizwan Syed, MBBS, FRCR, London, United Kingdom (*Abstract Co-Author*) Nothing to Disclose Sofia Michopoulou, London, United Kingdom (*Abstract Co-Author*) Nothing to Disclose Jamshed Bomanji, London, United Kingdom (*Abstract Co-Author*) Nothing to Disclose Ashley M. Groves, MBBS, Hitchin, United Kingdom (*Abstract Co-Author*) Investigator, GlaxoSmithKline plc; Investigator, General Electric Company; Investigator, Siemens AG; ; ;

PURPOSE

Many Neuroendocrine tumours (NET) show high somatostatin receptor avidity. The aim of this study is to compare 68Ga-DOTATATE PET/CT with 68Ga-DOTATATE PET/MRI imaging in patients with known NET, and assess the confidence in anatomic lesion detection and localization. Furthermore, the value of each sequence of MRI was separately evaluated.

METHOD AND MATERIALS

We analysed the data of 38 NET patients. Cross over of both 68Ga-DOTATE PET/CT and PET/MRI scans were performed. MR protocol was as follow: T1 MPR, pre and post gadolinium injection, T2 haste, DW1 (b0, 500, 1000). Two observers for 68Ga-DOTATATE PET/MRI and one observer for 68Ga-DOTATATE PET/CT, independently, reviewed the images and inter observer and inter modality correlation was assessed by using interclass correlation.

RESULTS

Our initial data showed good inter modality correlation between 68Ga-PET/CT and PET/MRI. All lesions considered as malignant in PET/CT were equally depicted in PET/MRI in the compared regions. Both modalities, revealed liver metastases in the same number of patients (18 patients), and bone metastases in 7 patients. However, counting the number of liver lesions in each patient, 68Ga-DOTATATE PET/MRI was able to recognize more lesions in 3 patients. On the other hand, more lung lesions were detected in the lung in the CT component compared to MRI component (7 lesions versus 4). The contrast and DWI sequence of PET/MRI did not have a significant effect on final outcome, but in a selected number of cases these images confirmed and helped to further characterize and detect more lesions. Inter observer reliability was equally very good in both modalities.

CONCLUSION

This study demonstrates the potential of 68Ga-DOTATOC PET/MRI in patients with NET, with special advantages in the characterization of liver lesions.

CLINICAL RELEVANCE/APPLICATION

68Ga-DOTATOC PET/MRI can help in diagnosis and staging of patients with NET, with special advantages in the characterization of liver lesions.

SSJ14-06 68Ga-DOTATOC Uptake in Somatostatin Expressing Tumors is Directly Related to Specific Activity: Implications for Receptor Quantitation Imaging

Tuesday, Dec. 1 3:50PM - 4:00PM Location: S504CD

Participants

Pedram Heidari, MD, Boston, MA (*Presenter*) Nothing to Disclose Dominik Berzaczy, MD, Vienna, Austria (*Abstract Co-Author*) Nothing to Disclose Alicia Leece, Boston, MA (*Abstract Co-Author*) Nothing to Disclose Shadi A. Esfahani, MD, MPH, Boston, MA (*Abstract Co-Author*) Nothing to Disclose Umar Mahmood, MD, PhD, Charlestown, MA (*Abstract Co-Author*) Research Grant, Sabik Medical Inc; Advisory Board, Blue Earth Diagnostics Limited;

PURPOSE

The importance of specific activity (SA) has been previously shown in functional PET imaging studies. We hypothesized that tracer uptake, measured using semiquantitative (SUV) or quantitative (Patlak plot) parameters, would vary considerably according to SA in cancer receptor imaging. This study aims to evaluate the effect of SA on PET parameters used for quantitation of 68Ga-DOTATOC uptake in somatostatin receptor (SSTR) tumor models.

METHOD AND MATERIALS

In-vitro, SSTR2 expression level was assessed using Western blot across multiple cancer lines including IMR32, Capan1, A549 and AR42J, and was normalized for B-actin expression. The SSTR2/B-actin ratio was correlated to in-vitro 68Ga-DOTATOC uptake normalized for cell counts. AR42J and IMR32 normalized 68Ga-DOTATOC uptake was plotted against 68Ga-DOTATOC SA ranging from 0.2 to 20 Ci/g and correlation was assessed. The in-vitro studies were performed in triplicate. For in-vivo studies Institutional Animal Care and Use Committees approval was obtained. Subcutaneous AR42J xenografts were implanted in Nu/Nu mice. Dynamic PET scans in list mode were acquired following injection of 68Ga-DOTATOC with a wide range of SAs (0.3 - 50 Ci/g). Net tracer influx (Ki), SUVmax and SUVmean were plotted against the SA to establish the correlation between quantitative parameters and SA. Patlak-plot was used to calculate the tracer influx constant for the tumor ((Ki= (k1 × k3 / k2 + k3)).

RESULTS

We observed a consistent ratio between 68Ga-DOTATOC uptake per cell and SSTR2/B-actin level across the cell lines (R2=0.95, p<0.024). In-vitro we demonstrated a linear correlation between SA and 68Ga-DOTATOC uptake per cell in IMR32 (R2=0.98, P<0.015) and AR42J (R2=0.99, P<0.005). We found that Ki, SUVmax, and SUVmean decreased in a linear fashion with reduction in SA. Quantitative 68Ga-DOTATOC PET parameters had a direct linear correlation with SA (R2=0.89, p<0.001 for Ki, R2=0.66, p<0.0001 for SUVmax and R2=0.82 and p<0.0001 for SUVmean).

CONCLUSION

68Ga-DOTATOC uptake is strongly correlated to SSTR2 expression for each given SA. However, 68Ga-DOTATOC uptake in SSTRexpressing tumors increases in a linear fashion with increase in SA, over the range studied.

CLINICAL RELEVANCE/APPLICATION

68Ga-DOTATOC uptake by tumors can vary widely with change in specific activity. Quantitation for radiotherapy dosimetry and response assessment is improved with correction for specific activity.

Musculoskeletal (Quantitative MR Applications)

Tuesday, Dec. 1 3:00PM - 4:00PM Location: E451A

MK BQ MR

AMA PRA Category 1 Credit ™: 1.00 ARRT Category A+ Credit: 1.00

FDA Discussions may include off-label uses.

Participants

Martin Torriani, MD, Boston, MA (*Moderator*) Nothing to Disclose Gregory Chang, MD, New York, NY (*Moderator*) Speaker, Siemens AG

Sub-Events

SSJ15-01 Quantitative MRI Perfusion Analysis of Osteoid Osteomas Pre- and Post Microwave Ablation using an Open Source Software Tool (UMMPerfusion)

Tuesday, Dec. 1 3:00PM - 3:10PM Location: E451A

Participants

Michael Kostrzewa, MD, Mannheim, Germany (*Presenter*) Nothing to Disclose Patricius Diezler, MD, Mannheim, Germany (*Abstract Co-Author*) Nothing to Disclose Thomas Henzler, MD, Mannheim, Germany (*Abstract Co-Author*) Nothing to Disclose Nils Rathmann, MD, Mannheim, Germany (*Abstract Co-Author*) Nothing to Disclose Stefan O. Schoenberg, MD, PhD, Mannheim , Germany (*Abstract Co-Author*) Institutional research agreement, Siemens AG Steffen J. Diehl, MD, Mannheim, Germany (*Abstract Co-Author*) Nothing to Disclose

PURPOSE

To quantitatively evaluate blood perfusion of osteoid osteomas prior and after percutaneous microwave (MW) ablation in timeresolved imaging with stochastic trajectories (TWIST) MRI sequences using an open source software tool.

METHOD AND MATERIALS

In 17 patients (11 males, 6 females, mean age 26y) with osteoid osteomas percutaneous, CT guided, MW ablation was performed (Medwaves, San Diego, California, USA). Lesions measured on average 5 ± 2 mm in diameter. Lesion diameter dependent MW ablation parameters were: 16 Watts, 915MHz, 80°C for 45 to 160 seconds. Prior to and after MW ablation 3D dynamic contrast enhanced MRI imaging was performed with 3D TWIST gradient echo sequences (Siemens Healthcare). Mean plasma flow (PF, ml/100ml/min), mean volume of distribution (VD, ml/100ml) and mean transit time (MTT, sec) were measured within the lesion in the pre and post MW ablation MRI TWIST data using an open source software tool for quantitative MRI perfusion analysis (UMMPerfusion, OpossUMM, Germany).

RESULTS

16 patients were free of symptoms within one week after treatment, one patient had decreased but persisting symptoms after MW ablation. No minor or major adverse events were observed according to SIR criteria. Mean PF, VD and MTT were 253 ± 226 ml/100ml/min, 63 ± 60 ml/100ml and 17 ± 7 sec prior to ablation and 55 ± 64 ml/100ml/min, 23 ± 39 ml/100ml and 17 ± 12 sec after ablation respectively. In a paired t-test there was no statistically significant change in MTT prior to and after ablation (p>0.05), whereas PF (p=0.002) and VD (p=0.02) decreased significantly. In the patient with persisting symptoms continuously high values for PF (229ml/100ml/min) and VD (118ml/100ml) were found in the MRI after MW ablation in a small portion of the lesion, this was attributed to imprecise needle placement and to too short ablation time.

CONCLUSION

Treatment success of percutaneous MW ablation of osteoid osteomas can be reliably quantified by MRI perfusion analysis, especially by evaluating pre and post procedural PF and VD within the lesion. MRI perfusion analysis helps to identify small remnants of perfused osteoid osteoma tissue after MW ablation.

CLINICAL RELEVANCE/APPLICATION

Quantitative MRI perfusion analysis is clinically valuable in the evaluation of treatment success of percutaneous MW ablation for osteoid osteomas.

SSJ15-02 A Phase I Study to Assess the Feasibility of Quantitative Molecular Imaging of ACL Grafts

Tuesday, Dec. 1 3:10PM - 3:20PM Location: E451A

Participants

Katherine Binzel, PhD, Columbus, OH (*Presenter*) Nothing to Disclose Robert Magnussen, Columbus, OH (*Abstract Co-Author*) Nothing to Disclose Wenbo Wei, Columbus, OH (*Abstract Co-Author*) Nothing to Disclose Melanie U. Knopp, Malibu, CA (*Abstract Co-Author*) Nothing to Disclose David Flanigan, MD, Columbus, OH (*Abstract Co-Author*) Consultant, Vericel; Consultant, Smith & Nephew plc Michael V. Knopp, MD, PhD, Columbus, OH (*Abstract Co-Author*) Nothing to Disclose Christopher C. Kaeding, MD, Columbus, OH (*Abstract Co-Author*) Consultant, Biomet, Inc

PURPOSE

Injury to the anterior cruciate ligament (ACL) commonly requires reconstruction with a graft to restore stability and function. The rate at which graft ligamentization occurs is not well delineated by magnetic resonance imaging (MRI). This initial study aims to

demonstrate the feasibility of combined MRI with dynamic positron emission tomography (PET) in order to evaluate the graft healing process following reconstructive surgery.

METHOD AND MATERIALS

MRI was performed on a 3T Achieva on 20 patients post-ACL reconstruction. Dynamic PET/CT was acquired on a Gemini TF 64 and/or new digital detector PET/CT system, Vereos TF (all Philips Healthcare, Cleveland, OH). An in-house fabricated cushion was used to match positioning during PET acquisitions to that of the dedicated MRI knee coil. A single bed position centered on the knees was acquired continuously for 75 minutes using an ultra-low dose 3 mCi 18F-fluorodeoxyglucose (FDG) protocol. Patients were grouped according to time since surgery, 0-6 months, 6-12 months, 12-24 months, and 24 months or greater. Standardized uptake values (SUVmax) were measured for regions of interest placed over the proximal, middle, and distal portions of the graft, the femoral and tibial tunnels, the posterior cruciate ligament (PCL), and quadriceps muscle for reference. Matched ROIs were drawn in the contralateral knee.

RESULTS

Dynamic PET images were readily co-registered to MRI for all patients. In the 0-6 month group, the average slope of the metabolic uptake curve was 0.20 in the distal graft, 0.21 in the mid graft, 0.27 in the proximal graft, and 0.28 in the femoral tunnel. In the 24+ month group the averages were 0.06, 0.05, 0.07, and 0.03, respectively. In addition to decreasing slopes of the uptake curves over time, patients with longer recovery times were seen to have SUVs more comparable to those in healthy knees than those who more recently had ACL repair.

CONCLUSION

We demonstrated that the quantitative evaluation of ACL graft ligamentization and healing is feasible by molecular PET imaging coregistered to MRI. Digital PET appears to enable further FDG dose reduction making a combined molecular imaging PET/MRI approach to assess ACL graft viability clinically feasible.

CLINICAL RELEVANCE/APPLICATION

A first-in-human study evaluating ACL graft healing with quantitative molecular imaging using combined PET/MRI

SSJ15-03 MRI Defined Ecologic Habitats in Extremity Soft Tissue Sarcomas: Characterization and Quantification of Tumor Heterogeneity and Potential Implications on Patient Outcomes-Early Experience

Tuesday, Dec. 1 3:20PM - 3:30PM Location: E451A

Participants

Meera Raghavan, MD, Tampa, FL (*Presenter*) Nothing to Disclose Hamidreza Farhidzadeh, Tampa, FL (*Abstract Co-Author*) Nothing to Disclose Lawrence O. Hall, PhD, Tampa, FL (*Abstract Co-Author*) Nothing to Disclose Dmitry Goldgof, PhD, Tampa, FL (*Abstract Co-Author*) Nothing to Disclose Robert J. Gillies, PhD, Tampa, FL (*Abstract Co-Author*) Nothing to Disclose Robert A. Gatenby, MD, Tucson, AZ (*Abstract Co-Author*) Nothing to Disclose

PURPOSE

We propose a novel computer-aided, spatially-explicit image analysis of magnetic resonance (MR) examinations to classify extremity STS based on radiologically defined spatial sub-regions, or "habitats." The identification of spatially distinct habitats can quantify and characterize the ecologic basis of intratumoral heterogeneity and may be helpful to guide targeted biopsy, tailor therapeutic options and offer prognostic information.

METHOD AND MATERIALS

T1-w gadolinium enhanced and fluid-sensitive MR images were assessed from pretreatment scans of 36 patients with extremity STS. There were three main steps: tumor segmentation based on pixel signal intensity; pixel and texture analysis within each distinctive habitat; and prediction of metastatic disease and histologic therapy response. Patient outcomes such as progression free survival (PFS), overall survival (OS), and presence of metastases were also assessed.

RESULTS

Habitat color maps (HCM) demonstrated spatially distinct intratumoral subregions (Fig. 1). Metastatic disease was classified correctly with 86.11% accuracy based on five texture features, and histologic necrosis with 75.75% accuracy based on four features. Specific subregions were also predictive for metastatic disease and histologic response to therapy. The post contrast T1 high/T2 low subregion was prognostic for overall survival (p= 0.036).

CONCLUSION

This technique can define distinct habitats within each STS based on MR imaging features and allows spatial variations to be assessed and quantified. We demonstrate the role of advanced clinical image analysis in providing critical insight into the evolutionary and ecologic landscape of STS. The preliminary results presented here show that distinct intratumoral subregions or habitats within STS can be identified and quantified and give useful clinical and prognostic information which can shape personalized and adaptive therapeutic regimens.

CLINICAL RELEVANCE/APPLICATION

Change in size alone does not accurately not reflect response to therapy and tumor biology of STS. We have developed an image analysis technique to non-invasively characterize and quantify tumor subregions on MR imaging. The identification of these radiologically defined habitats can give insight into the evolutionary and ecologic dynamics which are the basis of heterogeneity in STS. This can in turn offer more tailored personalized treatments to patients.

SSJ15-04 Quantitative Magnetic Resonance Imaging of Meniscal Pathology

Tuesday, Dec. 1 3:30PM - 3:40PM Location: E451A

Anthony S. Tadros, MD, San Diego, CA (*Presenter*) Nothing to Disclose Sheronda Statum, San Diego, CA (*Abstract Co-Author*) Nothing to Disclose Karen C. Chen, MD, San Diego, CA (*Abstract Co-Author*) Nothing to Disclose Won C. Bae, PhD, San Diego, CA (*Abstract Co-Author*) Nothing to Disclose Reni Biswas, San Diego, CA (*Abstract Co-Author*) Nothing to Disclose Betty Tran, San Diego, CA (*Abstract Co-Author*) Nothing to Disclose Jiang Du, PhD, San Diego, CA (*Abstract Co-Author*) Nothing to Disclose Eric Y. Chang, MD, San Diego, CA (*Abstract Co-Author*) Nothing to Disclose Christine B. Chung, MD, San Diego, CA (*Abstract Co-Author*) Nothing to Disclose

PURPOSE

To determine the capability of conventional and UTE quantitative MR values to detect meniscal pathology in cadaveric meniscal samples.

CLINICAL RELEVANCE/APPLICATION

Quantitative MR values may correlate with structural and biochemical meniscal alterations, complementing currently limited techniques in early diagnosis and postoperative evaluation of the meniscus.

SSJ15-05 Correlation of Age Dependent Whole Body Fat and Whole Body Skeletal Muscle Volume on DIXON MR Sequences in a Healthy Population with Normal BMI

Tuesday, Dec. 1 3:40PM - 3:50PM Location: E451A

Participants

Erika J. Ulbrich, MD, Zurich, Switzerland (*Presenter*) Nothing to Disclose Daniel Nanz, PhD, Zurich, Switzerland (*Abstract Co-Author*) Nothing to Disclose Olof Dahlqvist Leinhard, PhD, Linkoping, Sweden (*Abstract Co-Author*) Consultant, AMRA AB Magda Marcon, MD, Udine, Italy (*Abstract Co-Author*) Nothing to Disclose Michael A. Fischer, MD, Stockholm, Sweden (*Abstract Co-Author*) Nothing to Disclose

PURPOSE

To test a correlation of age- and gender-dependent reference standards of MR normative values of total adipose tissue (TAT), abdominal subcutaneous adipose tissue (ASAT) with the corresponding lean muscle tissue (LMT).

METHOD AND MATERIALS

Fat and water MR whole body images were acquired with a 2-point mDIXON sequence (Repetition time/echo time, 4,2 msec/1.2 msec, 3.1 msec) at 3 Tesla (Ingenia, Philips) in 80 healthy volunteers with normal BMI (18.5 to 25.5 kg/m2) aged between 20 and 60 years (10 men/10 women per decade). Volumes were measured from TAT, ASAT and LMT by a semi-automatic segmentation algorithm allowing separate quantification of each compartment (Advanced MR Analytics, AMRA, Linköping, Sweden). Pearson and Spearman correlations between Volume and several body measures were calculated. ANOVA was used to test for Volume differences among age subgroups. Prospective IRB approved study with written informed consent.

RESULTS

Overall mean Volume (liter) \pm standard deviation for women/men: 20.8 \pm 5.2/19.5 \pm 6.3 (TAT) and 15.7 \pm 2.2/23.2 \pm 2.3 (LMT). TAT/height2 and LMT/height2 didn`t show any age dependency for women/men (p = 0.973/0.557 and p = 0.483/0.539, respectively) nor TAT/height2 and LMT/height2 differences among age subgroups for both gender. There was significant correlation between TAT/height2 and body mass index (BMI) for women/men (p < 0.001 both), but not between LMT/height2 and BMI (p = 0.276/0.634). LMT/height2 correlated with TAT/height2 (p = 0.038/0.005) and ASAT/height2 (p = 0.011/0.002), but not with VAT/height2 (p = 0.205/0.252).

CONCLUSION

Women had higher TAT and lower LMT than men, but without significant age dependence. LMT/height2 correlated with TAT/height2 and ASAT/height2, but not with BMI.

CLINICAL RELEVANCE/APPLICATION

Normative values of LMT allow to determine muscular trophic in patients and might help to diagnose myopathy. Side Note for reviewer only please: Volunteers of this abstract are identical to Abstract number 15013444, but as the topic of fat quantification is very complex, we decided to put the data in two abstracts with the first dealing with the age dependent different fat volumes and the second abstract dealing with the correlation of the skeletal muscle volumes and the different fat volumes

SSJ15-06 Effect of Iterative Reconstruction Algorithms on Measurement of Trabecular Bone Microstructure with Clinical MDCT: A Cadaver Study Using Micro-CT as the Reference Standard

Tuesday, Dec. 1 3:50PM - 4:00PM Location: E451A

. . .

Participants

Miyuki Takasu, MD, Hiroshima, Japan (*Presenter*) Nothing to Disclose Chikako Fujioka, RT, Hiroshima, Japan (*Abstract Co-Author*) Nothing to Disclose Masao Kiguchi, RT, Hiroshima, Japan (*Abstract Co-Author*) Nothing to Disclose Chihiro Tani, MD, Hiroshima, Japan (*Abstract Co-Author*) Nothing to Disclose Yoko Kaichi, Hiroshima, Japan (*Abstract Co-Author*) Nothing to Disclose Kazuo Awai, MD, Hiroshima, Japan (*Abstract Co-Author*) Nothing to Disclose Kazuo Awai, MD, Hiroshima, Japan (*Abstract Co-Author*) Nothing to Disclose Kazuo Awai, KD, Hiroshima, Japan (*Abstract Co-Author*) Research Grant, Toshiba Corporation; Research Grant, Hitachi, Ltd; Research Grant, Bayer AG; Reseach Grant, DAIICHI SANKYO Group; Medical Advisor, DAIICHI SANKYO Group; Research Grant, Eisai Co, Ltd; Research Grant, Nemoto-Kyourindo; ; ; ; ; Nobuhito Nango, Tokyo, Japan (*Abstract Co-Author*) Nothing to Disclose Masafumi Machida, Musashimurayamashi, Japan (*Abstract Co-Author*) Nothing to Disclose

. . .

... _.

....

· ····

PURPOSE

Clinical multidetector computed tomography (MDCT) has been used to evaluate bone quality. The purpose of this study was to determine the efficacy of iterative reconstruction (IR) for measuring bone architecture through a comparison with micro-computed tomography (micro-CT) as the gold standard.

METHOD AND MATERIALS

L1 and L2 vertebrae of 10 fresh human cadavers were scanned by 64-section MDCT (LightSpeed VCT; reconstruction kernel, BONEPLUS; IR, ASiR; collimation, 64×0.625 mm), 80-section MDCT (Aquilion One Vision Edition; FC30, ADIR3D, 80×0.5 mm), and micro-CT (TOSCANER). Reconstructed voxel sizes were $0.2 \times 0.2 \times 0.16$ mm for MDCT and $0.052 \times 0.052 \times 0.072$ mm for micro-CT. Images were reconstructed using standard filtered back-projection and IR algorithms. Four patterns of CT images were reconstructed: without IR (IR (0%)), with 25-30% of IR (weak), with 50% of IR (mild), and with high-dose protocol without IR (120kV and 250mAs, HD).Trabecular parameters and tissue bone mineral density (tBMD) of the central 10-mm-thick portion of the vertebrae were calculated. Relationships between MDCT- and micro-CT-derived trabecular indices were compared using Pearson's correlation coefficient.

RESULTS

Metric parameters and tBMD measured by 64-section MDCT correlated better with micro-CT values with IR (mild) (r=0.611-0.948) than with IR (0%) (r=0.703-0.945). The correlation coefficients were significantly different (p<0.05). Non-metric parameters showed better correlations with micro-CT values with IR (0%) (r=0.712-0.883) than by IR (30% and 50%) (r=0.694-0.871). For 80-section MDCT, five of seven morphological parameters and tBMD correlated better with micro-CT values with IR (0%) (r=0.698-0.914) than with IR (25% and 50%) (r=0.663-0.888, p<0.05). For three of eight parameters by 64-section MDCT and six out of eight parameters with 80-section MDCT, the correlation coefficients were lowest with the HD protocol.

CONCLUSION

IR improved the correlation between 64-section MDCT and micro-CT-derived metric parameters. In the assessment of trabecular microstructure, IR algorithms showed different strengths according to the vendor and category of trabecular parameters.

CLINICAL RELEVANCE/APPLICATION

To ensure the accurate measurement of trabecular bone microstructure by clinical MDCT, it is important to select the appropriate reconstruction algorithm and imaging protocol.

Nuclear Medicine (Quantitative Imaging and Image Processing)

Tuesday, Dec. 1 3:00PM - 4:00PM Location: S505AB

BQ CT NM

AMA PRA Category 1 Credit ™: 1.00 ARRT Category A+ Credit: 1.00

FDA Discussions may include off-label uses.

Participants

Chadwick L. Wright, MD, PhD, Lewis Center, OH (*Moderator*) Nothing to Disclose Andrew C. Homb, MD, Louisville, KY (*Moderator*) Nothing to Disclose

Sub-Events

SSJ17-01 The Prognostic Value of Volumetric FDG PET/CT Parameters and Partial Volume Effect Correction in Patients with Locally Advanced Non-Small Cell Lung Cancer: A Secondary Analysis of ACRIN 6668/RTOG 0235 Trial

Tuesday, Dec. 1 3:00PM - 3:10PM Location: S505AB

Awards

Trainee Research Prize - Resident

Participants

Ali Salavati, MD, MPH, Philadelphia, PA (*Presenter*) Nothing to Disclose Fenghai Duan, PhD, Providence, RI (*Abstract Co-Author*) Nothing to Disclose Sina Houshmand, MD, Philadelphia, PA (*Abstract Co-Author*) Nothing to Disclose Benjapa Khiewvan, MD, Philadelphia, PA (*Abstract Co-Author*) Nothing to Disclose Adam Opanowski, Philadelphia, PA (*Abstract Co-Author*) Nothing to Disclose Bradley S. Snyder, MS, Providence, RI (*Abstract Co-Author*) Nothing to Disclose Bo Wei, Providence, RI (*Abstract Co-Author*) Nothing to Disclose Bo Wei, Providence, RI (*Abstract Co-Author*) Nothing to Disclose Burry A. Siegel, MD, Saint Louis, MO (*Abstract Co-Author*) Consultant, Merrimack Pharmaceuticals, Inc Consultant, Siemens AG Advisory Board, General Electric Company Stockholder, Radiology Corporation of America Spouse, Speaker, Siemens AG Mitchell Machtay, MD, Cleveland, OH (*Abstract Co-Author*) Consultant, Bristol-Myers Squibb Company; Speaker, AbbVie Inc; Speaker, Bristol-Myers Squibb Company; Speaker, Eli Lilly and Company; Speaker, AbbVie Inc;

Abass Alavi, MD, Philadelphia, PA (Abstract Co-Author) Nothing to Disclose

PURPOSE

There is a growing body of evidence supporting the application of volumetric PET/CT parameters and partial volume effect correction (PVC) in the prognostication of patients with non-small cell lung cancer (NSCLC). The aim of this secondary analysis was to assess the ability of pretreatment volumetric PET/CT measures, along with PVC, to predict locoregional control (LRC) and overall survival (OS) in patients enrolled in ACRIN 6668/RTOG 0235.

METHOD AND MATERIALS

Patients with inoperable stage IIB/III NSCLC and evaluable pretreatment FDG-PET/CT scans were included. Pretreatment Metabolic Tumor Volume(MTV),SUVmax,SUVmean,Total Lesion Glycolysis (TLG=SUVmean*MTV), pvcSUVmean and pvcTLG(pvcSUVmean*MTV) were quantified using semiautomatic adaptive contrast-oriented thresholding and local background PVC algorithms.The relationship between PET/CT indices and patient outcomes was assessed using Cox proportional hazards regression and time-varying models.

RESULTS

Of 234 eligible patients,38 were excluded mainly due to inadequate image quality, leaving 196-151 depending on the measured PET indices. PVC parameters were very highly correlated with their non-corrected counterparts (median correlation 0.98,range 0.96 to 0.997). Pretreatment MTV, TLG and pvcTLG (both primary tumor(PT) and whole body(WB)) were independent predictors of OS, while SUVmax, SUVmean and pvcSUVmean were not prognostic using either PT or WB measures.PVC and non-PVC indices yielded similar hazard ratios of 1.17(95%CI 1.05-1.31 p=0.004),1.20(95%CI1.06-1.34 p=0.003), 1.24(95%CI1.06-1.44 p=0.007), 1.27(95%CI1.08-1.50 p=0.004) for PT TLG, PT pvcTLG, WB TLG and WB pvcTLG,respectively.Similar results were observed after subsetting the entire cohort based on tumor size.Similar to OS, MTV and TLG were independent predictors of LRC, although their prognostic ability decreased during long-term follow-up.

CONCLUSION

Pretreatment volumetric PET/CT parameters including MTV and TLG are strong predictors of OS and LRC for NSCLC; however, the association with LRC appears to diminish over time. For this particular cohort, PVC did not appear to enhance the prognostic ability of PET/CT indices. The significance of PVC in treatment monitoring remains to be clarified.

CLINICAL RELEVANCE/APPLICATION

Pretreatment volumetric FDG-PET/CT parameters are strong independent predictors of overall survival and locoregional control in patients with locally advanced NSCLC treated with chemoradiation therapy.

SSJ17-02 Impact of Point-spread Function Reconstruction on Quantitative FDG-PET/CT Imaging Parameters and Inter Reader Reproducibility in Solid Tumors

Trainee Research Prize - Fellow

Participants Sara Sheikhbahaei, MD, MPH, Baltimore, MD (*Presenter*) Nothing to Disclose Charles Marcus, MD, Baltimore, MD (*Abstract Co-Author*) Nothing to Disclose Rick Wray, MD, Baltimore, MD (*Abstract Co-Author*) Nothing to Disclose Arman Rahmim, PhD, Baltimore, MD (*Abstract Co-Author*) Nothing to Disclose Martin A. Lodge, PhD, Baltimore, MD (*Abstract Co-Author*) Nothing to Disclose Rathan M. Subramaniam, MD, PhD, Baltimore, MD (*Abstract Co-Author*) Nothing to Disclose

PURPOSE

Recent studies suggest that implementation of the point spread function (PSF) in the reconstruction algorithm of positron emission tomography (PET) improves the spatial resolution of PET images. However, there is little known about the influence of PSF reconstruction on volumetric measurements in PET/CT. This study aims to determine the impact of PSF reconstruction on quantitative PET/CT indices and the inter-reader reproducibility of these measurements.

METHOD AND MATERIALS

Study was approved by the Institutional Review Board under a waiver of informed consent. A total of 42 oncology patients with 89 lesions (all \geq 2cm) were included. The PET/CT images were reconstructed with PSF (OSEM+TOF, 2i, 21s, all pass filter) and without PSF (OSEM+TOF, 2i, 21s, 5 mm Gaussian). For each lesion, the maximum, mean and peak standardized uptake values (SUV), total lesion glycolysis (TLG), and metabolic tumor volume (MTV) were measured by two readers (R1, R2) using a semi-automatic gradient segmentation method. Intra-class correlation coefficient (ICC) and Bland-Altman analyses were performed.

RESULTS

There was excellent correlation between non-PSF and PSF reconstruction PET/CT values [ICC \geq 0.950 for all parameters, P<0.0001]. Bland-Altman analyses comparing PSF with non-PSF images showed the average biases (%) of +11.14 (R1) and +11.1 (R2) for SUVmax, +7.04 (R1) and +7.54 (R2) for SUVmean, +7.03 (R1) and +7.06 (R2) for SUVpeak, -2.62 (R1) and -3.17 (R2) for TLG, and -9.61 (R1) and -10.43 (R2) for MTV. Percentage changes in PSF versus non-PSF indices were not related to the site of the lesions (P>0.05). Close agreement was observed between two readers [ICC ranged between 0.908-0.997, P<0.0001].

CONCLUSION

The PSF reconstruction increases the SUVmax, SUVmean and SUVpeak, as expected, while it tends to produce lower values for MTV and has variable effect on TLG. This can be attributed to the ability of PSF reconstruction to better discern tumor uptake from activity spill-out.

CLINICAL RELEVANCE/APPLICATION

Reconstruction method of PET/CT should be carefully considered in reporting quantitative parameters, subsequent lesion classifications and comparisons for therapy assessment.

SSJ17-03 Early Prediction of Chemotherapeutic Response with Volumetric FDG PET Parameters in Recurrent Gynecological Malignancies

Tuesday, Dec. 1 3:20PM - 3:30PM Location: S505AB

Participants

Mitsuaki Tatsumi, MD, PhD, Suita, Japan (*Presenter*) Nothing to Disclose Kayako Isohashi, Suita, Japan (*Abstract Co-Author*) Nothing to Disclose Hiroki Kato, Suita, Japan (*Abstract Co-Author*) Nothing to Disclose Masatoshi Hori, MD, Suita, Japan (*Abstract Co-Author*) Nothing to Disclose Noriyuki Tomiyama, MD, PhD, Suita, Japan (*Abstract Co-Author*) Nothing to Disclose Jun Hatazawa, MD, PhD, Osaka, Japan (*Abstract Co-Author*) Nothing to Disclose

PURPOSE

To evaluate if volumetric parameters(VPs) of FDG PET were useful in predicting treatment response early after chemotherapy in recurrent gynecological malignancies.

METHOD AND MATERIALS

This study included 35 patients with recurrent gynecological malignancies(19 uterine, 12 ovarian, 2 peritoneal, and 2 others). FDG PET/CT exam was performed before(pre) and after 1 cycle of chemotherapy(post1c). Metabolic tumor volume(MTV, SUV threshold 2.5) and total lesion glycolysis(TLG) were obtained as VPs in addition to SUVmax at the hottest lesion in each exam. MTV and TLG were also obtained for whole-body(wb) lesions. Pre, post1c, and changes(expressed as Δ) of VPs as well as SUVmax were compared each other and to the treatment response after last cycle of chemotherapy, which was decided with all clinical information available including imaging data.

RESULTS

PreSUVmax ranged from 1.9 to 22.4(median:7.0) and preMTV from 0 to 161(median:8.8). All preVPs exhibited a strong correlation with preSUVmax(Rho=0.78-0.88, p<0.001). Similar results were observed between post1cVPs and post1cSUVmax and between Δ VPs and Δ SUVmax. Post1cVPs and post1cSUVmax showed a strong(Rho=0.63-0.76) and moderate(Rho=0.40-0.57) correlation with Δ VPs and Δ SUVmax, respectively. Treatment response was observed in 14 of 35 pts and it correlated moderately with post1cVPs, Δ VPs, and Δ SUVmax. Among them, Δ wbMTV or Δ wbTLG was considered the best parameter to predict response from ROC analysis(AUC:0.79). A cutoff of Δ wbMTV 121% from ROC curve yielded the sensitivity, specificity, positive- , and negative predictive value of 57%, 100%, 100%, and 61%, respectively, if non-response was defined as positive. Mean Δ wbMTV was 31% and 287% respectively in response and non-response groups(p<0.05). No significant findings were noted between preVPs or preSUVmax and treatment response.

CONCLUSION

This study demonstrated early changes of VPs in FDG PET after 1 cycle of chemotherapy were more useful than changes of

SUVmax in predicting treatment response after the last cycle in pts with recurrent gynecological malignancies. Potential of MTV and TLG dealing with whole-body lesions was also demonstrated in this study.

CLINICAL RELEVANCE/APPLICATION

Early changes of volumetric FDG PET parameters after 1 cycle of chemotherapy were useful in predicting final treatment response in pts with recurrent gynecological malignancies.

SSJ17-04 Assessment of Whole-body Metabolic Tumor Burden of Nerve Sheath Tumors in Neurofibromatosis Type 1 Using 18F-FDG PET/CT

Tuesday, Dec. 1 3:30PM - 3:40PM Location: S505AB

Participants

Johannes M. Salamon, MD, Hamburg, Germany (*Presenter*) Nothing to Disclose Azien Laqmani, Hamburg, Germany (*Abstract Co-Author*) Nothing to Disclose Ivayla I. Apostolova, MD, Magdeburg, Germany (*Abstract Co-Author*) Nothing to Disclose Gerhard B. Adam, MD, Hamburg, Germany (*Abstract Co-Author*) Nothing to Disclose Victor F. Mautner, MD, Hamburg, Germany (*Abstract Co-Author*) Nothing to Disclose Thorsten Derlin, MD, Hannover, Germany (*Abstract Co-Author*) Nothing to Disclose

PURPOSE

To determine the metabolically active whole-body tumor volume and whole body total lesion glycolysis on 18F-fluorodeoxyglucose positron emission tomography/computed tomography (18F-FDG PET/CT) in individuals with neurofibromatosis type 1 (NF1) using a three-dimensional (3D) segmentation and computerized volumetry technique. And to compare these parameters in NF1 patients with benign (BPNSTs) and malignant peripheral nerve sheath tumors (MPNSTs).

METHOD AND MATERIALS

Eighteen NF1 patients with malignant PNSTs and 18 age- and sex-matched NF1 controls with benign PNSTs examined by 18F-FDG PET/CT were included (20 men; 16 women; age, 36.6 ± 12.3 years; range 16.5 to 68.7 years). Whole-body metabolic tumor burden (mTB), whole-body total lesion glycolysis (TLG) and a set of semi-quantitative imaging-based parameters were analyzed on a perpatient and a per-lesion basis. The Mann-Whitney U test, the Spearman correlation coefficient and ROC analysis were used for statistical analyses. Histopathological evaluation and clinical / radiological follow-up examinations served as the reference standards.

RESULTS

Whole-body mTB and whole-body TLG were significantly higher in NF1 patients with MPNSTs compared to patients with BPNSTs at different SUVmax cut-offs (2.0, 2.5, 3.5 and 4.0, p < 0.0001). MPNST demonstrated both a significantly higher metabolic tumor volume and TLG than BPNSTs (p < 0.0001). ROC analysis showed that metabolic tumor volume and TLG could be used to differentiate between benign and malignant tumors. Neither age nor gender were significantly correlated with whole-body mTB and whole-body TLG.

CONCLUSION

Whole-body mTB and whole-body TLG are different between NF1 patients with BPNST and MPNST. Moreover, malignant tumors have higher metabolic tumor volume and TLG than benign tumors. Further evaluation in prospective studies is required to determine the potential clinical impact and prognostic significance of these novel PET parameters in the context of NF1.

CLINICAL RELEVANCE/APPLICATION

New volumetric imaging parameters of peripheral nerve sheath tumors in NF1 such as mTB and TLG provide the basis for investigating biomarkers for early detection of MPNST and may help reducing unnecessary biopsies or surgery.

SSJ17-05 Determination of the Degree of Colorectal Carcinoma differentiation by Characterizing Tumor Heterogeneity with Textural Features on 18F-FDG PET/CT

Tuesday, Dec. 1 3:40PM - 3:50PM Location: S505AB

Participants

Wei Mu, Beijing, China (*Abstract Co-Author*) Nothing to Disclose Zhe Chen, Beijing, China (*Abstract Co-Author*) Nothing to Disclose Ying Liang, Beijing, China (*Abstract Co-Author*) Nothing to Disclose Ning Wu, MD, Beijing, China (*Abstract Co-Author*) Nothing to Disclose Jie Tian, PhD, Beijing, China (*Presenter*) Nothing to Disclose

PURPOSE

The aim of the study is to assess the usefulness of the tumor heterogeneity characterized by texture features and other commonly used semi-quantitative indices extracted from 18F-FDG PET images to determinate the differentiated degree of cancer cells in colorectal adenocarcinoma (CA) patients.

METHOD AND MATERIALS

We retrospectively studied the PET/CT images of 42 patients with pathologically proven CA (26 male and 15 female; mean age, 60±13 years), and the differentiation was graded on a scale of poor, moderate, or well differentiated. Firstly, the primary tumor was segmented with an improved level set method. Based on the traditional Chan-Vese (CV) model, we imposed gradient field constraint to exclude the effect of the adjacent bladder for some rectal tumors. Secondly, fifty-four 3D texture features (based on histogram analysis, concurrence matrix (CM), gray level size zone matrix (GLSZM), run length matrix (RLM), neibourhood gray level difference matrix(NGLD) and texture spectrum (TS)) were studied besides of SUVs (SUVmax, SUVmean, SUVpeak) and metabolic tumor volume (MTV). A 64-gray-level quantization was used, and local features (features based on CM and RLM) were computed over 13 directions. Then one-way analysis of variance (ANOVA) followed by multiple comparisons was employed to test the features for the statistical significance of group differences. In addition, the robustness of the features with respect to the segmentation methods was validated.

RESULTS

Three of the forty-eight features, difference variance (DV) and information correlation1 (IC1) based on CM and low gray level run emphasis (LGRE) based on GLSZM showed significant differences between any two groups (P<0.05). Through Student's test, there were no significant differences of the features between the manual segmentation and the proposed method (p>0.05).

CONCLUSION

Texture analysis of FDG PET could determinate the degree of colorectal carcinoma differentiation potentially, which also means the texture features may be another prognostic factors and can provide supplementary information for developing treatment plan.

CLINICAL RELEVANCE/APPLICATION

The texture features could determine the differentiated degree of cancer cells in colorectal adenocarcinoma (CA) patients, and could be another prognostic factors for personalized medicine.

SSJ17-06 Automatic PET Image Segmentation: A Cross-Platform and Cross-Method Evaluation

Tuesday, Dec. 1 3:50PM - 4:00PM Location: S505AB

Participants

Tram Nguyen, Odense, Denmark (*Presenter*) Nothing to Disclose Poul-Erik Braad, Odense C, Denmark (*Abstract Co-Author*) Nothing to Disclose Poul Flemming Hoilund-Carlsen, Odense, Denmark (*Abstract Co-Author*) Nothing to Disclose

PURPOSE

Quantitative PET relies on reproducible and accurate target delineation. This study investigated the unassessed variation between different commercial software packages that generally use threshold approaches. Method variability was also tested against inhouse implemented methods.

METHOD AND MATERIALS

PET scans of the NEMA/IEC phantom with different target-to-background ratios (TBRs) (5:1, 10:1, 20:1, infinite) and human 18F-NaF PET images (6 vertebrae of various shapes and inhomogeneity with/without bone abnormalities) were used. Region-of-interest (ROI) analysis with the ROVER (ABX, Radeberg, Germany) and PETVCAR (GE Healthcare) software was performed along with inhouse implementations. Cross-platform reproducibility was assessed by applying the same common 40% of peak value threshold method on all platforms. Cross-method variability was tested among the adaptive threshold (AT) method of ROVER, the estimated threshold (ET) by PETVCAR, and in-house implemented region growing with non-peak-based threshold (RG) and non-threshold level set (LS) methods.

RESULTS

Overall, consistent cross-platform results were obtained with some estimated mean activity deviations (\sim 0.1-0.3 kBq/mL) and volume variations (\sim 0.02-0.4 mL) at TBR5 and target size < 15 mm. At higher levels, ROVER deviated slightly from the other platforms with their near identical estimates. The peak-based method failed to segment inhomogeneous vertebrae well. Different methods yielded variations in estimated phantom activity (p \sim 0.6-0.9) and volumes (p \sim 0.8-0.95) that became marked at low contrast and targets < 35 mm. LS generally gave the best estimates, especially at high contrast and targets > 20 mm. Above TBR10, ET captured volumes the best, but overall underestimated activity levels the most. For vertebrae delineation, ET measurements, especially target volumes, deviated the most due to segmentation limitations.

CONCLUSION

Non-threshold or locally adaptive threshold methods had better performance range than peak-based thresholding across contrast, target size, and inhomogeneity. The cross-platform and cross-method variations introduced bias that has to be accounted for in any quantitative analysis design.

CLINICAL RELEVANCE/APPLICATION

Work like this is essential to elucidate critical aspects of quantification that will have decisive clinical impact along with the growing role of PET for prediction and therapy planning/evaluation.

Quantitative Imaging Mini-Course: Statistical Analysis/Metrology Issue

Tuesday, Dec. 1 4:30PM - 6:00PM Location: S403B

BQ PH

AMA PRA Category 1 Credits ™: 1.50 ARRT Category A+ Credits: 1.50

Participants

Michael F. McNitt-Gray, PhD, Los Angeles, CA (*Director*) Institutional research agreement, Siemens AG; Research support, Siemens AG; ; ; ; ;

Sub-Events

RC425A The Role of Metrology in Quantitative Imaging

Participants

Hyung J. Kim, PhD, Los Angeles, CA, (gracekim@mednet.ucla.edu) (Presenter) Nothing to Disclose

LEARNING OBJECTIVES

1) Understand the role of QI and its intended application. 2) Understand how to apply a study design for developing, evaluating, and validating a measurement of QI in a targeted population.

ABSTRACT

Many applications of using quantitative imaging biomarkers (QIB) have been reported in numerous scientific domains. Challenges are to obtain a universally consistent terminology or methods in reporting measurement variation of QIB under the various circumstances of scanners, readers, and software. Understanding variation of "measureland" (The quantity intended to be measured (VIM clause 2.3)) in radiological imaging is critical to set a clinically meaningful benchmark of a QI. To estimate a variation of measureland, the study design is a critical basis for developing, evaluating, and validating a QIB using a standard variation metric. Reporting an estimated measurement universally is an initialized step for combining the knowledge across studies and centers as part of evaluation and validation by an independent party. We will discuss the procedure starting from research question, study design, and the corresponding statistical methods toward development, evaluation, and validation of a measurement of QIB in a targeted population.

RC425B Methods for Technical Performance Assessment: What to Assess and How

Participants

Nicholas Petrick, PhD, Silver Spring, MD (Presenter) Nothing to Disclose

LEARNING OBJECTIVES

1) Understand how to apply bias/linearity, repeatability and reproducibility analyses in characterizing the technical performance of a quantitative imaging metric. 2) Understand how technical performance can affect the utility of a quantitative imaging biomarker or Radiomic signature.

ABSTRACT

Developments in extracting biological information from medical images have given rise to a number of proposed quantitative imaging biomarkers (QIBs) and the field of Radiomics. Critical to these research areas is the establishment of accurate and reproducible quantitative imaging (QI) metrics and the establishment of appropriate and widely accepted assessment methods. In this section of the refresher course, we will update the audience on the latest recommendations for assessing the technical performance of individual QI metrics. We will also present an example case in which we assess the technical performance of a lung nodule volume estimation tool.

RC425C Statistical Methods and Principles for Algorithm Comparison Assessment

Participants

Gene Pennello, PhD, Silver Spring, MD (Presenter) Nothing to Disclose

LEARNING OBJECTIVES

1) Understand objectives of algorithm comparison studies and study design principles. 2) Understand methods for testing hypotheses, estimating performance, and producing descriptive summaries for algorithm comparison. 3) Observe illustrations of how the methods are applied to real data.

Handout:Gene Pennello

http://abstract.rsna.org/uploads/2015/15003205/Gene RSNA 2015 Talk 2015 12 01.pdf

A Practical Approach for Beginning Radio-genomic Research

Tuesday, Dec. 1 4:30PM - 6:00PM Location: S501ABC



AMA PRA Category 1 Credits ™: 1.50 ARRT Category A+ Credits: 1.50

Participants

Maryellen L. Giger, PhD, Chicago, IL (*Presenter*) Stockholder, Hologic, Inc; Shareholder, Quantitative Insights, Inc; Royalties, Hologic, Inc; Royalties, General Electric Company; Royalties, MEDIAN Technologies; Royalties, Riverain Technologies, LLC; Royalties, Mitsubishi Corporation; Royalties, Toshiba Corporation; Researcher, Koninklijke Philips NV; Researcher, U-Systems, Inc Hui Li, MD, PhD, Chicago, IL (*Presenter*) Nothing to Disclose Karen Drukker, PhD, Chicago, IL, (kdrukker@uchicago.edu) (*Presenter*) Nothing to Disclose Elizabeth S. Burnside, MD, MPH, Madison, WI (*Presenter*) Stockholder, NeuWave Medical Inc Yuan Ji, Chicago, IL (*Presenter*) Nothing to Disclose Alexandra V. Edwards, Chicago, IL (*Presenter*) Nothing to Disclose John Papaioannou, MSc, Chicago, IL (*Presenter*) Nothing to Disclose Chun-Wai Chan, MS, Chicago, IL (*Presenter*) Nothing to Disclose Yitan Zhu, PhD, Evanston, IL (*Presenter*) Nothing to Disclose Robert Tomek, MSc, Darien, IL (*Presenter*) Employee, Quantitative Insights, Inc

LEARNING OBJECTIVES

1) Understand what planning and online resources are needed to create a successful cross-disciplinary radio-genomic research team that can efficiently meet hypothesis-generated imaging/genomic science objectives. 2) Comprehend what skill set distinctions are needed for a hypothesis-resolving radio-genomic research team and how those essential components can be assembled to investigate and/or discover a given disease signature. 3) Learn how to grasp a radio-genomic conceptual research framework that may at first seem unfamiliar to imaging scientists.

ABSTRACT

Neuroradiology Series: Brain Tumors

Wednesday, Dec. 2 8:30AM - 12:00PM Location: E451A

NR BQ MR

AMA PRA Category 1 Credits ™: 3.25 ARRT Category A+ Credits: 3.50

Participants

Rivka R. Colen, MD, Houston, TX, (rcolen@mdanderson.org) (*Moderator*) Nothing to Disclose James G. Smirniotopoulos, MD, Bethesda, MD (*Moderator*) Nothing to Disclose

Sub-Events

RC505-01 Beyond Enhancement and Histology: Molecular Markers for Diagnosis

Wednesday, Dec. 2 8:30AM - 8:55AM Location: E451A

Participants James G. Smirniotopoulos, MD, Bethesda, MD (*Presenter*) Nothing to Disclose

Active Handout: James G. Smirniotopoulos

http://abstract.rsna.org/uploads/2015/15000013/RC505-01 Smirniotopoulos(1).pdf

RC505-03 Radiogenomics Defines Key Genomic Network Driving GBM Invasion

Wednesday, Dec. 2 9:05AM - 9:15AM Location: E451A

Participants

Rivka R. Colen, MD, Houston, TX (*Presenter*) Nothing to Disclose Markus Luedi, Houston, TX (*Abstract Co-Author*) Nothing to Disclose Sanjay K. Singh, Houston, TX (*Abstract Co-Author*) Nothing to Disclose Islam S. Hassan, MBBCh, Houston, TX (*Abstract Co-Author*) Nothing to Disclose Joy Gummin, Houston, TX (*Abstract Co-Author*) Nothing to Disclose Erik P. Sulman, MD, PhD, Houston, TX (*Abstract Co-Author*) Nothing to Disclose Frederick F. Lang, MD, Houston, TX (*Abstract Co-Author*) Nothing to Disclose Pascal O. Zinn, MD, Boston, MA (*Abstract Co-Author*) Nothing to Disclose

PURPOSE

Clinical care and outcome in Glioblastoma (GBM) remains challenging due to the tumor's invasive grwoth. To establish personalized treatment options in GBM, discovery of genetic mechanisms essential for the tumor's invasion is needed. We have previously described radiogenomic approaches to diagnose gene networks non invasively by analyzing genomic data from TCGA. The purpose of the current reseach is to identify a genetic network that drives GBM invasion and can be targeted specifically.

METHOD AND MATERIALS

Using Kaplan-Meier statistics, the data of the two independent databases TCGA and REMBRANDT were used to validate the genetic netowork's impact on clinical outcome. The genes' staus was assessed in a panel of human glioma stem cells (GSCs) and conventional proneural, classical and mesenchymal GBM cell lines using RT-PCR. Differentiation potential (Tuj1+ve, S100A+ve, and GFAP+ve), self-renewal (limiting dilution assays), invasion (Boyden chamber) and proliferation (BrdU) were assessed. Gain (lentiviral vectors) and loss (SMARTchoice Inducible shRNA) of function experiments were performed. Orthotopic xenograft models (nude mice) were used to characterize the genes impact in vivo. Potential FDA approved therapeutics were identified using connectivity map.

RESULTS

Texture analysis based on radiogenomics significantly predicted the genes responsible for invasion of GBM in a non-invasive manner. Invasion in both, in vitro and in vivo was significantly decreased upun downregulation of this gene network. Transcriptome microarray analysis showed that an upregulation of the described genes results in class switching from proneural to mesenchymal subtypes. Cmap derived therapeutics could significantly inhibit the gene network's activity and hence invasion.

CONCLUSION

The describend genes could be essential drivers of molecular subtypes and invasion in GBM. The therapeutics defined with cmap offer a targetted therapy to adress these key features of GBM pathogenesis. Noninvasive radiogenomics-based identification of tumor subgroups and potential treatment approaches can significantly contribute to personalized therapy.

CLINICAL RELEVANCE/APPLICATION

The described gene network seems to be key for GBM pathogenesis. Noninvasive, radiogenomics-based subgroup identification and specific novel treatment approaches can significantly contribution to personalized GBM therapy.

RC505-04 Radiogenomic Analysis of TCGA/TCIA Diffuse Lower Grade Gliomas by Molecular Subtype

Wednesday, Dec. 2 9:15AM - 9:25AM Location: E451A

Participants Chad A. Holder, MD, Atlanta, GA (*Presenter*) Nothing to Disclose Laila M. Poisson, Detroit, MI (*Abstract Co-Author*) Nothing to Disclose Lee Cooper, Atlanta, GA (*Abstract Co-Author*) Nothing to Disclose

Erich Huang, PhD, Bethesda, MD (Abstract Co-Author) Nothing to Disclose James Y. Chen, MD, San Diego, CA (Abstract Co-Author) Research Consultant, EBM Technologies, Inc Research Consultant, Banyan Biomarkers, Inc Scott N. Hwang, MD, PhD, Memphis, TN (Abstract Co-Author) Nothing to Disclose Sugoto Mukherjee, MD, Charlottesville, VA (Abstract Co-Author) Nothing to Disclose Leo J. Wolansky, MD, Cleveland, OH (Abstract Co-Author) Nothing to Disclose Brent D. Griffith, MD, Detroit, MI (Abstract Co-Author) Nothing to Disclose Kristen W. Yeom, MD, Palo Alto, CA (Abstract Co-Author) Nothing to Disclose Michael Iv, MD, Stanford, CA (Abstract Co-Author) Nothing to Disclose Max Wintermark, MD, Lausanne, Switzerland (Abstract Co-Author) Advisory Board, General Electric Company; Rivka R. Colen, MD, Houston, TX (Abstract Co-Author) Nothing to Disclose Rajan Jain, MD, Northville, MI (Abstract Co-Author) Nothing to Disclose Justin Kirby, Bethesda, MD (Abstract Co-Author) Stockholder, Myriad Genetics, Inc John B. Freymann, BS, Rockville, MD (Abstract Co-Author) Nothing to Disclose Daniel L. Rubin, MD, MS, Palo Alto, CA (Abstract Co-Author) Nothing to Disclose C. Carl Jaffe, MD, Boston, MA (Abstract Co-Author) Nothing to Disclose Daniel J. Brat, MD, PhD, Atlanta, GA (Abstract Co-Author) Nothing to Disclose Adam E. Flanders, MD, Penn Valley, PA (Abstract Co-Author) Nothing to Disclose

PURPOSE

To investigate relationships between imaging phenotype and genetic classification of LGGs in the TCGA/TCIA database, we analyzed semi-quantitative MR features and IDH/1p19q classifications.

METHOD AND MATERIALS

Pre-operative MRIs of 72 TCGA/TCIA LGGs were reviewed by 3 neuroradiologists blinded to molecular status, using the VASARI LGG feature-set (standardized set of 26 MRI features). Data were compiled across 3 readers to define a single measure per sample. Clinical and molecular classifications were obtained from the LGG-AWG marker paper (TCGA Research Network.NEJM;2015, in press). Associations with histology, WHO grade and molecular type were assessed by Fisher's exact test (categorical features) and ANOVA/t-test (continuous features).

RESULTS

Of 70 tumors with IDH/1p19q classification, 16 were IDHmut-codel, 34 were IDHmut-non-codel, and 19 were IDHwt. IDHmut-codel tumors were preferentially centered in the frontal lobes (75%, FET p=0.026). IDHmut-non-codel tumors tended to arise in frontal (41%) and temporal lobes (41%), while IDHwt tumors did not show preference. Nonenhancing tumor margins were more well-defined for IDHmut LGGs (56% and 76% were well-defined) than for IDHwt tumors (32%, FET p=0.027). 66% of LGGs had an enhancing region, but this was not associated with molecular class (FET p=0.286), although enhancement was more likely in grade III than grade II (FET, p=0.043). 23% of these grade II/III tumors had MRI evidence of necrosis, with presence equally likely in any of the 3 molecular classes (FET p=0.931); however, 5/16 (31%) of LGGs with necrosis on MRI were grade II. IDHwt tumors tended to be smaller than IDHmut tumors (23.0 cm2 vs 39.7cm2, respectively, for maximal area, t-test p<0.001). Further differences were found in T1/FLAIR ratio (FET p=0.030), T2/FLAIR signal crossing the midline (FET p=0.007), and presence of hemorrhage (FET p=0.009), cysts (FET p=0.006), or satellites (FET p=0.030).

CONCLUSION

Review showed differential MR features between LGG molecular classes. IDHwt LGGs had association with aggressive features (e.g., small dimension with poorly-defined non-contrast-enhanced borders). Lack of association with necrosis or presence of an enhancing region suggests that the IDHwt class is not simply underdiagnosed GBM. An investigation of imaging profiles that align with molecular type or define further subclasses is underway.

CLINICAL RELEVANCE/APPLICATION

Differential MR features exist between LGG molecular classes.

Honored Educators

Presenters or authors on this event have been recognized as RSNA Honored Educators for participating in multiple qualifying educational activities. Honored Educators are invested in furthering the profession of radiology by delivering high-quality educational content in their field of study. Learn how you can become an honored educator by visiting the website at: https://www.rsna.org/Honored-Educator-Award/

Daniel L. Rubin, MD, MS - 2012 Honored Educator Daniel L. Rubin, MD, MS - 2013 Honored Educator

RC505-05 The Triple-Negative Low-Grade Glioma: MR Imaging Correlates of Aggressive Molecular Phenotype

Wednesday, Dec. 2 9:25AM - 9:35AM Location: E451A

Participants

Javier Villanueva Meyer, MD, San Francisco, CA (*Presenter*) Nothing to Disclose Byung Se Choi, MD, Seongnam-Si, Korea, Republic Of (*Abstract Co-Author*) Nothing to Disclose Matthew Wood, San Francisco, CA (*Abstract Co-Author*) Nothing to Disclose Tarik Tihan, San Francisco, CA (*Abstract Co-Author*) Nothing to Disclose Soonmee Cha, MD, San Francisco, CA (*Abstract Co-Author*) Nothing to Disclose

PURPOSE

Low-grade gliomas (LGGs) are a heterogeneous group of tumors with distinct clinical behavior and prognosis. One strategy to improve their characterization is with molecular biomarkers: P53, IDH 1/2, and 1p19q. These objective markers correlate with histologic classification and clinical outcomes. Specifically, the absence of IDH1/2 mutation or 1p19q deletion have been identified as indicative of a poor prognosis. The purpose of our study was to determine MR imaging parameters that can discriminate a, recently-described, aggressive subtype of LGG that is characterized by an absence of all three of these genetic alterations.

METHOD AND MATERIALS

A retrospective review of our medical records from 2010 to 2014 yielded 105 cases of pathologically-confirmed LGG that had molecular testing for P53 mutation, IDH1/2 mutation, and 1p/19q deletion. The MR imaging characteristics including tumor location, volume, infiltration pattern, cortical involvement, hemorrhage, contrast-enhancement, and quantitative diffusion and perfusion were assessed. Additionally, clinical data of patient treatment, disease course, and survival was collected.

RESULTS

There were 24 diffuse astrocytomas (23%), 36 oligoastrocytomas (34%) and 45 oligodendrogliomas (43%). P53 mutation was found in 21 (20%), IDH1/2 mutation was found in 70 (67%), and 1p19q deletion was found in 45 (43%). Thirteen cases (12%) did not have any of these genetic alterations. Triple-negative tumors showed a lower incidence of cortical involvement (p<0.05) and lower mean and minimum apparent diffusion coefficient (ADC) values (1.25 vs 1.45x10^-3 mm^2/s; 0.89 vs 1.09x10^-3 mm^2/s, p<0.01). Multiple logistic regression analysis showed low ADC value as an independent predictor of triple-negative LGG. With a cut-off of 1.0x10^-3 mm^2/s, ADC value provides a 73% sensitivity and a 72% specificity with an odds ratio of 7.0 (p<0.01). In cases with available clinical follow-up, triple-negative LGGs were found to have disease progression within 2 years in 50% compared to 16% in the non-triple-negative cohort.

CONCLUSION

Triple-negative LGGs are a clinically and biologically aggressive phenotype that exhibit lower mean ADC values and lack of cortical involvement on MR imaging.

CLINICAL RELEVANCE/APPLICATION

MR imaging features can be used alongside molecular biomarkers to assess the aggressiveness and prognosis of LGGs and subsequently may provide a means of guiding management as patient-tailored therapy.

RC505-06 Do Macrocyclic Gadolinium Based Contrast Agents(GBCA) Deposit Gd in Normal Brain Tissue in Patients Receiving Contrast Enhanced MRI?

Wednesday, Dec. 2 9:35AM - 9:45AM Location: E451A

Participants

Nozomu Murata, MD, PhD, Seattle, WA (*Presenter*) Nothing to Disclose Luis F Gonzalez-Cuyar, MD, Seattle, WA (*Abstract Co-Author*) Nothing to Disclose Kiyoko Murata, MD,PhD, Tokyo, Japan (*Abstract Co-Author*) Nothing to Disclose Corinne L. Fligner, MD, Seattle, WA (*Abstract Co-Author*) Nothing to Disclose Russell Dills, PhD, Seattle, WA (*Abstract Co-Author*) Nothing to Disclose Daniel S. Hippe, MS, Seattle, WA (*Abstract Co-Author*) Research Grant, Koninklijke Philips NV; Research Grant, General Electric Company Kenneth R. Maravilla, MD, Seattle, WA (*Abstract Co-Author*) Nothing to Disclose

PURPOSE

Based on T1 shortening on noncontrast MR, recent studies have suggested that small amounts of gadolinium(Gd) may accumulate in brain even in patients with normal renal function. Recently McDonald confirmed Gd deposition in postmortem human brain tissue. To date, studies have shown Gd brain deposition only with Group 1 linear agents. The purpose of this study was to determine whether Gd is deposited in brain among patients receiving more stable macrocyclic agents using postmortem tissue analysis with inductively coupled plasma mass spectrometry (ICP-MS).

METHOD AND MATERIALS

This study was approved by the IRB. Brain tissue was collected at autopsy from decedents with available medical records that document past history of MRIs with or without GBCA exposure. Decedents with no prior MRI or only nonGd MRI served as controls. Tissue samples were collected from white matter, putamen, globus pallidus, caudate nucleus, pons and dentate nucleus and analyzed for Gd using ICP-MS. Bone tissue from rib was also analyzed as a reference tissue in each case. Results were correlated with types of agent received, cumulative dose, time since dosing and clinical and laboratory data.

RESULTS

Among 21 cases obtained to date, 15 cases with normal renal function received 1 or more GBCA exposures and 6 cases had no exposure. ICP-MS showed measurable amounts of Gd deposition (range 0.003-3.54ng/mg) in all 15 cases receiving GBCA.A subset of these ,4 cases received only a macrocyclic GBCA(1 Gadavist ; 3 ProHance) with doses ranging from 10 to 126 ml and Gd was also detected in all macrocyclic cases (0.006-0.188 ng/mg). Gd in brain was detected after only a single dose and deposition was present among all brain regions sampled. Gd deposition in rib was also positive in all 15 cases and showed significantly higher levels than brain in each case. By comparison there was no detectable Gd in any control cases.

CONCLUSION

Gd deposition occurs in normal brain tissue in patients with normal renal function with a past history of GBCA exposure even in those receiving only macrocyclic agents. The clinical significance remains undetermined and we are pursuing further investigation.

CLINICAL RELEVANCE/APPLICATION

Gd deposition is present in normal brain tissue after only one dose even with macrocyclis agents. This important observation needs further investigation to determine potential toxic effects.

Handout:Nozomu Murata

http://abstract.rsna.org/uploads/2015/15004555/RSNA2015 RC505-06WF.pptx

RC505-07 Post-therapy Brain Tumors: Imaging Pitfalls and Strategy

Wednesday, Dec. 2 9:45AM - 10:10AM Location: E451A

Soonmee Cha, MD, San Francisco, CA (Presenter) Nothing to Disclose

LEARNING OBJECTIVES

1) Discuss biologic and pathologic complexity of post-therapy brain tumors. 2) Present latest advances in imaging methods to differentiate recurrent tumor and treatment effect. 3) Review strengths and pitfalls of imaging post-therapy brain tumors. 4) Describe imaging strategy to improve diagnosis and management of patients with treated brain tumor.

RC505-08 Directions, Protons and Flows - Practical Advanced Brain Tumor Imaging

Wednesday, Dec. 2 10:30AM - 10:55AM Location: E451A

Participants

Jeffrey L. Sunshine, MD, PhD, Pepper Pike, OH (*Presenter*) Research support, Siemens AG Travel support, Siemens AG Travel support, Koninklijke Philips NV Travel support, Sectra AB Travel support, Allscripts Healthcare Solutions, Inc

RC505-10 A Multiparametric Voxel-level Model for Prediction of Cellularity in Glioblastoma

Wednesday, Dec. 2 11:05AM - 11:15AM Location: E451A

Participants

Peter Chang, MD, Bronx, NY (*Presenter*) Nothing to Disclose Daniel S. Chow, MD, New York, NY (*Abstract Co-Author*) Nothing to Disclose Timothy Ung, New York City, NY (*Abstract Co-Author*) Nothing to Disclose Jennifer Soun, MD, New York, NY (*Abstract Co-Author*) Nothing to Disclose Christopher G. Filippi, MD, Grand Isle, VT (*Abstract Co-Author*) Research Consultant, Regeneron Pharmaceuticals, Inc; Research Consultant, Syntactx Angela Lignelli-Dipple, MD, New York, NY (*Abstract Co-Author*) Nothing to Disclose Peter Canoll, New York City, NY (*Abstract Co-Author*) Nothing to Disclose Lawrence H. Schwartz, MD, New York, NY (*Abstract Co-Author*) Committee member, Celgene Corporation; Committee member, Novartis AG; Committee member, ICON plc; Committee member, BioClinica, Inc

PURPOSE

To create a robust multiparametric model for prediction of cellular density in glioblastoma (GBM) using voxel-by-voxel analysis of T1W-postcontrast, FLAIR and ADC intensity values calibrated to biopsy-proven histopathologic data.

METHOD AND MATERIALS

As part of an IRB-approved protocol, MR-localized biopsies of GBM patients were obtained from both contrast-enhancing tumor (CE) and nonenhancing (nCE) peritumoral edema using Brainlab referenced to T1W-postcontrast images. Total cell counts were obtained after HandE slide preparation scanned at 400x magnification. FLAIR and ADC data were interpolated and coregistered to the reference T1W volume using affine transformation and a mutual information cost function. For each biopsy site, corresponding mean intensity was obtained on T1W-postcontrast, FLAIR and ADC sequences. Univariate linear regression was used to determine correlation between cell count and intensity for each MR sequence. Two multivariate linear regression models, one each for CE and nCE regions, were used to combine data from each MR sequence into a robust model for tumor cellularity.

RESULTS

A total of 58 biopsy sites were obtained. Overall, cellularity demonstrated moderate linear correlation with T1W-postcontrast (r = 0.76), FLAIR (r = 0.62) and ADC (r = 0.64, within nCE region only). Multiple linear regression combining all three variables yielded a model highly predictive of cellularity, both within the nCE (r = 0.93) and CE (r = 0.76) region. Within the nCE region, the model weighted ADC (p = 0.0072) and FLAIR (p = 0.058) more significantly than T1W (p = 0.83), as determined by analysis of variance (ANOVA). Within the CE region, T1W (p < 0.001) and FLAIR (p = 0.12) were weighted more significantly than ADC (p = 0.21).

CONCLUSION

A multiparametric model combining T1W-postcontrast, FLAIR and ADC values strongly predicts cell counts in GBM, notably with correlation >90% in the nCE region. By applying this model at each voxel within the tumor volume, a noninvasive map of cellular density can be generated.

CLINICAL RELEVANCE/APPLICATION

Cellularity maps of the peritumoral region in GBM localize tumor microinvasion and may be used as a tool to guide extended surgical resection or biopsy and to assess infiltrative tumor burden.

RC505-11 Receiver Operating Characteristic (ROC) and Logistic Fit Analysis for Detecting Brain Tumor Based on OEF Measurements Obtain by PET and MR

Wednesday, Dec. 2 11:15AM - 11:25AM Location: E451A

Participants

Parinaz Massoumzadeh, PhD, Saint Louis, MO (*Presenter*) Nothing to Disclose Jonathan E. McConathy, MD, PhD, Saint Louis, MO (*Abstract Co-Author*) Research Consultant, Eli Lilly and Company; Research Consultant, Blue Earth Diagnostics Ltd; Research Consultant, Siemens AG; Research support, GlaxoSmithKline plc Andrei Vlassenko, MD, PhD, Saint Louis, MO (*Abstract Co-Author*) Nothing to Disclose Yi Su, PhD, Saint Louis, MO (*Abstract Co-Author*) Nothing to Disclose Hongyu An, DSc, Chapel Hill, NC (*Abstract Co-Author*) Nothing to Disclose Charles F. Hildebolt, DDS, PhD, Saint Louis, MO (*Abstract Co-Author*) Nothing to Disclose Daniel S. Marcus, PhD, Saint Louis, MO (*Abstract Co-Author*) Nothing to Disclose Tammie S. Benzinger, MD, PhD, Saint Louis, MO (*Abstract Co-Author*) Nothing to Disclose Tammie S. Benzinger, MD, PhD, Saint Louis, MO (*Abstract Co-Author*) Research Grant, Eli Lilly and Company; Investigator, Eli Lilly and Company; Investigator, F. Hoffmann-La Roche Ltd; Receiver operating characteristic (ROC) curve and logistic fit analysis for detecting brain tumors using cerebral oxygen extraction fraction (OEF) measurement obtained by [15]O positron emission tomography (PET) and oxygen sensitive magnetic resonance (MR) imaging.

METHOD AND MATERIALS

30 participants (20 with brain tumors) were recruited. MRI included standard clinical sequences plus OEF-MR1; a two-dimensional multi-echo gradient spin echo sequence. Concurrent with the MR acquisition, subjects with brain tumors underwent PET scanning, which included 2 sets of 3 scans with serial inhalation of air with 40-75 mCi [15]O labeled carbon monoxide , 40-75 mCi [15]O labeled oxygen , and injection of 25-50 mCi [15]O labeled water. MR and PET data were post-processed off line and registered to the anatomic T1 pre-and post-contrast images. Regions of interest were drawn based upon contrast-enhancing tumor areas, contra-lateral normal white matter (NWM), and normal gray matter (NGM) Ratios of OEF (rOEF) were obtained for lesions compared to normal tissue. Statistical analyses, including Bland-Altman plot, ROC, and logistic fit, were performed.

RESULTS

Bivariate analyses results are: between two rOEF-PET measurements of all selected regions R=0.92 and P <0.0001, and tumor type R=0.68 and p<0.0001; and similarly betweenr rOEF-MR and rOEF-PET all selected regions R=0.3 and P <0.0413, and tumor type R=0.39 and p<0.173. Based on Bland-Altman analysis both MR and PET methods of obtaining OEF are in agreement (the measurements lie within range ± 1.96 xSD). However, the coefficient obtain for rOEF-MR covers much larger range which may not not be clinically acceptable. Area under ROC curve (AUC) has much higher value for PET (0.95) than MR (0.58).

CONCLUSION

Both MR and [15]O PET can measure OEF in brain tumors and in peritumoral edema. Variable OEF measurements for tumor and edema may be implication for tumor grade and prognosis. BOLD MR fails in regions with signal loss on SWI or T2*. Area under ROC Curve (AUC) has much higher value for PET (0.95) than MR (0.58). Based on logistic fit probablity of distinguing tumor with PET is much higher than MR.

CLINICAL RELEVANCE/APPLICATION

Both MR and PET techniques have tremendous potential and may offer new insight into the underlying physiology of brain tumors and their response to therapy without requiring radiation or injected contrast. BOLD MR fails in regions with signal loss on SWI or T2*.

RC505-12 What Does the Black Box Tell us? Risk and Benefit of Ferumoxytol as an MRI Contrast Agent

Wednesday, Dec. 2 11:25AM - 11:35AM Location: E451A

Participants

Csanad G. Varallyay, MD, PhD, Portland, OR (*Presenter*) Nothing to Disclose Rochelle Fu, Portland, OR (*Abstract Co-Author*) Nothing to Disclose Joao Prola Netto, MD, Portland, OR (*Abstract Co-Author*) Nothing to Disclose Edward Neuwelt, MD, Portland, OR (*Abstract Co-Author*) Nothing to Disclose

PURPOSE

Ferumoxytol, an ultrasmall iron oxide nanoparticle (USPIO) has been marketed as Feraheme® for iron replacement therapy in patients with chronic kidney disease. Due to its magnetic properties, and long plasma half-life, ferumoxytol uniquely allows MR imaging of the intravascular space early after injection, which is beneficial for high-resolution blood volume mapping of brain lesions. Delayed (24h) ferumoxytol enhancement may help in differential diagnosis. As of March 30, 2015, the FDA added a boxed warning to Feraheme® package insert, which strengthens existing warnings regarding potential fatal and serious hypersensitivity reactions including anaphylaxis, even in patients who received Feraheme® previously. It emphasizes the importance of trained personnel, monitoring at least 30 min post injection to properly treat hypersensitivity reactions.

METHOD AND MATERIALS

Our institution has been actively doing imaging research with ferumoxytol for over 10 years. In this study we evaluated early adverse events (occurring within 1 day), potentially related to ferumoxytol administration hypersensitivity, and qualitatively compared it with published data.

RESULTS

At the time writing this abstract we have analyzed a total of 553 ferumoxytol infusions in 298 patients and have not recorded any severe (grade 3, 4 or 5) hypersensitivity reactions occurring within 1 day. Early grade 1 and 2 reactions, were present, such as nausea/vomiting (5.1%), hypertension (3.3%), pruritus (1.3%). In published data, the frequency of severe hypersensitivity of Feraheme® was equivalent to ionic iodinated contrast media, and about 10x higher than gadolinium MR contrast agents and nonionic iodinated contrast agents.

CONCLUSION

Our results suggest less frequent severe hypersensitivity reactions compared to published data, and it may be due to the difference in patient population. A detailed toxicity evaluation of our data is in progress. The intended purpose of change in labeling by the addition of the boxed warning is to strengthen the warnings in the label and to mitigate the risk of serious hypersensitivity reactions including anaphylaxis in order to enhance patient safety.

CLINICAL RELEVANCE/APPLICATION

Ferumoxytol remains safe for MRI in the vast majority of patients, with a very small risk of serious adverse event, and personnel should be prepared to treat such reactions if they were to occur.

RC505-13 Moving Towards Quantitative Brain Tumor Imaging

Wednesday, Dec. 2 11:35AM - 12:00PM Location: E451A

Thomas L. Chenevert, PhD, Ann Arbor, MI (Presenter) Consultant, Koninklijke Philips NV

Radiogenomics of Lung Cancer-Changing Landscape and Challenges

Wednesday, Dec. 2 8:30AM - 10:00AM Location: S403A

CH BQ OI

AMA PRA Category 1 Credits ™: 1.50 ARRT Category A+ Credits: 1.50

Participants Sub-Events

RC518A Lung Cancer in the Radiogenomic Era-Implications for Imaging

Participants

Lawrence H. Schwartz, MD, New York, NY (*Presenter*) Committee member, Celgene Corporation; Committee member, Novartis AG; Committee member, ICON plc; Committee member, BioClinica, Inc

LEARNING OBJECTIVES

1) To understand the clinical needs for Radiogenomic Imaging in Lung Cancer. 2) To understand what imaging modalities and quantification techniques can be used in Radiogenomic Imaging in Lung cancer. 3) To illustrate examples of successes and failures in Radiogenomic Imaging approaches in Lung Cancer.

RC518B Qualitative Assessments of Lung Cancer for Radiogenomic Analysis

Participants

Hyun-Ju Lee, MD, PhD, Seoul, Korea, Republic Of (Presenter) Nothing to Disclose

LEARNING OBJECTIVES

1) To introduce the results of correlation between imaging features and genetic phenotypes of lung cancer. 2) To describe the implications of imaging traits on pathology, patient prognosis, and genetics. 3) To introduce the role of qualitative assessment for the next step high-throughput quantitative feature selection.

ABSTRACT

```
RC518C Quantitative Assessment in Lung Cancer Radiogenomics-Reproducibility and Reliability
```

Participants

Binsheng Zhao, DSc, New York, NY (*Presenter*) License agreement, Varian Medical Systems, Inc; License agreement, Keosys SAS; License agreement, Hinacom Software and Technology, Ltd; License agreement, ImBio, LLC; License agreement, AG Mednet, Inc

LEARNING OBJECTIVES

1) Familiarize the audience with quantitative image features that can be computed to characterize tumors. 2) Discuss reproducibility and reliability of image features due to, repeat CT scans, CT acquisition and reconstruction techniques, tumor segmentations.

ABSTRACT

The way tumors look on radiological images may also reveal their underlying cancer gene expressions. Tumor imaging phenotypes can be characterized not only qualitatively by the radiologist's eyeballing, but also quantitatively by computer through image feature analysis. Radiogenomics promises the ability to assess cancer genotype though the tumor's imaging phenotype. However, to date, little attention has been paid to the sensitivity of image features to repeat scans, imaging acquisition techniques, reconstruction parameters and tumor segmentations. This refresher course will first familiarize the audience with quantitative image features that can be computed to characterize tumor size, shape, edge and density texture statistics. Both phantom and in-vivo studies will be introduced to explain how repeat CT scans and CT imaging acquisition and reconstruction techniques affect the assessment of quantitative image features in lung cancer Radiogenomics studies. Last but not least, the effects of image segmentation on feature calculations will be addressed.

Molecular and Functional Imaging/Surrogate Markers in Radiation Oncology

Wednesday, Dec. 2 8:30AM - 10:00AM Location: S102C



AMA PRA Category 1 Credits ™: 1.50 ARRT Category A+ Credits: 1.50

Participants

Anca L. Grosu, MD, Freiburg, Germany (Moderator) Nothing to Disclose

LEARNING OBJECTIVES

1) To understand challenges of morphological radiological investigations for the detection and characterization of tumor biology and the timely assessment of tumor response in clinical cancer therapy and in clinical trials testing new therapy regimens. 2) To understand the role and the potential of functional and molecular imaging modalities and techniques used a. prior to therapy for tumor delineation and targeting, b. during cytotoxic therapy, such as radiation and chemotherapy for intra-treatment tumor response monitoring, and .) after cytotoxic therapy for response assessment. 3) To apply and integrate imaging modalities into the therapeutic management of cancer. 4) To review the role of imaging as predictors of tumor control and survival and their emerging role as short-term surrogate markers for long-term therapeutic outcome of cancer treatment regimens and its potential for adaptive therapy.

Sub-Events

RC520A Imaging Surrogate Markers in CNS Tumors

Participants

Anca L. Grosu, MD, Freiburg, Germany (Presenter) Nothing to Disclose

LEARNING OBJECTIVES

1) Clinical problem: Limitations of the morphological/radiological investigations (CT and MRI) for the detection of the gross tumor mass and visualization of tumor biology. 2) Gross Tumor Volume (GTV) Delineation: Amino- Acids PET (AA-PET) and SPECT: a. Sensitivity and specificity of MET-PET, FET-PET and IMT-SPECT b. Comparison MET-PET, FET-PET and IMT-SPECT c. AA-PET for GTV delineation in gliomas d. Future trials. 3) Tumor Biologys: a. Glucose metabolism: FDG-PET b. Tumor proliferation: FLT-PET c. Tumor hypoxia: F-MISO-PET d. Tumor angiogenesis: RGD-PET, MRI e. Visualization of tumor stemm cells in vivo: animal-PET f. Tumor heterogeneity: MRI.

ABSTRACT

1) Clinical problem: Limitations of the morphological/radiological investigations (CT and MRI) for the detection of the gross tumor mass and visualization of tumor biology. 2) Gross Tumor Volume (GTV) Delineation: Amino- Acids PET (AA-PET) and SPECT: a. Sensitivity and specificity of MET-PET, FET-PET and IMT-SPECT b. Comparison MET-PET, FET-PET and IMT-SPECT c. AA-PET for GTV delineation in gliomas d. Future trials. 3) Tumor Biologys: a. Glucose metabolism: FDG-PET b. Tumor proliferation: FLT-PET c. Tumor hypoxia: F-MISO-PET d. Tumor angiogenesis: RGD-PET, MRI e. Visualization of tumor stemm cells in vivo: animal-PET f. Tumor heterogeneity: MRI.

RC520B Imaging Surrogate Markers in Pelvic Tumors

Participants

Nina A. Mayr, MD, Seattle, WA (Presenter) Nothing to Disclose

LEARNING OBJECTIVES

View learning objectives under main course title.

RC520C Imaging Surrogate Markers in Lung Tumors

Participants Meng X. Welliver, MD, Columbus, OH (*Presenter*) Nothing to Disclose

LEARNING OBJECTIVES

View learning objectives under main course title.

RC520D Imaging Surrogate Markers in Head and Neck Cancer

Participants

Min Yao, MD, PhD, Cleveland, OH (Presenter) Nothing to Disclose

LEARNING OBJECTIVES

1) Prognostic indications of FDG PET in head and neck cancer. 2) How to use FDG PET in radiation treatment planning in head and neck cancer. 3) Further treatment decision based on PET. 4) Future prospectives including potential new tracers.

Radiomics Mini-Course: Promise and Challenges

Wednesday, Dec. 2 8:30AM - 10:00AM Location: S502AB

BQ PH

AMA PRA Category 1 Credits ™: 1.50 ARRT Category A+ Credits: 1.50

Participants

Sandy Napel, PhD, Stanford, CA (*Director*) Medical Advisory Board, Fovia, Inc; Consultant, Carestream Health, Inc; Scientific Advisor, EchoPixel, Inc

Sub-Events

RC525A An Overview of Radiomics

Participants

Maryellen L. Giger, PhD, Chicago, IL (*Presenter*) Stockholder, Hologic, Inc; Shareholder, Quantitative Insights, Inc; Royalties, Hologic, Inc; Royalties, General Electric Company; Royalties, MEDIAN Technologies; Royalties, Riverain Technologies, LLC; Royalties, Mitsubishi Corporation; Royalties, Toshiba Corporation; Researcher, Koninklijke Philips NV; Researcher, U-Systems, Inc

LEARNING OBJECTIVES

1) Understand the meaning of radiomics relative to computer-aided diagnosis and quantitative imaging. 2) Learn about the current state-of-the-art in radiomics. 3) Appreciate the existing and future potential role of radiomics with other -omics data and within precision medicine.

ABSTRACT

RC525B From Radiomics to Radiogenomics

Participants

Hugo Aerts, PhD, Boston, MA (Presenter) Nothing to Disclose

LEARNING OBJECTIVES

1) Understand the motivation for integrating imaging with genomic and clinical data. 2) Learn about the methodology for quantitative radiomic analysis Example biomarker quantification studies in Radiomics and Imaging-Genomics (Radiogenomics).

ABSTRACT

RC525C Challenges for Radiomics and Radiogenomics

Participants

Karen Drukker, PhD, Chicago, IL, (kdrukker@uchicago.edu) (Presenter) Nothing to Disclose

LEARNING OBJECTIVES

1) Recognizing potential pitfalls along the radiomics/radiogenomics pipeline. 2) Understanding the crucial role of statistics in the design and evaluation of radiomics/radiogenomics phenotypes and systems.

ABSTRACT

Handout:Karen Drukker

http://abstract.rsna.org/uploads/2015/15003209/referencesCited.docx

Chest (Emphysema)

Wednesday, Dec. 2 10:30AM - 12:00PM Location: S404CD



AMA PRA Category 1 Credits ™: 1.50 ARRT Category A+ Credits: 1.50

FDA Discussions may include off-label uses.

Participants

Brett M. Elicker, MD, San Francisco, CA (*Moderator*) Nothing to Disclose Santiago E. Rossi, MD, Capital Federal, Argentina (*Moderator*) Advisory Board, Koninklijke Philips NV Speaker, Pfizer Inc Royalties, Springer Science+Business Media Deutschland GmbH

Sub-Events

SSK05-01 A New Subtype of COPD in Cigarette Smokers

Wednesday, Dec. 2 10:30AM - 10:40AM Location: S404CD

Participants

David A. Lynch, MBBCh, Denver, CO (*Presenter*) Research support, Siemens AG; Scientific Advisor, PAREXEL International Corporation; Consultant, Boehringer Ingelheim GmbH; Consultant, Gilead Sciences, Inc; Consultant, F. Hoffmann-La Roche Ltd; Consultant, Veracyte, Inc;

Carla G. Wilson, Denver, CO (*Abstract Co-Author*) Nothing to Disclose Mustafa Al Qaisi, MD, Denver, CO (*Abstract Co-Author*) Nothing to Disclose Teresa Gray, Denver, CO (*Abstract Co-Author*) Nothing to Disclose Stephen Humphries, Denver, CO (*Abstract Co-Author*) Nothing to Disclose James D. Crapo, MD, Denver, CO (*Abstract Co-Author*) Nothing to Disclose

PURPOSE

Although quantitative CT measurement of % low attenuation areas less than -950 HU (%LAA-950) is commonly used as a surrogate for emphysema, there is a subgroup of patients who meet quantitative criteria for emphysema, but who do not have visual evidence of emphysema. The purpose of this study was to determine the demographic and physiologic features of this discordant group, compared with a control group that did not have either visual or quantitative evidence of emphysema.

METHOD AND MATERIALS

2099 cigarette smokers enrolled in the COPDGene study underwent visual analysis by two trained research analysts, according to the Fleischner Society categorization of emphysema. From this group, we selected all subjects who had quantitative evidence of emphysema (%LAA-950>5%) but did not have visual evidence of emphysema (n=165). The control group comprised subjects with no visual or quantitative CT evidence of emphysema (n=677). All subjects underwent inspiratory and expiratory CT evaluation, with quantitative CT metrics. Expiratory air trapping was assessed quantitatively by measuring the % LAA <856 HU on expiration. Followup spirometry was obtained 5 years after the initial CT in 128 discordant subjects and in 448 controls. Differences between groups were evaluated using Chi-Square and Student t test as appropriate.

RESULTS

Kappa value for presence or absence of emphysema was 0.84. Compared with the control group, the discordant group were older (mean \pm s.d. 62 \pm 9 vs 59 \pm 9 years, p=0.0001), more likely to be male (63% vs 38%, p<0.0001), and less likely to be African American (5% vs 21% p<0.0001). Although the FEV1 % at baseline was similar in the two groups, the FEV1/FVC ratio was significantly lower in the discordant group (0.71 \pm .10 vs 0.77 \pm .07 p<0.0001). On quantitative expiratory CT, the %LAA-856 was 23 \pm 12 % in the discordant group compared with 11 \pm 9% in the controls (p<0.0001). On 5 year followup, the mean decrease in FEV1 in the discordant group was 241 \pm 271 ml, compared with 178 \pm 259 ml in the control group (p=0.018).

CONCLUSION

Even in the absence of visual emphysema, quantitative CT densitometry identifies a subgroup of smokers with evidence of airway obstruction, who demonstrate progression in airway obstruction over time.

CLINICAL RELEVANCE/APPLICATION

The high proportion of LAA-950 in the discordant group may be due to sub-resolution emphysema (perhaps panlobular), or to lobular overinflation related to small airways abnormality.

SSK05-02 Optimal Threshold for Quantification of Air-trapping Using Non-Rigid Image Registration of Inspiration/Expiration CT Scans in COPD

Wednesday, Dec. 2 10:40AM - 10:50AM Location: S404CD

Participants

Sang Min Lee, Seoul, Korea, Republic Of (*Presenter*) Nothing to Disclose Joon Beom Seo, MD, PhD, Seoul, Korea, Republic Of (*Abstract Co-Author*) Nothing to Disclose Sang Min Lee, MD, Seoul, Korea, Republic Of (*Abstract Co-Author*) Nothing to Disclose Namkug Kim, PhD, Seoul, Korea, Republic Of (*Abstract Co-Author*) Stockholder, Coreline Soft, Inc Sang Young Oh, MD, Seoul, Korea, Republic Of (*Abstract Co-Author*) Nothing to Disclose Yeon-Mok Oh, MD, PhD, Seoul, Korea, Republic Of (*Abstract Co-Author*) Nothing to Disclose

PURPOSE

I o restrospectively investigate the optimal threshold for quantification of air-trapping using non-rigid registration of inspiration and expiration CT scans in COPD patients in correlation with FEF25-75% and RV/TLC

METHOD AND MATERIALS

Institutional review board approval was obtained. From June 2005 to October 2010, 195 patients (166 COPD patients, 29 nonsmoker control) were included in our study. Inspiration and expiration CT scans were performed in the same CT scanner followed by non-rigid registration using an in-house software. Subtraction value per voxel between inspiration and registered expiration CT was obtained and volume fraction of air-trapping (air-trapping index, ATI), using variable thresholds (from 30 to 120 HU), was calculated. Calculated ATI using variable thresholds, expiration/inspiration ratio of mean lung density (E/I MLD), and the percent of lung voxels below -856HU on expiration CT (gas-trapping index, Exp -856) were correlated with pulmonary function parameters for small airway disease or air-trapping (FEF25-75% and RV/TLC).

RESULTS

All of ATI with variable thresholds were significantly correlated with both FEF25-75% and RV/TLC (all P<0.001). When correlated with FEF25-75%, the highest correlation coefficient was -0.656, using the threshold of 80HU. As for RV/TLC, as threshold increased, the correlation coefficient decreased. The highest correlation coefficient was 0.664, using the threshold of 30HU. When plotting the relation between subtraction thresholds and FEF25-75% and RV/TLC, threshold of 60 HU was suitable (r= -0.649 and 0.651, respectively). Those correlation coefficients were comparable to the results with E/I MLD (r= -0.670 and 0.657 for FEF25-75% and RV/TLC, respectively) and Exp -856 (r= -0.604 and 0.565 for FEF25-75% and RV/TLC, respectively). When the optimal threshold of 60HU was applied, the measured ATI of 23 nonsmoker normal controls and COPD patients were 24.2% \pm 16.8 and 65.7% \pm 17.7 (P<0.001).

CONCLUSION

Optimal threshold for quantification of air-trapping using non-rigid registration of inspiration and expiration CT scans in COPD patients is 60 HU with significant correlation with FEF25-75% and RV/TLC, and is comparable to E/I MLD and Exp -856.

CLINICAL RELEVANCE/APPLICATION

Quantification of air-trapping using optimal subtraction threshold of 60 HU using non-rigid image registration of inspiration and expiration CT scans may be useful in assessing small airway dysfunction in COPD patients.

SSK05-03 Impact of Endobronchial Coiling on Segmental Bronchial Lumen in Treated and Untreated Lung Lobes: Correlation with Changes in Lung Volume, Clinical and Pulmonary Functional Tests

Wednesday, Dec. 2 10:50AM - 11:00AM Location: S404CD

Participants

Christopher Kloth, Tuebingen, Germany (*Abstract Co-Author*) Nothing to Disclose Wolfgang M. Thaiss, MD, Tuebingen, Germany (*Abstract Co-Author*) Nothing to Disclose Hendrik Ditt, Forchheim, Germany (*Abstract Co-Author*) Employee, Siemens AG Juergen Hetzel, Tuebingen, Germany (*Abstract Co-Author*) Nothing to Disclose Konstantin Nikolaou, MD, Tuebingen, Germany (*Abstract Co-Author*) Nothing to Disclose Speakers Bureau, Bayer AG Marius Horger, MD, Tuebingen, Germany (*Presenter*) Nothing to Disclose

PURPOSE

To assess the impact of endobronchial coiling on crossectional area of segment bronchi and corresponding lobe volumes both at end-inspiration and end-expiration in patients with chronic obstructive lung disease (COLD) grade IV (GOLD) by using quantitative chest-CT.

METHOD AND MATERIALS

From January 2010 to December 2014 30 patients (female=15, median age=65.36y; range 48-76y) underwent chest-CT both before and after endobronchial coiling for lung volume reduction (LVR). Two thin-slice (0.6mm) non-enhanced image data sets were acquired both at end-inspiration and end-expiration. Clinical response was defined as an increase in the walking distance (6MWT) after LVR-therapy. Additionally, we used also PFT measurements with forced expiratory volume in 1 second (FEV1), ratio of residual volume over total lung capacity (RV/TLC) and single-breath diffusion capacity for carbon monoxide (DLCOSB) for correlation

RESULTS

In the treated segment bronchi, the cross-sectional area of the lumen showed a significant reduction (p<0.05) in inspiration and a tendency to an increased lumen in expiration (p>0.05). In the other ipsilateral lobe, the segment bronchial lumens showed no significant changes. In the contralateral lung, we found at inspiration a strong tendency towards an increased lumen (p=0.06). The lung volumes of the treated lobes directly correlated with the treated segment bronchial lumen in expiration (r = 0.80, p < 0.001). Clinical correlation with 6 minutes walking test (6MWT) and pulmonary function test (PFT) showed only in responders a statistically significant decrease of volume in the treated lobe. Responders showed a increase of the 6 MWT (p < 0.0001) and non-responders a significant decrease of the 6MWT (p < 0.0078). The responder subgroup showed an increase of FEV1, TLC and VC however not statistically significant

CONCLUSION

Endobronchial coiling causes a significant decrease in the crossectional area of treated segmental bronchi in inspiration and also a slight increase in expiration accompanied by a volume reduction whereas in the non-treated lung lobes a slightly opposite tendency was observed. 6MWT and PFT minimally, but statistically significant improved after LVR.

CLINICAL RELEVANCE/APPLICATION

Our data support the current understanding of coiling effects which claim that they stabilize and stiffen the lung parenchyma thus compensating for the loss of elasticity in the interstitium and reducing bronchial motility/collapsing.

SSK05-04 Lung Morphology Assessment of Cystic Fibrosis Using Non Contrast Proton MRI with Submillimeter Details at 1.5 Tesla

Awards

Trainee Research Prize - Medical Student

Participants

Gael Dournes, MD, PhD, Pessac, France (*Presenter*) Nothing to Disclose Julie Macey, Bordeaux, France (*Abstract Co-Author*) Nothing to Disclose Fanny Menut, Bordeaux, France (*Abstract Co-Author*) Nothing to Disclose Marjorie Salel, Bordeaux, France (*Abstract Co-Author*) Nothing to Disclose Michel Montaudon, MD, Pessac, France (*Abstract Co-Author*) Nothing to Disclose Olivier Corneloup, MD, Bordeaux, France (*Abstract Co-Author*) Nothing to Disclose Valerie Latrabe, MD, Pessac, France (*Abstract Co-Author*) Nothing to Disclose Hubert Cochet, MD, Pessac, France (*Abstract Co-Author*) Nothing to Disclose Jean Francois Chateil, MD, Bourdeaux, France (*Abstract Co-Author*) Nothing to Disclose Michael Fayon, Bordeaux, France (*Abstract Co-Author*) Nothing to Disclose Patrick Berger, MD, PhD, Bordeaux, France (*Abstract Co-Author*) Nothing to Disclose Francois H. Laurent, MD, Pessac, France (*Abstract Co-Author*) Nothing to Disclose

PURPOSE

The aim of the study was to assess the concordance between CT and non-contrast proton MRI for evaluation of structural cystic fibrosis (CF) changes using a respiratory-gated PETRA, a T1-VIBE and a T2-HASTE sequences.

METHOD AND MATERIALS

All consecutive CF patients under stable condition were enrolled from July 2014 to January 2015 in a single institution. All patients or their parents gave written informed consent. Patients had to complete both CT and MRI the same day. The Helbich-Bhalla score was used to assess CF severity. Concordance between CT and MRI was assessed using intraclass correlation coefficient (ICC) and Bland-Altman analysis. Intra and inter-observer reproducibility were assessed.

RESULTS

24 CF patients were enrolled (mean age=22.6 \pm 9.6, ranging from 9 to 48-year-old). Mean Helbich-Bhalla score at CT was 13.6 \pm 5.5. The concordance in overall Helbich-Bhalla score was very good using PETRA (ICC=0.99) while it was found good using VIBE and HASTE sequences (ICC=0.69 and 0.62, respectively). Bland-Altman plots showed that agreement between CT and PETRA was independent from the magnitude of score (mean difference (MD =-0.3 [-1.7; 1.3]), whereas there was systematic underestimation using VIBE (MD=-4.9 [-0.5; -9.3] and HASTE (MD=-5.6 [-0.4; -10.9]). Intra and interobserver reproducibility were very good for the whole imaging modalities (ICC=0.86-0.98).

CONCLUSION

In this pilot study, the Helbich-Bhalla score using PETRA matched closely with that of CT and showed higher level of concordance than either conventional T1-weighted or T2-weighted sequences. Further improvement in respiratory synchronization and acquisition time are expected, whereas future combination with functional information is warranted.

CLINICAL RELEVANCE/APPLICATION

Implication for patient care - PETRA is a clinically available sequence which provides assessment of lung structural-CF alterations with submillimeter details - Using lung MRI, non-invasive structural assessment of CF may no longer be restricted due to radiation concern for routine follow-up or under treatment.

SSK05-05 Different Progression of CT Defined Emphysema Depending of Trends in Smoking Habit in the ITALUNG Screening Trial

Wednesday, Dec. 2 11:10AM - 11:20AM Location: S404CD

Participants

Chiara Romei, Pisa, Italy (*Presenter*) Nothing to Disclose Barbara Conti, Pisa, Italy (*Abstract Co-Author*) Nothing to Disclose Laura Carrozzi, Pisa, Italy (*Abstract Co-Author*) Nothing to Disclose Franscesca Carozzi, Firenze, Italy (*Abstract Co-Author*) Nothing to Disclose Antonio Palla, Pisa, Italy (*Abstract Co-Author*) Nothing to Disclose Fabio Falaschi, MD, Pisa, Italy (*Abstract Co-Author*) Nothing to Disclose

PURPOSE

To evaluate with low dose computed tomography (LDCT) densitometric analysis, changes in pulmonary emphysema over 2 years, in subjects with different trends in smoking habit enrolled in the ITALUNG trial of lung cancer screening.

METHOD AND MATERIALS

284 subjects (male 69.7%; mean age 60.2±4.2) enrolled in the active arm of ITALUNG trial of lung cancer screening underwent to LDCT esamination at first (T1) and third (T3) annual screening round.LDCT evaluated parameters were: total lung volume (ml); % of Relative Areas (RA) at -910, -950, -960 Hounsfield Units (HU); 15th percentile density (PD15, g/L). Lung function tests (VC, FVC, FEV1, FEV1/VC, FEV1/FVC, FRC, RV, TLC, RV/TLC and DLCO) were performed.Four subgroups were identified based on the trends in smoking habit during the 2 years of follow-up: persistent current smokers, former smokers, quitters and re-starter. A predictive model for longitudinal variation of CT parameters during the study was applied, considering as independent variables: age, sex, smoking variation, lung function tests and total lung volume.

RESULTS

Longitudinally, an increase of the median value of %RA was observed: %RA-960 = 9.8 at T1 and 10.2 at T3, (p<.0001); %RA-950=13 at T1 and 13.5 at T3 (p<.0001); %RA-910=29.2 at T1 and 29.5 at T3 (p<.0003).On the contrary, PD15 g/l decreased (33.4 at T1 and 30 at T3, p<.0001). No functional tests and diffusion capacity demonstrated significant evolution in the 2 years of follow-up except FEV1/FVC (p=0.031).In the 142 current smokers, in the 93 former smokers and in the 42 quitters PD15 g/l

decreased respectively from 38.2 ± 20 at T1 to 39.21 ± 17.4 at T3 (p<.00504), from 24.2 ± 21.5 at T1 to 20 ± 18.6 at T3 (p=0.0063), from 36.6 ± 12.4 at T1 to 26.8 ± 16.2 al T3 (p<.0001). On the contrary in the 7 re-starter PD15 g/l increased without statistical relevance (38.6 ± 23.4 at T1 and 48.4 ± 18.6 at T3, p=0.1897).

CONCLUSION

LDCT densitometric analysis allows a short-term evaluation of progression of pulmonary emphysema in screened subjects. The different trends in smoking habit during the follow-up seems to independently determine the lung density change with the major decrease in quitters and former smokers, possibly dependent to the absence of inflammatory smoking induced effects.

CLINICAL RELEVANCE/APPLICATION

The short-term progression of emphysema can be evaluated by LDCT analysis in asymptomatic subjects and differ depending of trends in smoking habit in the period of follow-up.

SSK05-06 Assessment of Healthy Volunteers with COPD High Risk Factors by Quantitative CT: Correlation with Pulmonary Functional Tests

Wednesday, Dec. 2 11:20AM - 11:30AM Location: S404CD

Participants

Yi Xia, MD, Shanghai, China (*Presenter*) Nothing to Disclose Yu Guan, MD, Shanghai, China (*Abstract Co-Author*) Nothing to Disclose Li Fan, Shanghai, China (*Abstract Co-Author*) Nothing to Disclose Shiyuan Liu, PhD, Shanghai, China (*Abstract Co-Author*) Nothing to Disclose

PURPOSE

To investigate the association of quantitative CT (QCT) with spirometric measurements in healthy volunteers with COPD high risk factors between non-smoking group and smoking group.

METHOD AND MATERIALS

Seventy-four healthy volunteers were examined by PFT, inspiratory and expiratory CT. Inclusion criteria: 1. age>45y; 2. cigarette>10 pack*year; or chronic cough,sputum or dyspnea symptom; or emphysema on CT; 3. spirometry: FEV1%pred<95% and FEV1/FVC>70%; 4. informed consent acquired. The subjects were classified into 2 groups: non-smoking group(n=40) and smoking group(n=34). QCT parameters contained trachea volume, total lung volume (TLV) and emphysema index of threshold of lung area with attenuation lower than -950 HU (EI-950) on inspiratory CT; air trapping, defined as the percentage of attenuation area lower than -856 HU (LAA-856) on expiratory CT. To evaluate the correlation between QCT parameters and PFT values, Spearman correlation analysis was used. Compare the difference between non-smoking group and smoking group, t-test was used.

RESULTS

The TLV showed good correlation with FEV1, FVC and TLC(r=0.575, P<0.001;r=0.590, P<0.001;r=0.714, P<0.001)for all subjects. For non-smoking group, there were strong correlation between TLV and FEV1, FVC, TLC(r=0.498, P=0.001;r=0.580, P<0.001;r=0.757, P<0.001). However, there was no correlation between TLV and FEV1, FVC for smoking group. In addition, there was a correlation between total lung capacity (TLC) and EI-950 (r=0.236, P=0.043), between TLC and LAA-856 (r=0.265, P=0.026), respectively. For non-smoking group, the TLC had strong correlation with LAA-856(r=0.526, P=0.001); But, there was no statistical difference between TLC and EI-950 or LAA-856 for smoking group. Compared with smoking group, TLV (4.79±0.98 L vs. 3.75±1.06 L) and trachea volume(62.3±13 cm3 vs.43.3±18 cm3) were reduced significantly in non-smoking group. Smoking group [(2.69±0.33) L and (3.51±0.45) L] showed higher FEV1 and FVC vs. non-smoking group[(2.28±0.52)L and 2.95±0.69](P<0.001).

CONCLUSION

There were different correlations and features between PFT and CT volume in non-smoking group and smoking group for subjects with COPD high risk factors.

CLINICAL RELEVANCE/APPLICATION

Assessment of healthy volunteers with COPD high risk factors by QCT indicate that non-smoking group and smoking group have different features, which could guide clinical management.

SSK05-07 The Airway Remodelling and Emphysema Alteration as Determined by Quantitative CT Measurement: Correlations with the Frequency of COPD Exacerbation

Wednesday, Dec. 2 11:30AM - 11:40AM Location: S404CD

Participants

Yu Guan, MD, Shanghai, China (*Presenter*) Nothing to Disclose Li Fan, Shanghai, China (*Abstract Co-Author*) Nothing to Disclose Yi Xia, MD, Shanghai, China (*Abstract Co-Author*) Nothing to Disclose Shiyuan Liu, PhD, Shanghai, China (*Abstract Co-Author*) Nothing to Disclose

PURPOSE

We aimed to evaluate the change of airway remodelling and emphysema in COPD exacerbations as determined by quantitative CT measurement. We aslo study the relationship between COPD exacerbation frequency and quantitative CT measures of airway remodelling and emphysema.

METHOD AND MATERIALS

Volumetric CT was acquired for 80 patients who visited the emerency department for AECOPD. All images were reconstructed with 1mm slice and retrospectively analyzed using a software program with fully-automated 3D airway extraction and emphysema analysis. Total lung emphysema index were calculated automatically at the threshold of -950HU. Airway parameters including wall thickness(WT), luminal diameter(LD) and wall area percentage(WA%) were measured in the six segmetal bronchus as follows, RB1, RB4, RB10, LB1 and LB10. The frequency of COPD exacerbation in the prior year was determined by using a questionnaire.Statistical analysis was performed to examine evaluate the change of airway remodelling and emphysema in COPD exacerbations and the relationship of exacerbation frequency with quantitative CT measurements.

RESULTS

Emphysema index alteration was not influenced by the frequency of COPD exacerbation in the same patient. There was no significant correlations between emphysema index alteration and COPD exacerbation frequency(r=0.46, P=0.06). However, the wall area percentage(WA%) and wall thickness(WT) were measured in the six segmetal bronchus were associated with COPD exacerbation frequency(r=0.74, P=0.02; r=0.65, p=0.03, respectively). No significant correlations was found between luminal diameter(LD) and COPD exacerbation frequency(r=0.53, P=0.08).

CONCLUSION

Quantitative CT can identify the change of airway remodelling and emphysema index in COPD exacerbations. The small airway alterlation was associated with COPD exacerbations frequency.

CLINICAL RELEVANCE/APPLICATION

Quantitative CT can identify the change of small airway and emphysema of COPD exacerbations which may contributed to individual treatment.

SSK05-08 Meta-analysis of Repeatability of CT Lung Density Measures

Wednesday, Dec. 2 11:40AM - 11:50AM Location: S404CD

Participants

Sean B. Fain, PhD, Madison, WI (*Presenter*) Research Grant, General Electric Company Research Consultant, Marvel Medtech, LLC Heather Chen-Mayer, PhD, Gaithersburg, MD (*Abstract Co-Author*) Nothing to Disclose
Alfonso Rodriguez JR, MS, Madison, WI (*Abstract Co-Author*) Nothing to Disclose
Jered Sieren, Coralville, IA (*Abstract Co-Author*) Consultant, Vida Diagnostics, Inc
Matthew K. Fuld, PhD, Iowa City, IA (*Abstract Co-Author*) Researcher, Siemens AG
Bernice E. Hoppel, PhD, Vernon Hills, IL (*Abstract Co-Author*) Research support, Siemens AG; Scientific Advisor, PAREXEL International
Corporation; Consultant, Boehringer Ingelheim GmbH; Consultant, Gilead Sciences, Inc; Consultant, F. Hoffmann-La Roche Ltd;
Consultant, Veracyte, Inc;
Frank N. Ranallo, PhD, Madison, WI (*Abstract Co-Author*) Nothing to Disclose

PURPOSE

To determine the clinically relevant change of lung density CT metrics.

METHOD AND MATERIALS

The most established measures of lung parenchymal density are "RA950" and "Perc15". The RA950 is defined here as the relative lung area (or lung voxels) at total lung capacity (TLC) with CT attenuation below -950 Hounsfield units (HU). The Perc15 is defined as the HU value at which 15 percent of all voxels have a lower density. These measures are the most common, based on studies comparing to tissue histology in resected lung and established in longitudinal studies of emphysema progression. Literature review was conducted on recent clinical studies involving repeat scans of non-diseased or stable subjects to determining bias and repeatability. A meta-analysis was performed on the repeatability coefficient (RC) inclusive of recent studies that met three major criteria: 1) The study was performed using 16 or 64 slice architectures with 3D volumetric scanning similar to the specifications. 2) The study performed CT in subjects for at least two time points in identical CT scanners with \leq 4 months separating the two time points to mitigate the degree of possible disease progression. 3) The Perc15 and/or RA950 metrics were used to assess lung parenchymal density.

RESULTS

Most studies show that performing volume adjustment (VA) to compensate for the state of the lung inflation will improve the RC. Mean RCs were determined from the meta-analysis using the random effects model, shown in a summary Forest plot (Fig. 1), for before and after VA. Each study reported limits of agreement (LOA), defined as 1.96SDbias, from which the RC can be calculated. The RC is deemed the Smallest Real Difference (SRD), a reference for making clinical decisions.

CONCLUSION

Result of the meta-analysis suggests that without lung VA, a decrease in Perc 15 of at least 18 HU, is required for detection of an increase in the extent of emphysema, with 95% confidence. With lung VA, this SRD value is narrowed down to 11 HU. For RA 950 without VA, an increase of at least 3.7% constitutes a real change. There are insufficient studies to support a meta-analysis of RA950 with VA.

CLINICAL RELEVANCE/APPLICATION

Volume adjustment should be considered to improve repeatability and increase precision for longitudinal studies of emphysema progression in COPD using lung density CT.

SSK05-09 Quantitative Analysis of Pulmonary Peripheral Vessels Using CT in Healthy Subject and COPD Patients

Wednesday, Dec. 2 11:50AM - 12:00PM Location: S404CD

Participants

Sang Min Lee, MD, Seoul, Korea, Republic Of (*Abstract Co-Author*) Nothing to Disclose Joon Beom Seo, MD, PhD, Seoul, Korea, Republic Of (*Abstract Co-Author*) Nothing to Disclose Hyun Jung Koo, MD, Seoul, Korea, Republic Of (*Presenter*) Nothing to Disclose Namkug Kim, PhD, Seoul, Korea, Republic Of (*Abstract Co-Author*) Stockholder, Coreline Soft, Inc Jangpyo Bae, MS, Seoul, Korea, Republic Of (*Abstract Co-Author*) Nothing to Disclose Yeon-Mok Oh, MD, PhD, Seoul, Korea, Republic Of (*Abstract Co-Author*) Nothing to Disclose

PURPOSE

To analyze peripheral vascular changes at CT of COPD with new method and correlate them with emphysema index (EI) and pulmonary function tests.

METHOD AND MATERIALS

Non-contrast, inspiration volumetric CT of 30 healthy subjects (M:F = 25:5; 50.6 ± 7.6 yrs) and 73 COPD patients (M:F = 71:2; 64.3 ± 6.6 yrs) were included. Using in-house software, all pulmonary vessels were extracted automatically. Three imaging planes, which are 1cm, 2cm and 3cm distant from lung surface, respectively, were generated. The numbers of all vessels in each plane and per cm2 (No, No_rel, respectively) were counted. The mean area of each vessel and the percentage of vessel area at image plane (Ar, Ar%, respectively) were measured. The results were compared between two groups and correlated with emphysema index (EI) and PFT.

RESULTS

At imaging plane 1cm apart from the surface, the No, No_rel and Ar% in COPD patients were significantly smaller than healthy subjects (No: 2265 ± 650 vs. 2597 ± 741 ; No_rel: 1.08 ± 0.35 /cm² vs. 1.27 ± 0.40 /cm²; Ar%: 4.84 ± 1.61 vs. 5.75 ± 1.88). In addition, No_rel and Ar% at all planes showed significant negative correlation with EI (1cm: r = -0.344, -0.353; 2cm: r = -0.438, -0.414; 3cm: r = -0.423, -0.412, respectively), FEV1 (1cm: r = 0.224, 0.211; 2cm: r = 0.222, 0.231; 3cm: r = 0.226, 0.208, respectively), FEV1/FVC (1cm: r = 0.287, 0.276; 2cm: r = 0.260, 0.274; 3cm: r = 0.270, 0.281, respectively) and DLco (1cm: r = 0.351, 0.347; 2cm: r = 0.306, 0.325; 3cm: r = 0.282, 0.325, respectively).

CONCLUSION

In COPD patients, number of pulmonary vessels and vessel area percent are significant smaller than those in healthy subjects. Quantified number per cm2 and area percent of vessels significantly correlated with FEV1, FEV1/FVC and DLco.

CLINICAL RELEVANCE/APPLICATION

Detailed analysis of analysis of peripheral vascular changes is possible using volumetric CT and dedicated software. It may be helpful in the understanding of vascular changes in COPD.

Radiomics Mini-Course: Oncologic Applications

Thursday, Dec. 3 8:30AM - 10:00AM Location: S103AB

BR CH NR BQ CT NM OI RO PH

AMA PRA Category 1 Credits ™: 1.50 ARRT Category A+ Credits: 1.50

Participants

Sandy Napel, PhD, Stanford, CA (*Director*) Medical Advisory Board, Fovia, Inc; Consultant, Carestream Health, Inc; Scientific Advisor, EchoPixel, Inc

Sub-Events

RC625A Breast Cancer with PET-CT

Participants

Richard L. Wahl, MD, Saint Louis, MO (Presenter) Research Consultant, Nihon Medi-Physics Co, Ltd;

LEARNING OBJECTIVES

1) Describe the FDG pet uptake characteristics before therapy of 'triple - negative' breast cancers vs other subtypes.

ABSTRACT

Honored Educators

Presenters or authors on this event have been recognized as RSNA Honored Educators for participating in multiple qualifying educational activities. Honored Educators are invested in furthering the profession of radiology by delivering high-quality educational content in their field of study. Learn how you can become an honored educator by visiting the website at: https://www.rsna.org/Honored-Educator-Award/

Richard L. Wahl, MD - 2013 Honored Educator

RC625B Radiogenomics of Lung Cancer

Participants

Michael D. Kuo, MD, Los Angeles, CA (Presenter) Nothing to Disclose

LEARNING OBJECTIVES

1) To discuss the principles behind lung cancer radiogenomics. 2) Highlight clinical applications of lung cancer radiogenomics.

ABSTRACT

RC625C Brain Cancer: Radiomics, Radiogenomics, and Big Data

Participants Rivka R. Colen, MD, Houston, TX, (rcolen@mdanderson.org) (*Presenter*) Nothing to Disclose

LEARNING OBJECTIVES

1) Define the field of radiomics and imaging genomics. 2) Apply radiomics and imaging genomics in brain tumors. 3) Describe the use of MRI as a biomarker for genomic signatures and profiles. 4) Define role of MRI in personalized medicine for target discovery of therapeutic targets. 5) Explain the use of MRI in drug development and clinical trials. 6) Assess the research available in imaging genomics and radiomics. 7) Define and describe the integration of radiomics and imaging genomics into big data platforms.

ABSTRACT

This objective of this course is to introduce the recently emerged field of radiomics and imaging genomics (radiogenomics) in brain tumors, specifically glioblastoma (GBM). Emphasis will be on radiomics with regards to the high-dimensional, high-throughput feature extraction of imaging features from medical images, specifically MRI; the second emphasis will be on the use of imaging in relation to underlying tumor genomics, how to use MRI as a biomarker, surrogate and correlate of tumor genomics as well as the use of MRI as a genomic target discovery tool and its application in therapeutic discovery and drug development. The role of radiomics and imaging genomics in the era of big data and how we can leverage the imaging-omic data will also be discussed.

Quantitative Imaging and Informatics (In Association with the Society for Imaging Informatics in Medicine)

Thursday, Dec. 3 8:30AM - 10:00AM Location: S501ABC

IN BQ

AMA PRA Category 1 Credits ™: 1.50 ARRT Category A+ Credits: 1.50

Participants

Adam E. Flanders, MD, Penn Valley, PA, (adam.flanders@jefferson.edu) (*Moderator*) Nothing to Disclose Luciano M. Prevedello, MD,MPH, Columbus, OH (*Moderator*) Nothing to Disclose

LEARNING OBJECTIVES

1) Develop an understanding of what quantitative imaging is and how it may revolutionize the way we practice diagnostic radiology today. 2) Learn the research advances and the current clinical applications of this technology. 3) Appreciate the current challenges involved in using these tools clinically and understand the steps required for a successful clinical implementation.

ABSTRACT

Medicine has undergone a gradual evolution in which diagnostic imaging has become the centerpiece in establishing a clinical diagnosis and in assessing disease response. In recent years, the focus has changed such that for some disease categories (e.g. oncology) we now perceive medical imaging as a phenotypic expression of the genetic makeup of that disease. To that end, imaging now serves as a biomarker of genetic disease subtypes with features that may offer clues to understanding the natural behavior of the disease and specific changes that may occur as part of a therapeutic response. It is now well recognized that there is a substantial amount of objective information contained within diagnostic imaging studies that can be exploited beyond the level of simple measurements. The extraction of quantitative and semi-quantitative information from imaging studies that is both useful and reproducible is the challenge and opportunity for clinical trials research and radiologic reporting today and in the future. This session will explore the revolution and evolution of quantitative imaging; providing attendees with research advances, clinical applications, and the challenges of clinical implementation.

Sub-Events

RCC51A What is Quantitative Imaging?

Participants

Katherine P. Andriole, PhD, Dedham, MA (Presenter) Advisory Board, McKinsey & Company, Inc;

LEARNING OBJECTIVES

1) Be able to describe what is meant by quantitative imaging. 2) Understand existing issues in implementing quantitative imaging techniques in the clinical arena as well as in the research realm, and see how informatics tools may help. 3) Be aware of on-going international efforts to address current challenges and to move quantitative imaging forward.

ABSTRACT

Quantitative imaging has rapidly evolved in recent years from a promising research activity to an essential clinical tool. Physicians consider the objective metrics obtained from imaging studies, in making critical patient management decisions. What is meant by quantitative imaging will be described using illustrative real-world use cases. Existing issues including technical as well as workflow challenges will be discussed. An introduction to imaging informatics tools and techniques such as standards, integration, data mining, cloud computing, ontologies, data visualization and navigation tools, and business analytics applications that may assist in filling current gaps in the clinical implementation of quantitative imaging will be given. An overview of activities of the RSNA's Quantitative Imaging Biomarkers Alliance (QIBA), an international initiative whose goal is to optimize the potential of quantitative imaging, including a description of the data warehouse project will be provided.

RCC51B Informatics Approaches to Enable Quantitative Imaging in Real World Radiology Practice

Participants

Daniel L. Rubin, MD, MS, Palo Alto, CA (Presenter) Nothing to Disclose

LEARNING OBJECTIVES

1) To highlight limitations in current radiological quantitative imaging practice and identify opportunities for improvement through informatics. 2) To introduce Annotation and Image Markup (AIM) as a new standard for capturing and sharing quantitative imaging metadata. 3) To demonstrate new AIM-enhanced tools that can streamline and improve quantitative imaging assessment and workflow for the radiologist.

ABSTRACT

Radiology practice is increasingly a quantitative endeavor. Radiologists frequently need to measure the length of lesions to track treatment response or measure the size of structures to for diagnostic assessment. Current practices of quantitation are cumbersome; measurements are recorded as screen captures that cannot be processed by machine, and the numbers must be transcribed into a radiology report. It is currently exceedingly difficult to create structured databases of quantitative image information for discovery about how, say, change in tumor size over time relates to drug treatment. Quantitative imaging is currently at best a labor-intensive process and at worst error-prone. We have been developing informatics methods to streamline the electronic capture of quantitative imaging results as "image metadata" in structured format that can be easily processed by computers. Tools that we are producing will allow the radiologist to perform quantitative imaging assessment in their current routine workflow-measuring lesions on the PACS, while simultaneously their measurements will be captured and transmitted in standardized formats to applications that can automate accurate reporting, analysis, and decision support. In the future such tools will even help researchers to discover new ways that quantitative signals in images can improve assessment of treatment and prediction of

disease course.

Honored Educators

Presenters or authors on this event have been recognized as RSNA Honored Educators for participating in multiple qualifying educational activities. Honored Educators are invested in furthering the profession of radiology by delivering high-quality educational content in their field of study. Learn how you can become an honored educator by visiting the website at: https://www.rsna.org/Honored-Educator-Award/

Daniel L. Rubin, MD, MS - 2012 Honored Educator Daniel L. Rubin, MD, MS - 2013 Honored Educator

RCC51C QI Clinical Use Cases Outside of Oncology

Participants

Eliot L. Siegel, MD, Severna Park, MD (*Presenter*) Research Grant, General Electric Company; Speakers Bureau, Siemens AG; Board of Directors, Carestream Health, Inc; Research Grant, XYBIX Systems, Inc; Research Grant, Steelcase, Inc; Research Grant, Anthro Corp; Research Grant, RedRick Technologies Inc; Research Grant, Evolved Technologies Corporation; Research Grant, Barco nv; Research Grant, Intel Corporation; Research Grant, Dell Inc; Research Grant, Herman Miller, Inc; Research Grant, Virtual Radiology; Research Grant, Anatomical Travelogue, Inc; Medical Advisory Board, Fovia, Inc; Medical Advisory Board, Toshiba Corporation; Medical Advisory Board, McKesson Corporation; Medical Advisory Board, Carestream Health, Inc; Medical Advisory Board, Bayer AG; Research, TeraRecon, Inc; Medical Advisory Board, Bracco Group; Researcher, Bracco Group; Medical Advisory Board, Merge Healthcare Incorporated; Medical Advisory Board, Microsoft Corporation; Researcher, Microsoft Corporation

LEARNING OBJECTIVES

List the current greatest challenges to quantitative imaging from an informatics perspective.
 Describe how data from clinical trials and the electronic medical record can provide decision support tools associated with the application of quantitative imaging.
 Be able to articulate the requirements for 'next generation' quantitative imaging and opportunities for improvement of the current generation of CAD software.

ABSTRACT

In the current and future era of Big Data and advanced algorithms to model and diagnose complex disease, structured reporting, natural language processing and quantitative imaging have become essential elements for diagnostic imaging. Additionally it is absolutely essential that our imaging reports including scanning parameters, diagnosis, findings, recommendations, etc. as well as quantitative measurements and impressions from the pixel data be made available for the next generation of diagnostic, staging, and treatment algorithms. Currently there are several major challenges to making these imaging data accessible in a machine recognizable manner and these will be listed, including the application of a method to 'tag' medical images and a means of structuring and classifying findings made by radiologists and other human interpreters as well as computer algorithms that make quantitative measurements and computer aided detection and diagnosis. Once these data are available they can be utilized for decision support in radiology such as determination of which patients should be screened, estimation of the likelihood of malignancy when a nodule is detected, and refinement of CAD algorithms based on a priori estimates of likelihood of disease.

Chest (Diffuse Lung Disease/Funtional Imaging)

Thursday, Dec. 3 10:30AM - 12:00PM Location: S404CD



FDA Discussions may include off-label uses.

Participants

Yoshiharu Ohno, MD, PhD, Kobe, Japan (*Moderator*) Research Grant, Toshiba Corporation; Research Grant, Koninklijke Philips NV; Research Grant, Bayer AG; Research Grant, DAIICHI SANKYO Group; Research Grant, Eisai Co, Ltd; Research Grant, Terumo Corporation; Research Grant, Fuji Yakuhin Co, Ltd; Research Grant, FUJIFILM Holdings Corporation; Research Grant, Guerbet SA; Hiroto Hatabu, MD, PhD, Boston, MA (*Moderator*) Research Grant, Toshiba Corporation Research Grant, AZE, Ltd Research Grant, Canon Inc

Sub-Events

SSQ05-01 Distribution and Associated High-Resolution CT findings Predict Survival in Chronic Hypersensitivity Pneumonitis

Thursday, Dec. 3 10:30AM - 10:40AM Location: S404CD

Participants

Jonathan H. Chung, MD, Denver, CO (*Presenter*) Research Grant, Siemens AG; Royalties, Reed Elsevier Tilman Koelsch, MD, Phoenix, AZ (*Abstract Co-Author*) Nothing to Disclose Xi Zhan, MD,PhD, Beijing, China (*Abstract Co-Author*) Nothing to Disclose David A. Lynch, MBBCh, Denver, CO (*Abstract Co-Author*) Research support, Siemens AG; Scientific Advisor, PAREXEL International Corporation; Consultant, Boehringer Ingelheim GmbH; Consultant, Gilead Sciences, Inc; Consultant, F. Hoffmann-La Roche Ltd; Consultant, Veracyte, Inc;

Evans R. Fernandez Perez, Denver, CO (Abstract Co-Author) Nothing to Disclose

PURPOSE

It is unknown if the presence of air-trapping and disease distribution on chest CT, which may be a clue to the diagnosis, predicts mortality among patients with chronic hypersensitivity pneumonitis (CHP).

METHOD AND MATERIALS

The earliest CT chest scans from subjects with HP were scored. Fibrotic HP on CT was defined as presence of reticulation with associated traction bronchiectasis and/or bronchielectasis. The predominant zonal and axial distribution of lung disease, the presence or absence as well as total percentage of lung involvement (to the nearest 5%) for air-trapping was scored. The most likely diagnosis with level of confidence (possible, probable, or definite) was also determined. A Cox proportional hazards (PH) model was used to identify independent predictors in time-to death analysis.

RESULTS

Of 82 subjects, 60 (73%) had fibrotic HP, and 22 (27%) had non-fibrotic HP on chest CT. The most common patterns were HP (43, 52%), UIP (19, 23%), NSIP (11, 13%), and other (9, 10%). Compared to other CT patterns, the HP pattern was most often zonally diffuse or upper and axially diffuse or peripheral (p<0.01). Compared with survivors, patients who died had lower FVC% predicted, were more likely to have pulmonary fibrosis, and were less likely to have ground-glass opacity on CT. In a Cox PH model, the presence of UIP pattern of fibrosis, axially diffuse disease, and absence of air-trapping/mosaic perfusion were independent predictors of survival (Hazard ratios 2.82 [p-value 0.02], 2.46 [p-value 0.01], and 0.39 [p-value 0.01]; respectively).

CONCLUSION

Chest CT has prognostic value in the setting of CHP.

CLINICAL RELEVANCE/APPLICATION

Chest CT may be a valuable biomarker in HP, aside from diagnosis and follow-up.

Honored Educators

Presenters or authors on this event have been recognized as RSNA Honored Educators for participating in multiple qualifying educational activities. Honored Educators are invested in furthering the profession of radiology by delivering high-quality educational content in their field of study. Learn how you can become an honored educator by visiting the website at: https://www.rsna.org/Honored-Educator-Award/

Jonathan H. Chung, MD - 2013 Honored Educator

SSQ05-02 Prevalence of Pulmonary Fibrosis in Asymptomatic 1st Degree Relatives of Patients with Familial Pulmonary Fibrosis (FPF)

Thursday, Dec. 3 10:40AM - 10:50AM Location: S404CD

Participants

Jonathan H. Chung, MD, Denver, CO (*Presenter*) Research Grant, Siemens AG; Royalties, Reed Elsevier Anna Peljto, Aurora, CO (*Abstract Co-Author*) Nothing to Disclose Tasha Fingerlin, Denver, CO (*Abstract Co-Author*) Nothing to Disclose Marvin I. Schwarz, MD, Denver, CO (*Abstract Co-Author*) Nothing to Disclose David Schwartz, Denver, CO (Abstract Co-Author) Nothing to Disclose

David A. Lynch, MBBCh, Denver, CO (*Abstract Co-Author*) Research support, Siemens AG; Scientific Advisor, PAREXEL International Corporation; Consultant, Boehringer Ingelheim GmbH; Consultant, Gilead Sciences, Inc; Consultant, F. Hoffmann-La Roche Ltd; Consultant, Veracyte, Inc;

PURPOSE

The purpose of this study was to determine the prevalence and pattern of HRCT pulmonary fibrosis in asymptomatic 1st degree relatives of patients with FPF.

METHOD AND MATERIALS

HRCT scans of 250 1st degree relatives of patients with FPF were scored by two thoracic radiologists using a variation of a sequential reading method previously described (Washko GR, et al. N Engl J Med. 2011 Mar 10;364(10):897-906). CT scans were scored as no, equivocal for, suspicious for, or definite pulmonary fibrosis. Presence of honeycombing and ground-glass opacity as well as extent of disease to the nearest 10% was also scored. HRCT diagnosis was also collected with level of confidence (possible, probable, definite).

RESULTS

222 of the 250 CT scans were considered technically adequate. In 15.3% (34/222), pulmonary fibrosis was present (definite or probable). In an additional 3.2% (7/222), presence of pulmonary fibrosis was scored as equivocal. In those with pulmonary fibrosis, an average of 6% (+/-7%) of the lung was involved. Honeycombing in these subjects was present in 14.7% (5/34) while ground-glass opacity was present in 23.5% (8/34). The extent of honeycombing was very small and on average closest to 0% in all subjects with honeycombing. The extent of ground-glass opacity was on average 9% (+/-8%). A high confidence pattern was identified in 38.2% (13/34) of subjects with pulmonary fibrosis: 6 UIP, 3 NSIP, 2HP, and 1 asbestosis.

CONCLUSION

Pulmonary fibrosis is common in asymptomatic relatives of patients with FPF.

CLINICAL RELEVANCE/APPLICATION

HRCT screening of asymptomatic relatives of patients with FPF should be considered.

Honored Educators

Presenters or authors on this event have been recognized as RSNA Honored Educators for participating in multiple qualifying educational activities. Honored Educators are invested in furthering the profession of radiology by delivering high-quality educational content in their field of study. Learn how you can become an honored educator by visiting the website at: https://www.rsna.org/Honored-Educator-Award/

Jonathan H. Chung, MD - 2013 Honored Educator

SSQ05-03 Prediction of Survival with Baseline Extent and 1-year Change of Regional Disease Patterns at Thin Section CT in Idiopathic Pulmonary Fibrosis

Thursday, Dec. 3 10:50AM - 11:00AM Location: S404CD

Participants

Sang Min Lee, MD, Seoul, Korea, Republic Of (*Abstract Co-Author*) Nothing to Disclose Joon Beom Seo, MD, PhD, Seoul, Korea, Republic Of (*Abstract Co-Author*) Nothing to Disclose Sang Min Lee, Seoul, Korea, Republic Of (*Presenter*) Nothing to Disclose Namkug Kim, PhD, Seoul, Korea, Republic Of (*Abstract Co-Author*) Stockholder, Coreline Soft, Inc Jin Woo Song, Seoul, Korea, Republic Of (*Abstract Co-Author*) Nothing to Disclose

PURPOSE

To know if the baseline extent and 1-year change of regional disease patterns at thin-section CT (TSCT), which is measured with texture-based automated quantification system, can predict survival of idiopathic pulmonary fibrosis (IPF)

METHOD AND MATERIALS

Total 194 IPF patients (M:F = 153:41; 63.3 ± 7.8 yrs) with TSCT scans at the time of diagnosis and 1 year after were included. Mean follow-up period of survival was 36.0 ± 18.9 months. Using in-house, texture-based automated system, the area percent of five regional disease patterns, including ground glass opacity (GGO), reticular opacity (RO), honeycomb (HC), emphysema (EM) and consolidation (CON) were quantified. The area percent of abnormal lung (AbN) and fibrosis (FIB) were calculated. The survival analyses were performed by constructing Kaplan-Meier disease-free survival curves. The association of baseline extent and 1-year change of TSCT measures with survival was assessed with Cox proportional hazards regression. Both univariable and multivariable analyses including age, sex, smoking, baseline and change of FVC%pred, DLCO%pred and SpO2% were performed.

RESULTS

Measured relative extents of AbN, HC, GGO, CON, EM, RO and FIB at baseline and 1-year follow-up TSCT were as follows; baseline: $43.0\% \pm 17.1$, 7.0 ± 6.7 , 12.3 ± 11.9 , 2.9 ± 1.3 , 3.9 ± 5.5 , 16.8 ± 9.8 , 23.9 ± 12.3 ; follow-up: 45.3 ± 19.5 , 7.2 ± 7.6 , 13.8 ± 11.6 , 3.2 ± 1.5 , 3.6 ± 5.6 , 17.6 ± 11.6 , 24.8 ± 14.4 , respectively. Survival analysis indicate that disease-free survival of patients with higher baseline extent of AbN, HC, RO, FIB (cut-off value 35%, 10%, 25%, 20%, respectively) and increased extent of AbN, HC, RO, FIB at follow-up TSCT (cut-off value 5%) were significantly shorter than in patients with lower baseline extent and stable or decreased extent of those regional patterns (all p<0.001). Univariable analysis revealed that baseline FVC%pred, DLCO%pred, SpO2%, AbN, HC, RO, FIB, change of AbN, HC, RO, FIB were predictive of survival, After adjustment, the baseline extent of RO and change in extent of AbN were predictive of survival.

CONCLUSION

The baseline extent and 1-year change of regional disease patterns at TSCT, which is measured with texture-based automated quantification system, can predict survival of IPF patients.

CLINICAL RELEVANCE/APPLICATION

The baseline extent and change of regional disease patterns quantified with texture-base automated quantification system is useful in predicting survival of IPF patients.

SSQ05-04 Parallel Bands of Lung Involvement Along the Direction of Ribs: A New Sign of Systemic Sclerosis on Volume-rendered Computed Tomography of the Chest

Thursday, Dec. 3 11:00AM - 11:10AM Location: S404CD

Participants Hanan Sherif, MD, Doha, Qatar (*Abstract Co-Author*) Nothing to Disclose Ahmed-Emad Mahfouz, MD, Doha, Qatar (*Abstract Co-Author*) Nothing to Disclose Maysa A. Mohamed, MBBS, Doha, Qatar (*Abstract Co-Author*) Nothing to Disclose Ahmed Sayedin, MBBCh, Doha, Qatar (*Presenter*) Nothing to Disclose

PURPOSE

To differentiate between systemic sclerosis-related interstitial lung disease and usual interstitial pneumonia on volume-rendered computed tomography (CT) of the chest.

METHOD AND MATERIALS

The multi-detector CT examinations of the chest of 50 patients with systemic sclerosis and 50 patients with usual interstitial pneumonia have been post-processed to obtain volume-rendered images of the lungs. On these images, normally aerated lung parenchyma has been encoded blue and increased attenuation of lung parenchyma has been encoded white. The images have been randomized and provided to an experienced radiologist to note the presence or absence of parallel bands of increased attenuation of the lung parenchyma along the direction of the ribs (the parallel-band sign). Statistical analysis has been done by the chi-square test.

RESULTS

The parallel-band sign has been seen in 32 patients with systemic sclerosis-associated interstitial lung disease and in none of the patients with usual interstitial pneumonia. The parallel-band sign has sensitivity of 64.0%, specificity of 100.0%, positive predictive value of 100.0%, negative predictive value of 73.5%, and accuracy of 82.0% for the diagnosis of systemic sclerosis-associated interstitial lung disease on volume-rendered CT of the chest.

CONCLUSION

Lung involvement in systemic sclerosis-related interstitial lung disease may take the characteristic distribution of parallel bands at the surface of the lungs along the direction of the ribs. The parallel-band sign differentiates systemic sclerosis-related interstitial lung disease from usual interstitial pneumonia with high specificity on volume-rendered CT of the chest.

CLINICAL RELEVANCE/APPLICATION

The use of the parallel-band sign may help differentiate systemic sclerosis-associated interstitial lung disease from usual interstitial pneumonia, particularly if the interstitial lung disease precedes other manifestations of systemic sclerosis such as skin involvement, cardiac disease, or esophageal dilatation.

SSQ05-05 Regional Variation in Ventilation in the Asthmatic Human Lungs Using Magnetic Resonance Imaging and Computed Tomography

Thursday, Dec. 3 11:10AM - 11:20AM Location: S404CD

Participants

Wei Zha, PhD, Madison, WI (*Abstract Co-Author*) Nothing to Disclose
Stan Kruger, MD, Madison, WI (*Abstract Co-Author*) Nothing to Disclose
Robert V. Cadman, PhD, Philadelphia, PA (*Abstract Co-Author*) Nothing to Disclose
David Mummy, MS, MBA, Madison, WI (*Presenter*) Nothing to Disclose
Nizar Jarjour, Madison, WI (*Abstract Co-Author*) Nothing to Disclose
Ronald L. Sorkness, Madison, WI (*Abstract Co-Author*) Nothing to Disclose
Scott K. Nagle, MD, PhD, Madison, WI (*Abstract Co-Author*) Nothing to Disclose
Scott K. Nagle, MD, PhD, Madison, WI (*Abstract Co-Author*) Stockholder, General Electric Company Research Consultant, Vertex
Pharmaceuticals Incorporated
Sean B. Fain, PhD, Madison, WI (*Abstract Co-Author*) Research Grant, General Electric Company Research Consultant, Marvel
Medtech, LLC

PURPOSE

To investigate regional patterns of ventilation abnormalities in asthmatics with both automated and manual methods.

METHOD AND MATERIALS

A total of 83 asthmatic subjects (normal/moderate/severe: n=14/49/20) underwent hyperpolarized (HP) 3He magnetic resonance imaging (MRI), spirometry, and computed tomography (CT). The right and left lungs were segmented from proton MRI using a region-growing algorithm written in MATLAB and further separated into the lung lobes (right upper-RUL, middle-RML and lower-RLL; left upper-LUL and lower-LLL) by a deformable registration to lobar segmentation derived from CT (VIDA Diagnostics, IA). 3He was registered to proton using a rigid registration method. Ventilation defects were identified independently using both manual segmentation and an automated approach which corrected for B1 inhomogeneity, excluded pulmonary vasculature and determined defects adaptively. A linear mixed-effects model was used to perform the pairwise comparison of percent defect volume (PDV) amongst lobes. Spearman correlation was used to evaluate the association between PDV and spirometry. A p<0.05 is considered significant.

RESULTS

The automated defect quantification took \sim 3min versus 20min per study for manual segmentation. The two method yielded similar whole lung PDV (p=0.12). The whole lung PDV measured by both methods correlated inversely with the percent predicted forced

expiratory volume in 1 second (% FEV1) (manual/automated: p = -0.41, p = 0.0002/p = -0.24, p = 0.040) and % FEV1 over forced vital capacity (p = -0.46, p < 0.0001/p = -0.32, p = 0.0045). Both methods found PDV was significantly larger in the RML (automated: 8.21±13.64%) than all other lobes (all p < 0.013). The RUL (5.52±8.83%) was less ventilated than the RLL (3.55±5.24%) and LLL (2.62±3.82%) with p < 0.047. The automated method also suggested a more defected RUL than LUL (3.26±4.76%) with p = 0.011 whereas the difference was not significant by manual measurements.

CONCLUSION

Compared to manual assessment, the automated approach provides comparable PDV measurements and similar association to spirometic measures. Both methods suggest the RML is most affected in asthmatic lungs and that the RUL is measurably more defected than RLL and LLL.

CLINICAL RELEVANCE/APPLICATION

The automated defect quantification can facilitate the application of HP 3He MRI as a potential tool for guiding bronchoscopic assessment of cellular and molecular markers of asthma progression.

SSQ05-06 Lobar Analysis of Hyperpolarised Xenon MR Lung Imaging (Xe-MRI) in Chronic Obstructive Pulmonary Disease (COPD)

Thursday, Dec. 3 11:20AM - 11:30AM Location: S404CD

Participants

Tahreema N. Matin, MBBS, Oxford, United Kingdom (*Presenter*) Nothing to Disclose Mitchell Chen, DPhil,MBBS, Oxford, United Kingdom (*Abstract Co-Author*) Nothing to Disclose Xiaojun Xu, MSc, DPhil, Oxford, United Kingdom (*Abstract Co-Author*) Nothing to Disclose Tom Doel, DPhil, Oxford, United Kingdom (*Abstract Co-Author*) Nothing to Disclose Najib Rahman, MSc, DPhil, Oxford, United Kingdom (*Abstract Co-Author*) Nothing to Disclose Vicente Grau, PhD, Oxford, United Kingdom (*Abstract Co-Author*) Nothing to Disclose Annabel Nickol, Oxford, United Kingdom (*Abstract Co-Author*) Nothing to Disclose Fergus V. Gleeson, MBBS, Oxford, United Kingdom (*Abstract Co-Author*) Consultant, Alliance Medical Limited; Consultant, Blue Earth Diagnostics Limited; Consultant, Polarean, Inc;

PURPOSE

To determine lobar ventilation and apparent diffusion coefficient (ADC) values acquired using hyperpolarised xenon MR lung imaging (Xe-MRI) in subjects with chronic obstructive pulmonary disease (COPD), and to correlate these with quantitative CT (QCT) and pulmonary function tests (PFTs).

METHOD AND MATERIALS

Eighteen patients with COPD (stage II - IV GOLD criteria classification) underwent Xe-MRI at 1.5T, QCT and PFTs.Whole lung and lobar Xe-MRI parameters were obtained using semi-automated segmentation of multi-slice Xe-MRI ventilation images and Xe-MRI diffusion-weighted images (b =20.855sec/cm2) following co-registration to CT using in-house software. Percentage predicted PFT results were established.Whole lung and lobar QCT-derived emphysema was calculated from percentage of lung tissue with density of <-950 HU.Pearson's correlation coefficients were used to evaluate the relationship between imaging measures and PFTs.

RESULTS

Lobar Xe-MRI percentage ventilated volume and lobar Xe-MRI average ADC showed significant correlation with lobar QCT percentage emphysema (r=0.61, P<<0.001 and r=0.72, P<<0.001 respectively). Whole lung Xe-MRI average ADC showed significant correlation with the PFTs: percentage predicted transfer factor of the lung of carbon monoxide (TLCO) (r=-0.69, P<0.03) and percentage predicted functional residual capacity (FRC) (r=0.65, P<0.007). Whole lung QCT percentage emphysema showed a similar significant correlation with percentage predicted TLCO (r=-0.71, P<<0.001) and percentage predicted FRC (r=0.48, P<0.05).

CONCLUSION

This is the first study to generate lobar analysis of Xe-MRI ventilation and ADC. The excellent correlation of whole lung Xe-MRI average ADC with PFTs and lobar Xe-MRI derived measures with lobar QCT percentage emphysema provide supportive evidence for employment of this technique in patients with COPD. This is particularly relevant for those undergoing regional treatments, where Xe-MRI has the potential to accurately guide treatment options or predict post-treatment lung function.

CLINICAL RELEVANCE/APPLICATION

The potential clinical value of Xe-MRI regional lung assessment is becoming increasingly relevant with the possibility of regional lung treatments e.g. lung volume reduction surgery, endobronchial valve placement and radiotherapy. The excellent correlation of Xe-MRI with QCT-derived measures of COPD and PFTs suggests it may be of value in patients considered for these treatments.

SSQ05-07 MR Perfusion Parameters and Apparent Diffusion Coefficient in Lung Cancer: Relation to Microvessel Density Based on Surgical Specimen

Thursday, Dec. 3 11:30AM - 11:40AM Location: S404CD

Participants

Chin A Yi, MD, PhD, Seoul, Korea, Republic Of (*Presenter*) Nothing to Disclose Jae-Hun Kim, PhD, Seoul, Korea, Republic Of (*Abstract Co-Author*) Nothing to Disclose Hyeok-Jun Won, Seoul, Korea, Republic Of (*Abstract Co-Author*) Nothing to Disclose

PURPOSE

Microvessel density is a direct biomarker of tumor angiogenesis. Perfusion parameters of dynamic contrast-enhanced MRI (DCE-MRI) and apparent diffusion coefficient (ADC) of diffusion-weighted MR imaging (DWI) can be measured as a quantitative, non-invasive, and repetitive method for the estimation of tumor angiogenesis in the lung cancer. The purpose of this study was to correlate MR perfusion parameters and ADC with microvessel density in lung cancers patients who underwent surgical resection.

METHOD AND MATERIALS

Ninety three patients (53 men, 40 women; age range, 40-79 years) with non-small cell lung cancers underwent diffusion-weighted and dynamic contrast-enhanced MR imaging before surgery. Surgical specimens were obtained and microvessel density was measured with immunohistochemistry staining for CD 31. Perfusion parameters (Ktrans; volume transfer coefficient, ve; fraction of extravascular extracellular space, vp; fraction of plasma space, T0; the time lag between bolus arrival times of arterial input function and tissue concentration) and ADC were measured and compared with quantitative histologic microvessel density by using the Pearson correlation test.

RESULTS

The significant positive correlations were found between microvessel density and Ktrans (r=0.22, P=0.03) and vp (r=0.29, P < .01). An inverse correlation was found between T0 and microvessel density (r=-0.34, P < .01), whereas no significant correlation was found between ADC and microvessel density.

CONCLUSION

Perfusion parameter such as Ktrans, ve, and T0 showed significant correlation with microvessel density in lung cancers, whereas no correlation was found between ADC and microvessel density.

CLINICAL RELEVANCE/APPLICATION

Perfusion parameter such as Ktrans, ve, and T0 may play a role as indirect biomarkers indicating the extent of microvessel density in lung cancers.

SSQ05-08 Pulmonary Perfusion Phase Imaging using Self-Gated Fourier Decomposition MRI Reveals Perfusion Inhomogeneities in Patients with Cystic Fibrosis

Thursday, Dec. 3 11:40AM - 11:50AM Location: S404CD

Participants

Simon Veldhoen, MD, Wurzburg, Germany (*Presenter*) Nothing to Disclose Daniel Stab, St Lucia, Australia (*Abstract Co-Author*) Nothing to Disclose Andreas M. Weng, Wurzburg, Germany (*Abstract Co-Author*) Nothing to Disclose Andreas Kunz, Wurzburg, Germany (*Abstract Co-Author*) Nothing to Disclose Andre Fischer, DIPLPHYS, PhD, Wurzburg, Germany (*Abstract Co-Author*) Nothing to Disclose Clemens Wirth, MD, Wuerzburg, Germany (*Abstract Co-Author*) Nothing to Disclose Helge Hebestreit, MD, Wuerzburg, Germany (*Abstract Co-Author*) Nothing to Disclose Thorsten A. Bley, MD, Hamburg, Germany (*Abstract Co-Author*) Nothing to Disclose Herbert Koestler, PhD, Wuerzburg, Germany (*Abstract Co-Author*) Nothing to Disclose

PURPOSE

Fourier Decomposition (FD) MRI provides site-resolved functional lung imaging without application of contrast media. Perfusion and ventilation-weighted images are reconstructed using a Fourier analysis of a non-triggered time series of morphologic lung images. In this work, we demonstrate that perfusion-weighted data also carries information regarding the pulmonary perfusion phase.

METHOD AND MATERIALS

Lung perfusion measurements were performed using SENCEFUL, an advancement of the FD technique, obtaining morphologic image series by cardiac and respiratory self-navigation of data sampled in quasi-random fashion. Signal variations over the cardiac cycle allow for determining perfusion-weighted images (perfusion amplitude) and the perfusion phase, which indicates the phase shift in the lungs in relation to a reference voxel in a central vessel (e.g. pulmonary trunk). Pulmonary perfusion amplitude and phase measurements on 3 volunteers and 3 cystic fibrosis patients were performed on a 1.5T system. A 2D FLASH sequence providing a DC signal acquisition for self-navigation was used.

RESULTS

Perfusion amplitude maps of the healthy subjects revealed homogeneous lung perfusion. In the perfusion phase maps, the perfusion-induced signal changes exhibited similar behavior in all lung parts. In contrast, the maps of the cystic fibrosis patients showed areas with reduced perfusion and a significantly higher phase dispersion. The attached image example of a 27 year old cystic fibrosis patient shows reduced perfusion e.g. in the upper lobes and the perfusion phase map reveals an higher phase dispersion when compared to the healthy volunteer. Similar results were found in the other examined volunteers and cystic fibrosis patients.

CONCLUSION

Signal intensities in lung MRI are pulsatile as a function of the cardiac triggered inflow. While a balanced perfusion phase in healthy volunteers indicates a homogeneous pulse wave velocity throughout the lungs, results in patients with cystic fibrosis show regionally varying delays.

CLINICAL RELEVANCE/APPLICATION

Based on a time series' FD, the maps describe a new contrast in pulmonary MRI. First measurements revealed that perfusion phase maps of cystic fibrosis patients differ from those of healthy subjects. Hence, the perfusion phase may contain valuable diagnostic information. Detailed examination of the diagnostic capabilities of FD based perfusion phase MRI is subject to future work.

SSQ05-09 Functional Evaluation of Chronic Lung Allograft Dysfunction with Novel Computed Tomography Lung Deformation Algorithms

Thursday, Dec. 3 11:50AM - 12:00PM Location: S404CD

Participants

Miho Horie, MSc, Toronto, ON (*Presenter*) Research Grant, Toshiba Corporation Tomohito Saito, MD, PhD, Toronto, ON (*Abstract Co-Author*) Nothing to Disclose Joanne Moseley, Toronto, ON (*Abstract Co-Author*) Royalties, RaySearch Laboratories AB; Shafique Keshavjee, MD, Toronto, ON (*Abstract Co-Author*) Nothing to Disclose Narinder S. Paul, MD, Richmond Hill, ON (*Abstract Co-Author*) Research Grant, Toshiba Corporation; Research Grant, Carestream Health, Inc

PURPOSE

Lung transplantation is the destination therapy for end stage chronic lung disease. Chronic lung allograft dysfunction (CLAD) limits the 5-year survival after lung transplantation (Tx). It is important to diagnose and distinguish the CLAD subtypes: Bronchiolitis Obliterans Syndrome (BOS) and Restrictive Allograft Syndrome (RAS). CLAD diagnosis with conventional techniques is limited, deformable registration provides qualitative and quantitative assessment of focal and global lung function. The purpose of this study is to determine the utility of using deformable registration CT data in the diagnosis of CLAD.

METHOD AND MATERIALS

A retrospective study of 30 patients post bilateral Tx followed with PFT and low dose lung CT (conventional tests) scheduled every 3mths. The study cohort had confirmed diagnosis, based on conventional tests and pathology: No-CLAD (n=10); BOS (n=10); RAS (n=10). The CT data was assessed qualitatively and quantitatively using finite element based image registration software (MORFEUS) to document changes in lung deformation between baseline and disease onset. Surface vector analysis was performed and indicated expansion (+) or contraction (-) of regional lung volume; the mean and percentage change for inward and outward vectors was compared using the Mann-Whitney U test.

RESULTS

Qualitative analysis: Upper lobe deformation; No-CLAD 20% (2/10); BOS 20% (2/10) and RAS 70% (7/10). Quantitative analysis: mean vector change from baseline (% change from baseline); for the right (R) and left (L) lungs. No-CLAD: R = +4.0mm (55%); L = +3.2mm (59%). BOS: R = +3.8mm (61%); L = +3.4mm (57%). RAS: R = -8.6mm (71%); L = -9.9mm (74%).

CONCLUSION

Deformable lung registration can quantitatively detect and distinguish between No-CLAD/BOS and RAS.

CLINICAL RELEVANCE/APPLICATION

Lung deformation analysis is a promising technique in evaluating the subtypes of CLAD and in assessing regional change when conventional techniques are limited.

Gastrointestinal (Quantitative Imaging)

Thursday, Dec. 3 10:30AM - 12:00PM Location: E350



AMA PRA Category 1 Credits ™: 1.50 ARRT Category A+ Credits: 1.50

FDA Discussions may include off-label uses.

Participants

Claude B. Sirlin, MD, San Diego, CA (*Moderator*) Research Grant, General Electric Company; Speakers Bureau, Bayer AG; Consultant, Bayer AG; ;

Alexander R. Guimaraes, MD, PhD, Portland, OR (*Moderator*) Speakers Bureau, Siemens AG; Expert Witness, Rice, Dolan, Kershaw Andrew D. Smith, MD, PhD, Jackson, MS (*Moderator*) Research Grant, Pfizer Inc; President, Radiostics LLC; President, Liver Nodularity LLC; President, Color Enhanced Detection LLC; Pending patent, Liver Nodularity LLC; Pending patent, Color Enhanced Detection LLC; Pending patent, Liver Nodularity LLC; Pending patent, Color Enhanced Detection LLC; Pending patent, Liver Nodularity LLC; Pending patent, Color Enhanced Detection LLC; Pending patent, Liver Nodularity LLC; Pending patent, Color Enhanced Detection LLC; Pending patent, Liver Nodularity LLC; Pending patent, Color Enhanced Detection LLC; Pending Patent, Liver Nodularity LLC; Pending patent, Color Enhanced Detection LLC; Pending Patent, Liver Nodularity LLC; Pending Patent, Color Enhanced Detection LLC; Pending Patent, Liver Nodularity LLC; Pending Patent, Color Enhanced Detection LLC; Pending Patent, Liver Nodularity LLC; Pending Patent, Color Enhanced Detection LLC; Pending Patent, Color Enhanced Patent, C

Sub-Events

SSQ06-01 3D Vibe-Dixon MR Sequence in Hepatic Fat Quantification: Inter-reader Reproducibility and Correlation to MRS Results in a Liver Donor Cohort

Thursday, Dec. 3 10:30AM - 10:40AM Location: E350

Participants

Chiara Pozzessere, MD, Siena, Italy (*Presenter*) Nothing to Disclose Xiangyu Zhu, Baltimore, MD (*Abstract Co-Author*) Nothing to Disclose Celia P. Corona-Villalobos, MD, Baltimore, MD (*Abstract Co-Author*) Nothing to Disclose Lorenzo Righi, Siena, Italy (*Abstract Co-Author*) Nothing to Disclose Sandra L. Castanos Gutierrez, MD, Baltimore, MD (*Abstract Co-Author*) Nothing to Disclose Fatemeh Sobhani, Baltimore, MD (*Abstract Co-Author*) Nothing to Disclose Neda Rastegar, MD, Baltimore, MD (*Abstract Co-Author*) Nothing to Disclose Li Pan, Baltimore, MD (*Abstract Co-Author*) Nothing to Disclose Ii Pan, Baltimore, MD (*Abstract Co-Author*) Nothing to Disclose

PURPOSE

Liver steatosis is the most common liver disease in Western Countries and it may progress to steatohepatis and cirrhosis. Magnetic Resonance Spectroscopy (MRS) has been shown to strongly correlate with histology in fat quantification. However, MRS has some limitations such as breathing artifact and difficulties in avoiding vessels or bile ducts within the voxel. 3D VIBE-Dixon is a MR sequence which can quantify fat content. The aim of this study was to compare fat quantification of liver using 3D VIBE-DIXON to that using MRS.

METHOD AND MATERIALS

IRB approved this prospective, HIPAA compliant study. Thirty potential liver donors (14 males, 12 females; mean age 38 yo) underwent liver MR, including single voxel MRS, within the right (RL) and left lobe (LL) and axial 3D VIBE-Dixon. Liver biopsy was performed in 8 patients. Fat percentage (FP) was generated by MRS. Two readers blinded to MRS results independently quantified the FP on 3D VIBE-Dixon by drawing a ROI in both lobes in the same locations of the MRS voxels.Lin's concordance correlation was used to assess concordance between MRS and 3D VIBE-Dixon, for the two readers. Intraclass correlation coefficient was used to compare 3D VIBE-Dixon to histology. Inter-observer agreement was calculated. A $p \leq 0.05$ was considered statistically significant.

RESULTS

In the RL, mean FP was 5.8% by MRS, and 4.8% and 4.8% by 3D VIBE-Dixon for readers 1 and 2, respectively, with a strong concordance between the two technique (rho= 0.78 and 0.76 for reader 1 and 2, respectively, p<0.001). In the LL, mean FP was 5.2% by MRS, and 4.2% and 4% by 3D VIBE DIXON for readers 1 and 2, respectively, with medium concordance between the two sequences (rho=0.44 and 0.38 for readers 1 and 2, respectively). Inter-observer agreement was excellent in both RL and LL (rho=0.96 and 0.92, respectively, p<0.001). In the 8 patients who underwent biopsy FP by 3D VIBE-DIXON highly correlated to histological results (ICC=0.85).

CONCLUSION

In this prospective study, fat quantification using 3D VIBE-DIXON was highly reproducible, with strong correlation to MRS in the RL. Correlation was moderate in the LL, probably due to artifacts on MRS.

CLINICAL RELEVANCE/APPLICATION

3D VIBE-DIXON is a highly reproducible MR sequence, which may allow non-invasive fat quantification in the liver. Further studies with larger cohort and pathology comparison are required.

Honored Educators

Presenters or authors on this event have been recognized as RSNA Honored Educators for participating in multiple qualifying educational activities. Honored Educators are invested in furthering the profession of radiology by delivering high-quality educational content in their field of study. Learn how you can become an honored educator by visiting the website at: https://www.rsna.org/Honored-Educator-Award/

Ihab R. Kamel, MD, PhD - 2015 Honored Educator

Adults

Thursday, Dec. 3 10:40AM - 10:50AM Location: E350

Participants

William Haufe, San Diego, CA (Presenter) Nothing to Disclose Curtis N. Wiens, PhD, Madison, WI (Abstract Co-Author) Nothing to Disclose Catherine A. Hooker, BS, San Diego, CA (Abstract Co-Author) Nothing to Disclose Tanya Wolfson, MS, San Diego, CA (Abstract Co-Author) Nothing to Disclose Alan B. McMillan, Madison, WI (Abstract Co-Author) Nothing to Disclose Paul Manning, MSc, La Jolla, CA (Abstract Co-Author) Nothing to Disclose Kang Wang, PhD, San Diego, CA (Abstract Co-Author) Nothing to Disclose Scott B. Reeder, MD, PhD, Madison, WI (Abstract Co-Author) Institutional research support, General Electric Company Institutional research support, Bracco Group Michael S. Middleton, MD, PhD, San Diego, CA (Abstract Co-Author) Consultant, Allergan, Inc Institutional research contract, Bayer AG Institutional research contract, sanofi-aventis Group Institutional research contract, Isis Pharmaceuticals, Inc Institutional research contract, Johnson & Johnson Institutional research contract, Synageva BioPharma Corporation Institutional research contract, Takeda Pharmaceutical Company Limited Stockholder, General Electric Company Stockholder, Pfizer Inc Institutional research contract, Pfizer Inc Claude B. Sirlin, MD, San Diego, CA (Abstract Co-Author) Research Grant, General Electric Company; Speakers Bureau, Bayer AG;

Consultant, Bayer AG;;

PURPOSE

To assess the inter-site reproducibility of 2D magnetic resonance elastography (MRE) analysis for hepatic stiffness in obese adults

METHOD AND MATERIALS

In this HIPAA compliant, IRB approved study, obese (BMI \ge 30 kg/m²) adults underwent 2D MRE on a 1.5T or 3.0T GE scanner at one of two sites. A passive driver produced 60 Hz acoustic shear waves through the liver, and MRE-generated wave images, magnitude images, and stiffness maps (elastograms) were transferred offline for manual analysis. Analysts at each of the two separate sites evaluated all exams from both sites. Analysts drew regions of interest (ROIs) on the elastograms in areas of the liver where parallel wave propagation was observed on the corresponding wave image. From these ROIs, stiffness values were recorded. Weighted average was applied to obtain a single per-liver stiffness value. Bland-Altman plot and intraclass correlation coefficient (ICC) were used to assess inter-site reproducibility. Paired t-test was used to examine systematic shifts.

RESULTS

87 adults (74 female, 13 male) underwent MRE. The mean (± standard deviation) age and BMI were 48.3 (± 12.5) years and 42.6 (± 5.8) kg/m2 respectively. Fourteen scans were considered unanalyzable by at least one of the two sites due to low signal-tonoise or poor wave propagation. Hence, data from 73 subjects were used in reproducibility analyses. ICC for the two sites was .833 [0.724, 0.898]. Mean (± standard deviation) stiffness values for site A and site B were 2.90 (± 1.06 kPa) and 3.13 (±1.15 kPa) respectively. A small, clinically non-meaningful, but statistically significant bias was observed (mean difference .23 kPa, paired ttest p=0.0016).

CONCLUSION

MRE analysis for hepatic stiffness from independent analysts at two separate sites had high reproducibility. There was a small systematic bias observed between the two participating study sites, which was not clinically meaningful in the context of staging liver fibrosis.

CLINICAL RELEVANCE/APPLICATION

In order for 2D MRE to be clinically useful in the staging of hepatic fibrosis, liver stiffness results must be analyst and site independent. Studies such as this will help demonstrate the reproducibility of MRE stiffness values.

sSQ06-03 ¹H-Magnetic Resonance Spectroscopy is Superior to Controlled Attenuation Parameter (CAP) in Assessing Liver Fat Content in Human Non-alcoholic Fatty Liver Disease (NAFLD)

Thursday, Dec. 3 10:50AM - 11:00AM Location: E350

Awards

Trainee Research Prize - Resident

Participants

Jurgen H. Runge, MD, PhD, Amsterdam, Netherlands (Presenter) Nothing to Disclose Loek P. Smits, MD, MSc, Amsterdam, Netherlands (Abstract Co-Author) Nothing to Disclose Joanne Verheij, Rotterdam, Netherlands (Abstract Co-Author) Nothing to Disclose Aart N. Nederveen, PhD, Amsterdam, Netherlands (Abstract Co-Author) Nothing to Disclose U Beuers, Amsterdam, Netherlands (Abstract Co-Author) Nothing to Disclose Jaap Stoker, MD, PhD, Amsterdam, Netherlands (Abstract Co-Author) Research Consultant, Robarts Clinical Trials

PURPOSE

Non-alcoholic fatty liver disease (NAFLD) is an increasingly recognized health problem worldwide. Liver biopsy is the diagnostic standard, but liver fat content is preferably assessed noninvasively and quantitatively. Recently, the Controlled Attenuation Parameter (CAP) technique was introduced on the FibroScan®, a transient elastography device with FDA approval since 2013. Only limited data are available regarding CAP's accuracy compared to established quantitative measures. Therefore, we prospectively compared CAP and 1H-Magnetic Resonance Spectroscopy (1H-MRS) derived fat fractions (FF) against liver biopsy in a cohort of patients with NAFLD.

METHOD AND MATERIALS

Forty NAFLD patients (M/F: 29/11) with median (IQR) age of 52.6 (48.5-57.3) and BMI of 27.1 (25.4-33.1) were included in this IRB-approved study. Same-day 3T MRI and CAP measurement were performed by a single examiner within 27 (17-50) days of liver biopsy, assessed by a single pathologist. ¹H-MRS derived FF and CAP values were compared between Brunt steatosis grades S0-S3 using Kruskall-Wallis and Mann-Whitney-U tests. Correlations were assessed with Spearman's. Diagnostic accuracies of CAP and FF to identify \geq S1 on biopsy were compared with ROC analyses.

RESULTS

Median FF differed (p<0.0001) between all histological steatosis grades at 1.0%(0.7-1.4), 6.1%(3.9-8.8), 17.4%(11.3-21.1) and 26.3%(25.0-30.1). Median CAP only differed between grades S0 and S2 (p=0.025) and S1 and S2 (p=0.006) at 260 dB/m (221-320), 281 dB/m (249-331), 330 dB/m (305-378) and 348 dB/m (321-353). FF (rs 0.90;95%-CI:0.81-0.95) correlated better (P=0.0002) with steatosis grades than CAP (rs 0.53;95%-CI:0.25-0.73). The area under the ROC curve (AUROC) to identify \geq S1 was higher (P=0.04) for ¹H-MRS at 0.98 (95%-CI:0.93-1.0) than for CAP at 0.76 (95%-CI:0.56-0.95). Optimal cut-off values of 4.1% and 261 dB/m resulted in sensitivity/ specificity/positive/negative predictive values of 89%/100%/100%/56% for ¹H-MRS and 89%/60%/ 94%/43% for CAP.

CONCLUSION

¹H-MRS derived FF differed between all four steatosis grades on biopsy, while CAP did not. Better correlation with histological features and superior AUROC to identify steatosis stage \geq S1 reaffirm ¹H-MRS as preferred method for noninvasive liver fat content assessment.

CLINICAL RELEVANCE/APPLICATION

¹H-MRS derived liver fat fractions show better diagnostic accuracy than CAP values for accurate noninvasive liver fat content assessment.

SSQ06-04 Assessment of Liver and Pancreas Iron Overload with a 3T MRI Multiecho GRE Sequence in Diffuse Liver Disorders: Rorrelation with Serum Ferritin and Liver Biopsy

Thursday, Dec. 3 11:00AM - 11:10AM Location: E350

Participants

Manuela Franca, MD, Porto, Portugal (*Presenter*) Nothing to Disclose Angel Alberich-Bayarri, MD, Valencia, Spain (*Abstract Co-Author*) Nothing to Disclose Luis Marti-Bonmati, MD, PhD, Godella, Spain (*Abstract Co-Author*) Nothing to Disclose Graca Porto, Porto, Portugal (*Abstract Co-Author*) Nothing to Disclose Helena Pessegueiro Miranda, Porto, Portugal (*Abstract Co-Author*) Nothing to Disclose Joao A. Oliveira, Porto, Portugal (*Abstract Co-Author*) Nothing to Disclose Francisca E. Costa, MD, Porto, Portugal (*Abstract Co-Author*) Nothing to Disclose Jose Ramon Vizcaino Vazquez, Porto, Portugal (*Abstract Co-Author*) Nothing to Disclose

PURPOSE

Iron overload is associated with hereditary hemochromatosis, chronic transfusions, hemolytic conditions and diffuse liver diseases such as chronic hepatitis C, alcoholic liver disease and NAFLD. Pancreatic iron can be also found in some of these conditions. Our objective was to assess $R2^*$ values of the liver and pancreas in patients with chronic diffuse liver diseases, comparing the $R2^*$ values with serum ferritin levels and liver biopsy.

METHOD AND MATERIALS

A total of 99 consecutive patients with chronic diffuse liver disorders who underwent liver biopsy and abdominal MR examination were included. The 3T MR examination included a single breath-hold multiecho GRE sequence with 12 echoes. Iron related-R2* quantification was performed with a dedicated software selecting a ROI within the biopsied liver segment and also in the pancreas (head, body and tail). Liver biopsy was used as gold standard for liver iron deposits grading (0-4).

CONCLUSION

There is an excellent relationship between liver R2*-iron quantification against liver biopsy and serum ferritin, in different chronic liver disorders. Pancreas R2* is significantly correlated with serum ferritin, liver R2* and histologic iron grading.

CLINICAL RELEVANCE/APPLICATION

In patients with diffuse chronic liver disorders, pancreas R2* correlate with liver R2* and biopsy-proved liver iron overload.

SSQ06-05 Liver Volume-assisted Estimation of Liver Function Based on Gd-EOB-DTPA- enhanced MR-Relaxometry

Thursday, Dec. 3 11:10AM - 11:20AM Location: E350

Awards

RSNA Country Presents Travel Award

Participants

Michael Haimerl, Regensburg, Germany (*Presenter*) Nothing to Disclose Niklas Verloh, Regensburg, Germany (*Abstract Co-Author*) Nothing to Disclose Claudia Fellner, MD, PhD, Regensburg, Germany (*Abstract Co-Author*) Nothing to Disclose Marcel D. Nickel, Erlangen, Germany (*Abstract Co-Author*) Employee, Siemens AG Christian R. Stroszczynski, MD, Regensburg, Germany (*Abstract Co-Author*) Nothing to Disclose Philipp Wiggermann, Regensburg, Germany (*Abstract Co-Author*) Nothing to Disclose

PURPOSE

To determine whether liver function as determined by indocyanine green (ICG) clearance can be estimated quantitatively from gadoxetic acid (Gd-EOB-DTPA)-enhanced magnetic resonance (MR)- Relaxometry and to estimate the impact of liver liver volumes.

METHOD AND MATERIALS

132 patients underwent an ICG clearance test and Gd-EOB-DTPA-enhanced MRI, including MR-Relaxometry at 3 Tesla. A transverse

3D VIBE sequence with an inline T1 calculation was acquired prior to and 20 minutes post-Gd-EOB-DTPA administration. Volumetric analysis of respective livers was performed on Aquarius iNtuition Viewer (TeraRecon Inc.). The reduction rate of T1 relaxation time (rrT1) between pre- and post-contrast images and the liver volume-assisted index of T1 reduction rate (LVrrT1) were evaluated. The plasma disappearance rate of ICG (ICG-PDR) was correlated with the liver volume (LV), rrT1 and LVrrT1, providing an MRI-based estimated ICG-PDR value (ICG-PDRest).

RESULTS

Regression model showed a significant log-linear correlation of ICG-PDR with LV (r = 0.31; p = 0.001), T1post (r = 0.62; p < 0.001) and rT1 (r = 0.85; p < 0.001). Assessment of LV and consecutive evaluation of multiple linear regression model revealed a stronger log-linear correlation of ICG-PDR with LVrrT1 (r = 0.91; p < 0.001), allowing for the calculation of ICG-PDRest.

CONCLUSION

Liver function as determined using ICG-PDR can be estimated quantitatively from Gd-EOB-DTPA-enhanced MR-Relaxometry. Volumeassisted MR-Relaxometry has a stronger correlation with liver function than does MR-Relaxometry.

CLINICAL RELEVANCE/APPLICATION

Global and regional liver function may be visualized by Gd-EOB-DTPA-enhanced MRI, which might be of importance for planning liver resections.

SSQ06-06 Liver Volume Predicts the Clinical Outcome of Patients with Decompensated Alcoholic Steatohepatitis

Thursday, Dec. 3 11:20AM - 11:30AM Location: E350

Participants

Maxime Ronot, MD, Clichy, France (*Abstract Co-Author*) Nothing to Disclose Romain Breguet, MD, Geneva, Switzerland (*Abstract Co-Author*) Nothing to Disclose Catrina Hansen, Geneve, Switzerland (*Abstract Co-Author*) Nothing to Disclose Christoph D. Becker, MD, Thonex, Switzerland (*Abstract Co-Author*) Nothing to Disclose Laurent Spahr, Geneve, Switzerland (*Abstract Co-Author*) Nothing to Disclose Sylvain Terraz, MD, Geneva, Switzerland (*Abstract Co-Author*) Nothing to Disclose Matthieu Lagadec, MD, Clichy, France (*Presenter*) Nothing to Disclose

PURPOSE

To evaluate the prognostic value of abdominal multidetector computed tomography (MDCT) in patients with decompensated alcoholic steatohepatitis (ASH).

METHOD AND MATERIALS

This ancillary study was based on the analysis of data collected during a randomized trial on ASH treatment. Response to treatment was defined as the improvement of the baseline MELD score \geq 3 points at 3 months. All patients underwent contrast-enhanced MDCT of the abdomen. The following parameters were measured: 1/ liver (DL) and spleen (DS) density on unenhanced images, and DL/DS ratio, 2/ liver volume-to-body weight ratio (VLBW), 3/ subcutaneous fat (FSC), visceral fat (FV) and muscular (M) surfaces at the level of L3-L4. Responders and non-responders were compared with uni-, multivariate and ROC analyses. Results were compared with a validation cohort of patients, clinically and biologically similar to the study cohort.

RESULTS

Fifty-eight patients (34 males; mean age, 56 years) were analyzed, including 34 (59%) responders. Baseline mean MELD and ABIC scores were 19 (13-28) and 8.3 (6.5-10.3). On multivariate analysis, VLBW (OR=3.73; 95%CI, 1.64-8.46; p=0.002) and FSC (OR=1.01; 95%CI, 1.00-1.02; p=0.022) were associated with response to treatment, with AUROC curves of 0.78±0.06 (p<0.001) and 0.66±0.07 (p=0.043), respectively. BMI, baseline MELD and ABIC scores, gender, DL/DS, FV and M were not different between the two groups. VLBW \geq 2.4% predicted response with 88% and 63% sensitivity and specificity. In the validation cohort (n=24, 75% responders), the same cut-off value predicted response with 83% and 67% sensitivity and specificity.

CONCLUSION

In patients suffering from decompensated ASH, the liver volume appears to be a major positive prognostic factor. This simple morphometric parameter may be added to the initial evaluation of the liver disease to improve patient management.

CLINICAL RELEVANCE/APPLICATION

The liver volume-to-body weight ratio appears to be a major prognostic factor in patients with ASH. This morphometric parameter could be added to the initial workup of patients, to better predict the response to treatment and improve the management.

SSQ06-07 MRI Based Quantification of Hepatic Uptake and Excretion of Gadoxetic Acid: Preliminary Results

Thursday, Dec. 3 11:30AM - 11:40AM Location: E350

Participants

Daniel Truhn, MD, Cologne, Germany (*Presenter*) Nothing to Disclose Alexander Ciritsis, Aachen, Germany (*Abstract Co-Author*) Nothing to Disclose Nienke L. Hansen, MD, Aachen, Germany (*Abstract Co-Author*) Nothing to Disclose Alexandra Barabasch, MD, Aachen, Germany (*Abstract Co-Author*) Nothing to Disclose Burkhard Maedler, Bonn, Germany (*Abstract Co-Author*) Nothing to Disclose Burkhard Maedler, Bonn, Germany (*Abstract Co-Author*) Researcher, Koninklijke Philips NV Christiane K. Kuhl, MD, Bonn, Germany (*Abstract Co-Author*) Nothing to Disclose Nils A. Kraemer, Aachen, Germany (*Abstract Co-Author*) Nothing to Disclose

PURPOSE

Recent research in liver MRI has shown that quantification of hepatic uptake of gadoxetic acid is a promising method for determination of local liver function and correlates well with established clinical measures of liver function. The aim of this study was to evaluate a method for combined measurement of hepatic uptake and excretion.

METHOD AND MATERIALS

After intravenous administration of gadoxetic acid, signal enhancement of liver tissue in 14 healthy patients was measured over the time course of 30 minutes. First, the data was assessed using previously published methods that do not consider excretion. Then, a dual inlet two compartment model was appended by a parameter describing the excretion of contrast medium into the bile. A least squares fit was performed to extract the following parameters: extra- and intracellular volume fraction, uptake and excretion rates, arterial and portal venous flow fractions. Results for the models without and with consideration of excretion were subsequently compared.

RESULTS

The dual inlet two compartment model provided the best agreement between modeled and measured signal values when compared to previously published methods that do not consider excretion of contrast agent. The mean value for the uptake rate in healthy liver tissue was 4.76+-0.54 /100/min. Excretion half-time was 21.9+-2.4 min.Inter-patient variance was significantly greater when conventional models (uptake only) models were applied. We found a significant deviation between modeled and measured signal values with an uptake rate of 3.56+-1.34 /100/min. Excretion rates could only be obtained with the dual inlet two compartment model.

CONCLUSION

The model not considering the excretion was only valid in the first 5 minutes of hepatic signal enhancement and failed over the course of 30 minutes. Accurate modeling of gadoxetic acid induced hepatic enhancement over a longer time course requires a dual inlet two compartment model. Including this parameter into models of liver tissue might lead to a more precise correlation between hepatic function and MRI.

CLINICAL RELEVANCE/APPLICATION

When aiming to measure hepatic function using MRI not only the hepatic uptake, but also the excretion should be taken into account to get better correlations between MRI and liver function.

SSQ06-08 The Attenuation Distribution Across the Long Axis (ADLA): Evaluation of Predictive Performance in a Large Clinical Trial

Thursday, Dec. 3 11:40AM - 11:50AM Location: E350

Awards

Trainee Research Prize - Medical Student

Participants Nikita Lakomkin, Nashville, TN (*Presenter*) Nothing to Disclose Allison Hainline, Nashville, TN (*Abstract Co-Author*) Nothing to Disclose Hakmook Kang, Nashville, TN (*Abstract Co-Author*) Nothing to Disclose M. S. Hutson, Nashville, TN (*Abstract Co-Author*) Nothing to Disclose Carlos L. Arteaga, Nashville, TN (*Abstract Co-Author*) Nothing to Disclose Richard G. Abramson, MD, Nashville, TN (*Abstract Co-Author*) Consultant, ICON plc;

PURPOSE

Novel methods of image feature analysis may be a useful adjunct to standard methods of cancer treatment response assessment. The attenuation distribution across the long axis (ADLA) is a simple, easily extractable measure of lesion heterogeneity; in a recent preliminary study, ADLA measurements predicted overall survival (OS) better than RECIST 1.1. The purpose of this study was to evaluate the ability of the ADLA method to predict OS in a larger clinical trial.

METHOD AND MATERIALS

Under a data sharing agreement from Genentech (San Francisco, CA) and an IRB waiver from our institution, we obtained deidentified imaging and clinical data from RIBBON-1, a multi-site phase 3 trial of bevacizumab (Avastin) in metastatic breast cancer. We analyzed all RIBBON-1 patients treated with Avastin who had at least 1 liver metastasis measuring \geq 15 mm on baseline contrast-enhanced CT. For each patient at every time point, up to 2 target liver lesions were evaluated using both RECIST 1.1 criteria and ADLA. The ADLA was obtained as the standard deviation of the post-contrast CT attenuation values in the portal venous phase across a long-axis diameter function. To define a treatment response using ADLA, Brier scores were computed to establish the optimal percent decrease for separating patients with longer OS. Using Kaplan-Meier survival analysis, the log-rank test was then used to evaluate the ability of a treatment response by ADLA measurements to predict OS. The ADLA method was then compared to RECIST 1.1 using a bootstrapping technique that generated 95% confidence intervals on the Brier scores for both approaches.

RESULTS

165 patients met inclusion criteria. Median OS was 461 days (range 60-916). The ADLA method discriminated patients with longer OS at an optimal threshold of a 21.5% decrease from baseline. At this threshold, a treatment response by the ADLA method successfully separated patients with longer OS (p<0.001). Furthermore, a treatment response by ADLA was superior to a response by RECIST 1.1 for discriminating patients with longer OS (95% confidence interval for the Brier score difference: [0.070-0.52]). Kaplan-Meier survival curves are shown below.

CONCLUSION

In retrospective data analysis from a large clinical trial, the ADLA method was superior to RECIST 1.1 for predicting overall survival.

CLINICAL RELEVANCE/APPLICATION

The ADLA measurement is an easily extractable parameter that may be useful for assessing cancer treatment response.

SSQ06-09 Differences of Target Lesion Selection Drives Variability of Response Assessment According to RECIST 1.1

Awards RSNA Country Presents Travel Award

Participants

Yunus Alparslan, Aachen, Germany (*Presenter*) Nothing to Disclose Jonas Schmoe, Aachen, Germany (*Abstract Co-Author*) Nothing to Disclose Hanna Witte, Aachen, Germany (*Abstract Co-Author*) Nothing to Disclose Annika Keulers, MD, Aachen, Germany (*Abstract Co-Author*) Nothing to Disclose Christiane K. Kuhl, MD, Bonn, Germany (*Abstract Co-Author*) Nothing to Disclose Sebastian Keil, MD, Aachen, Germany (*Abstract Co-Author*) Nothing to Disclose

PURPOSE

To conduct a prospective systematic analysis of factors contributing to variability of response classification in RECIST1.1 beyond factors related to disease measurement, i.e. variability that persists even if dedicated software for response assessment is used.

METHOD AND MATERIALS

63 patients (60 \pm 9 years) underwent a total 132 contrast-enhanced CT studies for initial staging or follow-up after systemic chemotherapy. A target or non-target lesion satisfying RECIST1.1 criteria could be identified in 52/63 patients (82.5%) and 113/132 (85.6%) of (re-)staging CT studies. Data were independently interpreted by three radiologists with > 4 years of experience who used specialized software (MintMedical) for standardized response assessment. Response was classified in complete or partial response (CR, PR), or stable or progressive disease (SD, PD), and stratified as progressive (PD) vs. non-progressive (CR, PR, SD).

RESULTS

Overall, readers agreed in terms of response classification in 58.4% of studies (66/113) and disagreed in 41.6% (47/113). In 50/113 studies, readers had chosen the same, and in 63/113 studies, readers had chosen different target lesions. Selection of the same target lesions was associated with an 88% rate (44/50) of agreement; selection of different target lesions was associated with a 74.6% rate (47/63) of disagreement. After dichotomizing response classes according to their therapeutic implication in PD vs. non-PD RECIST1.1 response classes, disagreement was observed in 17/113 staging examinations (15%). In 13 of these 17 patients (76.5%), readers had chosen different target lesions.

CONCLUSION

The basic assumption of standardized response assessment is that different readers should yield the same response classification for a given patient. In fact, however, different readers disagree in almost half of patient cases, and in 15%, they disagree even with regards to the basic distinction between PD vs. non-PD. Major source of variability appears to be the fact that different readers may choose different target lesions. The resulting variability between readers will not be compensated for by software tools for automated response assessment.

CLINICAL RELEVANCE/APPLICATION

Even with standardized RECIST readings and use of dedicated automated software, different radiologists will yield different results with regards to response classification, even with regards to broadly different categories (PD vs. non-PD).

Hot Topic Session: Molecular Neuroimaging in Dementia: State-of-the-Art and Emerging Techniques

Thursday, Dec. 3 3:00PM - 4:00PM Location: E350



FDA Discussions may include off-label uses.

Participants

Satoshi Minoshima, MD, PhD, Salt Lake City, UT (*Moderator*) Royalties, General Electric Company; Consultant, Hamamatsu Photonics KK; Research Grant, Hitachi, Ltd; Research Grant, Nihon Medi-Physics Co, Ltd; Research Grant, Astellas Group; Research Grant, Seattle Genetics, Inc;

Alexander Drzezga, MD, Cologne, Germany (*Moderator*) Research Grant, Eli Lilly and Company; Speakers Bureau, Siemens AG; Speakers Bureau, General Electric Company; Speakers Bureau, Piramal Enterprises Limited; Research Consultant, Eli Lilly and Company; Research Consultant, Piramal Enterprises Limited; ; ; ; ; ;

Sub-Events

SPSH52A Potential of Amyloid Imaging versus MRI in the Diagnostic Workup of Dementia

Participants

Clifford R. Jack JR, MD, Rochester, MN (Presenter) Stockholder, Johnson & Johnson; Research Consultant, Eli Lilly and Company; ;

LEARNING OBJECTIVES

1) Explain the utility of structural MRI and amyloid PET in characterizing the pattern of neurodegeneration and pathologic involvement in dementia syndromes. 2) Identify the advanced MRI techniques that provide information on disease pathophysiology in dementia. 3) Discuss cases for which MRI and amyloid PET would provide critical information for clinical assessment.

ABSTRACT

Development of molecular imaging agents for fibrillar β -amyloid (A β) positron emission tomography (PET), brought molecular imaging of Alzheimer's disease (AD) pathology into the spotlight. Large cohort studies with longitudinal follow-up in cognitively normal, mild cognitive impairment and AD patients indicate that A β deposition can be detected many years, even decades before the onset of symptoms with molecular imaging and its progression can be followed longitudinally. The role of molecular imaging in AD clinical trials is growing rapidly especially in an era when preventive interventions are designed towards eradicating the pathology targeted by molecular imaging agents. The utility of A β PET in differential diagnosis of AD is greatest when there is no pathologic overlap between the two dementia syndromes such as in frontotemporal lobar degeneration and AD. However A β PET alone may be insufficient in distinguishing dementia syndromes that commonly have overlapping A β pathology, such as dementia with Lewy bodies and vascular dementia, which represent the two most common dementia pathologies after AD. MRI is recommended during the initial evaluation of dementia, in order to determine potentially treatable causes such as tumors, subdural hematoma or normal pressure hydrocephalus. In addition, presence and extent of cerebrovascular disease, which may contribute to cognitive impairment and dementia, can be determined during this initial MRI evaluation. Pattern of structural MRI changes reflect neurodegenerative pathology and are closely associated with the clinical disease severity in AD. Although A β deposition is the most common pathologic process observed in dementia patients, other pathologic processes such as loss of neuronal integrity and connectivity can be measured with the advanced MRI techniques and complement A β PET.

URL

SPSH52B Imaging Inflammation and Molecular Pathology in Dementia

Participants

Ana M. Catafau, MD, PhD, Barcelona, Spain, (ana.catafau@piramal.com) (Presenter) Employee, Piramal Imaging GmbH

LEARNING OBJECTIVES

1) Explain potential clinical applications of different molecular pathology PET tracers. 2) List different targets for neuroinflammation PET imaging. 3) Describe advantages and disadvantages of different PET targets for neuroinflammation imaging. 4) Identify challenges for the development of molecular pathology tracers for neurodegenerative disorders.

ABSTRACT

Clinical classifications of neurodegenerative disorders are often based on neuropathology. The term "proteinopathies" includes disorders that have in common abnormal proteins as a hallmark, e.g. amyloidoses, tauopathies, synucleopathies, ubiquitinopathies. Different proteins can also co-exist in the same disease. To further complicate the pathophysiology scenario, not only different proteins, but also cells are believed to play an active role in neurodegeneration, in particular those participating in neuroinflammatory processes in the brain, such as activated microglia and astrocytes. In clinical practice, differentiating pathophysiology from clinical symptoms to allow accurate clinical classification of these disorders during life, becomes difficult in absence of biomarkers for these pathology hallmarks. PET imaging can be a useful tool in this context. Using PET tracers targeting misfolded proteins it will be possible to identify the presence or absence of the target, to depict the cerebral distribution and to quantify the protein load in different cerebral regions, as well as to monitor changes over time. Beta-amyloid is one of the proteins involved in neurodegenerative disorders, which is currently suitable to be imaged by means of PET. Research efforts are currently ongoing in order to identify new PET tracers targeting non-amyloid PET tracers for neurodegeneration. This presentation will focus on the investigational PET tracers targeting tau and alpha-synuclein as misfolded proteins, and activated microglia and astrocytes as cellular targets for neuroinflammation.

SPSH52C Tau Imaging. Scientific Tool or Diagnostic Biomarker?

Participants

Jonathan E. McConathy, MD, PhD, Saint Louis, MO (*Presenter*) Research Consultant, Eli Lilly and Company; Research Consultant, Blue Earth Diagnostics Ltd; Research Consultant, Siemens AG; Research support, GlaxoSmithKline plc

LEARNING OBJECTIVES

1) Participants will be familiar with the current status of PET tracers targeting tau that are being used in human research studies and understand their potential roles in therapeutic trials and clinical neuroimaging.

ABSTRACT

Imaging biomarkers for Alzheimer's disease (AD) and other neurodegenerative diseases are playing an increasingly important role in both research and patient care. Abnormal deposition of the tau and beta-amyloid proteins are pathologic hallmarks of AD, and several PET tracers targeting tau are now available for human research studies. The optimal use and sequencing of imaging biomarkers in the evaluation of cognitive impairment and dementia are active areas of investigation. In this presentation, current and potential future applictions of tau-PET will be discussed in the context of both research studies and possible clinical applications.

Imaging Tumor Response: Old and New Challenges

Thursday, Dec. 3 4:30PM - 6:00PM Location: S102AB

BQ MR OI

AMA PRA Category 1 Credits ™: 1.50 ARRT Category A+ Credits: 1.50

Participants

Sub-Events

RC718A Reporting Cancer Response-Practical Perspective

Participants

Elena K. Korngold, MD, Portland, OR (Presenter) Nothing to Disclose

LEARNING OBJECTIVES

1) Define important terms and concepts in tumor response assessment. Describe the current use of imaging for evaluating response of GI cancers. 2) Understand the rationale for the creation of standardized and structured criteria for imaging evaluation of tumor response to therapy in research trials. 3) Understand the basic concept and organization of the RECIST (Response Evaluation Criteria in Solid Tumors) criteria. Understand the limitations of RECIST and other standardized reporting methods. 4) Recognize the reason for use of alternate criteria in specific diseases (i.e., Cheson for lymphoma, EASL/mRECIST for HCC), biomarkers, and the evolving role of imaging in evaluation of tumor response with novel therapeutic interventions.

RC718B Prostate Cancer Treatment Assessment

Participants

Hedvig Hricak, MD, PhD, New York, NY (Presenter) Nothing to Disclose

LEARNING OBJECTIVES

1) Understand the clinical challenges of prostate cancer post-treatment follow-up and the role of imaging in detecting local recurrence. 2) Know how MRI protocols for detecting local recurrence should be adjusted depending on the prior treatment and the questions being asked. 3) Understand standard and emerging uses of bone scanning, PET/CT and MRI/PET for detecting metastasis.

ABSTRACT

MRI has emerged as the key modality for assessing local recurrence of prostate cancer after radical prostatectomy (RP) or radiation therapy (RT). Early detection of local recurrence is important to allow potentially curative salvage therapy. The efficacy of MRI in detecting local recurrence is treatment dependent, and MRI protocols need to be adjusted to the questions being asked. After RT, T2-weighted MRI is limited due to post-radiation effects on the prostate such as glandular shrinkage, loss of normal zonal anatomy, and reduced contrast between cancer and normal tissue caused by glandular atrophy and fibrosis. MRI should include both T2weighted and diffusion-weighted sequences; a recent study suggested that in most patients, dynamic contrast-enhanced (DCE)-MRI could be omitted after RT without lowering diagnostic performance, thereby eliminating the risks and costs associated with the use of contrast. If salvage treatment is an option after RT, MRI offers loco-regional staging. Post-RT MRI can evaluate the length of the urethra and may show urethral shortening (which has been associated with incontinence after primary RP), decreased urethral margin definition and other tissue changes that could conceivably affect treatment selection and planning. After surgery, in addition to DWI, the use of DCE-MRI is essential, as it can show small lesions and differentiate tumor from scarring. MRI may help to determine whether post-RP local recurrence is amenable to salvage RT and may aid RT planning. Assessment of recurrence after emerging focal therapies remains problematic, since methods for reliably differentiating necrosis or scarring from tumor are lacking. In the future, PET/CT with targeted tracers may be able to address this need. PET/CT and bone scanning are valuable in the search for nodal and osseous metastases, respectively. The implementation of clinical MRI/PET and the use of new tracers will likely open new horizons in the assessment of recurrence.

RC718C Evaluating Response in Targeted Therapy of Abdominal Malignancy

Participants

Yves M. Menu, MD, Paris, France (Presenter) Nothing to Disclose

LEARNING OBJECTIVES

1) Understand the main challenges in abdominal tumors treated with targeted chemotherapies in clinical situations like neoadjuvant therapy, tumor down staging or palliative treatment. 2) Know the specific situations of most common abdominal malignancies like liver primary and secondary tumors, pancreatic adenocarcinoma and colorectal cancer. 3) Understand how the Radiologist should manage the imaging techniques (CT, MRI, PET) in order to meet the clinical objectives and if targeted therapies require changes over cytotoxic chemotherapies.

ABSTRACT

Abdominal malignancies are very common. Imaging is pivotal for detection, staging and evaluation of tumor response to treatment. As targeted therapies are increasingly administered, the necessity for an update of tumor response criteria has become obvious. Tumor size and anatomy is still required important information, but evaluation of tissue viability is increasingly needed. Another specificity of abdominal malignancies is the increasing number of patients who are candidates for an integrated approach including systemic therapies, local therapies, radiation therapy and surgery. This underlines the necessity of a team approach and the major role of the radiologist within this group. In Hepatocellular Carcinoma (HCC), targeted therapies are widely used and mainly aimed at palliation, although potential downstaging may lead to reconsider this position. mRECIST criteria have been developed specifically for HCC and are considered as the international standard nowadays. In secondary liver tumors, targeted therapies are usually administered in association with cytotoxic drugs. As up to 30% of patients with liver metastases from colon cancer might become resectable, the evaluation is not limited to volumetric response. The report should mention in addition relevant information on tumor viability and aggressiveness and also comment on useful elements for guidance of potential surgery or intervention. In other abdominal advanced malignancies, targeted therapies are not yet standard. However, due to the poor prognosis of these diseases, very active research develops in this field and interestingly favors a better selection of patients. Imaging may play a role with this issue, like classifying locally advanced vs metastatic patients as well as highly vs less agressive tumors. In summary, the Radiologist should have knowledge of the main clinical challenges, of ongoing and potential treatments in order to provide relevant information to the Multi Disciplinary Team.

RC718D Evaluation of Lung Cancer Response

Participants

Jeremy J. Erasmus, MD, Houston, TX (Presenter) Nothing to Disclose

LEARNING OBJECTIVES

1) To understand the applicability of anatomic imaging using World Health Organization (WHO) criteria and Response Evaluation Criteria in Solid Tumors (RECIST 1.1) in the assessment of tumor response in patients with non-small cell lung cancer (NSCLC). 2) To be aware of the limitations of World Health Organization (WHO) criteria and Response Evaluation Criteria in Solid Tumors (RECIST 1.1) in the assessment of tumor response. 3) To understand the potential role of metabolic tumor response assessment with 18F-FDG PET (PET Response Criteria in Solid Tumors (PERCIST)) in patients with NSCLC.

ABSTRACT

NSCLC commonly presents with advanced disease and chemotherapy is often an integral component in;treatment. However, following initiation of chemotherapy, tumor progression can occur in up to 33% of patients. Early determination of this therapeutic failure can be important in management and can assist clinical decisions concerning discontinuation of ineffective treatment and institution of alternative therapy. Additionally, an essential component of evaluating the results of cancer treatment in patients on clinical trials is the reporting of the response rate. Because small differences in the response rate can affect the outcome clinical trials, it is important that the criteria used to make this determination are meaningful and consistent. While the antitumor effect of a treatment in patients with solid tumors can be determined clinically or by surgical pathologic re-staging, image-based serial measurements based on WHO criteria or Response Evaluation Criteria in Solid Tumors (RECIST) provide uniform criteria for reporting response. However, morphological alterations detected by CT may not correlate with pathological response and tumor viability. Furthermore, the assessment of objective response has also been complicated by the development of treatment protocols that target tumor biology including tumor cell proliferation and invasion, angiogenesis and metastasis. Anti-tumor effect in many of these regimens is cytostatic and, unlike anticancer cytotoxic agents, may not cause regression in tumor size. FDG-PET may allow an early and sensitive assessment of the effectiveness of anticancer chemotherapy as FDG uptake is not only a function of proliferative activity but is also related to viable tumor cell number. This talk will review the status and limitations of anatomic and metabolic tumor response metrics in NSCLC including WHO criteria, RECIST 1.1 and PET Response Criteria in Solid Tumors (PERCIST).

Honored Educators

Presenters or authors on this event have been recognized as RSNA Honored Educators for participating in multiple qualifying educational activities. Honored Educators are invested in furthering the profession of radiology by delivering high-quality educational content in their field of study. Learn how you can become an honored educator by visiting the website at: https://www.rsna.org/Honored-Educator-Award/

Jeremy J. Erasmus, MD - 2015 Honored Educator

Radiomics Mini-Course: From Image to Radiomics

Thursday, Dec. 3 4:30PM - 6:00PM Location: S404AB

BQ PH

AMA PRA Category 1 Credits ™: 1.50 ARRT Category A+ Credits: 1.50

Participants

Sandy Napel, PhD, Stanford, CA (*Director*) Medical Advisory Board, Fovia, Inc; Consultant, Carestream Health, Inc; Scientific Advisor, EchoPixel, Inc

Sub-Events

RC725A Image Annotation and Semantic Labeling

Participants

Daniel L. Rubin, MD, MS, Palo Alto, CA (Presenter) Nothing to Disclose

LEARNING OBJECTIVES

1) To understand the new Big Data paradigm in Radiology and learn about new tools that can help Radiologists to leverage images more effectively. 2) To become acquainted with the Annotation and Image Markup (AIM) format that makes image metadata (radiologist observations and quantitative image features) machine-accessible. 3) To learn how AIM can support radiology clinical workflow, enable research discovery, support regulatory objectives, facilitate new biomarker development, and improve clinical practice.

ABSTRACT

The Annotation and Image Markup (AIM) format for collecting and storing measurements and other information in images brings tremendous benefits to clinical radiology. AIM standardizes iamge annotations, making the semantic descriptors and quantitative information in images machine-accessible, searchable, and minable. AIM allows more specific and customizable searching of annotations, enabling objective and computable analysis of measurements, and helps clinicians to more easily leverage images in a variety of application such as automated reporting, report summaries, lesion tracking, content based image retrieval, and decision support. AIM also enables trials that collect image measurements, and it facilitates integrating image data with non-image data, such as molecular and clinical data. Finally, by standardizing measurement data and permitting aggregating image annotations across multiple sites, AIM will allow for new imaging biomarker discovery and validation that might lead to better response criteria for use both clinically and in the approval of new medical products. AIM currently underlies an interconnected suite of tools that allows researchers to easily generate minable structured image metadata for research, and it is being used in several national projects and at a variety of institutions nationally.URLs:(a) https://wiki.nci.nih.gov/display/AIM/Annotation+and+Image+Markup++AIM(b) http://epad.stanford.edu

Honored Educators

Presenters or authors on this event have been recognized as RSNA Honored Educators for participating in multiple qualifying educational activities. Honored Educators are invested in furthering the profession of radiology by delivering high-quality educational content in their field of study. Learn how you can become an honored educator by visiting the website at: https://www.rsna.org/Honored-Educator-Award/

Daniel L. Rubin, MD, MS - 2012 Honored Educator Daniel L. Rubin, MD, MS - 2013 Honored Educator

RC725B Image Feature Computation and Considerations

Participants

Sandy Napel, PhD, Stanford, CA (*Presenter*) Medical Advisory Board, Fovia, Inc; Consultant, Carestream Health, Inc; Scientific Advisor, EchoPixel, Inc

LEARNING OBJECTIVES

Learn about processing pipelines that extract features from regions within images. 2) Learn about different classes of features.
 Learn about feature interactions and influence of segmentation.

ABSTRACT

Images can be two-dimensional (2D), 3D, time varying, and/or vector valued (when, e.g., multiple acquisitions of the same volume are acquired). Computation of features from images requires delineation (also called segmentation) of regions or volumes within these multidimensional images, and then applying computer algorithms to the data within these regions to characterize them and, perhaps, their surroundings, with numbers. This session will cover the structure of feature computation pipelines and various factors that influence their outputs. Classes of features include shape (values characterize region boundary smoothness and compactness), margin (values characterize how sharp the transition is from inside to outside the region), and texture (variation of gray values or color within and possibly nearby to the region). In addition, specialized features may be computed when prior research has described important implications of observations (e.g., %-ground glass opacities in lung nodules at CT). It is important to recognize that computed features may be influenced by data acquisition and reconstruction methods (e.g., sharp vs. smooth reconstruction kernels in CT, contrast agent on board, variation in pulse sequences across vendors), aspects of the region they are not designed to characterize (e.g., shape influenced by texture causing segmentation irregularities, histogram statistics influenced by nearby structures (e.g., bone within the segmentation of a lung nodule near a rib). Attention to these details can result in improved utility of extracted features, and more significance in associations of features with other clinical variables.

RC725C Correlating Image Features with Multi-Omics Data

Participants

Olivier Gevaert, PhD, Stanford, CA (Presenter) Nothing to Disclose

LEARNING OBJECTIVES

Understand how to model the relationship between image features and genomic data using univariate and multivariate methods.
 Implement dediciated preprocessing for image feature data and for genomic data, each requiring their own statistical modeling.

ABSTRACT

Vast amounts of molecular data characterizing the genome, epi-genome and transcriptome are becoming available for a wide range of cancers. In addition, new computational tools for quantitatively analyzing medical and pathological images are creating new types of phenotypic data. Now we have the opportunity to integrate the data at molecular and tissue scale to create a more comprehensive view of key biological processes underlying cancer. Moreover, this integration can have profound contributions toward predicting diagnosis and treatment. I will discuss current work in progress to model multi-omics data and how to integrate it with medical imaging data. I will show examples for non-small cell lung cancer and glioblastoma.

Quantitative Measures in Cardiac CT and MR Imaging-Do They Matter?

Friday, Dec. 4 8:30AM - 10:00AM Location: E350

CA BQ CT MR

AMA PRA Category 1 Credits ™: 1.50 ARRT Category A+ Credits: 1.50

FDA Discussions may include off-label uses.

Participants

LEARNING OBJECTIVES

ABSTRACT

Sub-Events

RC803A Quantitative Assessment of the Cardiac Chambers and Its Clinical Significance

Participants

Bernd J. Wintersperger, MD, Toronto, ON, (bernd.wintersperger@uhn.ca) (*Presenter*) Speakers Bureau, Siemens AG; Research support, Siemens AG

LEARNING OBJECTIVES

1) Describe the approach of cardiac MR and CT in assessment of cardiac function and size 2) Understand important differences between varies imaging strategies 3) Understand the impact and role of cardiac size and function on treatment decisions

ABSTRACT

Introduction: Cardiac performance is generally assessed by volumetric quantifications such as size and output. Follow-up and changes over time may allow identification of early disease onset, may trigger specific therapies and may allow prediction of patient prognoses and general outcome. While CT & MR imaging provide more accurate results, echocardiography remains the first line modality. CT for functional evaluation should be considered a 3rd line option based on the added radiation exposure.Methods:Most important measures of cardiac function are end-diastolic volume (EDV), stroke volume (SV) and ejection fraction (EF). While the acoustic window may limit echocardiography, CT & MRI can easily cover all aspects of the atria and ventricles. While results of clinical echocardiography may only allow a categorization of ventricular EF (grade 1-4) with large variations related to assumptions, CT and MRI allow highly accurate results in normal & abnormal ventricles. In order to maintain accuracy and precision adequate imaging parameters with respect to coverage, spatial resolution and temporal resolution are required. Today's functional cardiac MR imaging is based on cine SSFP methods with cardiac short axis orientation for the left ventricle and short axis or transverse orientation for the right ventricle. Atrial volumetric assessment is performed rarely but might especially be of interest in patients with AV valve dysfunction or atrial sources of arrhythmia. While quantitative assessment of regional motion was previously limited to echocardiography or specific MR techniques (e.g. MR tagging), recent software developments also allow this information being derived from standard cine MRI. ConclusionBased on its accuracy cardiac MR plays an increasingly important role in assessment of patients with cardiac diseases. Accurate and precise quantification of cardiac function is increasingly important in therapy decisions and therapy monitoring.

Handout:Bernd J. Wintersperger

http://abstract.rsna.org/uploads/2015/14000904/RSNA 2015 RC803A Quantitative Measures in Cardiac CT and MR Imaging_ Quantitative Assessment of the Cardiac Chambers and Clinical Significance.pdf

RC803B Quantitative Assessment Cardiac Valves on MRI

Participants

Jens Bremerich, MD, Basel, Switzerland, (jens.bremeric@usb.ch) (Presenter) Nothing to Disclose

LEARNING OBJECTIVES

1) Apply CMR for morphometry and quantification of valvular function. 2) Compare various CMR approaches for assessment of cardiac valves. 3) Analyse flow data in stenotic or incompetent valves.

ABSTRACT

Introduction: Echocardiography remains first line modality for imaging cardiac valves. In specific cases, however, MR provides complementary quantitative data. Methods: Most relevant sequences for valve imaging are: 1) Black blood, 2) CineSSFP, and 3) VENCine. Black blood images are fast spin echo sequences. CineSSFP are used for quantification of valvular morphology and motion. Temporal resolution is typically 50ms for a segmented breath hold sequence but may be further shortened by means of parallel imaging or non-breath hold sequences. VENCine is an excellent tool for flow volume and velocity quantification. Volumes are relevant to calculate regurgitant fraction of incompetent valves, velocities are used to calculate degree of stenosis relying on modified Bernoulli equation. Results: Aortic regurgitation is difficult to evaluate with Echocardiography but easily quantified on VENCine with excellent reproducibility. Regurgitant fraction is defined as Volume_{antegrade}/Volume_{retrograde}*100 [%]. Aortic stenosis may also be quantified with MR by measuring the opening area on CineSSFP or by measuring peak velocity in the valve on VENCine and calculation with modified Bernoulli equation ($\Delta P = 4 * Vmax2$). Mitral regurgitation may also be quantified by MRI. Echocardiographic quantification relies predominantely on the extent of the regurgitant jet into the left atrium which is not a reliable sign on MRI, since extent of regurgitant jets depend on various sequence parameters such as field strength and echo time. Pulmonary regurgitation can also be quantified with MRI which is relevant in congenital heart disease such as after surgical repair in tetralogy of Fallot. Pulmonary stenosis, Tricuspid stenosis and regurgitation are no routine indications for MRI but are rather evaluated by echocardiography. Conclusion: Aortic regurgitation is an excellent indication for MRI, it enables accurate and

reproducible quantification.

RC803C How to Quantify Valve Function on Cardiac CT

Participants

Paul Schoenhagen, MD, Cleveland, OH, (schoenp1@ccf.org) (Presenter) Nothing to Disclose

LEARNING OBJECTIVES

1) Describe the limited role of CT for assessment of valvular function. 2) Discuss clinical indications where anatomic and functional valvular with CT is indicated. 3) Describe data acquisition and analysis approach for valvular assessment.

ABSTRACT

CT is a predominantly anatomic imaging modality. Compared to predominantly functional modalities its temporal resolution is limited. In addition, functional/4-D imaging requires retrospective gated data acquisition and is associated with higher radiation exposure. The role of CT for functional valvular analysis is therefore limited to few clinical scenarios, where it can provide complementary information. The strength of CT in these situations is the ability for reconstruction in the acquired 3-D/4-D volume. A prominent example is transcatheter valve replacement/implantation but also assessment of prosthetic valves.

URL

Handout: Paul Schoenhagen

http://abstract.rsna.org/uploads/2015/14000907/schoenhagen_RSNA2015 - valve function 11_30.pdf

RC803D 4D Flow MRI Quantification?

Participants

Christopher J. Francois, MD, Madison, WI (Presenter) Research support, General Electric Company

LEARNING OBJECTIVES

1) Describe MRI physics of 4D flow MRI. 2) Illustrate use of 4D flow MRI for basic hemodynamic function. 3) Demonstrate potential futures uses of 4D flow MRI for advanced hemodynamic analyses.

ABSTRACT

MRI flow imaging is based on flow-sensitive, phase contrast sequences. This presentation will introduce the basic MRI physics responsible for imaging flow, extending 1-directional flow imaging to 3-directional flow imaging used in 4D flow MRI.Examples from valvular and congenital heart disease will be used to illustrate the use of 4D flow MRI to quantify flow velocities and volumes. Although 4D flow MRI is still very much in the early developmental phase, published data comparing 4D flow MRI to established techniques for quantifying flow will be reviewed.The future potential for 4D flow MRI to be used to non-invasively quantify more advanced hemodynamic parameters will be demonstrated. Specifically, the use of 4D flow MRI to measure pressure gradients, pulse wave velocity, wall shear stress and kinetic energy will be covered.

Active Handout: Christopher Jean-Pierre Francois

http://abstract.rsna.org/uploads/2015/14000908/RC803D.pdf

The Biology of Breast Cancer

Friday, Dec. 4 8:30AM - 10:00AM Location: S406B

BR BQ

AMA PRA Category 1 Credits ™: 1.50 ARRT Category A+ Credits: 1.50

Participants Sub-Events

RC815A Breast Cancer Genomics

Participants

Cherie M. Kuzmiak, DO, Chapel Hill, NC (Presenter) Research Grant, FUJIFILM Holdings Corporation;

LEARNING OBJECTIVES

1) Understand the molecular classification of breast cancer and comparisont with clinical definitions. 2) Learn some of the main genomic features and clinical and treatment outcomes that stratify with the molecular subtypes.

RC815B Genetic Risk and Cancer Biology with Imaging

Participants

Elizabeth S. Burnside, MD, MPH, Madison, WI (Presenter) Stockholder, NeuWave Medical Inc

LEARNING OBJECTIVES

1) Understand the different types of genetic information that are being measured and used for the clinical care of breast cancer. 2) Convey that cancer development and evolution depends on both genetics and environment influences. 3) Demonstrate that imaging has the potential to better understand biology, capturing the complex combined influence of genetics and environment. 4) Illustrate the move toward personalized medicine in breast cancer and the role of imaging.

ABSTRACT

RC815C Imaging Breast Cancer Subtypes

Participants

Sheryl G. Jordan, MD, Chapel Hill, NC, (Sheryl_jordan@med.unc.edu) (Presenter) Nothing to Disclose

LEARNING OBJECTIVES

1) Master the move beyond classifying breast cancer as DCIS, IDC, ILC, or Other/Rare. 2) Understand imaging features for four breast cancer molecular subtypes, namely luminal A, luminal B, HER2-enriched, and basal subtypes. 3) Recognize molecular subtypes' clinical patterns and outcomes in case-based presentations, to include sufficient length of patient follow-up as to reinforce prognosis.

ABSTRACT

Radiomics Mini-Course: Informatics Tools and Databases

Friday, Dec. 4 8:30AM - 10:00AM Location: S404AB

BQ IN PH

AMA PRA Category 1 Credits ™: 1.50 ARRT Category A+ Credits: 1.50

Participants

Sandy Napel, PhD, Stanford, CA (*Director*) Medical Advisory Board, Fovia, Inc; Consultant, Carestream Health, Inc; Scientific Advisor, EchoPixel, Inc

LEARNING OBJECTIVES

ABSTRACT

Sub-Events

RC825A The Role of Challenges and Their Requirements

Participants

Jayashree Kalpathy-Cramer, MS, PhD, Charlestown, MA (Presenter) Nothing to Disclose

LEARNING OBJECTIVES

1) Understand the role of challenges and benchmarks in image analysis, radiomics and radiogenomics. 2) Learn about challenge infrastructure and requirements to host and participate in challenges. 3) Learn about past and upcoming challenges that focus on topics in radiology, radiomics and radiogenomics.

ABSTRACT

Challenges and benchmarks have been used successfully in a number of scientific domains to make significant advances in the field by providing a common platform for collaboration and competition. By provide a common dataset and common set of evaluation metrics, they also facilitate a fair and rigorous evaluation of algorithms. Challenge organizers often sequester the test data from the training data, further enhancing the rigor of the evalation. These efforts can introduce problems in medical imaging to experts in other domains such as image processing and machine learning and serve as a means to bring in to medical images a range for expertise from other domains. They also serve to allow computer scientists access to clinical data which they may not otherwise have. Many challenges have also highlighted the need for collaboration as the best results are often obtained by combining a range of complementary techniques. We will discuss recent challenges from a number of domains including imaging and bioinformatics, explore the informatics infrastructure to host and participate in challenges and discuss the needs for future challenges including those in radiomics and radiogenomics.

RC825B Quantitative Image Analysis Tools: Communicating Quantitative Image Analysis Results

Participants

Andriy Fedorov, PhD, Boston, MA, (andrey.fedorov@gmail.com) (Presenter) Nothing to Disclose

LEARNING OBJECTIVES

1) Review the meaning and importance of interoperability for quantitative image analysis tools. 2) Review specific use cases motivating standards-based interoperable communication of the analysis results. 3) Learn about free open source tools that can facilitate interoperable communication of analysis results using DICOM standard.

ABSTRACT

Quantitative imaging holds tremendous but largely unrealized potential for objective characterization of disease and response to therapy. Quantitative imaging and analysis methods are actively researched by the community. Certain quantitation techniques are gradually becoming available both in the commercial products and clinical research platforms. As new quantitation tools are being introduced, tasks such as their integration into the clinical or research enterprise environment, comparison with similar existing tools and reproducible validation are becoming of critical importance. Such tasks require that the analysis tools provide the capability to communicate the analysis results using open and interoperable mechanisms. The use of open standards is also of utmost importance for building aggregate community repositories and data mining of the analysis results. The goal of this course is to build the understanding of the interoperability as applied to quantitative image analysis, with the focus on clinical research applications.

Handout: Andriy Fedorov

http://abstract.rsna.org/uploads/2015/15003220/rc825fedorov.pdf

RC825C Public Databases for Radiomics Research: Current Status and Future Directions

Participants

Justin Kirby, Bethesda, MD (Presenter) Stockholder, Myriad Genetics, Inc

LEARNING OBJECTIVES

1) Understand the importance of using digital object identifiers and public databases to facilitate reproducible radiomics research. 2) Become familiar with publicly available databases where you can. a) download existing radiomic and radiogenomic data sets. b) request to upload new radiomic/radiogenomic data sets. 3) Learn about new data-centric journals which help enable researchers to receive academic credit for releasing well-annotated data sets to the public.

ABSTRACT

Lack of reproducibility in scientific research, particularly in healthcare, has become an increasing issue in recent years. The National Insitutes of Health (NIH) and many major publishers have since called for increased sharing of raw data sets so that new findings can be easily validated in a transparent way. This is especially important in the emerging field of radiomics where large data sets and huge numbers of image features lead to an increased risk of spurious correlations which are not actually driven by biology. A number of public databases have since been created by governments and other organizations to help facilitate the sharing of data sets. Publishers have developed new 'data journals' and services specifically designed to encourage researchers to annotate and share their data sets. It is now up to the imaging research community to begin taking advantage of these resources. Other disciplines such as genomics and proteomics are significantly leading imaging in the adoption of these new open-science workflows. Significant engagement with NIH and other organizations providing open databases and related services is critical to enabling imaging researchers to successfully shift to a culture of data sharing and transparency.

Gastrointestinal (New MRI Techniques)

Friday, Dec. 4 10:30AM - 12:00PM Location: E353A

GI MR BQ

AMA PRA Category 1 Credits ™: 1.50 ARRT Category A+ Credits: 1.50

Participants

Vamsi R. Narra, MD, FRCR, Saint Louis, MO (*Moderator*) Consultant, Biomedical Systems; Bobby T. Kalb, MD, Tucson, AZ (*Moderator*) Nothing to Disclose

Sub-Events

SST04-01 Improving the Quality of 2D GRE MR Elastography of Chronic Liver Diseases Using a Shorter, In-Phase Echo Time

Friday, Dec. 4 10:30AM - 10:40AM Location: E353A

Participants

Jin Wang, Rochester, MT (*Presenter*) Nothing to Disclose

Nan Zhang, MS, MD, Beijing, China (Abstract Co-Author) Nothing to Disclose

Jun Chen, PhD, Rochester, MN (*Abstract Co-Author*) The Mayo Clinic and Jun Chen have intellectual property rights and a financial interest in MRE technology.

Kevin J. Glaser, Rochester, MN (Abstract Co-Author) Intellectual property, Magnetic Resonance Innovations, Inc; Stockholder, Resoundant, Inc

Bogdan Dzyubak, PhD, Rochester, MN (Abstract Co-Author) Nothing to Disclose

Roger C. Grimm, MS, Rochester, MN (Abstract Co-Author) Nothing to Disclose

Meng Yin, Rochester, MN (Abstract Co-Author) The Mayo Clinic and MY have intellectual property rights and a financial interest in MRE technology.

Richard L. Ehman, MD, Rochester, MN (Abstract Co-Author) CEO, Resoundant, Inc; Stockholder, Resoundant, Inc; Research Grant, Resoundant, Inc

PURPOSE

The purpose of this study was to validate the improvement in image quality of 2D GRE MR elastography (MRE) using a shorter, inphase echo time (TE) for patients with chronic liver diseases, steatosis, and iron deposition.

METHOD AND MATERIALS

With IRB approval and patient authorization, 308 consecutive patients with clinically indicated chronic liver diseases underwent MRE exams using a 2D GRE MRE sequence on 1.5T. They were randomly separated into 2 groups based on the TE used. Group 1 used an in-phase TE of 18 ms (160/308, 52%) and Group 2 used the current standard TE of 21 ms (148/308, 48%). Hepatic relative fat fraction (RFF) was measured by using a two-point Dixon method. The iron concentration in blood samples analyzed in standard laboratory tests was used to assess the iron deposition in liver. Clinical information collected at the same time as the MRE exam included blood pressures, and pulse rate. The fraction of the acquired liver volume with an MRE inversion-derived confidence level of over 95%, as well as the average SNR within the liver were computed for each patients and compared between the short TE and long TE groups with analysis of variance (ANOVA). The effect of age, gender, BMI, Total.Iron.Bind.Capacity, iron, systolic pressure, diastolic pressure, FOV, TE, fat concentration (%), and pulse rate on SNR and ROI volume were evaluated by a mixed-effect model.

RESULTS

No significant differences were found in epidemiological and etiological parameters between the two groups (P>0.05). The SNR of MRE images in Group 1 was significantly higher than that in Group 2 (23.73 ± 0.61 vs. 18.01 ± 0.63 , p<.0001). ROI volume for reporting hepatic tissue stiffness was significantly larger in Group 1 (323.70 ± 9.36 cm³ vs. 255.53 ± 9.73 cm³, p<.0001). Only TE had a statistically significant effect on SNR (p < .0001); only fat (p<.0001) and iron (p=0.0379) were statistically significant effects on volume.

CONCLUSION

The SNR and reliable ROI volume of 2D GRE MRE can be significantly improved by using a shorter, in-phase TE of 18 ms compared to the current standard of 21 ms.

CLINICAL RELEVANCE/APPLICATION

The quality of 2D GRE MRE can be significantly improved by using a shorter, in-phase TE. A direct measurement of fat and iron disposition in the liver might provide better statistical significance.

SST04-02 Intravoxel Incoherent Motion MR Imaging of the Abdomen: The Effect of Data Fitting Altorithms on the Measurement Repeatability

Friday, Dec. 4 10:40AM - 10:50AM Location: E353A

Participants

Hyojung Park, Seoul, Korea, Republic Of (*Presenter*) Nothing to Disclose Seung Soo Lee, MD, Seoul, Korea, Republic Of (*Abstract Co-Author*) Nothing to Disclose Yu Sub Sung, Seoul, Korea, Republic Of (*Abstract Co-Author*) Nothing to Disclose Hyun Hee Cheong, Seoul, Korea, Republic Of (*Abstract Co-Author*) Nothing to Disclose Yedaun Lee, MD, Busan, Korea, Republic Of (*Abstract Co-Author*) Nothing to Disclose Cheol Mog Hwang, MD, Daejeon, Korea, Republic Of (*Abstract Co-Author*) Nothing to Disclose So Yeon Kim, MD, Seoul, Korea, Republic Of (*Abstract Co-Author*) Nothing to Disclose Moon-Gyu Lee, MD, Seoul, Korea, Republic Of (Abstract Co-Author) Nothing to Disclose

PURPOSE

To evaluate the effect of fitting algorithms and number of b-values on the measurement repeatability of intravoxel incoherent motion(IVIM) parameters of the abdominal organs.

METHOD AND MATERIALS

The institutional review board approved the study protocol, and informed consent was obtained. Twelve healthy volunteers(M:F = 6:6; mean age, 30 years) underwent navigator-triggered DWI twice on an 1.5T system using nine different b values (0,30,60,100,150,200,400,600,900). DWI data were processed using full-biexponential fitting algorithm which estimates slow diffusion(Ds), fast diffusion(Df), and perfusion fraction(f) simultaneously and using segmented fitting algorithm which estimates Ds with higher b-value(≥ 200) data and subsequently estimates f and Df. IVIM parameters were measured on the right lobe of the liver, spleen, pancreas, right renal cortex, and right renal medulla on each set of IVIM parameters over two repeated by full-biexponential and segmented fitting algorithms. Measurement repeatability of IVIM parameters over two repeated scans were evaluated using the within-subject coefficient of variation(wCV).

RESULTS

For all abdominal organs and two fitting algorithms, Df showed the poorest repeatability(the range of wCV, 29.5%-144.1%) among IVIM parameters(wCV for Ds, 4.1%-16.9%; wCV for f, 8.5% -46.2%). For spleen, pancreas, renal medulla, segmented fitting resulted in better repeatability of Ds(wCV, 4.9%-11.9% vs. 8.0%-16.9%) and f(wCV, 8.5%-37.9% vs. 17.3% - 46.2%) than full-biexponential fitting. For liver, full-biexponential fitting resulted in better repeatability of all IVIM parameters(wCV, 4.1%, 29.5%, and 9.7% for Ds, Df, and f, respectively) than segmented fitting(wCV, 4.8%, 43.0%, 12.8% for Ds, Df, and f, respectively). For renal cortex, the measurement repeatability of Ds was better with full-biexponential fitting, but that of f was better with segmented fitting.

CONCLUSION

Df is not a reliable parameter for the evaluation of abdominal organs. Despite some inconsistent results across different organs, segmented fitting algorithm generally results in better repeatability of Ds and f than full-biexponential fitting algorithm.

CLINICAL RELEVANCE/APPLICATION

Segmented fitting is a preferred fitting algorithm for IVIM analysis of abdominal organs.

SST04-03 Fast Advanced Spin Echo Diffusion-Weighted Imaging in the Abdomen

Friday, Dec. 4 10:50AM - 11:00AM Location: E353A

Participants

Takeshi Yoshikawa, MD, Kobe, Japan (*Abstract Co-Author*) Research Grant, Toshiba Corporation Yoshiharu Ohno, MD, PhD, Kobe, Japan (*Presenter*) Research Grant, Toshiba Corporation; Research Grant, Koninklijke Philips NV; Research Grant, Bayer AG; Research Grant, DAIICHI SANKYO Group; Research Grant, Eisai Co, Ltd; Research Grant, Terumo Corporation; Research Grant, Fuji Yakuhin Co, Ltd; Research Grant, FUJIFILM Holdings Corporation; Research Grant, Guerbet SA; Katsusuke Kyotani, RT, Kobe, Japan (*Abstract Co-Author*) Nothing to Disclose Yoshimori Kassai, MS, Otawara, Japan (*Abstract Co-Author*) Employee, Toshiba Corporation Hisanobu Koyama, MD, PhD, Kobe, Japan (*Abstract Co-Author*) Nothing to Disclose Keitaro Sofue, Kobe, Japan (*Abstract Co-Author*) Nothing to Disclose Kouya Nishiyama, Kobe, Japan (*Abstract Co-Author*) Nothing to Disclose Kazuro Sugimura, MD, PhD, Kobe, Japan (*Abstract Co-Author*) Nothing to Disclose Kazuro Sugimura, MD, PhD, Kobe, Japan (*Abstract Co-Author*) Nothing to Disclose Kazuro Sugimura, MD, PhD, Kobe, Japan (*Abstract Co-Author*) Nothing to Disclose

PURPOSE

To assess values of Fast Advanced Spin Echo (FASE)-diffusion-weighted imaging in evaluation of abdominal diseases

METHOD AND MATERIALS

Fifty-two patients (32 men and 20 women, mean: 69.4 years), who were suspected to have hepato-biliary-pancreatic malignancy and underwent 3T-MRI, were enrolled. FSE-T2WI, SE-EPI-DWI (b=1000), and FASE-DWI (600) were obtained in all patients. Amount of abdominal gas and ascites on images was recorded for each patient using a 5-point scale. Anteroposterior (AP) and right-to-left (RL) abdominal diameters were measured on the slice with most severe image distortion and diameters of the right upper liver near the diaphragm were measured for each sequence and each patient, and correlation analyses were performed. Overall image quality and severity of image distortion were visually assessed using a 5-point scale on EPI-DWI and FASE-DWI, and compared. Regression analyses were done to estimate factors for low image quality and severe distortion. Malignant lesion (n=39) conspicuity was visually assessed separately on EPI-DWI and FASE-DWI, and compared. Diagnostic confidence levels were compared between EPI-DWI alone and EPI-DWI+FASE-DWI sets.

RESULTS

Correlation coefficient was the highest between T2WI and FASE-DWI for all the diameters, indicating less image distortion on FASE-DWI. Lower correlation coefficients, indicating more severe distortion, were observed in abdominal AP direction and right liver RL direction on EPI-DWI. Image distortion was significantly more severe on EPI-DWI (p<0.0001). There was no significant difference between overall image quality and malignant lesion conspicuity. Age, sex, and gas were found to be significant factors for image quality on EPI-DWI (0.047, 0.004, 0.018), and sex and AP diameter were significant factors for image quality on FASE-DWI (0.005, 0.043). Diagnostic confidence level for malignant lesion was significantly higher on EPI-DWI +FASE-DWI set (0.022).

CONCLUSION

FASE-DWI can provide additional diagnostic information in evaluation of various abdominal diseases and be used as an alternative to EPI-DWI.

CLINICAL RELEVANCE/APPLICATION

FASE-DWI can provide additional diagnostic information in evaluation of various abdominal diseases and be used as an alternative to

EPI-DWI.

SST04-04 Techniques to Generate High-accuracy Computed Diffusion-weighted Images (cDWIs) of the Liver

Friday, Dec. 4 11:00AM - 11:10AM Location: E353A

Participants Toru Higaki, PhD, Hiroshima, Japan (Presenter) Nothing to Disclose Yuko Nakamura, MD, Bethesda, MD (Abstract Co-Author) Nothing to Disclose Yuji Akiyama, Hiroshima, Japan (Abstract Co-Author) Nothing to Disclose Tatsuya Ohkubo, Otawara, Japan (Abstract Co-Author) Employee, Toshiba Corporation Yoshimori Kassai, MS, Otawara, Japan (Abstract Co-Author) Employee, Toshiba Corporation Kazuo Awai, MD, Hiroshima, Japan (Abstract Co-Author) Research Grant, Toshiba Corporation; Research Grant, Hitachi, Ltd; Research Grant, Bayer AG; Research Grant, DAIICHI SANKYO Group; Medical Advisor, DAIICHI SANKYO Group; Research Grant, Eisai Co, Ltd; Research Grant, Nemoto-Kyourindo; ; ; ; ;

Yoshiko Iwakado, Hiroshima, Japan (Abstract Co-Author) Nothing to Disclose

Background

Computed diffusion-weighted images (cDWIs) are virtual DWIs calculated from actual DWIs using two arbitrarily selected low bvalues. cDWI is advantageous because images can be generated on MR scanners that do not allow the acquisition of high b-value DWIs. cDWI can also reduce the scan time and lower the image noise when DWIs are acquired with routinely-used b-values. However, the image quality of cDWIs may be degraded without adequate image processing. We propose techniques to generate high-accuracy cDWIs.

Evaluation

Six healthy volunteers (4 males, 2 females, age 31-52 years) underwent hepatic MRI on a 3T MR scanner (Vantage Titan 3T, Toshiba Medical Systems, Tokyo, Japan). We obtained 21 DWIs at b-values raised at 50 s/mm2 (from 0 to 1000 s/mm2). We developed software to generate cDWIs via plug-in into NIH ImageJ (http://www.nih.gov/ij/). cDWIs at b=1000 were generated from various combinations of input b-values and the optimal combination was determined quantitatively. We applied some preprocessing as this can reduce artifacts or image noise. One method was non-rigid image registration of DWIs with two input b-values. The other used an image filter to remove abnormal values from the ADC map. Images generated with/without preprocessing were evaluated qualitatively.

Discussion

For the input image of low b-value, we employed image with b=150 because effect of micro-perfusion which strongly arises at b=0 is disappeared at b=150. Quantitative comparisons between cDWIs and actual DWIs obtained at b=1000 showed that the fewest errors in signal intensity were recorded when the combination of input b-values was 150 and 600. Qualitative comparisons revealed that the image quality of the proposed cDWIs obtained with non-rigid image registration and image filtering was superior to that of conventional cDWIs (see attached figures).

Conclusion

When generating cDWIs at b=1000 sec/mm2, the optimal combination of b-values for the cDWI input was b=150 and 600. The proposed preprocessing techniques, non-rigid image registration, and image filtering contributed to the improved image quality of cDWIs.

SST04-05 Accuracy of MR-determined Hepatic Proton Density Fat Fraction (PDFF) and Histology-determined Fat Fraction for Estimation of Triglyceride Concentration in Twenty-one Ex-vivo Human Livers

Friday, Dec. 4 11:10AM - 11:20AM Location: E353A

Participants

Kevin A. Zand, MD, San Diego, CA (Abstract Co-Author) Nothing to Disclose Elhamy R. Heba, MBBCh, MD, San Diego, CA (Presenter) Nothing to Disclose Tanya Wolfson, MS, San Diego, CA (Abstract Co-Author) Nothing to Disclose Amol Shah, MD, La Jolla, CA (Abstract Co-Author) Nothing to Disclose Gavin Hamilton, PhD, San Diego, CA (Abstract Co-Author) Nothing to Disclose Michael Peterson, San Diego, CA (Abstract Co-Author) Nothing to Disclose Lisa Clark, MPH, PhD, San Diego, CA (Abstract Co-Author) Nothing to Disclose Anthony Gamst, PhD, San Diego, CA (Abstract Co-Author) Nothing to Disclose Michael S. Middleton, MD, PhD, San Diego, CA (Abstract Co-Author) Consultant, Allergan, Inc Institutional research contract, Bayer AG Institutional research contract, sanofi-aventis Group Institutional research contract, Isis Pharmaceuticals, Inc Institutional research contract, Johnson & Johnson Institutional research contract, Synageva BioPharma Corporation Institutional research contract, Takeda Pharmaceutical Company Limited Stockholder, General Electric Company Stockholder, Pfizer Inc Institutional research contract, Pfizer Inc Jeffrey B. Schwimmer, MD, San Diego, CA (Abstract Co-Author) Nothing to Disclose

Claude B. Sirlin, MD, San Diego, CA (Abstract Co-Author) Research Grant, General Electric Company; Speakers Bureau, Bayer AG; Consultant, Bayer AG;;

PURPOSE

To assess the accuracy of magnetic resonance (MR)-determined hepatic proton density fat fraction (PDFF) and histologydetermined fat fraction (histology-FF) for estimation of triglyceride concentration ([TG]) in ex-vivo human liver using biochemicallydetermined liver [TG] as a reference standard.

METHOD AND MATERIALS

Twenty-one postmortem whole livers were obtained from the National Disease Research Interchange and scanned at 3T using a cardiac coil within 48 hours of death. Donors $(31 - 67 \text{ [mean } 55 \pm 11 \text{] yrs}; 11 \text{ female})$ had or were at risk for hepatic steatosis based on medical history. Five 1.5-cm radius circular locations were selected in each specimen. Unenhanced two-dimensional axial spoiled gradient-recalled-echo images of the specimens were obtained. Using published MR techniques, MR spectroscopy (MRS), magnitude-based MRI (M-MRI), and complex-based MRI (C-MRI) hepatic PDFF estimations were computed at each location. Six

biopsies were also obtained at each location (thirty biopsies per liver): three for histologic analysis to determine histology-FF and three for biochemical analysis to determine [TG]. The average of [TG] at each location was used as a reference standard for that location. Regression analyses were performed for [TG] versus MRS-PDFF, M-MRI-PDFF, C-MRI-PDFF, and histology-FF. R²'s with bootstrap-based bias-corrected, accelerated 95% confidence intervals were computed and served as metrics of accuracy. Pairwise comparisons of the R²'s were performed using bootstrap-based tests to adjust for within-liver dependence.

RESULTS

MRS-PDFF, M-MRI-PDFF, C-MRI-PDFF, histology-FF and [TG] of liver specimens ranged from 0.1 - 23.5%, -7.4 - 26.3%, 1.3 - 21.2%, 0 - 70 %, and 1.2 - 31.3 mg/100g respectively. The R²'s from the regression models between [TG] and MRS-PDFF, M-MRI-PDFF, C-MRI-PDFF, and histology-FF were 0.95 (0.86 - 0.98), 0.90 (0.62 - 0.97), 0.92 (0.55 - 0.99), and 0.92 (0.78 - 0.94) respectively. The differences between R²'s were not statistically significant (all p>0.05).

CONCLUSION

In this ex-vivo study, using biochemically-determined liver [TG] as a reference standard, MR-determined hepatic PDFF and histology were accurate for estimation of hepatic [TG].

CLINICAL RELEVANCE/APPLICATION

This study helps to validate the MR-determined hepatic PDFF as an accurate biomarker of hepatic steatosis.

SST04-06 Multiecho Single Voxel Spectroscopy and 3-D GRE MR Based Estimation of Liver Fat Correlates Well with Dichotomized Histologic Steatosis Grades

Friday, Dec. 4 11:20AM - 11:30AM Location: E353A

Participants

Sonal Krishan, MD, Gurgaon, India (Presenter) Nothing to Disclose

PURPOSE

To evaluate the diagnostic performance of Multiecho Single voxel spectroscopy and 3-D GRE sequences in predicting dichotomised histologic steatosis grades.

METHOD AND MATERIALS

This prospective, IRB approved, HIPAA-compliant single-center study was conducted in 71 consecutive adults who also had simultaneous liver biopsy. MR imaging fat fraction was estimated at 1.5 T by using T1-VIBE low-flip-angle multiecho gradient-recalled-echo imaging with T2* correction and multipeak modeling as well as multiecho single voxel spectroscopy. Steatosis was graded histologically on a semi-quantitative scale as the percentage of hepatocytes with macrovesicular steatosis (grades 0:5%, 1:5-10%, 2:10-20%, and 3:>20%). Sensitivity, specificity, and binomial confidence intervals were calculated for proposed MR imaging fat percentage threshold.

RESULTS

The proposed MR imaging fat fraction threshold of 5% to diagnose grade 1 or higher steatosis had 88% sensitivity (95% confidence interval [CI]: 83, 93) and 89% specificity (95% CI: 78, 100). The diagnostic performance to diagnose grade 2 or higher steatosis had 84% sensitivity (CI: 74, 94) and 92% specificity (95% CI: 85, 99). Accuracy to diagnose grade 3 steatosis had 81% sensitivity (95% CI: 71, 91) and 90% specificity (95% CI: 83, 97).

CONCLUSION

The fat fraction thresholds provided high sensitivity and specificity for diagnosis of grade 1 or higher, grade 2 or higher, and grade 3 steatosis. More clinical and longitudnal studies are now needed to further validate these high-specificity thresholds for inclusion in the clinical practise.

CLINICAL RELEVANCE/APPLICATION

MR based evaluation of liver fat fraction is an accurate technique across all histologic grades of hepatic steatosis.

SST04-07 Feasibility of Magnetic Resonance Elastography for the Pancreas

Friday, Dec. 4 11:30AM - 11:40AM Location: E353A

Participants

Yohei Ito, MD, Hamamatsu, Japan (*Presenter*) Nothing to Disclose Yasuo Takehara, MD, Hamamatsu, Japan (*Abstract Co-Author*) Nothing to Disclose Toshihiro Kawase, Kakegawa, Japan (*Abstract Co-Author*) Nothing to Disclose Kenichi Terashima, Tokyo, Japan (*Abstract Co-Author*) Nothing to Disclose Yoshihisa Ohkawa, Kakegawa, Japan (*Abstract Co-Author*) Nothing to Disclose Yuko Hirose, Hmamatsu, Japan (*Abstract Co-Author*) Nothing to Disclose Yuko Hirose, Hmamatsu, Japan (*Abstract Co-Author*) Nothing to Disclose Ai Koda, Hamamatsu, Japan (*Abstract Co-Author*) Nothing to Disclose Naoko Hyodo, Hamamatsu, Japan (*Abstract Co-Author*) Nothing to Disclose Takasuke Ushio, Hamamatsu, Japan (*Abstract Co-Author*) Nothing to Disclose Yuki Hirai, MD, Hamamatsu, Japan (*Abstract Co-Author*) Nothing to Disclose Nobuko Yoshizawa, MD, Hamamatsu, Japan (*Abstract Co-Author*) Nothing to Disclose Shuhei Yamashita, MD, Hamamatsu, Japan (*Abstract Co-Author*) Nothing to Disclose Hatsuko Nasu, Hamamatsu, Japan (*Abstract Co-Author*) Nothing to Disclose Hatsuko Nasu, Hamamatsu, Japan (*Abstract Co-Author*) Nothing to Disclose Naoki Ooishi, Hamamatsu, Japan (*Abstract Co-Author*) Nothing to Disclose Hatsuko Nasu, Hamamatsu, Japan (*Abstract Co-Author*) Nothing to Disclose Naoki Ooishi, Hamamatsu, Japan (*Abstract Co-Author*) Nothing to Disclose Naoki Ooishi, Hamamatsu, Japan (*Abstract Co-Author*) Nothing to Disclose Harumi Sakahara, MD, Hamamatsu, Japan (*Abstract Co-Author*) Nothing to Disclose

PURPOSE

The purposes are three-folds, 1) to assess the usefulness of elastic belt bracing the upper abdomen for reducing the miscalculated areas (cross-hatches) of the pancreas on the stiffness map of MR elastography (MRE), 2) to establish the stiffness of normal

pancreas in normal subjects and 3) to investigate the feasibility of MRE in differentiating between normal pancreas and the focal pancreatic diseases.

METHOD AND MATERIALS

First, 8 normal volunteers were examined with MRE with or without elastic belt. On the stiffness map, the pancreatic areas with or without cross-hatches were measured by drawing the region of interest and were compared between MRE with and without belt. Second, 14 normal volunteers were examined with MRE with elastic belt for the measurements of normal pancreas stiffness. Third, consecutive 11 adult patients suspected of having pancreatic lesions underwent MR examination at 3.0T including MRE with elastic belt for the assessment of the lesion stiffness. A spin-echo based echo planar MRE utilized MEG of 80Hz, external driver frequency/amplitude of 60Hz/50% and temporal phase of 6.

RESULTS

The median percentages of measurable areas of pancreatic stiffness of 8 normal volunteers were 57.4 % with elastic belt and 35.3 % without the belt (p = 0.0078). The mean stiffness of the pancreatic areas of the 14 normal volunteers was 2.37 ± 0.16 kPa for the head, 2.46 ± 0.17 kPa for the body, 2.58 ± 0.26 kPa for the tail and 2.47 ± 0.11 kPa for the overall area. Of 11 patients, 8 patients were diagnosed as having solid pancreatic lesions consisted of 7 pancreatic cancers and 1 inflammatory pseudotumor. The mean stiffness of 7 pancreatic cancers was 6.06 ± 0.49 kPa that was significantly higher than normal pancreatic stiffness. The mean stiffness of inflammatory pseudotumor was 6.2 kPa and it was also higher than normal pancreatic parenchyma.

CONCLUSION

With elastic belt, miscalculation of the pancreatic stiffness was reduced. MRE implicates its potential to differentiate between normal pancreas and pancreatic diseases namely desmoplastic pancreatic lesions.

CLINICAL RELEVANCE/APPLICATION

With improved accuracy with elastic belt, MRE shows a potential to differentiate between normal pancreatic parenchyma and desmoplastic pancreatic lesion based on the stiffness value.

SST04-08 Balanced Steady State Free Precession Sequences for Efficient 3D Whole Organ Liver Iron Content Determination Using MRI: Proof of Principle

Friday, Dec. 4 11:40AM - 11:50AM Location: E353A

Participants

Arthur P. Wunderlich, PhD, Ulm, Germany (*Presenter*) Nothing to Disclose Stefan A. Schmidt, Ulm, Germany (*Abstract Co-Author*) Nothing to Disclose Holger Cario, Ulm, Germany (*Abstract Co-Author*) Nothing to Disclose Meinrad J. Beer, MD, Wuerzburg, Germany (*Abstract Co-Author*) Research Consultant, Shire plc

PURPOSE

Current MRI based methods for determining liver iron content (LIC) suffer from multiple restrictions, one of them incomplete liver coverage. 3D balanced steady state free precession (bSSFP) has the potential to overcome this limitation, but was not yet tested for 3D LIC analysis.

METHOD AND MATERIALS

34 patients (8f, 26m, age 23 \pm 12.9 y) suspected for liver iron overload were investigated by 1.5 T MRI (Siemens Avanto, Siemens Healthcare, Iselin, NY). To reduce banding artefacts, shim volume was placed over the liver. A transversal volume was acquired with bSSFP using the whole-body resonator as receiver coil with flip angle (FA) of 7, 10, 17 and 30 and TR/TE 3.5/1.75 ms. Acquisition was performed in free breathing with 3 long-term averages at matrix size 192x192x20 yielding a resolution of 2.2x2.2x4 mm in 35 s acquisition time per FA. Liver-to-muscle signal intensity ratio (SIR) and its uncertainty was calculated by manually placing ROIs in artefact-free liver parenchyma and paraspinal muscles. Results were correlated to LIC determined by Ferriscan® as reference method.

RESULTS

3D whole liver coverage was possible in 27/34 patients. Liver was imaged without visible artefacts in 30/34 patients.SIR uncertainty was below 10% in all FA except 30°, where it remained below 15%. Correlation was best for SIR vs. logarithm of reference LIC at 30° FA with $R^2 = 0.815$.

CONCLUSION

bSSFP is known as MRI sequence with highest efficiency, capable of contiguous 3D acquisition. Short TR/TE allow for whole organ coverage, and high SNR is useful for LIC determination at low uncertainty. Free breathing was chosen because it has the potential of reducing pulsation artefacts by long-term averaging, and is useful in sedated and uncooperative patients. However, bSSFP is prone to susceptibility artefacts, which we handled to a stage of invisibility by shim optimisation in most patients. Probably invisible banding caused only moderate correlation. Results are promising, even with the simple SIR approach. Increasing scan length in head-feet direction will allow for coverage of the entire liver in all patients at the cost of slightly longer measurement times. Quantitative analysis to evaluate tissue T2 is under way, however, challenging due to inhomogeneous liver tissue.

CLINICAL RELEVANCE/APPLICATION

Whole-organ MRI based contiguous 3D LIC determination using the efficient bSSFP sequence is a promising new approach. However, optimization is needed.

ssT04-09 Magentic Resonance Performance in Quantifying Activity of Small Bowel Crohn's Disease

Friday, Dec. 4 11:50AM - 12:00PM Location: E353A

Participants Michal M. Amitai, Ramat Gan, Israel (*Abstract Co-Author*) Nothing to Disclose Eyal Klang, Ramat Gan, Israel (*Presenter*) Nothing to Disclose Shomron Ben-Horin, Ramat Gan, Israel (*Abstract Co-Author*) Nothing to Disclose Doron Yablecovitch, Ramat Gan, Israel (*Abstract Co-Author*) Nothing to Disclose Adi Lahat, Ramat Gan, Israel (*Abstract Co-Author*) Nothing to Disclose Sandra Neuman, Ramat Gan, Italy (*Abstract Co-Author*) Nothing to Disclose Noa Rozendorn, Ramat Gan, Israel (*Abstract Co-Author*) Nothing to Disclose Nina Levhar, Ramat Gan, Israel (*Abstract Co-Author*) Nothing to Disclose Uri Kopylov, Ramat Gan, Israel (*Abstract Co-Author*) Nothing to Disclose Rami Eliakim, Ramat Gan, Israel (*Abstract Co-Author*) Nothing to Disclose

PURPOSE

Magnetic Resonance Index of Activity (MaRIA), is a Magnetic Resonance Enterogrpahy (MRE)-based score in the evaluation of distal small bowel and colonic Crohn's disease. The gold standard for quantifying mucosal inflammation is with capsule endoscopy either by Lewis score (LS) or, Capsule Endoscopy Crohn's Disease Activity Index (CECDAI). The aim of this study was to compare the quantification of distal small bowel inflammation using MRE, capsule endoscopy and inflammatory markers.

METHOD AND MATERIALS

Patients with small bowel Crohn's disease in clinical remission or mild symptoms (CDAI<220) were prospectively recruited and underwent MRE and capsule endoscopy, after approval by our institutional review board and signing an informed consent.MaRIA, LS and CECDAI scores were calculated for the distal small bowel. C-reactive protein (CRP) and fecal calprotectin (FCP) levels were evaluated in association with the clinical scores.

RESULTS

Active inflammation was detected in 47/56 patients. A significant correlation was demonstrated between MaRIA and capsule endoscopy scores. The correlation between the MaRIA and either the LS and CECDAI was similar (r=0.51, p=0.0001 and r=0.54, p=0.0001, respectively). The mean MaRIA score was significantly lower in patients with mucosal healing, defined as LS<135 (18.8±10.7 vs 10.7±7.1, p=0.002). CRP did not correlate with either MaRIA or capsule endoscopy indices. FCP demonstrated stronger correlation with the MaRIA (r=0.49, p=0.0001) in comparison to capsule endoscopy scores (r=0.36, p=0.007 and r=0.45, p=0.001 for LS and CECDAI, respectively).

CONCLUSION

Significant correlation was observed between quantitative MRE and capsule endoscopy based indices of inflammation in the distal small bowel. FCP correlated better with MRE than with capsule endoscopy scores.

CLINICAL RELEVANCE/APPLICATION

The MaRIA score can be used to non-invasively quantify distal small bowel Crohn's disease, and thus help guide clinical decisions regarding prognosis and treatment.

Neuroradiology/Head and Neck (New Techniques in Head and Neck Imaging)

Friday, Dec. 4 10:30AM - 12:00PM Location: N227



Gaurang V. Shah, MD, Ann Arbor, MI (Moderator) Nothing to Disclose

Sub-Events

SST10-01 Using Semi-quantitative Dynamic Contrast-enhanced Magnetic Resonance Imaging Parameters to Evaluate Tumor Hypoxia: A Preclinical Feasibility Study in a Maxillofacial VX2 Rabbit Model

Friday, Dec. 4 10:30AM - 10:40AM Location: N227

Participants

Lin-Feng Zheng, MD, PhD, Shanghai, China (*Presenter*) Nothing to Disclose Yujie Li, Shanghai, China (*Abstract Co-Author*) Nothing to Disclose Zhuoli Zhang, MD, PhD, Chicago, IL (*Abstract Co-Author*) Nothing to Disclose Gui-Xiang Zhang, MD, Shanghai, China (*Abstract Co-Author*) Nothing to Disclose

PURPOSE

To test the feasibility of semi-quantitative dynamic contrast-enhanced magnetic resonance imaging (DCE-MRI) parameters for evaluating tumor hypoxia in a maxillofacial VX2 rabbit model.

METHOD AND MATERIALS

Eight New Zealand rabbits were inoculated with VX2 cell solution to establish a maxillofacial VX2 rabbit model. DCE-MRI were carried out using a 1.5 Tesla scanner. Semi-quantitative DCE-MRI parameters, maximal enhancement ratio (MER) and slope of enhancement (SLE), were calculated and analyzed. The tumor samples from rabbits underwent hematoxylin-eosin (HE), pimonidazole (PIMO) and vascular endothelial growth factor (VEGF) immunohistochemistry (IHC) staining, and the PIMO area fraction and VEGF IHC score were calculated. Spearman's rank correlation analysis was used for statistical analysis.

RESULTS

The MER values of eight VX2 tumors ranged from 1.132 to 1.773 (1.406 ± 0.258) and these values were negatively correlated with the corresponding PIMO area fraction (p = 0.0000002), but there was no significant correlation with the matched VEGF IHC score (p = 0.578). The SLE values of the eight VX2 tumors ranged from 0.0198 to 0.0532 s-1 (0.030 ± 0.011 s-1). Correlation analysis showed that there was a positive correlation between SLE and the corresponding VEGF IHC score (p= 0.0149). However, no correlation was found between SLE and the matched PIMO area fraction (p = 0.662). The VEGF positive staining distribution predominantly overlapped with the PIMO adducts area, except for the area adjacent to the tumor blood vessel.

CONCLUSION

The semi-quantitative parameters of DCE-MRI, MER and SLE allowed for reliable measurements of the tumor hypoxia, and could be used to noninvasively evaluate hypoxia during tumor treatment.

CLINICAL RELEVANCE/APPLICATION

This preclinical feasibility study shows that DCE-MRI could serve as a potentially non-invasive and translational tool for tumor pathophysiological feature evaluation in clinical practice.

SST10-02 Improved Image Quality in Head and Neck CT Using a 3D Iterative Approach to Reduce Metal Artifacts

Friday, Dec. 4 10:40AM - 10:50AM Location: N227

Participants

Wolfgang Wust, MD, Erlangen, Germany (Presenter) Speakers Bureau, Siemens AG

Michael M. Lell, MD, Erlangen, Germany (*Abstract Co-Author*) Research Grant, Siemens AG; Speakers Bureau, Siemens AG; Research Grant, Bayer AG; Speakers Bureau, Bayer AG; Research Consultant, Bracco Group; ;

Michael Uder, MD, Erlangen, Germany (*Abstract Co-Author*) Speakers Bureau, Bracco Group; Speakers Bureau, Siemens AG; Research Grant, Siemens AG;

Matthias S. May, Erlangen, Germany (Abstract Co-Author) Speakers Bureau, Siemens AG

PURPOSE

Metal artifact from dental fillings and other devices degrades image quality and may compromise the CT detection and evaluation of lesions in the oral cavity and oropharynx. The aim of this study was to evaluate the effect of iterative metal artifact reduction (IMAR) on CT of the oral cavity and oropharynx.

METHOD AND MATERIALS

Data from 50 consecutive patients with metal artifact from dental hardware were reconstructed with standard filtered backprojection (FBP), linear interpolation metal artifact reduction (MAR) and IMAR. The image quality of slices containing metal was analyzed for the severity of artifacts and diagnostic value.

RESULTS

A total of 455 slices, 9.1±4.1 slices per patient, contained metal and were evaluated with each reconstruction method. Slices without metal were not affected by the algorithms and demonstrated identical image quality. 38% of the slices were considered nondiagnostic with FBP, 31% with MAR, but only 7% with IMAR. 33% of slices had poor image quality with FBP, 46% with MAR, and 10% with IMAR. 13% of slices with FBP, 17% with MAR and 22% with IMAR were of moderate, 16% of slices with FBP, 5% with MAR and 30% with IMAR were of good and 1% of slices with MAR and 31% with IMAR of excellent image quality.

CONCLUSION

IMAR yields the highest image quality in comparison to FBP and MAR in patients with metal hardware in the head and neck area.

CLINICAL RELEVANCE/APPLICATION

The 3D iterative approach to metal artifact reduction can significantly improve the imaging of the head and neck region whenever dental hardware might disturb clinical imaging.

SST10-03 Role of Arterial Spin Labelling in Characterizing Skull-Base Lesions

Friday, Dec. 4 10:50AM - 11:00AM Location: N227

Participants

Nadya Pyatigorskaya, Paris, France (*Presenter*) Nothing to Disclose Stephanie Trunet, MD, Paris, France (*Abstract Co-Author*) Nothing to Disclose Sophie Gerber, Paris, France (*Abstract Co-Author*) Nothing to Disclose Bruno Law-Ye, JD, Paris, France (*Abstract Co-Author*) Nothing to Disclose Melika Sahli Amor, Paris, France (*Abstract Co-Author*) Nothing to Disclose Samia Belkacem, MD, Paris, France (*Abstract Co-Author*) Nothing to Disclose Peggy Bienvenot, MD, Paris, France (*Abstract Co-Author*) Nothing to Disclose Damien P. Galanaud, MD, PhD, Paris, France (*Abstract Co-Author*) Nothing to Disclose Delphine Leclercq, MD, Paris, France (*Abstract Co-Author*) Nothing to Disclose

PURPOSE

Classical dynamic susceptibility-contrast MRI (DSC-MRI) is a challenging technique in studying the skull base because of the airinterface artefacts. This work was aimed at investigating whether the pseudo-continuous Arterial Spin Labeling (pcASL)-MRI perfusion method can be used to adequately evaluate tumor perfusion of skull base tumors, as well as evaluating the diagnostic value of characterizing tumors by the ASL method.

METHOD AND MATERIALS

Forty-eight patients with skull baselesions were retrospectively enrolled. The lesions found were meningiomas (n=10), schwannomas (n=4), paragangliomas (3), chondrosarcoma (1), plasmocytomas (4), metastatic lesions (4), parotid lesions (4), epidermoid carcinomas (5), pituitary adenomas (5), cholesteatoma (1), hemangioblastoma (1), lymphoma (1), cystic lesions (3), and infections (2). Relative Tumor Blood Flow (rTBF) was calculated based on the pcASL data. Two expert neuroradiologists analyzed all the images. PcASL imaging was correlated to the pathology results for the lesions that underwent surgical resection (33), to other post-contrast enhancement perfusion methods (9), to the lesion morphology, and to follow up results (10). The normalized rTBF values for the lesions in the same anatomical region were compared, at the significant level set to p<0.05.

RESULTS

The pcASL method allowed characterizing all the enrolled lesions. Moreover, there was a significant rTBF difference between cerebellopontine angle schwannoma and meningioma and between schwannoma and metastasis. For pituitary lesions, there was a significant difference between pituitary adenoma and meningioma. For jugular foramen region, there was a significant difference between paraganglioma, chondrosarcoma, and cholesteatoma.Interestingly, one case of osteomyelitis, showed a pseudotumoral increased rTBF, and a plasmocytoma under treatment, showed low rTBF, in relation with treatment response.

CONCLUSION

The present preliminary study shows the interest of pcASL-MRI in evaluating tumor perfusion in the tumors that are located in the skull-base region. Moreover, pcASL can be helpful in the differential diagnosis of the tumors in this region without using contrast materials.

CLINICAL RELEVANCE/APPLICATION

This study shows that pcASL-MRI can be a powerful tool for detecting and characterizing skull-base lesions; it can be easily implemented in clinical practice.

SST10-04 Feasibility and Preliminary Experience of Quantitative T2 Star Mapping in the Differentiation of Benign and Malignant Thyroid Nodules in Comparison with Diffusion-weighted Imaging

Friday, Dec. 4 11:00AM - 11:10AM Location: N227

Participants

Lianming Wu, Shanghai, China (Presenter) Nothing to Disclose

PURPOSE

To investigate the feasibility of T2 star relaxation time for distinguishing benign from malignant thyroid node in comparison with diffusion-weighted (DW) imaging.

METHOD AND MATERIALS

A total of 56 consecutive patients (43 women and 13 men; age range, 23-76 years; mean [+SD] age, 51+12.3 years) with thyroid nodules, who were referred for fine-needle aspiration biopsy by endocrinology or general surgery clinics, were prospectively underwent 3.0T magnetic resonance imaging by using a multi-echo T2 star and DW imaging (maximum b value, 800 sec/mm2).

Parametric maps were obtained for apparent diffusion coefficient (ADC) and T2 star value. Two radiologists reviewed these maps and measured ADC and T2 star value. Data were analyzed by using mixed-model analysis of variance and receiver operating characteristic curves.

RESULTS

The T2 star values of the cancerous node (mean: 23.21+0.87ms) were significantly lower (P <0.001) than those of benign node (mean: 5.08+0.32ms). Adopting a threshold value of 12.35 ms. Quantitative T2 star mapping resulted in 91.2% sensitivity, 79.3% specificity in the identification of thyroid cancer. The ADC values of the cancerous node (mean: 0.83+0.37ms) were significantly lower (P <0.001) than those of benign node (mean: 1.53+0.28ms). Adopting a threshold value of 1.03 ms, ADC mapping resulted in 90.3% sensitivity, 73.2% specificity. Quantitative T2 star mapping showed significantly greater specificity for differentiating cancerous node from benign node than ADC mapping 79.3% vs 73.2%, P<.001), with equal sensitivity (91.2% vs 90.3%, P>0.05).

CONCLUSION

Preliminary findings suggest the feasibility of performing T2 star mapping of the thyroid node acquired by using mulit-echo T2 star that may provide increased sensitivity to the diagnostic performance of thyroid cancer compared with DWI. Further larger studies to confirm these preliminary findings are warranted.

CLINICAL RELEVANCE/APPLICATION

Preliminary findings suggest the feasibility of performing T2 star mapping of the thyroid node may provide increased sensitivity to the diagnostic performance of thyroid cancer compared with DWI.

SST10-05 Quantitative Diffusion-weighted Imaging for Evaluating Papillary Thyroid Carcinoma at 3T MRI: Optimal b Value

Friday, Dec. 4 11:10AM - 11:20AM Location: N227

Participants

Ruo Yang Shi, Shanghai, China (*Presenter*) Nothing to Disclose Lianming Wu, Shanghai, China (*Abstract Co-Author*) Nothing to Disclose

PURPOSE

To assess the quantitative diffusion-weighted imaging (DWI) in distinguish papillary thyroid carcinoma (PTC) from benign thyroid nodules, and to evaluate the efficiency of DWI under different b values in discriminating between PTC and benign thyroid nodules, with pathologic analysis after surgery as reference standard.

METHOD AND MATERIALS

DWI was performed in 32 patients with thyroid nodules followed by surgery. DWI was examined by single-shot echo planar imaging (SE-EPI) under different b values including 0, 250, 500, 750, 1000, 1500, 2000s/mm². The diffusion-weighted image quality of six b value groups was evaluated. Apparent diffusion coefficient (ADC) values were counted in region of interest (ROI) for b values of 0 and for each b value from 250 to 2000 s/mm². Mean ADC values in ROI and the difference between PTC regions and benign thyroid nodules were calculated using two independent sample t-test. Sensitivity, specificity and area under the curve (AUC) were acquired by ROC curve.

RESULTS

The contrast-to-noise ratio (CNR) and signal-to-noise ratio (SNR) were not satisfied when b value 1500 or 2000s/mm² was adopted. The qualitative image quality was not enough to meet diagnostic requirement. The mean ADC values (\pm standard deviation) of the PTC regions were 1.33 ± 0.47 , 0.92 ± 0.35 , 0.69 ± 0.31 , 0.57 ± 0.26 , 0.43 ± 0.20 , and $0.32 \pm 0.15 \times 10^{-3}$ mm²/s and were significantly lower than those of benign thyroid nodules (P<.005). b=500 acquired the highest AUC among all the b values. Applying a threshold ADC value of 1.32×10^{-3} mm²/s at b=500, the sensitivity is 73.7% and the specificity is 92.3%.

CONCLUSION

Quantitative DWI can distinguish PTC from benign thyroid nodules. The optimal b value for DWI at 3T MRI to identify PTC may be 500s/mm².

CLINICAL RELEVANCE/APPLICATION

Quantitative DWI for thyroid can play important role in the diagnose of the thyroid nodules. The optimal b value may be 500s/mm².

SST10-06 Multi-parametric Advanced MR Imaging (IVIM, DCE-MR, 2D and 3D Tumor Metrics) as a Predictive Tool of Treatment Response in HPV Positive Oropharyngeal Squamous Cell Carcinoma Patients

Friday, Dec. 4 11:20AM - 11:30AM Location: N227

Participants

Ahmed Elakkad, MBBCh, MSc, Houston, TX (*Abstract Co-Author*) Nothing to Disclose Nabil A. Elshafeey, MD, Houston, TX (*Presenter*) Nothing to Disclose Masumeh Hatami, Houston, TX (*Abstract Co-Author*) Nothing to Disclose Aikaterini Kotrotsou, PhD, MEng, Houston, TX (*Abstract Co-Author*) Nothing to Disclose Mohamed G. Elbanan, MD, Houston, TX (*Abstract Co-Author*) Nothing to Disclose Vinodh A. Kumar, MD, Houston, TX (*Abstract Co-Author*) Nothing to Disclose Ashok J. Kumar, MD, Houston, TX (*Abstract Co-Author*) Nothing to Disclose Rivka R. Colen, MD, Houston, TX (*Abstract Co-Author*) Nothing to Disclose

PURPOSE

Human papilloma virus (HPV) positive tumors carry a better prognosis than HPV negative ones. Although HPV positivity is proven to be independent of other known prognostic factors including age and TNM staging, yet treatment failure has been recorded. In our study we used Intra Voxel Incoherent Motion, dynamic contrast enhanced magnetic resonance perfusion imaging (DCEMRI) and 2D, 3D volumetric parameters to find out which is the best predictor of treatment response in HPV positive oropharyngeal squamous

METHOD AND MATERIALS

Patients with pathologically proven HPV positive oropharyngeal SCC were included in this study under an IRB approved protocol with signed study specific informed consent forms as a part of prospective ongoing clinical trial. All patients underwent two MRI studies, baseline scan within 1week before treatment and mid-treatment scan. According to response to treatment, patients were then categorized into 2 groups; complete responders (CR) in whom the primary has completely disappeared and partial responders (PR) where there was still a residual tumoral tissue. All morphological image analyses and segmentation were done using 3D Slicer 4.3.1 (slicer.org) and reviewed in consensus by 2 neuroradiologists. Multiple quantitative imaging features were identified including IVIM (D, D*, and f), MR-Perfusion (Ktrans, Vp, Ve, and Kep) as well as 2D and 3D volumes of the primary tumor at the first time point.

RESULTS

Median of the time between the two MRI was 25 days. Based on the second MRI, 75% of patients hadcomplete response to treatment. Mann-Whithny U Exact test was used to compare baseline variables between patient with complete and partial response to therapy. Kep mean and Ktrans mean significantly higher in patients who showed partial response to treatment. Logistic Regression analysis was performed to determine the association between each of the perfusion parameters and response to treatment. Higher Ktrans had a significant association with partial response to treatment.

CONCLUSION

Treatment response in HPV positive oropharyngeal squamous cell carcinoma patients can be reliably predicted through different advanced MRI parameters.

CLINICAL RELEVANCE/APPLICATION

HPV positive OPCC response to treatment are detected using multiple advanced and conventional MRI

SST10-07 Differentiation of the Metastatic Lymph Nodes from Thyroid Carcinoma and Squamous Cell Carcinoma and Lymphoma with Dual-Energy CT Monoenergetic Imaging

Friday, Dec. 4 11:30AM - 11:40AM Location: N227

Participants

Yang Yaying I, MD, Kunming, China (*Presenter*) Nothing to Disclose Li Qing, MD, Kunming, China (*Abstract Co-Author*) Nothing to Disclose Zhao Wei, MD, Kunming, China (*Abstract Co-Author*) Nothing to Disclose Yang Bin, MD, Dali, China (*Abstract Co-Author*) Nothing to Disclose

Background

Objective To explore the value of dual-energy CT monoenergetic imaging in differential diagnosis of the metastatic cervical lymph nodes in thyroid carcinoma, squamous cell carcinoma and lymphoma.

Evaluation

The spectrum curve slope of arterial phase and parenchymal phase can be used to differentiate lymph node metastasis of in thyroid carcinoma, the metastatic lymph nodes from lymphoma in the neck.

Discussion

Results Of 79 enlarged lymph nodes, 23 were metastatic lymph nodes from thyroid carcinoma, 24 from squamous cell carcinoma and 32 were lymphoma. With the increase of keV values (from 60 to 180 keV), the corresponding CT values of the three kinds of malignant lymph nodes were decreased. The higher the keV value, the smaller the CT value decrease, and the spectrum curve appeared as "drop type". The spectrum slope curve of the metastatic lymph nodes of thyroid carcinoma in arterial phase (1.23 ± 0.41) and parenchymal phase (0.85 ± 0.33) are maximal and the slope curve of lymphoma in arterial phase (0.40 ± 0.16) and parenchymal phase (0.47 ± 0.09) are the lowest. The spectrum slope curve of metastatic lymph nodes from the squamous cell carcinoma in arterial phase and parenchymal phase is 0.88 ± 0.10 and 0.62 ± 0.28 , respectively. The spectrum curve slope of the three kinds of malignant lymph nodes have statistical significance. Comprehensive analysis showed, if 0.36 > K > 0.24 in arterial phase, it is most probably lymphoma; If $0.81\geq K\geq0.78$, it is most probably the metastatic lymph nodes; and if $1.65\geq K>0.98$, it is most probably lymph node metastasis from thyroid carcinoma; in parenchymal phase, if $0.38 > K\geq0.34$, it is most probably the metastatic lymph nodes; and if $1.65\geq K>0.98$, it is most probably lymph nodes. If $0.52 > K\geq0.38$, it is most probably lymphoma, if $1.18\geq K\geq0.56$, it is most probably lymph node metastasis from thyroid carcinoma.

Conclusion

The spectrum curve slope of arterial phase and parenchymal phase can be used to differentiate lymph node metastasis of in thyroid carcinoma, the metastatic lymph nodes from lymphoma in the neck.

SST10-08 High Resolution Diffusion Weighted Imaging of Thyroid Gland Using Reduced FOV Technique: A Preliminary Clinical Application at 3T MRI

Friday, Dec. 4 11:40AM - 11:50AM Location: N227

Participants

Hao Yonghong, MD, Wuhan, China (*Presenter*) Nothing to Disclose Wenzhen Zhu, MD, PhD, Wuhan, China (*Abstract Co-Author*) Nothing to Disclose Jianpin Qi, PhD, Wuhan, China (*Abstract Co-Author*) Nothing to Disclose

PURPOSE

DWI has been shown to be useful for differentiation between benign and malignant thyroid nodules. However, due to severe susceptibility and distortion artifacts and image blurring, the diagnostic value of clinical thyroid DWI is limited. The purpose of this study was to evaluate the performance of reduced field of view (r-FOV) diffusion weighted imaging and compare the diagnostic value of r-FOV diffusion imaging and conventional diffusion imaging in patients with thyroid nodules.

METHOD AND MATERIALS

79 consecutive patients who were clinically suspected with thyroid malignant lesions by ultrasound or/and scintigraphy and 12 healthy controls were included in this study. All participants underwent r-FOV diffusion imaging and f-FOV diffusion imaging with a 3T MRI scanner. Image quality and lesion identifications were visually evaluated by two independent reviewers and image properties (SNR, CNR, geometric distortion) were quantified. The apparent diffusion coefficient values of thyroid lesions and normal thyroid parenchyma were calculated and compared between two diffusion methods. The ROC analyses for both DWI methods were performed and differences in the area under the curve were assessed.

RESULTS

Agreement between two reviewers was good for image quality and lesion identification. The image quality and lesion identification of r-FOV diffusion imaging was rated higher than that of f-FOV DW imaging(p<0.001). The geometric distortions for f-FOV DW imaging were significant higher than that for r-FOV imaging, while SNR of r-FOV imaging was slightly lower than that of conventional DW imaging. The mean ADCs of r-FOV diffusion imaging were lower than that of f-FOV diffusion imaging ignore of different tissue types (1.42 \pm 0.44 ×10-3 mm2/s vs 1.54 \pm 0.45×10-3 mm2, p<0.001). There was significant difference among the ADCs of different tissue groups obtained from both r-FOV and f-FOV DWI. The areas under the curve for r-FOV (0.962) and conventional DW imaging (0.951) were not statistically different.

CONCLUSION

r-FOV diffusion imaging provide higher image quality and lesion identification than f-FOV diffusion imaging by reducing susceptibility artifacts, spatial distortion, image blurring, and were of comparable diagnostic values in nodules thyroid.

CLINICAL RELEVANCE/APPLICATION

high resolution DWI of thyroid could improve the identification and interpretation of nodules, especially for microcarcinoma.

SST10-09 The Optimization Weighting Factors of Linear Image Blending in Dual-Energy Computed Tomography for the Diagnosis of Laryngeal Carcinoma

Friday, Dec. 4 11:50AM - 12:00PM Location: N227

Participants

Mengxi Jiang, Beijing, China (*Presenter*) Research Grant, General Electric Company Jian Jiang, MD, Beijing, China (*Abstract Co-Author*) Research Grant, General Electric Company Yuan Jiang, MD, Beijing, China (*Abstract Co-Author*) Nothing to Disclose Xiaoying Wang, MD, Beijing, China (*Abstract Co-Author*) Nothing to Disclose

PURPOSE

To evaluate the linear image-blending of varying weighting factors in dual-energy computed tomography of laryngeal carcinoma regarding subjective and objective image quality.

METHOD AND MATERIALS

Patients with biopsy-proven untreated primary laryngeal carcinoma who underwent DECT scan (100kVp/Sn140 kVp) of neck were retrospectively evaluated.Ten (9 men, 1 woman; age range, 46-76 years old) cases were enrolled. Linearly blended images series with 11 weighting factors (0 to 1.0 in steps of 0.1) were reconstructed. For objective assessment, attenuation of lesion, various anatomic landmarks, image noise, lesion contrast-to-noise ratio and signal-to-noise ratio were compared between different image datasets. For subjective assessment, two independent blinded radiologists rated overall image quality, lesion delineation, image sharpness, and image noise of each image dataset on a 5-point grading scale.

RESULTS

The mean attenuation of lesion, sternocleidomastoid muscle, internal jugular vein, and submandibular gland increased stepwise with decreasing tube voltage from Sn140 kVp through 100 kVp. CNR was the highest in the weighting factors of 0.8 (M_0.8; 12.5 \pm 5.7). M_0.8 images showed no significant differences between linearly blended image series M_0.6 (11.7 \pm 5.5; P=0.123), M_0.7 (12.3 \pm 5.6; P=1.000), M_0.9 (12.5 \pm 5.6; P=1.000) and M_1.0 (12.2 \pm 5.5; P=1.000), but differed significantly compared to the linearly blended image series M_0, M_0.1, M_0.2, M_0.3, M_0.4 and M_0.5 (P<0.05). SNR was the highest in the weighting factors of 0.7 (35.0 \pm 6.1). M_0.7 images showed no significant differences between linearly blended image series M_0.6 (34.7 \pm 6.1; P=1.000). Overall image quality was higher in M_0.9 (4.7) and M_1.0 (4.7) images, although differences to the M_0.8 (4.4) images did not reach statistical significance (P=0.083). Delineation of the tumour was rated significantly better in M_0.9 (4.4) and M_1.0 (4.5) images compared to other linearly blended image series. Scoring of the image sharpness revealed equally good results in all image series.

CONCLUSION

The linear-blending images of DECT data at the weighting factors of 0.9 and 1.0 can provide higher image quality for the diagnosis of laryngeal carcinoma.

CLINICAL RELEVANCE/APPLICATION

Linear image blending in DECT could provided more information about laryngeal carcinoma, which improved diagnostic confidence in the assessment of laryngeal carcinoma.

Neuroradiology (Quantitative Neuroimaging)

Friday, Dec. 4 10:30AM - 12:00PM Location: N230

NR BQ MR

AMA PRA Category 1 Credits ™: 1.50 ARRT Category A+ Credits: 1.50

Participants

Pratik Mukherjee, MD, PhD, San Francisco, CA (*Moderator*) Research Grant, General Electric Company; Medical Adivisory Board, General Electric Company;

Sub-Events

SST11-01 Repeatability of the Volume of Interest Placement Using Edited Magnetic Resonance Spectroscopy

Friday, Dec. 4 10:30AM - 10:40AM Location: N230

Participants

Fei Gao, Jinan, China (*Presenter*) Nothing to Disclose Guangbin Wang, MD, Jinan, China (*Abstract Co-Author*) Nothing to Disclose Bin Zhao, MD, Jinan, China (*Abstract Co-Author*) Nothing to Disclose Fuxin Ren, Jinan, China (*Abstract Co-Author*) Nothing to Disclose

PURPOSE

Edited magnetic resonance spectroscopy (MRS), using the MEGA-PRESS sequence, is the most widely used technique for detecting gamma-aminobutyric acid (GABA) in the human brain. However, this method required a relatively large volume of interest (VOI), so the accuracy of VOI placement is important to ensure the reliability of GABA quantification. In this study the MRS voxels overlap of intra- and inter-subject were evaluated.

METHOD AND MATERIALS

Fifteen healthy volunteers (8 men and 7 women, 44.87±3.42 years) underwent MRS examinations. All subjects were examined on a 3T scanner using MEGA-PRESS sequence and T1-weighted 3D TFE images were used as a localizer. The unsuppressed water signal was obtained for quantification. The VOI was chosen in the parietal region (3x3x3 cm3). MEGA-PRESS was analyzed using 'Gannet' in Matlab with Gaussian curve fitting to the GABA peaks. GABA levels (institutional units) were calculated for each subject. In one subject, four continuous scans were conducted within a period of 3 weeks. The VOI was chosen in the three areas: frontal region (3x3x3 cm3), parietal region (3x3x3 cm3) and temporal region (4x2x2 cm3). Each pixel in the T1-weighted images was segmented as gray matter, white matter, or cerebrospinal fluid using the FSL software. VOIs were co-registered to the anatomical images using the "Re-creation of VOI" Matlab tool. The VOIs and anatomical images were registered to the baseline images (intra-subject) or standard space (inter-subject) using the SPM software. The Dice overlap coefficient was used to calculate the MRS voxels overlap of intra- and inter-subject.

RESULTS

The MRS voxels overlap of inter-subject was $78.87\% \pm 8.85\%$ in parietal region. No correlation between GABA levels and gray matter volume within VOI was found in parietal region for all subjects (r=0.13, p=0.64). The MRS voxels overlap of intra-subject was $85.88\% \pm 5.36\%$ in frontal region, $88.86\% \pm 2.45\%$ in parietal region and $81.31\% \pm 3.38\%$ in temporal region.

CONCLUSION

The high degree of MRS voxels overlap of intra- and inter-subject and low correlation between gray matter volume and GABA levels, suggesting that VOI placement using MEGA-PRESS has great repeatability, and the small variations in VOI placement and subject anatomy do not affect the GABA levels.

CLINICAL RELEVANCE/APPLICATION

VOI placement using MEGA-PRESS has great repeatability and MEGA-PRESS is recommended to measure GABA levels in vivo in the human brain.

SST11-02 Does Gadolinium Change the Relaxometry of the Dentate Nuclei? A Quantitative Multi-parametric MRI Study

.

.

Friday, Dec. 4 10:40AM - 10:50AM Location: N230

Participants

Enrico Tedeschi, MD, Napoli, Italy (*Presenter*) Nothing to Disclose Carmela Russo, Naples, Italy (*Abstract Co-Author*) Nothing to Disclose Sirio Cocozza, MD, Napoli, Italy (*Abstract Co-Author*) Nothing to Disclose Giuseppe Palma, PhD, Naples, Italy (*Abstract Co-Author*) Nothing to Disclose Antonietta Canna, Naples, Italy (*Abstract Co-Author*) Nothing to Disclose Pasquale Borrelli, Naples, Italy (*Abstract Co-Author*) Nothing to Disclose Roberta Lanzillo, Naples, Italy (*Abstract Co-Author*) Nothing to Disclose Valentina Angelini, Naples, Italy (*Abstract Co-Author*) Nothing to Disclose Emanuela Postiglione, Naples, Italy (*Abstract Co-Author*) Nothing to Disclose Vincenzo Brescia Morra, Naples, Italy (*Abstract Co-Author*) Nothing to Disclose Arturo Brunetti, MD, Naples, Italy (*Abstract Co-Author*) Nothing to Disclose Marco Salvatore, MD, Napoli, Italy (*Abstract Co-Author*) Nothing to Disclose

PURPOSE

Repeated intravenous administration of Gadolinium-based contrast agents (Gd-CA) has been associated with increased MRI signal intensity in T1-weighted sequences in dentate nuclei (DN). Our aim is to perform, for the first time, a quantitative MRI (qMRI) assessment of DN relaxometry in patients receiving multiple doses of Gd-CA using 0.7x0.7x1.3 mm3 resolved Gradient-Echo (GRE) sequences.

METHOD AND MATERIALS

From a total of 92 Multiple Sclerosis patients with normal renal function, we retrospectively selected 21 patients [Group A, M/F=5/16, age: 41±11 years, disease duration (DD): 15.9±8.1 years] who had performed, during the course of the disease, 9 or more contrast-enhanced (CE) MRI scans, and 28 patients (Group B, M/F=14/14, age: 36±11 years, DD: 7.8±6.8 years) who underwent less than 4 CE-MRI scans. A group of 28 age/sex-matched healthy controls (HC, M/F=11/17, age: 38±13 years), who underwent only unenhanced MRI, was also studied. In patients and HC, GRE sequences (TR=28ms, TE=[7,22]ms, FA=[3,20]°) were acquired at 3T and processed with an in-house software, providing quantitative estimates of R1, R2* and magnetic susceptibility (QSM) of the brain. ROIs were hand-drawn on the axial slice with the best representation of DN. Group differences in qMRI data were tested both in terms of absolute DN values and of ratios between DN and a brainstem (BS) ROI, used as internal reference.

RESULTS

The DN/BS ratio for R1 was significantly higher in Group A (1.17 ± 0.09) when compared to Group B (1.10 ± 0.08) and HC (1.11 ± 0.07), p-values being 0.008 and 0.009, respectively. Instead, the DN/BS ratio for R1 did not differ between Group B and HC (p=0.79). Also, no significant differences were found between the 3 groups in terms of R2* or QSM DN/BS ratios, nor of R1, R2* and QSM absolute DN values.

CONCLUSION

Our in vivo high-resolution quantitative relaxometric MRI analysis showed higher R1 values in patients undergoing repeated CE-MRI scans, supporting the hypothesis that Gd-CA accumulate in DN. Further longitudinal quantitative analysis of the mechanisms of Gd-CA clearance in the brain are warranted.

CLINICAL RELEVANCE/APPLICATION

Repeated administration of Gd-based contrast agents is associated with long-term changes in brain relaxometry, thus indirectly confirming the concerns about the stability of Gd-chelation over time.

SST11-03 Metabolic Changes in the Bilateral Visual Cortex of Monocular Blindness Macaque Monkeys: A Multivoxel Proton Magnetic Resonance Spectroscopy Study

Friday, Dec. 4 10:50AM - 11:00AM Location: N230

Participants

Lingjie Wu, MD, Shanghai, China (*Abstract Co-Author*) Nothing to Disclose Zuohua Tang, PhD, MD, Shanghai, China (*Presenter*) Nothing to Disclose

PURPOSE

To study adaptive plasticity and reorganization in the visual cortex of the monocular blind macaque using multi-voxel proton magnetic resonance spectroscopy study (1H-MRS).

METHOD AND MATERIALS

Four healthy neonatal macaques were randomly divided into 2 groups. One group served as control group (group A). Optic nerve transecting was performed in the right eye of the other group (group B), to establish the monocular blind model. Sixteen (group B16M) and thirty-two (group B32M) months after monocular optic nerve transecting, multi-voxel 1H-MRS was performed on the bilateral visual cortex of all monkeys, respectively. We compared NAA/Cr, Ins/Cr, Cho/Cr and Glx/Cr in the visual cortex between group A and group B as well as between the left and right visual cortices of group A and B in each time points, respectively. All of the metabolic changes detecting by multi-voxel 1H-MRS were further compared with the hematoxylin-eosin and immunofluorescent staining findings.

RESULTS

Compared with group A, in bilateral visual cortex, NAA/Cr in both group B16M and group B32M, as well as Glx/Cr in group B32M were all significant decrease (p<0.05), whereas the Cho/Cr and Ins/Cr of group B32M were significant increase (p<0.05). Meanwhile, significant difference of NAA/Cr in group B32M was found between the left and right visual cortex, whereas no statistical difference of Ins/Cr, Cho/Cr and Glx/Cr between the left and right visual cortex was found in both group B16M and group B32M. All of these findings were further confirmed by the hematoxylin-eosin and immunofluorescent staining using anti-NeuN antibody, anti-Choline Acetyltransferase antibody and anti-EAAT3 antibody.

CONCLUSION

Multi-voxel 1H-MRS was able to detect the different metabolic changes in the visual cortex, which was valuable for investigating its adaptive plasticity and reorganization.

CLINICAL RELEVANCE/APPLICATION

Such alterations in the metabolism of the bilateral visual cortex could provide valuable information for future studies of adaptive plasticity and reorganization in visual loss or other sensory deprivation in animal models and human beings.

SST11-04 Physiology-based MRI Assessment of CSF Flow in Chiari I Malformation (CMI)

Friday, Dec. 4 11:00AM - 11:10AM Location: N230

Participants

Rafeeque A. Bhadelia, MD, Chestnut Hill, MA (*Presenter*) Nothing to Disclose Neel Madan, MD, Boston, MA (*Abstract Co-Author*) Consultant, Near Infrared Imaging, LLC; Board Member, Quindec Inc Carl B. Heilman, Boston, MA (*Abstract Co-Author*) Nothing to Disclose David B. Khatami, MD, PhD, Boston, MA (*Abstract Co-Author*) Nothing to Disclose Yansong Zhao, Boston, MA (*Abstract Co-Author*) Researcher, Koninklijke Philips NV Samuel Patz, PhD, Boston, MA (Abstract Co-Author) Nothing to Disclose

PURPOSE

Invasive pressure studies have suggested that in patients with Chiari I malformation (CMI), CSF flow across the foramen magnum transiently decreases after coughing in the presence of a clinically significant obstruction. The purpose of this study was to demonstrate this phenomenon non-invasively by assessing CSF flow response to coughing in CMI patients using MR pencil beam imaging (PBI) and compare it to healthy participants.

METHOD AND MATERIALS

7 CMI patients and 6 healthy participants were studied using PBI with a temporal resolution of ~50ms. Patients and participants were scanned for 90-seconds to continuously record cardiac-cycle related CSF flow waveforms as well as the heart rate and respiratory motion during resting, coughing and post-coughing periods. CSF flow waveform amplitude (ACSF), CSF stroke volume (SVCSF), and CSF flow rate (FRCSF; SVCSF x heart rate)in resting and immediate post-coughing periods were determined. Post-coughing values of all three parameters were calculated as a percentage of resting values, and compared between patients and healthy participants.

RESULTS

There was no significant difference in ACSF, SVCSF and FRCSF between CMI patients and healthy participants during rest. However, after coughing, a significant decrease in ACSF (p<0.001), SVCSF (p=0.001) and FRCSF (p=0.001) was observed in CMI patients compared to healthy participants.

CONCLUSION

Coughing decreases CSF flow across the foramen magnum in CMI patients but not in healthy participants. Real-time MRI measurement of CSF flow response to coughing may provide objective quantitative assessment of foramen magnum obstruction in CMI patients.

CLINICAL RELEVANCE/APPLICATION

Physiology-based MRI measurement of CSF flow may provide objective assessment of foramen magnum obstruction in CMI patients

SST11-05 Cerebral Perfusion Relates to Regional Cortical Thickness in the General Population

Friday, Dec. 4 11:10AM - 11:20AM Location: N230

Participants

Hazel I. Zonneveld, MD, MSc, Rotterdam, Netherlands (Presenter) Nothing to Disclose

Wiro Niessen, PhD, Rotterdam, Netherlands (*Abstract Co-Author*) Co-founder, Quantib BV; Scientific Director, Quantib BV; Shareholder, Quantib BV

Aad Van Der Lugt, MD, PhD, Rotterdam, Netherlands (Abstract Co-Author) Nothing to Disclose

Gabriel P. Krestin, MD, PhD, Rotterdam, Netherlands (*Abstract Co-Author*) Consultant, General Electric Company; Research Grant, General Electric Company; Research Grant, Bayer AG; Research Grant, Siemens AG; Speakers Bureau, Siemens AG Mohammad A. Ikram, Rotterdam, Netherlands (*Abstract Co-Author*) Nothing to Disclose Meike W. Vernooij, MD, Rotterdam, Netherlands (*Abstract Co-Author*) Nothing to Disclose

PURPOSE

To investigate whether cerebral perfusion is associated with regional cortical thickness on magnetic resonance imaging (MRI) in community-dwelling persons free of stroke and a clinical diagnosis of dementia.

METHOD AND MATERIALS

2,961 persons (mean age 59.6 years; 54.5% women) from a prospective population-based study underwent brain MRI on a 1.5tesla MRI system, yielding cortical thickness of 34 cortical regions using automated segmentation technique (FreeSurfer). Total cerebral blood flow (tCBF) was determined using 2D phase-contrast MRI by adding flow rates for the carotid arteries and the basilar artery and expressed in ml/min. Parenchymal CBF (mL/min/100mL) was calculated by dividing tCBF by each individual's brain volume (mL) multiplied by 100. We used multivariable linear regression models to investigate the association between cerebral perfusion and regional cortical thickness.

RESULTS

Both lower tCBF and pCBF were associated with thinner regions of the cortex predominantly involving the frontal lobe, and the medial posterior regions. Strongest association was found for tCBF with cortical thickness of the superior-frontal and rostral-middle-frontal region.

CONCLUSION

In community-dwelling persons, cerebral perfusion relates to cortical thickness variations in different brain regions.

CLINICAL RELEVANCE/APPLICATION

Our findings provide further insight into the pathophysiological role of cerebral perfusion in neurodegeneration in aging.

SST11-06 A Diffusional Kurtosis Imaging Study of Type-2 Diabetic Brain

Friday, Dec. 4 11:20AM - 11:30AM Location: N230

Participants

Ying Xiong, MD, Chicago, IL (*Presenter*) Nothing to Disclose Yi Sui, PhD, Chicago, IL (*Abstract Co-Author*) Nothing to Disclose Jinliang Niu, MD, PhD, Shanxi, China (*Abstract Co-Author*) Nothing to Disclose Qiang Zhang, PhD, Wuhan, China (*Abstract Co-Author*) Nothing to Disclose Kejia Cai, PhD, Chicago, IL (*Abstract Co-Author*) Nothing to Disclose Wenzhen Zhu, MD, PhD, Wuhan, China (*Abstract Co-Author*) Nothing to Disclose

PURPOSE

Diffusional kurtosis imaging (DKI) is an extension of diffusion tensor imaging (DTI) by taking non-Gaussian diffusion behavior into consideration, allowing more comprehensive characterization of diffusion in tissues. This study aims at investigating brain microstructural changes in both white matter (WM) and gray matter (GM) of type-2 diabetes mellitus (T2DM) patients using DKI.

METHOD AND MATERIALS

DKI (b=0, 1250, 2500 s/mm2; 25 directions) was performed at 3T on 30 T2DM patients (60.6±6.3 years old; 13 males) and 28 healthy controls (58.5±5.9 years old; 11 males). FMRIB Software Library (FSL) with tract-based spatial statistics (TBSS) was utilized to analyze the DKI metrics, including mean kurtosis (MK), axial kurtosis (Ka), and radial kurtosis (Kr) of multiple WM regions and specific GM structures in the bilateral thalamus, followed by a Pearson's correlation between MK values of selected WM fiber tracts and disease duration.

RESULTS

In the whole-brain TBSS analysis, the T2DM patients exhibited abnormalities in 35.4%, 10.5%, and 26.0% of WM regions as measured by MK, Ka, and Kr, respectively, when compared to the controls. A reduction in MK of the T2DM patients was caused primarily by the decreased Kr, suggesting compromised myelin sheath in the WM regions. MK and Ka also decreased in the bilateral thalamus, while Kr did not show statistically significant difference. This can be related to the compromised synapse in the thalamus, which is a sensory and movement relay between cerebral cortex and other regions of the brain and spinal cord. Atlas-based MK analyses on individual fiber tracts showed that pronounced MK reduction occurred in the internal capsule, corona radiata, cingulum (hippocampus), superior longitudinal fasciculus, corpus callosum, as well as the thalamus. Decreased MK values in the genu of the corpus callosum and anterior corona radiata were correlated with increased disease duration (R=-0.473 and -0.400 respectively, p<0.05) of the T2DM patients.

CONCLUSION

DKI can complement conventional DTI by providing new information to characterize and pinpoint brain microstructural changes in both WM and GM of T2DM patients.

CLINICAL RELEVANCE/APPLICATION

DKI can probe microstructural changes in WM and GM in patients with T2DM, and potentially provide valuable information to study diabetic encephalopathy, including cognitive impairment.

SST11-07 Adaptive Tissue Cluster Tracking on Quantitative MRI for Fully Automatic Brain Segmentation on Young Children

Friday, Dec. 4 11:30AM - 11:40AM Location: N230

Participants

Marcel Warntjes, Linkoping, Sweden (*Presenter*) Employee, SyntheticMR AB Suraj Serai, PhD, Cincinnati, OH (*Abstract Co-Author*) Nothing to Disclose James L. Leach, MD, Cincinnati, OH (*Abstract Co-Author*) Nothing to Disclose Blaise V. Jones, MD, Cincinnati, OH (*Abstract Co-Author*) Nothing to Disclose

PURPOSE

Multi-parametric quantitative MRI of longitudinal T1 relaxation, transverse T2 relaxation and proton density (PD) can be achieved within a clinically acceptable scan time. It has been shown that values of T1, T2 and PD rapidly change during the first years of life. The purpose of this study was to create an algorithm that adaptively tracks the grey matter and white matter tissue properties in qMRI data, in order to segment grey matter, white matter and cerebrospinal fluid volumes of the brain, independent of age.

METHOD AND MATERIALS

A group of 23 quantified datasets at 3T of paediatric clinical cases in the range 0-20 years old was used to develop an algorithm to automatically track the mean T1, T2 and PD values of GM, myelinated WM and CSF. The positions of the tissue clusters were then used to define GM, myelinated WM and CSF partial volume. The sum of all partial volumes in the intracranial volume resulted in an estimation of total GM, WM and CSF volumes.

RESULTS

The observed T1/T2 relaxation times for GM changed from 1850/110 ms to 1360/86 ms in the first two years of life, whereas myelinated WM changed from 1080/98 ms to 720/70 ms. After two years the T1 and T2 relaxation were relatively constant. CSF had T1/T2 = 4200/1600 ms for all ages. Application of adaptive tissue cluster tracking on GM and WM showed that myelinated WM volume, an average, increased from 0 to 252 mL, CSF decreased from 241 mL to 40 mL and total brain volume increased from 403 mL to 1225 mL in the first 4 years of life. Without tissue cluster tracking the estimated WM volume was significantly lower and CSF volume was significantly higher.

CONCLUSION

Using adaptive tissue cluster tracking the differences in T1 and T2 relaxation between young children and adults can be corrected for, allowing fully automatic brain segmentation on all ages.

CLINICAL RELEVANCE/APPLICATION

Quantitative MRI provides absolute values and improved means of statistics in clinical MRI. Automatic brain segmentation using qMRI may provide more precise monitoring and follow-up throughout life.

SST11-08 Radiomic Texture Analysis Mapping Predicts Areas of True Functional MRI Activation

Friday, Dec. 4 11:40AM - 11:50AM Location: N230

Islam S. Hassan, MBBCh, Houston, TX (*Presenter*) Nothing to Disclose Aikaterini Kotrotsou, PhD, MEng, Houston, TX (*Abstract Co-Author*) Nothing to Disclose Ali S. Bakhtiari, Houston, TX (*Abstract Co-Author*) Nothing to Disclose Jeffrey S. Weinberg, MD, Houston, TX (*Abstract Co-Author*) Nothing to Disclose Ashok J. Kumar, MD, Houston, TX (*Abstract Co-Author*) Nothing to Disclose Raymond Sawaya, MD, Houston, TX (*Abstract Co-Author*) Nothing to Disclose Markus Luedi, Houston, TX (*Abstract Co-Author*) Nothing to Disclose Pascal O. Zinn, MD, Boston, MA (*Abstract Co-Author*) Nothing to Disclose Rivka R. Colen, MD, Houston, TX (*Abstract Co-Author*) Nothing to Disclose

PURPOSE

To develop an automated robust method using MR texture analysis to accurately predict areas of true functional activity

METHOD AND MATERIALS

10 right-handed (5 male, 5 female) healthy individuals underwent a functional MRI study using the sentence completion task. IRB approval and informed consent were obtained in this HIPAA compliant study. fMRI data analysis was performed using statistical parametric mapping approach (SPM8). The resultant functional map was individually thresholded to optimize visualization of language area. A board-certified neuroradiologist classified different clusters into Expected (E) and Non-Expected (NE) based on their anatomical locations. Texture Analysis was performed using the mean EPI volume for each individual, and 20 rotation-invariant texture features were obtained. Logistic regression and treebagging models were used to identify significant discriminatory texture features and build predictive models for the E versus NE ROIs

RESULTS

We identified 65 ROIs (23 E versus 42 NE). Logistic regression model identified specific texture features (sum variance p=0.014, sum average p=0.019, cluster shade p=0.028, cluster prominence p=0.046, correlation p=0.09) related with the homogeneity that allowed discrimination between E and NE ROIs. The AUC of the logistic regression model was 93.59% (86.58% cross-validated), specificity/sensitivity of 97.31%/74.17%. Tree-bagging model resulted in an AUC of 88.19% and specificity/sensitivity of 80.95%/86.96%.

CONCLUSION

Radiomic texture analysis of fMRI can be a useful tool for detecting areas of true functional activity and serve as a tool for eliminating false-positive or non-task related activity

CLINICAL RELEVANCE/APPLICATION

Radiomic texture analysis can discriminate those areas of true functional task-related activity and thus allow for precise presurgical detection and mapping of areas of true functional eloquence in order that maximal extent of neurosurgical resection can occur while simultaneously maintaining intact neurological function.

SST11-09 Non-Invasive Determination of Epidermal Growth Factor Receptor Variant III Expression in Glioblastoma through Analysis of Multi-Parametric Magnetic Resonance Imaging

Friday, Dec. 4 11:50AM - 12:00PM Location: N230

Participants

Hamed Akbari, MD, PhD, Philadelphia, PA (*Presenter*) Nothing to Disclose Spyridon Bakas, Philadelphia, PA (*Abstract Co-Author*) Nothing to Disclose Martin Rozycki, Philadelphia, PA (*Abstract Co-Author*) Nothing to Disclose Xiao Da, Philadelphia, PA (*Abstract Co-Author*) Nothing to Disclose Jared Pisapia, Philadelphia, PA (*Abstract Co-Author*) Nothing to Disclose Michel Bilello, MD, PhD, Philadelphia, PA (*Abstract Co-Author*) Nothing to Disclose Donald M. O'Rourke, MD, Philadelphia, PA (*Abstract Co-Author*) Nothing to Disclose Christos Davatzikos, Philadelphia, PA (*Abstract Co-Author*) Shareholder, Gliomics LLC

PURPOSE

Epidermal growth factor receptor variant III (EGFRvIII) is the target of ongoing investigational drug trials for the treatment of glioblastoma (GB). However, tissue-based genetic testing of the EGFRvIII status is costly and not widely available. The goal of this study is to combine multi-parametric magnetic resonance imaging (MRI) data, with the intention of non-invasively determining the mutation status of EGFRvIII in patients with GB. We hypothesize that quantification of subtle, yet important, imaging phenotypes of GB from multiple MRI modalities may lead to non-invasively determining expression of molecular tumor characteristics, and particularly of the EGFRvIII oncogene.

METHOD AND MATERIALS

Preoperative multi-parametric MRI data (i.e. T1, T1-Gad, T2, T2-FLAIR, rCBV, DTI, and DSC) from 41 solitary de novo GB patients were retrospectively analyzed. Appropriate imaging features were extracted to create an integrative predictive model of EGFRvIII mutation, based on Support Vector Machines. The utilized features comprise the age of the patient, the size of the enhancing tumor, non-enhancing tumor, and edema; the tumor location, the mass-effect parameters, and the distribution of intensities of each region across all MRI modalities. Leave-one-out cross validation was used to test how well the predictive model generalizes on new unseen patient data. The results were compared with the EGFRvIII status obtained through tissue-based diagnostics.

RESULTS

The output of the predictive model is a value between -1 and 1. Values closer to 1 indicate higher probability for the subject to harbor the mutation, and values closer to -1 the opposite. A receiver operating characteristic (ROC) curve was calculated by changing the threshold in the range of the model's output values. The accuracy of the model was calculated for the threshold equal to 0. The proposed method successfully identified the EGFRvIII mutation, with 83% accuracy and the area under the ROC curve equal to 0.82.

CONCLUSION

Computational analysis of multi narametric MDI data can load to the avtraction of informative and comprehensive features

computational analysis of multi-parametric mist data can lead to the extraction of informative and comprehensive reatures, representative of the distinctive imaging phenotypes related to the EGFRvIII mutation status in patients with GB.

CLINICAL RELEVANCE/APPLICATION

Analysis of multi-parametric MRI data reveals EGFRvIII mutation phenotypes in GB, hence assists in personalizing treatment whilst avoiding costly and not widely-available tissue-based genetic testing.